

**Design, Synthesis, Characterization and Applications of  
Polyimides, Sulphonated Copolyimides and their Composites  
with Protic Ionic Liquids**



**By**  
**Aalia Manzoor**

Department of Chemistry  
Quaid-i-Azam University  
Islamabad  
2024

**Design, Synthesis, Characterization and Applications of  
Polyimides, Sulphonated Copolyimides and their Composites  
with Protic Ionic Liquids**



A dissertation submitted to the Department of Chemistry, Quaid-i-Azam University, Islamabad, in fulfilment of the requirements for the degree of

**Doctor of Philosophy**

In

**Organic Chemistry**

By

**Aalia Manzoor**

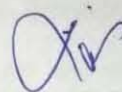
Department of Chemistry  
Quaid-i-Azam University  
Islamabad

2024

## DECLARATION

This is to certify that this dissertation entitled "*Design, Synthesis, Characterization and Applications of Polyimides Sulphonated Copolyimides and their Composites with Protic Ionic Liquids*" submitted by *Ms. Aalia Manzoor*, is accepted in its present form by the Department of Chemistry, Quaid-i-Azam University, Islamabad, Pakistan, as satisfying the partial requirement for the award of degree of *Doctor of Philosophy in Organic Chemistry*.

External Examiner (I):



---

**Prof. Dr. Zahid Shafiq**  
Institute of Chemical Sciences  
Bahauddin Zakariya University  
Multan

External Examiner (II):



---

**Prof. Dr. Naseem Iqbal**  
USPCAS-E NUST  
H-12 Islamabad

Supervisor & Head of Section:



---

**Prof. Dr. Mrs. Humaira Masood Siddiqi**  
Department of Chemistry  
Quaid-i-Azam University  
Islamabad.

Chairman:



---

**Prof. Dr. Aamer Saeed Bhatti**  
Department of Chemistry  
Quaid-i-Azam University  
Islamabad.


### Certificate of Approval

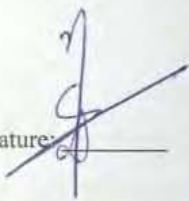
This is to certify that the research work presented in this thesis, entitled "Design, Synthesis, Characterization and Applications of Polyimides Sulphonated Copolyimides and their Composites with Protic Ionic Liquids" was conducted by Ms. Aalia Manzoor under the supervision of Prof. Dr. Mrs. Humaira Masood Siddiqi


No part of this thesis has been submitted anywhere else for any other degree. This thesis, is submitted to the Department of Chemistry Quaid-i-Azam University Islamabad in partial fulfillment of the requirements for the Doctor of Philosophy in Field of Organic Chemistry, Department of Chemistry, Quaid-i-Azam University, Islamabad.


Student Name Ms. Aalia Manzoor Signature: 

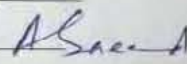
Examination Committee:

1. External Examiner: Prof. Dr. Zahid Shafiq Signature:   
Institute of Chemical Sciences  
Bahauddin Zakariya University  
Multan

2. External Examiner: Prof. Dr. Naseem Iqbal Signature:   
USPCAS-E NUST  
H-12 Islamabad

3. Internal Examiner: Prof. Dr. Mrs. Humaira Masood Siddiqi Signature:   
Department of Chemistry  
Quaid-i-Azam University  
Islamabad.

Supervisor: Prof. Dr. Humaira Masood Siddiqi Signature: 

Head of Department: Prof. Dr. Aamer Saeed Bhatti Signature: 

### **PLAGIARISM UNDERTAKING**

I solemnly declare that, the research work presented in the thesis titled "**Design, Synthesis, Characterization and Applications of Polyimides Sulphonated Copolyimides and their Composites with Protic Ionic Liquids**" is solely my research work with no significant contribution from any other person. Small contribution/help wherever taken has been duly acknowledged and that complete thesis has been written by me.

I understand the zero tolerance policy of the HEC and **Quaid-i-Azam University Islamabad** towards plagiarism. Therefore, I as an Author of the above titled thesis declare that no portion of my thesis has been plagiarized and any material used as reference is properly referred/cited.

I undertake that if I am found guilty of any formal plagiarism in the above titled thesis even after award of Ph.D. degree, the university reserves the rights to withdraw/revoke my Ph.D. degree and that HEC and the University has the right to publish my name on the HEC/University website on which names of students are placed who submitted plagiarized thesis.

Student/Author Signature: \_\_\_\_\_



Name: **Ms. Aalia Manzoor**

### **AUTHOR'S DECLARATION**

I, Ms. Aalia Manzoor hereby state that my Ph.D. thesis titled "**Design, Synthesis, Characterization and Applications of Polyimides Sulphonated Copolyimides and their Composites with Protic Ionic Liquids**" is my own work and has not been submitted previously by me for taking any degree from this University (Quaid-i-Azam University Islamabad) or anywhere else in the country/world.

At anytime if my statement is found to be incorrect even after my Graduation the University has the right to withdraw my Ph.D. degree.



Name of student: Ms. Aalia Manzoor

بِسْمِ اللَّهِ الرَّحْمَنِ الرَّحِيمِ

*This dissertation is Dedicated To my  
Loving Abu G (Manzoor Hussain  
Khan), Ammi (Azra Manzoor),  
Brothers and Sister*

*Who supported, encouraged and prayed  
for me throughout my life.*

*May ALLAH Almighty bless them all. Aameen!!*



## Table of Contents

---

---

<b>Preamble.....</b>	<b>vi</b>
<b>Acknowledgements.....</b>	<b>viii</b>
<b>Abstract.....</b>	<b>x</b>
<b>Index of tables .....</b>	<b>xii</b>
<b>Index of Figures .....</b>	<b>xiii</b>
<b>Index of Schemes .....</b>	<b>xvi</b>
<b>List of Abbreviations .....</b>	<b>xvii</b>
<b>1: Introduction .....</b>	<b>1</b>
1.1: Polyimides.....	1
1.1.1: Synthesis of polyimides .....	2
1.1.1.1: Synthesis of polyamic acid and its mechanism.....	4
1.1.1.1.1: The impact of monomer reactivity.....	6
1.1.1.1.2: The impact of reaction conditions and solvent.....	8
1.1.1.2: The thermal imidization.....	9
1.1.1.3: The chemical imidization .....	9
1.2: Sulphonated polyimides.....	11
1.3: Ionic Liquids .....	14
1.3.1: Properties of ionic liquids .....	14
1.3.2: Classification of ionic liquids.....	15
1.3.2.1: Protic ionic liquids.....	16
1.3.2.2: Aprotic ionic liquids.....	16

1.4: Sulphonated copolyimide/protic ionic liquid (SPI/IL) composites .....	17
1.5: Applications of sulphonated polyimides and protic ionic liquid composites .....	17
1.5.1: Sulphonated copolyimides as chemosensors.....	18
1.5.2: Sulphonated copolyimides for adsorption of toxic metal ions from water.....	19
1.5.3: Polymer electrolyte membrane fuel cells (PEMFCs) .....	21
1.6: Literature Review on sulphonated copolyimides and composites .....	24
1.7: Scope and Objective of Work .....	29
1.8: Plan of work .....	30
<b>2: Experimental.....</b>	<b>35</b>
2.1: Materials.....	35
2.2: Purification of solvents .....	36
2.3: Characterization methods.....	36
2.3.1: Thin layer chromatography (TLC) .....	36
2.3.2: Fourier transform infrared spectroscopy (FTIR).....	36
2.3.3: Ultraviolet-visible absorption spectroscopy.....	36
2.3.4: Gel permeation chromatography (GPC) .....	37
2.3.5: Thermal analysis.....	37
2.3.6: Atomic absorption spectroscopy (AAS) .....	37
2.3.7: Four probe proton conductivity measurement .....	37
2.3.8: Single fuel cell test.....	39
2.4: Synthesis.....	41
2.4.1: Synthesis of diamine monomers.....	41
2.4.1.1: General method for the synthesis dinitro compounds.....	41
2.4.1.1.1: Synthesis of DN2.....	42
2.4.1.1.2: Synthesis of DN3.....	42

2.4.1.2: General method for the reduction of dinitro compounds.....	42
2.4.1.2.1: Synthesis of A2.....	43
2.4.1.2.2: Synthesis of A3.....	43
2.4.2: General procedure for the synthesis of polyimides.....	43
2.4.2.1: Synthesis of polyimides from 6FDA.....	44
2.4.2.1.1: Synthesis of neat polyimide FM.....	44
2.4.2.1.2: Synthesis of neat polyimide FA.....	45
2.4.2.1.3: Synthesis of neat polyimide FA2 .....	45
2.4.2.1.4: Synthesis of neat polyimide FA3.....	46
2.4.2.1.5: Synthesis of neat polyimide FI.....	46
2.4.2.2: Synthesis of polyimides from ODPA.....	47
2.4.2.2.1: Synthesis of neat polyimide OM.....	47
2.4.2.2.2: Synthesis of neat polyimide OA.....	48
2.4.2.2.3: Synthesis of neat polyimide OA2 .....	48
2.4.2.2.4: Synthesis of neat polyimide OA3.....	49
2.4.2.2.5: Synthesis of neat polyimide OI.....	49
2.4.3: General procedure for the synthesis of sulphonated copolyimides.....	50
2.4.3.1: Synthesis of triethyl ammonium salt of benzidine-2, 2' -disulphonic acid (BDSA).....	51
2.4.3.2: Synthesis of sulphonated copolyimides from 6FDA.....	51
2.4.3.2.1: Synthesis of sulphonated copolyimides (FBM (10, 20, 30, 40, 50)).	52
2.4.3.2.2: Synthesis of sulphonated copolyimides (FBA (10, 20, 30, 40, 50)).	52
2.4.3.2.3: Synthesis of sulphonated copolyimides (FBA2(10, 20, 30, 40, 50)).	53

2.4.3.2.4: Synthesis of sulphonated copolyimides (FBA3 (10, 20, 30, 40, 50))	54
2.4.3.2.5: Synthesis of sulphonated copolyimides (FBI(10, 20, 30, 40, 50))	55
2.4.3.3: Synthesis of sulphonated copolyimides from ODPA	55
2.4.3.3.1: Synthesis of sulphonated copolyimides (OBM (10, 20, 30, 40, 50))	56
2.4.3.3.2: Synthesis of sulphonated copolyimides (OBA (10, 20, 30, 40, 50))	56
2.4.3.3.3: Synthesis of sulphonated copolyimides (OBA2 (10, 20, 30, 40, 50))	57
2.4.3.3.4: Synthesis of sulphonated copolyimides (OBA3 (10, 20, 30, 40, 50))	58
2.4.3.3.5: Synthesis of sulphonated copolyimides (OBI (10, 20, 30, 40, 50))	59
2.4.4: General procedure for the synthesis of protic ionic liquids (PILs)	59
2.4.4.1: Synthesis of protic ionic liquids using methane sulphonic acid (MsOH)	60
2.4.4.1.1: Synthesis of trimethylammonium methane sulphonate (TMMs)	60
2.4.4.1.2: Synthesis of dimethylethylammonium methane sulphonate (DMMs)	
2.4.4.1.3: Synthesis of diethylmethylammonium methane sulphonate (DEMs)	
2.4.4.1.4: Synthesis of triethylammonium methane sulphonate (TEMs)	61
2.4.4.2: Synthesis of protic ionic liquids using trifluoromethane sulphonic acid (TfOH)	61
2.4.4.2.1: Synthesis of trimethylammonium trifluoromethane sulphonate (TMTf)	61
2.4.4.2.2: Synthesis of dimethylethylammonium trifluoromethane sulphonate (DMTf)	62
2.4.4.2.3: Synthesis of diethylmethylammonium trifluoromethane sulphonate (DETf)	62
2.4.4.2.4: Synthesis of triethylammonium trifluoromethane sulphonate (TETf)	

2.4.5: Synthesis of sulphonated copolyimides/protic ionic liquid (SPI/IL) composites.....	63
---	----

**3. Results and discussion.....64**

3.1: Synthesis of diamines, polyimides, protic ionic liquids and composites.....	64
--	----

3.1.1: Synthesis of diamines.....	64
-----------------------------------	----

3.1.2: Synthesis of homo and copolyimides.....	66
--	----

3.1.2.1: Synthesis of polyimides (PIs).....	68
---	----

3.1.2.1.1: FTIR studies of polyimides.....	70
--	----

3.1.2.1.2: Morphological studies of polyimides.....	71
---	----

3.1.2.1.3: Thermal properties of polyimides.....	72
--	----

3.1.2.1.4: Solubility and viscosities of polyimides.....	74
--	----

3.1.2.2: Synthesis of sulphonated copolyimides (SPIs).....	75
--	----

3.1.2.2.1: Free standing film formation.....	81
--	----

3.1.2.2.2: FTIR studies of sulphonated copolyimides.....	82
--	----

3.1.2.2.3: Morphological studies of sulphonated copolyimides.....	83
---	----

3.1.2.2.4: Thermal properties of sulphonated copolyimides.....	83
--	----

3.1.2.2.5: Solubility and viscosities of sulphonated copolyimides.....	86
--	----

3.1.2.2.6: Gel permeation chromatographic analysis of copolyimides.....	87
---	----

3.1.2.2.7: UV-Visible spectrophotometric studies of copolyimides.....	87
---	----

3.1.2.2.8: Computational studies of sulphonated copolyimides.....	88
---	----

3.1.3: Synthesis of protic ionic liquid composites.....	90
---	----

3.1.3.1: Synthesis of protic ionic liquids.....	90
---	----

3.1.3.2: Synthesis of composites.....	91
---------------------------------------	----

3.1.3.2.1: FTIR studies of composite membranes.....	93
3.1.3.2.2: Morphological studies of composite membranes.....	94
3.1.3.2.3: Gel permeation chromatographic analysis of composites.....	94
3.2: Heavy metal sensing studies of SPI (OBM-20).....	95
3.2.1: Electronic absorption variations of OBM-20 by divalent and trivalent metal ions.....	95
3.2.1.1: Effect of pH.....	98
3.2.1.2: Effect of interfering ions.....	98
3.2.1.3: Limit of Detection (LOD).....	100
3.3: Lead ions adsorption studies of SPIs (FBM-50 and OBM-50).....	102
3.3.1: Optimization of parameters.....	102
3.3.2: Adsorption kinetics of lead ions.....	105
3.3.2.1: Adsorption kinetics and contact time effects.....	106
3.3.3: Theoretical calculations for adsorption.....	108
3.4: Four probe proton conductivity measurements.....	110
3.5: Single fuel cell test.....	113
3.6: Half Cell Gas Diffusion Electrode (GDE) measurement.....	114
<b>Conclusions.....</b>	<b>117</b>
<b>Future Recommendations.....</b>	<b>120</b>
<b>References.....</b>	<b>121</b>
<b>List of Publications.....</b>	<b>139</b>
<b>Annexures.....</b>	<b>140</b>

Water shortage and fossil fuels depletion are threatening universal problems of modern society therefore wastewater treatment and power generation with environmental protection is worldwide urgency. To cope with these challenges, polymer-based adsorbents and electrolytes are under investigation. Among polymeric materials, polyimides (PIs) having excellent chemical resistance and thermal stability and can work very well in required conditions. Thanks to these outstanding properties polyimides are under investigation for decades.

However, the weak hydrophilicity of PIs is a major hurdle in their use for these applications. This shortcoming can be overcome by converting polyimides into sulfonated copolyimides with the introduction of sulfonic acid group in the polymeric backbone, which makes the polymer chains hydrophilic. Introduction of hydrophilic sulphonate groups into the PI main chain, improves material's hydrophilicity and results in better ion exchange properties. The hydrophilic sulphonic acid group being anionic functional group, bears strong affinity towards positive charges. Hence, sulphonated polyimides are of great interest in research for exploiting their possible applications in removal of toxic metal ions from water and as proton conducting electrolytes for polymer electrolyte membrane fuel cells (PEMFCs). To improve the proton conductivity of sulphonated copolyimides another widely explored approach is the incorporation of protic ionic liquids (PILs) in the sulphonated polyimide (SPI) matrix. For compatibility and good dispersion of an additive in the matrix, the same structural moieties are introduced in both phases. It is believed that the presence of these structural units might lead to increased interfacial interactions.

Development of an iterative approach for defining the successful sulfonation of polyimides while still retaining other important properties such as flexibility, strength and hydrolytic stability has been the goal of this research work. For this purpose, the synthesis and characterization of fully cyclized, soluble, good film forming sulphonated copolyimides for efficient sensing and removal of toxic metal ions from water and good ionic conductivity for polymer electrolyte membrane fuel cells will be discussed in the dissertation.

Two series of high molecular weight homo and copolyimides with varying degree of sulphonation were prepared. Oxydiphthalic anhydride (ODPA) and 4,4'-(hexafluoroisopropylidene) diphthalic anhydride (6FDA), flexible linkages bearing unsulphonated diamines (two synthesized and three commercial) and commercial sulphonated diamine 4,4'-diamino-2,2'-biphenyldisulfonic acid (BDSA). The latter diamine (BDSA) was used in various molar amounts (10-50 mol %) as a sulfonic acid source in the polyimide backbone of sulphonated copolyimides. For composites synthesis, the protic ionic liquid was added in various weight percentages (10-50 wt %) as an additive in the sulphonated copolyimide matrix for enhanced proton conductivity. For both of the polymer series, high molecular weights were achieved as judged by intrinsic viscosity measurements and good film forming characteristics.

This thesis is demarcated into three main chapters. The first chapter presents a relevant literature review and highlights the significance and objectives of the present work. In addition, the synthetic methodology of the diamine monomers, polyimide, sulphonated copolyimides, protic ionic liquids and composites has also been described.

The second chapter outlines the materials, characterization techniques and procedures for the synthesized diamines, polyimides, protic ionic liquids as well as preparation of composites.

The last chapter presents a discussion about the structural characterization of monomers, polyimides, sulphonated copolyimides and the composites. Furthermore, this chapter details the physical properties of polyimides and their composites such as molecular weight, thermal, electrochemical, proton conductivity, metal sensing and metal adsorption.

Finally, the thesis is concluded and future recommendations are made at the end of third chapter.

References and reprints of publications from this study have been given at the end of thesis.



## Acknowledgements

---

My first and foremost thanks to *Almighty Allah* the most beneficent and the most merciful without whose blessing it would have been impossible for me to complete this dissertation. Peace and blessings of Allah be upon His Prophet *Muhammad (P.B.U.H)* who guided the mankind to the path of rightness, who is the true source of wisdom, knowledge and whose love is the only way to reach Allah.

I would like to extend my sincere gratitude to all those people who made this thesis possible. I am heartily thankful to my dignified and respectable supervisor, **Dr. Humaira Masood Siddiqi**, Professor and head of organic section, Department of Chemistry, QAU Islamabad Pakistan, whose supervision, encouragement and endless support from the preliminary to the concluding level enabled me to develop an understanding of the subject. She gave me the freedom to work on projects which were of interest to me. Her expertise, valuable suggestions and patience, added considerably to my experience and enabled me to complete this research project. The amount of lab space which I was permitted to use is also gratefully acknowledged. I am extremely grateful for having Humaira Masood Siddiqi as my advisor. I am highly obliged to **Prof. Dr. Aamer Saeed Bhatti**, Chairman Department of Chemistry for providing me research facilities and promotive environment in the said department.

I sincerely express my gratitude to **Dr. Afzal Shah**, Professor Department of Chemistry, QAU Islamabad Pakistan, who unofficially functioned as my advisor. He was an absolutely outstanding advisor. He very generously gave of his time during our meetings and was very patient in explaining concepts to me which I was frequently slow to grasp. I owe my deepest gratitude to **all dignified teachers** of the Department especially **Organic section** (Dr Aamer Saeed Bhatti, Dr Humaira Masood Siddiqi, Dr Shahid Hameed, Dr Muhammad Farman, Dr Moazzam Nasir, Dr Abbas Hassan, Dr Ahsan Ullah, Dr Farzana Latif Ansari and Dr Zaidi (Late)) for their very kind behaviour, guidance, motivation, and encouragement throughout my educational career in this department since MSc (2011). I am greatly indebted to **Dr Shangfeng Du**, Associate Professor, University of Birmingham, UK, for warm welcome, introduction to fuel cell chemistry, lab facilities, weekly meetings, quick response to e. mails, valuable time and suggestions.

I am grateful to Higher Education Commission of Pakistan for NRPU 6160 and financial support for my visit to University of Birmingham, UK, under “International Research Support Initiative Program”. I express my sincere gratitude to colleagues at University of Birmingham, UK namely Mingshue Yao, Milan, Yang, Yichang, Dhua, Haotian and especially Pushpa for their support, help and full time availability. I owe my deepest gratitude to my lab fellows for their cooperation during my research work. The time spent in the company of these people has become a memorable part of my life. I would like to apprehend the cooperation of all employees of the Department of Chemistry. The lively company of my friends **Shagufta Jabeen, Kalsoom Fatima, Umama Bint-e-Irshad and Sheheen Gul** relieved my mood in the time of tension and stress. I thank them for their pleasant company, unconditional support, love and care.

Last but not the least, my heartiest gratitude and appreciation goes to my unconditionally loving family. I am most indebted to my sweet father **Manzoor Hussain Khan**, my mother **Azra Manzoor**, my caring brothers **Imran Manzoor and especially Nouman Manzoor (Biya)** for his never ending support and care, my lovely sister **Asma Manzoor**, for their endless prayers, matchless love and care. Words become meaningless when I have to say thanks to my parents and family; their prayers gave me strength and hope to accomplish this task and to pursue my goals.

**Aalia Manzoor**

Polyimides belong to a distinct class of polymers with unique properties and diverse uses. Over the past few decades, a variety of approaches have been suggested to improve the properties of polyimides by optimizing the polymer architecture. The thesis focuses on improving the properties of polyimides, sulphonated copolyimides and their composites with protic ionic liquids by optimizing the synthetic methodology. To improve the flexibility of polyimides, flexible linkages bearing monomers were targeted. For this purpose, two aromatic diamine monomers, A2 and A3, containing two and three carbon alkyl chains respectively were synthesized successfully in good yield and high purity. The synthesized and commercial unsulphonated diamines (A2, A3, A, I, M) and a sulphonated diamine (BDSA) were reacted with dianhydrides (oxydiphthalic anhydride (ODPA) and 4,4'-(hexafluoroisopropylidene)diphthalic anhydride (6FDA)) to prepare two series of ten homo and fifty sulphonated copolyimides. The sulphonated diamine (BDSA) was used in different mole percentages (10-50 mol %) to obtain varying degree of sulphonation in sulphonated copolyimides. The conventional two step thermal imidization procedure was followed for the preparation of polyimides.

Different characterization techniques were employed to assess the structure, morphology and thermal stability of sulphonated copolyimides. FTIR spectroscopic technique gave convincing evidence of the presence of all expected functional groups in the proposed structure of synthesized polyimides and composites. GPC analysis demonstrated the achievement of reasonably high molecular weight polyimides (12379 - 42726 g/mol) whereas XRD studies revealed their amorphous nature. The thermal stability of the synthesized polyimides was assessed using TGA and DSC analyses. For polyimides the onset degradation temperature and glass transition temperatures ranged between 290 - 550 °C and 190 - 220 °C respectively and for sulphonated copolyimides these values varied between 230 - 280 °C and 170 - 236 °C respectively.

In addition to the synthesis and characterization, this work explores the potential applications of sulphonated copolyimides in diverse fields. It highlights their metal ions interaction and toxic metal ions adsorption abilities, where their unique properties enable selective adsorption of toxic metal ions from water. Metal sensing application of ODPA

based sulphonated copolyimide (OBM-20) was explored by UV-Visible spectroscopy which showed its ability to sense the nanomolar concentration of toxic metal ions (0.01 nm). Atomic absorption spectroscopic (AAS) studies along with theoretical studies (MOE software) demonstrated good lead ions adsorption potential of sulphonated copolyimides suggesting the heavy metal adsorption properties of prepared materials.

Additionally, the thesis investigates the potential application of sulphonated copolyimides as proton exchange membranes (PEMs) for efficient energy conversion in proton exchange membrane fuel cells (PEMFCs). The research evaluates the performance of sulphonated copolyimide PEMs, focusing on key parameters such as proton conductivity, thermal stability and chemical resistance. The findings from this investigation provide valuable insights into the practical suitability of sulphonated copolyimides for fuel cell applications. To improve the proton conductivity of synthesized sulphonated copolyimides, sulphonated polyimide/protic ionic liquid (SPI/IL) composites were prepared. Different weight percentages of synthesized protic ionic liquids (10-50 wt%) were added in the sulphonated copolyimide matrices. The dispersion of protic ionic liquid was improved by like-like chemical interactions ensured by the presence of similar structural units i.e, triethyl amine unit in both the matrix and additive. The increase in the flexibility of the membranes with increasing wt % of ionic liquids confirmed the plasticizing behaviour of ionic liquid. Four probe proton conductivity measurements depicted good proton conducting potential of sulphonated copolyimides and composites up to 100 °C. The enhanced proton conductivity values of composites (0.1 S/cm) obtained at 80 °C were attributed to the presence and improved interactions of protic ionic liquids into SPI matrix.

Half cell *ex-situ* tests and single cell tests depicted the catalyst coating behaviour of sulphonated copolyimides and their composites with appreciably good catalyst binding potential.

## Index of Tables

---

<b>Table 2.1:</b> Synthesized composites.....	63
<b>Table 3.1:</b> Physical data of dinitros and diamines.....	66
<b>Table 3.2:</b> Codes for polyimides .....	70
<b>Table 3.3:</b> Thermal properties of polyimides.....	74
<b>Table 3.4:</b> Viscometric data of polyimides .....	75
<b>Table 3.5:</b> Codes and percentage compositions of 6FDA based sulphonated copolyimides (SPIs) .....	79
<b>Table 3.6:</b> Codes and percentage compositions of ODPA based sulphonated copolyimides (SPIs) .....	80
<b>Table 3.7:</b> Thermal properties of sulphonated copolyimides .....	85
<b>Table 3.8:</b> Viscometric data of sulphonated copolyimides.....	86
<b>Table 3.9:</b> GPC data of sulphonated copolyimides .....	87
<b>Table 3.10:</b> Molecular descriptors for FBM-50 and OBM-50 complexes.....	89
<b>Table 3.11:</b> Codes for PILs .....	91
<b>Table 3.12:</b> Codes and percentage compositions of composites.....	92
<b>Table 3.13:</b> GPC data of composites FBM20/IL(50) and FBA-20/IL(20).....	94
<b>Table 3.14:</b> Comparison of the absorbance intensities of OBM-20 in the absence and presence of Ni (II), Co (II) and Cr (III) .....	97
<b>Table 3.15:</b> Kinetic parameters for Pb (II) ions adsorption on SPIs.....	107
<b>Table 3.16:</b> Comparison of lead ions adsorption capacity of different materials in literature .....	108
<b>Table 3.17:</b> Molecular descriptors for FBM-50 and OBM-50 complexes.....	110

## Index of figures

---

<b>Figure 1.1:</b> The general structure of polyimide.....	1
<b>Figure 1.2:</b> Structure and physical appearance of commercial polyimides.....	2
<b>Figure 1.3:</b> One step synthetic procedure of polyimide.....	4
<b>Figure 1.4:</b> Two step synthetic procedure of polyimide.....	4
<b>Figure 1.5:</b> Mechanism of Polyamic acid synthesis.....	6
<b>Figure 1.6:</b> Chemical structure of Nafion.....	12
<b>Figure 1.7:</b> Interaction of polymers with water a) hydrophobic polymer and b) hydrophilic polymers.....	19
<b>Figure 1.8:</b> Swelling behaviour of polymer in water.....	20
<b>Figure 1.9:</b> Interaction of sulphonic acid group with metal ions.....	21
<b>Figure 1.10:</b> Pictorial representation of a fuel cell.....	21
<b>Figure 1.11:</b> Types of fuel cells.....	22
<b>Figure 1.12:</b> Schematic diagram of a polymer electrolyte membrane fuel cell.....	23
<b>Figure 2.1:</b> Four probe proton conductivity setup.....	39
<b>Figure 2.2:</b> Single cell test setup.....	40
<b>Figure 2.3:</b> Half cell gas diffusion electrode (GDE) test setup.....	41
<b>Figure 3.1:</b> Structures of dinitro compounds.....	65
<b>Figure 3.2:</b> Structures of diamines.....	65
<b>Figure 3.3:</b> Monomers used for synthesis of polyimides and sulphonated copolyimides.....	67
<b>Figure 3.4:</b> General structure of polyimide.....	70
<b>Figure 3.5:</b> Full range and elaborated FTIR spectra of FM and OM.....	71
<b>Figure 3.6:</b> XRD patterns of FM and OM.....	72
<b>Figure 3.7:</b> TGA patterns of FM and OM.....	73
<b>Figure 3.8:</b> DSC curves of FM and OM.....	74
<b>Figure 3.9:</b> Comparative FTIR spectra of BDSA.TEA and BDSA.....	76
<b>Figure 3.10:</b> General structure of sulphonated copolyimide.....	78
<b>Figure 3.11:</b> Physical appearance of sulphonated copolyimide films.....	81
<b>Figure 3.12:</b> Full range and elaborated FTIR spectra of FBM-50 and OBM-50.....	82
<b>Figure 3.13:</b> XRD of 50% sulphonated FBM-50 and OBM-50.....	83

<b>Figure 3.14:</b> TGA patterns of FBM-50 and OBM-50 .....	84
<b>Figure 3.15:</b> DSC curves of FBM-50 and OBM-50 .....	85
<b>Figure 3.16:</b> (a) UV-Vis spectra of OBM-20 and (b) corresponding plot showing time dependent changes in absorbance at $\lambda_{max}$ in aqueous solution of neutral pH at 25 °C ...	88
<b>Figure 3.17:</b> 3D view of (a) FBM-50 (b) OBM-50 in ball and stick and their electrostatic surface map .....	89
<b>Figure 3.18:</b> Structures of Brønsted acids, Brønsted bases and triethyl amine ionic liquids .....	91
<b>Figure 3.19:</b> FTIR spectra of FBM-20 and FBM-20/IL (20%).....	93
<b>Figure 3.20:</b> XRD patterns of FBM-20, FBM-20/IL(20%) and FBM-20/IL(50%).....	94
<b>Figure 3.21:</b> (a) UV-Vis spectra of OBM-20 in the presence of Co (II) and (b) corresponding plot showing time dependent changes in absorbance at $\lambda_{max}$ in aqueous solution.....	96
<b>Figure 3.22:</b> (a) UV-Vis spectra of OBM-20 in the presence of Cr (III) and (b) corresponding plot showing time dependent changes in absorbance at $\lambda_{max}$ in aqueous solution.....	96
<b>Figure 3.23:</b> (a) Changes in absorption spectrum of OBM-20 in the presence of Ni (II) and (b) corresponding plot showing time dependent variation in absorbance at $\lambda_{max}$ .....	97
<b>Figure 3.24:</b> Absorption spectra of OBM-20 in the presence of Ni (II) a) at pH 2.0 b) at pH 8.0-9.0 .....	98
<b>Figure 3.25:</b> Selectivity of OBM-20 towards Ni (II) in the presence of interfering ions (Na (I), K (I), Ca (II), Mg (II), Fe (II)) .....	99
<b>Figure 3.26:</b> Selectivity of OBM-20 towards a) Co (II) b) Cr (III) in presence of interfering ions (Ca (II), Mg (II), Fe (II)) .....	100
<b>Figure 3.27:</b> Absorption spectra of OBM-20 in various concentrations (0.01 nM-0.01 M) of Ni (II).....	101
<b>Figure 3.28:</b> Absorption spectra of OBM-20 in various concentrations of a) Co (II) (1 nM-0.01 M) b) Cr (III) (0.01 nM-0.01 M) .....	101
<b>Figure 3.29:</b> (a) Effect of adsorbent dose (b) initial ions concentration on the adsorption capacity of sulphonated copolyimides (FBM-50 and OBM-50).....	103

<b>Figure 3.30:</b> Time course for the adsorption of heavy metal ions on sulphonated polyimides (a) 40 ppm concentration, (b) 60 ppm concentration.....	103
<b>Figure 3.31:</b> The effect of pH of adsorption medium on the adsorption capacity of sulphonated copolyimides (FBM-50 and OBM-50).....	104
<b>Figure 3.32:</b> Adsorption kinetics (a) Time course for the adsorption of heavy metal ions on sulphonated polyimides and (b) Pseudo 2nd order model for metal ions adsorption.	107
<b>Figure 3.33:</b> : (a) 3D view of complex of FBM with Pb in ball and stick (b) Hydrophobic (green dots) and hydrophilic part (blue & purple) of FBM complex with Pb .....	109
<b>Figure 3.34:</b> (a) 3D view of complex of OBM with Pb in ball and stick (b) Hydrophobic (green dots) and hydrophilic part (blue & purple) of OBM complex with Pb.....	109
<b>Figure 3.35:</b> Proton conductivity of FBA2-40 at 60 °C, 80 °C and 100 °C .....	110
<b>Figure 3.36:</b> Proton conductivity of FBA2 (20) and FBA2-20/IL (20) at 80 °C .....	112
<b>Figure 3.37:</b> Proton conductivity of FBA2 (20), Nafion 212 and FBA2-20/IL (20) at 80 °C .....	112
<b>Figure 3.38:</b> Polarization curve of FBA2-50 at 80 °C and 100 % RH coated platinum nanorods.....	113
<b>Figure 3.39:</b> Power density of FBA2-50 coated platinum nanorods.....	114
<b>Figure 3.40:</b> EIS of FBA2-50 coated platinum nanorods .....	112
<b>Figure 3.41:</b> Comparative cyclic voltammograms of Nafion and FBA2-50 coated Pt/C .....	115
<b>Figure 3.42:</b> Comparative cyclic voltammograms of FBM-20 and FBM-20/IL (50) coated Pt/C.....	115



## Index of schemes

---

<b>Scheme 1.1:</b> General synthesis of 4-((4-aminophenoxy)alkoxy)benzenamines .....	32
<b>Scheme 1.2:</b> General synthesis of homopolyimides .....	32
<b>Scheme 1.3:</b> General synthesis of triethyl ammonium salt of benzidine-2, 2'-disulphonic acid.....	33
<b>Scheme 1.4:</b> General synthesis of sulphonated copolyimide in triethyl ammonium sulfate form .....	33
<b>Scheme 1.5:</b> General synthesis of protic ionic liquids (PILs) .....	34
<b>Scheme 1.6:</b> General synthesis of protic ionic liquid composites .....	34
<b>Scheme 3.1:</b> Synthesis of 4-((4-aminophenoxy)alkoxy)benzenamines.....	65
<b>Scheme 3.2:</b> Synthesis of homopolyimides.....	69
<b>Scheme 3.3:</b> Synthesis of triethyl ammonium salt of benzidine-2, 2'-disulphonic acid... 76	
<b>Scheme 3.4:</b> Synthesis of sulphonated copolyimide in triethyl ammonium sulfate form. 77	
<b>Scheme 3.5:</b> Synthesis of protic ionic liquids (PILs).....	90
<b>Scheme 3.6:</b> Synthesis of protic ionic liquid composites.....	91

## List of abbreviations

---

AAS	Atomic absorption spectroscopy
BDSA	4,4'-Diamino-2,2'-biphenyldisulfonic acid
DEMA	Diethylmethyl amine
DMEA	Dimethylethyl amine
DMF	<i>N,N'</i> -Dimethylformamide
ECSA	Electrochemical surface area
FC	Fuel cell
6FDA	4,4'-(Hexafluoroisopropylidene) diphthalic anhydride
GDE	Gas diffusion electrode
GDL	Gas diffusion layer
MEA	Membrane electrode assembly
MDA	4,4'-Methylene dianiline
MOE	Molecular operating environment
MsOH	Methane sulphonic acid
NTDA	1,4,5,8 Naphthalene tetracarboxylic dianhydride
ODA	4,4'-Diaminodiphenyl ether
ODPA	Oxydiphthalic anhydride
Pd/C	Palladium charcoal
PEM	Polymer electrolyte membrane
PEMFC	Polymer electrolyte membrane fuel cell
PI	Polyimide
PIL	Protic ionic liquids
PMDA	Pyromellitic dianhydride

PPA	Polyamic acid
SPI	Sulphonated copolyimide
SPI/PIL	Sulphonated copolyimide/protic ionic liquid composites
TEA	Triethylamine
TfOH	Trifloromethane sulphonic acid
TMA	Trimethylamine
$T_g$	Glass transition temperature
$T_{10}$	Temperature at 10% weight loss
$T_{max}$	Temperature at maximum decomposition
$X_n$	Degree of polymerization

## 1 Introduction

This chapter presents a brief introduction of polyimides, sulphonated copolyimides, protic ionic liquids and protic ionic liquids based composites.

### 1.1 Polyimides (PIs)

Polyimides, a class of scientifically and commercially valuable polymers, are often based on stiff aromatic backbones and are formed by the condensation reaction of dianhydride and diamine monomers resulting in imide rings formation. The imide ring consists of two carbonyl groups (C=O) covalently bonded with a nitrogen atom in their structure as depicted in **Figure 1.1**. PIs are highly stable materials possessing excellent chemical, thermal, mechanical, oxidative and thermo-oxidative stability due to the chemical nature of rigid aromatic construction and imide rings. Additionally, they are also known for their good film forming ability. The polyimide films can withstand harsh chemical and thermal conditions and are capable of maintaining their dimensional properties at high temperature. <sup>1, 2</sup>

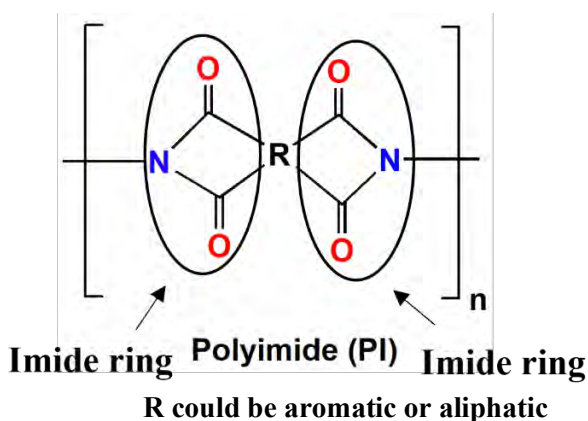


**Figure 1.1:** The general structure of polyimide.

Bogert and Renshaw, the pioneers of this field, firstly reported these extraordinary polymers in 1908. <sup>3</sup> Dupont opened new doors of research in this field in 1960 by introducing the outstanding thermo-oxidative stability of polyimides. <sup>4</sup> Kapton™, one of the most successfully commercialized PI films, was first synthesized by Sroog in 1965 with pyromellitic dianhydride (PMDA) and 4,4'-diaminodiphenyl ether (ODA) (**Figure 1.2**).

Subsequently, it was industrialized and named Kapton™ by DuPont. Other successfully commercialized PI films include Novax (Mitsubishi) and Upilex R (Ube Industries).<sup>5</sup>

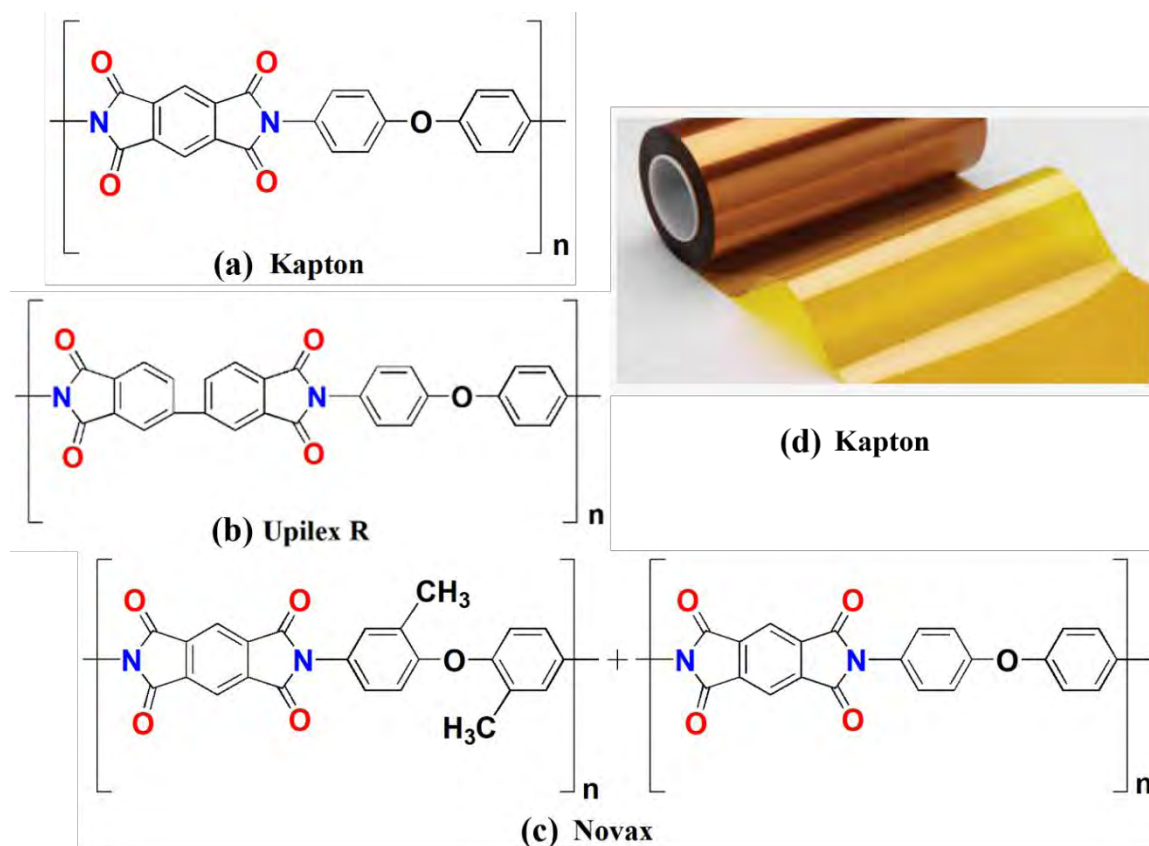


**Figure 1.2:** Structures of (a) Kapton (b) Upilex R (c) Novax and (d) physical appearance of Kapton (Dupont) polyimide film.<sup>5</sup>

Polyimides have been widely used in the fields of aerospace, microelectronic devices, gas separation technology and polymer electrolyte membranes.<sup>6-8</sup> Preparation of innovative polyimides and improvement of current systems is inevitable for the achievement of desired properties and applications.

### 1.1.1 Synthesis of polyimides

The synthetic methodology plays key role in the development of high performance polyimide material.

There are two well-known methods for the synthesis of polyimides.<sup>9</sup>

- a) One step polymerization
- b) Two step polymerization

### a) One step polymerization

In one step polymerization polyamic acid and polyimide are formed at the same time. The method consists of stirring the stoichiometric amounts of dianhydride and diamine in a high boiling solvent in the presence of acidic and basic catalysts at high temperature (180-220 °C). An acidic catalyst such as benzoic acid promotes the formation of *trans*-isoimide which is converted into polyimide by basic catalyst such as isoquinoline. Under these conditions chain growth and imidization occur spontaneously (**Figure 1.3**).<sup>9</sup>

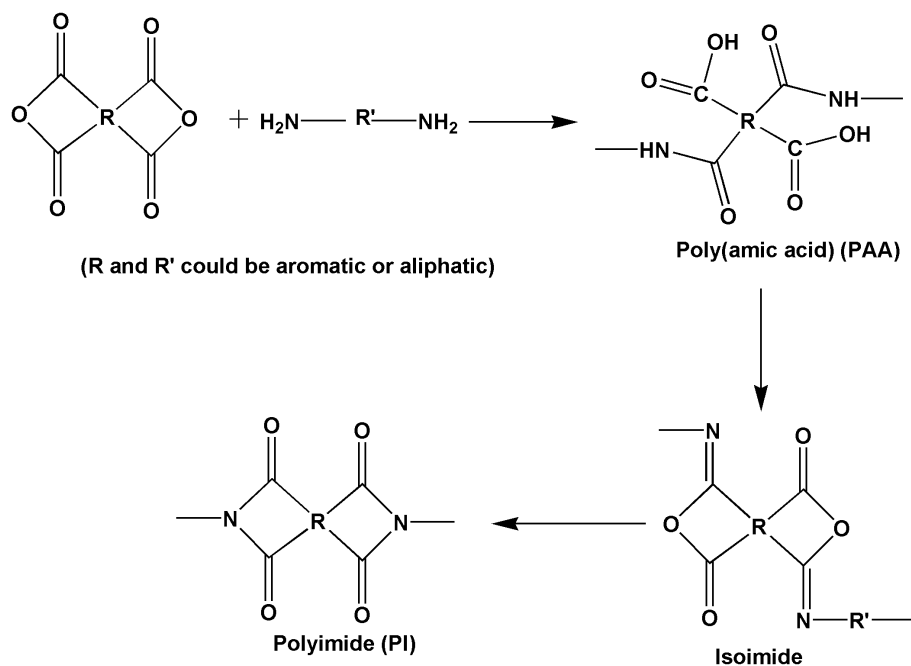


**Figure 1.3:** One step synthetic procedure of polyimide.

The one step polymerization is especially effective for processing monomers of moderate reactivity. This method is obviously more convenient than the conventional two step synthesis via polyamic acid. However, its application has been restricted, because there are very few inexpensive monomers that could result in the formation of soluble high performance polyimides. Most of the polyimides are infusible and insoluble due to their planar aromatic and hetero-aromatic structures and thus usually need to be processed from the solvent route. The two step method provided the first such solvent based route to process these polyimides. The process also enabled the first polyimide of significant commercial importance, Kapton<sup>TM</sup>, to enter the market.<sup>10</sup>

## b) Two step polymerization

Two step polymerization is commonly used typical procedure for the synthesis of polyimides. In two step method, the synthesis is done in two steps, first of all the soluble PAA is synthesized in first step followed by its conversion to the polyimide in second step (**figure 1.4**).<sup>11</sup> The first step for the preparation of polyamic acid is carried out by adding equimolar amount of dianhydride monomer in solution of diamine monomer in a polar solvent. In the second step, the resulting PAA having high molecular weight is cyclodehydrated (imidized) in the form of film utilizing glass slide or glass petri dish as a substrate either by thermal dehydration using a heating cycle (thermal imidization) or by using any chemical dehydrating agent (chemical imidization). The process involves various interrelated elementary reactions in a complex reaction scheme.<sup>12</sup>

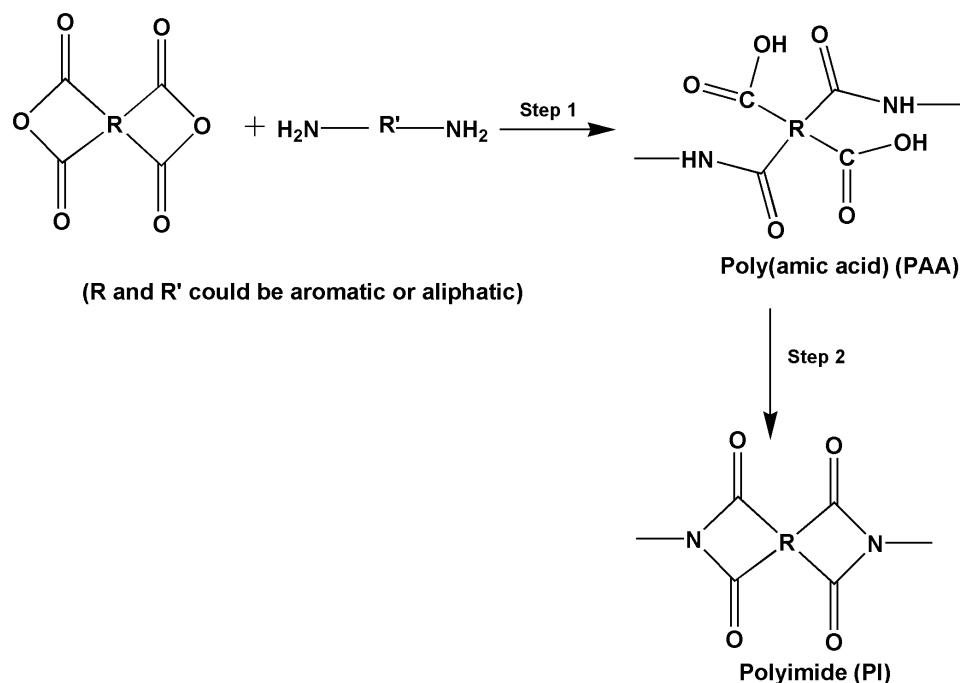


**Figure 1.4:** Two step synthetic procedure of polyimide.

### 1.1.1.1 Synthesis of polyamic acid and its mechanism

In classical two-step reaction, generally polyamic acid is formed when difunctional dianhydride is added to a difunctional diamine in a polar solvent at ambient temperature by a reversible nucleophilic acyl substitution. The attack of unshared pair of electrons of the nitrogen of diamine, on either of the carbonyl carbons of tetracarboxylic acid anhydride,

resulting in the displacement of the carboxylate functionality followed by proton transfer and results in the formation of amic acid.<sup>13</sup>

An accepted polyamic acid formation reaction mechanism is given in **Figure 1.5**. A cyclic intermediate is formed between the dianhydride carbonyl carbon and nitrogen atom of diamine by the shifting of pi electrons on the adjacent oxygen. The back shifting of electron pair to carbonyl group to reform double bond results in bond breaking among carbon and “leaving group” as it occurs simultaneously therefore this intermediate is very short lived. However, reverse reaction to give the starting species (anhydride and free amine) can take place if the bond between nitrogen and developing sp<sup>2</sup> carbon breaks. To obtain, the polyamic acid having high molecular weight, the forward reaction rate must be faster as compared to the reverse reaction rate. In general, the rate constant of forward reaction is quite larger as compared to the reverse reaction therefore normally this reaction appears irreversible if pure reagents are used. It is essential to investigate the driving forces that favor the forward reaction because the high molecular weight polyimide synthesis depends on the difference in reaction rate constants. The attack of carboxyl group on adjacent nitrogen atom of polyamic acid will result in reverse reaction therefore any reagent that can hinder this attack will decrease the rate of reverse reaction and as a result shifts the equilibrium towards right. Polarity of solvent plays very important role, polar solvents form strong hydrogen bonds with free carboxyl groups of polyamic acid resulting in hydrogen bonded complexes and favouring the forward reaction at ambient conditions.<sup>14</sup> However, significant differences are observed in equilibrium constants when the polymerization reactions are carried out in non-polar solvents (ether or hydrocarbon solvents), depending upon the basicity of amines and electrophilicity of dianhydrides.<sup>15</sup>

The equilibrium is shifted towards right at lower temperature because the formation of polyamic acid is exothermic in nature. However, at ambient temperature the shift in equilibrium towards right is so appreciable that further decrease in temperature normally do not affect the reaction rate. Alongwith this, the concentration of monomer is an important parameter influencing the equilibrium of reaction. As the forward reaction is bimolecular and follows 2<sup>nd</sup> order kinetics whereas the reverse reaction is unimolecular, therefore concentration of each of the monomeric units is equally significant in the



determination of PAA formation rate and successful production of polyamic acid having high molecular weight. The effect of concentration becomes particularly important for very dilute solutions where it leads to appreciable decrease in the molecular weight of polyamic acid.<sup>16</sup>

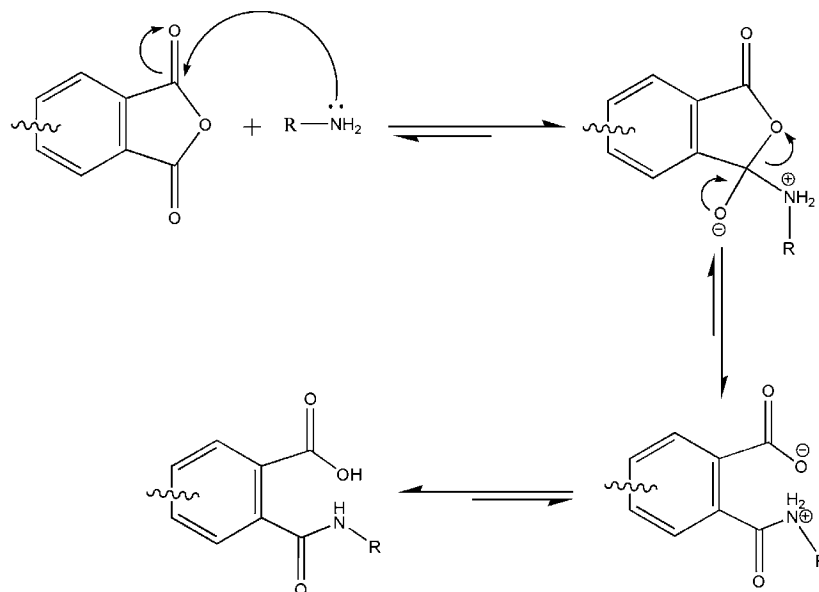


**Figure 1.5:** Mechanism of polyamic acid synthesis.

#### 1.1.1.1.1 The impact of monomer reactivity

The formation of polyamic acid follows the nucleophilic substitution reaction, where a diamine (nucleophile) attacks the carbonyl carbon (electrophile) of dianhydride. Therefore, the reaction depends upon the nucleophilicity of nitrogen of diamine and electrophilicity, electron accepting ability, of carbonyl groups of dianhydride. The greater the electrophilicity i.e; the higher electron affinity of dianhydride the faster will be the reaction rate with a given nucleophile. Electron accepting ability of dianhydride is generally evaluated corresponding to the electron affinity (Ea) of the molecule.<sup>16</sup>

Nearly all tetracarboxylic acid anhydrides contain bridging groups between two phthalic anhydride units and electron accepting ability is greatly influenced by the presence of bridging group. The bridging group with electron-withdrawing effect, such as  $-C=O$  and  $-SO_2$ , decreases the delocalization of electrons and the electron density of carbonyl carbon of anhydride, substantially increasing its electron affinity (Ea) as compared to 3, 3', 4, 4'-

biphenyltetracarboxylic dianhydride (BPDA), lacking a bridging group. As a result, the carbonyl carbons of anhydride experience an enhanced positive environment that results in an accelerated addition of an attacking nucleophile. Whereas, electron donating bridging groups such as ether decrease the  $E_a$  value of anhydride by reducing the affinity of carbonyl carbons for more electrons by donating electrons into the rings. Therefore, dianhydrides having ether groups are less affected by the moisture in atmosphere, whereas pyromellitic dianhydride (PMDA) having highest  $E_a$  resulting in highest reactivity, should be handled carefully in precisely moisture free environments. Efforts to correlate the nucleophilicity and reactivity of aromatic diamines remained less productive. However, the rates of reactions of the diamines generally increase with increase in their ionization potential and it is observed that it correlates with their basicity (pKa) such as, the amine having higher basicity will react more rapidly. Quantitative correlation between diamine basicity and reactivity has been achieved successfully, with the outcome, the rate constant increases with increasing value of pKa. <sup>16,17</sup>

The reaction rate is significantly affected by the structure of diamines as compared to changes in dianhydride structure. Electron-withdrawing bridging units influence the rate of acylation of diamines, resulting in decreased acylation rate and pKa. Generally, it is observed that magnitude of rate constant for electron withdrawing substituted diamines differs by four orders of magnitude as compared to electron donating ones. <sup>17</sup>

To control the equilibrium for favorable formation of polyamic acid, monomer reactivity is very important. The reaction between less reactive diamines and dianhydrides yields a lower molecular weight polyimide, whereas high molecular weight polyimide is obtained when the reactivity of both the diamine and dianhydride is high. According to Carother's equation,  $X_n$  (degree of polymerization, number of monomer units in a polymer) is related to  $1/(1-p)$ , and  $p$  (fractional monomer conversion) corresponds to the reaction extent. To obtain PAA having high molecular weight, dianhydride possessing high electron affinity is used with highly basic diamine. It is quite evident from the above discussion that polyamic acid formation is principally based on electron affinity and basicity of utilized monomers. PAA formation is also affected by the temperature of reaction and the used solvents. As the synthesis of PAA is exothermic in nature therefore polyamic acid of higher

molecular weight are achieved at lower temperatures. However, at lower temperatures the solid dianhydride dissolves slowly in reaction mixture. Therefore, it is assumed that the polymerization may take place more significantly at the interface (solid/liquid) at lower temperatures. Therefore, PAA having high molecular weight may be obtained rapidly in the interfacial type reaction before the complete dissolution of dianhydride. This results in high  $M_w$  and a wide molecular weight distribution.<sup>17</sup>

#### **1.1.1.1.2 The impact of reaction conditions and solvents on polyimide synthesis**

Research in polyimide synthesis proved that higher concentration of monomers results in production of higher molecular weight polyamic acid. Final molecular weight is also strongly affected by the order and mode of monomers addition, with the attainment of highest molecular weight upon addition of solid dianhydrides in the solution of diamines in polar solvent. The achievement of high molecular weights was credited entirely to the inhibition of side reactions. Highly reactive aromatic dianhydrides are prone to react immediately with water or any other impurity in solvents, however, dianhydrides react considerably faster with diamines as compared to other reagents. To obtain high molecular weight polyimides, these side reactions must be minimized, therefore, dianhydride is added in solid mode to reduce its readiness for competing side reactions due to water or any other impurity. Another key factor to achieve high molecular weight polyimide is the use of slight stoichiometric excess of dianhydride. Smaller quantity of solvent ensures less impurities that can interfere with main reaction resulting in high molecular weight polyimides. As dianhydrides are normally added as solids therefore, their dissolution rate is slow and depends on monomer concentration due to this solid mode of addition. The process becomes diffusion controlled due to low dianhydride solubility as well as low monomer reactivities, above a certain critical concentration. Like solid-liquid interfacial polymerization, quite high molecular weight polymer is obtained at the start of reaction, well before the complete dissolution of dianhydride and the attainment of stoichiometric balance. Broad distribution of molecular weight is often obtained in this type of polymerization.<sup>17,18</sup>

It is found by early researchers that the viscosities of polyamic acid are affected by storage in the form of solution after preparation and are decreased rapidly. Firstly, the

decrease in viscosity with passage of time was assigned to the sensitive nature of polyamic acid towards hydrolysis but later on, this change in viscosity was linked with reversible nature of the propagation reaction. Even though rate constants of reverse reactions are quite smaller, but some of these reactions may occur and can significantly affect the  $M_w$  of polyimides.<sup>14, 18, 19</sup>

The effect of utilized solvents is quite imperative in the synthesis of PAA as the solvent stabilizes the intermediates and favours the rate of forward reaction. Less polar solvents, like ether solvents, lack the ability of hydrogen bonding with the carboxyl group therefore, the rate of reaction is slower as compared to the polar solvents. Therefore, faster reaction rate is expected in polar solvent as it retards backward reaction rate at ambient temperature and shifts the reaction towards right side.<sup>18, 19</sup>

The main polymerization reaction is accompanied by several side reactions. The most detrimental side reaction in polyamic acid formation is the hydrolysis of dianhydride monomer resulting in the formation of diacid moieties which disturbs equilibrium balance of amine and anhydride end groups. Consequently, the hydrolytic cleavage of polyamic acid results in the degradation of amide-acid linkages to reform the monomers. The presence of water in monomers and solvents is the main driving force for these side reactions. These hydrolysis reactions result in the preparation of PAA having low molecular weight which in turn affects and lowers the film forming capability of the PAA upon thermal imidization. Therefore, the removal of water from the monomers and reaction solvent is essential for the preparation of higher molecular weight PAA and polyimides. Normally, careful drying of monomers and distillation of solvents is carried out for this purpose.<sup>19, 20</sup>

#### **1.1.1.2 The thermal imidization of PAA**

Thermal imidization is utilized for the conversion of intermediate polyamic acid to final polyimide. This method is particularly employed for the fabrication of films or a coating form. Glass substrate is normally used for casting the films and then undertaken through a heating cycle with temperature ranging between 100 °C to 350 °C. To achieve 100% imidization of polyamic acid considerable debate has been carried out in the literature.<sup>20.</sup>

<sup>21</sup> Many types of thermal cycles have been carried out by researchers however, basically they can be classified into two different types:

- 1) Heating the polyamic acid solution gradually, depending on heat stability and glass transition temperature (T<sub>g</sub>) of the polyimide to 250-350 °C. <sup>20</sup>
- 2) Heating polyamic acid solution using a glass petri dish to 100 °C and holding for one hour, then gradually increasing the temperature and heating from 100-200 °C by holding this temperature for one hour, followed by heating from 200-300 °C by holding this temperature for one hour and then cooled down slowly to room temperature from 300 °C. <sup>21</sup>

Imidization reaction is a quite complicated phenomenon and overall process comprises of numerous interconnected elementary reactions and number of dynamic physical properties like solvation, chain mobility, acidity and diffusion rate. Therefore, a simple kinetic expression is often not possible for the imidization reaction. During the initial stages, rate of imidization is usually faster because of the presence of solvent and increased chain mobility due to shorter chain sizes. <sup>21</sup> However, rate of reaction tapers off during the later stages due to the reasons listed below:

- 1) Extended heating resulting in loss of residual solvent.
- 2) Increase in T<sub>g</sub> as the imidization reaction proceeds and rate slows down evidently due to decrease in chain mobility.

For cyclodehydration, suitable conformations of amic acid groups are required, therefore, the rate of imidization reaction seems to depend on the availability of appropriate conformations. The slower reaction rate during last stages of imidization, can be assigned to the improper conformations that are required to rearrange to appropriate conformations so that imidization can occur. These conformational rearrangements are feasible if adjoining polymer chains and bounded solvent molecular rotations occur. <sup>22</sup>

#### **1.1.1.3 The chemical imidization of PAA:**

For the synthesis of molding powders, chemical imidization is a significant technique. Although, this is a low energy process but due to the involvement of dangerous reagents it is rarely employed for different applications. In this method, PAA is treated

with dianhydride and tertiary amine mixture at room temperature. Commonly utilized chemicals are acetic anhydride, triethylamine and pyridine. <sup>23</sup>

In chemical imidization, finally formed polyimide precipitates out because it is insoluble in the imidization mixture. There is possibility of precipitation to occur before the complete cyclization of PAA groups into polyimides. Therefore, the complete imidization is mainly based on solubility profile of PI in reaction mixture resulting in higher degrees of imidization for more soluble polyimides.

It has been postulated that during chemical imidization reverse reaction does not occur in comparison with the thermal imidization process. This reflects that mechanical properties of polyimide will not be affected much during imidization process, an important factor for imidization and fabrication of films. However, the main drawback of chemical imidization is, it may result in significantly higher 'isoimide' moieties percentage in the final product. <sup>24</sup>

## **1.2 Sulphonated polyimides: The ionomers**

Polyimides containing covalently bonded sulfonic acid group on their backbone are named as sulphonated polyimides. The sulfonic acid group possess an ionic bond where  $\text{SO}_3\text{H}$  can be perceived as an  $\text{SO}_3^-$  ion bonded to  $\text{H}^+$  ion. The specified nomenclature of these sulphonated polymers as ionomers (an abbreviation of ionic polymers) originated due to this ionic bond. These sulfonic acid group ionomers exhibit phase-separated domains consisting of a hydrophobic backbone and the hydrophilic sulfonic acid group. The hydrophilicity of the polyimide i.e, the interactions with water is determined by the hydrophilic domains whereas the mechanical and thermal properties are determined by the hydrophobic backbone. <sup>25</sup> The mechanical stability and water uptake affect each other and the most important parameter affecting both these factors is the concentration of sulfonic acid groups in an ionomer. <sup>26</sup>

The sulfonic acid groups functionalized perfluorinated ionomers form the subcategory of perfluorosulfonic acids (PFSA). These perfluorosulfonic acids (PFSA) are widely used materials for various applications. <sup>27</sup> The exceptional chemical stability of these materials is the main reason of their popularity. The strong and chemically inert bonds between carbon and fluorine (C-F) are the main reason of this extraordinary chemical

stability. Nafion is the most famous and widely used representative of this group. It was discovered by Walter Grot under the trademark of DuPont in 1960s. <sup>28</sup> The chemical structure of Nafion is shown in **Figure 1.6**.

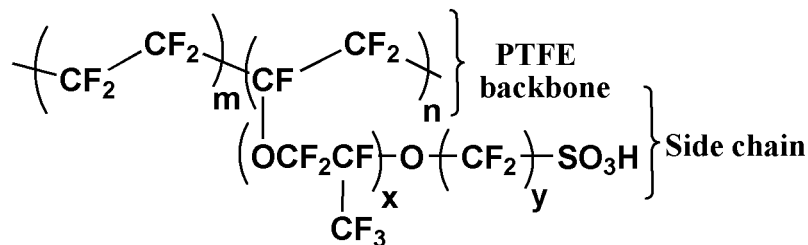


**Figure 1.6:** Chemical structure of Nafion.

From the **Figure 1.6**; it can be seen that the Nafion's backbone is derived from the tetrafluoroethylene (TFE) and the sulfonic acid group is attached via side-chain and is not attached directly to the backbone. Fluorine chemistry is involved in the synthesis of Nafion which includes highly exothermic reactions and management of flammable and explosive compounds. Due to these reasons, the preparation of PFSA ionomers is restricted to a few manufacturers globally. The disposal of Nafion implicates environmental risks meanwhile ignition for disposal, recommended by DuPont, releases perfluorocarboxylic acids, a chemical considered as environmental pollutant and relentless in the atmosphere. <sup>29, 30</sup>

The hydrocarbons based ionomers are generally inexpensive, widely accessible and their monomers and production routes are well established. <sup>31</sup> The hydrocarbons based ionomers are economically attractive for extensive application in different fields due to the advantages in fabrication. However, hydrocarbon ionomers contain C-H bonds in contrast to perfluorinated ionomers, which are prone to chemical degradation. Research focuses on aromatic hydrocarbon ionomers because the aromatic hydrocarbons containing aromatic rings, are chemically more stable than aliphatic hydrocarbons, containing straight chains or branched trains of carbon and hydrogen bonds. The mechanical stability of hydrocarbon membranes is a challenge, due to the rigid nature of aromatic polymer chains, that needs to be addressed as well. The aromatic rings are usually bridged with various flexible molecular units to improve the flexibility of aromatic polymer chains. <sup>32</sup>

Polyimides can be converted into aromatic hydrocarbon ionomers with the introduction of sulfonic acid group in polymer backbone. To date, the synthesis of sulphonated copolyimide has been carried out by direct copolymerization technique. The method involves the use of sulfonated monomer along with nonsulphonated one, a different strategy than post sulfonation of parent polyimide. For the synthesis of sulfonated copolyimide, stoichiometric amounts of sulfonated diamine is utilized relative to nonsulphonated diamine. To get high molecular weight sulphonated copolyimide, 1:1 stoichiometric ratio of total dianhydride to diamines is utilized. To control the degree of sulfonation various ratios (percentages) of sulfonated to nonsulphonated diamine were used. *m*-Cresol was used as solvent for copolymerization reactions in all cases. To synthesize high molecular weight sulphonated copolyimides, triethylammonium salt of sulfonated diamine, soluble in reaction media, is used.<sup>31, 32, 33</sup> Most sulphonated diamines are insoluble in *m*-cresol in their acid and sodium sulfonate forms. Several different sulfonated diamines have been reported for their usage for the synthesis of sulfonated copolymers, out of which 4,4'-diamino-biphenyl-2,2'-disulfonic acid (BDSA) is the most studied sulphonated diamine. It is commercially available and various groups have used this diamine for the synthesis of copolymers.<sup>32, 33</sup>

Cornet et al. introduced a synthetic strategy for the preparation of segmented (block) sulfonated copolyimides. The first step involved the preparation of sulphonated block of 4,4'-diamino-biphenyl-2,2'-disulfonic acid (BDSA) with 1,4,5,8 naphthalene tetracarboxylic dianhydride (NTDA). The sulfonation degree was controlled, in second step, by the modification of the molar ratio of unsulfonated diamine and BDSA in SPI. The nonsulphonated diamine used was 4,4'-oxydianiline (ODA). The high percentage of sulfonation usually results in high swelling and even the dissolution of polyimide membrane, therefore, controlling the degree of sulfonation is very important. All monomers may be added at the start of reaction to get a statistically random copolymer.<sup>33</sup>

The solubility of polyimides was also enhanced significantly by the introduction of phenyl ether bonds and bulky groups in the backbones of polymers. Random sulfonated copolyimides exhibited improved solubility in organic solvents as compared to the sequenced ones. This improvement in solubility was due to the nonsulphonated diamine and



the induced microstructures of the copolymer chain. The increased water uptake for a specific copolymer structure occurs with increased ionic content. However, the number of water molecules per ionic group remained constant, which suggested that water molecules were primarily located in the hydrophilic domains. For random copolyimides, both the number of water molecules per ionic group and conductivity were systematically lower than for the block copolyimides. It was reported that greater interchain spacing can be achieved by introducing bulky nonsulfonated diamines in the polymer backbone. It was indicated that increase in interchain spacing can improve proton conductivity at lower relative humidity. Incorporation of larger comonomers result in a comparatively more exposed structure by inhibiting frequent close parallel packing of polymer chains as indicated by x-ray diffraction patterns. As a result water can occupy more available free volume with greater interchain spacings. This scenario leads to higher conductivity due to higher water uptake values especially at low humidity.<sup>31-33</sup>

### **1.3 Ionic Liquids**

Ionic liquids are a fascinating class of materials, entirely composed of mobile ions and are molten, organic salts. They possess a wide liquid range and can be liquids at very low temperatures such as minus 90 °C. ILs are not the solutions of ionic compounds in a solvent rather they are ionic solutions having completely different properties.<sup>34</sup>

#### **1.3.1 Properties of ionic liquids**

An extensive study on ILs is emerging, including chemistry, chemical engineering, materials science and environmental science. As insights into the nature of ILs become deeper it is found that now some significant basic beliefs are quite different from the original theories. Broad physicochemical properties of ILs are now established. This can be assigned to various combinations of cations and anions that fulfill the description of ILs, resulting in a diverse collection of behaviors. Ionic liquids remain liquid over extremely large ranges of temperature and they do not evaporate and burn. They possess excellent lubricating and hydraulic properties along with high electrochemical stability and high ionic conductivity. Ionic liquids are more suitable than typical volatile solvents and catalysts in different physical and chemical processes, frequently showing “green” and “designer” properties to a practical extent.<sup>34,35</sup>

In a completely different area, Watanabe et al, discussed the use of ionic liquids (ILs) in energy storage and conversion materials and devices. They evaluated the application of ILs as electrolytes for Li/Na ion, Li/S, and Li/ O<sub>2</sub> batteries, fuel cell electrolytes, and electrode materials, particularly the ionic liquids derived N-doped carbons. Several ionic liquids (ILs) can meet the required standards imposed by several energy applications because of their exceptional properties such as nonflammability, high electrochemical stability, and high ionic conductivity.<sup>35</sup>

Ionic liquids (ILs) are liquids at ambient temperatures due to their chemical structure. The cation and anion are selected precisely to destabilize the solid-phase crystal. Although, in general there are no set rules for making an IL, it can be attained within a relatively large window of ions by balancing the symmetry and ion-ion interactions. For example, as the cation alkyl chain affects the coulombic forces and disrupts the lattice packing therefore, it must be long enough to reduce these two factors. On the other hand, it will increase the melting point of salt because the cohesive interactions increase with the increase in the length of nonpolar groups as per linear alkanes, therefore the alkyl chain should not be too long ( $\sim n < 12$ ). However, recently Davis et al. produced salts with low melting points and having very long chain ( $> C16$ ) by the introduction of a *cis* double bond “kink” in the alkyl group.<sup>36</sup> This is comparable to homeoviscous adaptation in cell membranes and shows the complex array of packing and chemical factors that controls IL melting point.<sup>37</sup>

### 1.3.2 Classification of ionic liquids

Ionic liquids are typically classified on the basis of their chemical structures, like solvents. However, they contain structural features similar to the molten salts, ionic crystals, ionic surfactants and molecular liquids. There are enormous number of ILs.<sup>38,39</sup>

The classification of ionic liquids is quite challenging, because various labels appear suitable for a given ionic liquid, depending upon the considered importance of cation, anion, or a functional group. The most common classification being; protic<sup>40</sup> and aprotic<sup>41</sup> depending on the well recognised division between protic (proton donating) and aprotic (nonproton-donating) molecular solvents.<sup>42</sup> However, this definition would not

seem so strict because Davis et al. evaluated dicationic ionic liquids having both functionalities; protic as well as aprotic charge centers in the same molecule.<sup>43</sup>

### **1.3.2.1 Protic ionic liquids (PILs)**

Protic ionic liquids (PILs) are formed by proton transfer between an equimolar combination of a Brønsted acid and a Brønsted base. This depicts that the synthesis of PILs is usually simpler and cheaper as compared to other ionic liquid classes and there are no byproducts as well. Protic ionic liquids may be treated as pure mixtures of ions. The reason behind this is; nearly all PILs show “good” ionic behavior in comparison with ideal aqueous KCl solutions from Walden plots of molar conductivity versus fluidity.<sup>44</sup> The possibility of hydrogen bonding, due to the presence of active protons, imparts unique applications to PILs.

The proton transfer results in the creation of H-bond donor and acceptor sites on ions. The proton transfer mechanism in PILs is still unclear, but it is proposed that it may be similar to Grotthuss-like behavior with labile protons “hopping” between ions along H-bonds as in molecular protic solvents.<sup>45, 46</sup> Proton transfer abilities of protic ionic liquids have been associated with many properties (thermal stability, vapor pressure, catalytic activity, conductivity and protein stabilization).<sup>47, 48</sup> Therefore, better understanding of the H-bonding structures may provide deep insight into PIL solvent behavior.

### **1.3.2.2 Aprotic ionic liquids (APILs)**

Aprotic ionic liquids (AILs) are quite different and do not share common structural feature to the PILs. AILs are composed of a large number of cation and anion chemical structures, some of them form H-bond while others do not. In the beginning, most of the AILs were confined to halometallate ions, but now this area has been expanded including a massive range of chemical structures.<sup>49</sup> The preparation of AIL is usually more complicated and expensive than PILs, often comprising of multistep reactions because ions are formed by covalent bond formation between two functional groups.<sup>50</sup> Mostly this leads to more thermal and electrochemical stable solvent than its corresponding protic ionic liquid; Walden plots (the plots relating conductivity of an ionically conducting liquid to its viscosity) frequently show “good” ionic behavior for AILs.<sup>51</sup>

#### **1.4 Sulphonated copolyimide/protic ionic liquid (SPI/IL) composites**

Protic ionic liquids (PILs) alone cannot work effectively in different applications related to the energy harvesting devices. To make use of unique properties of ionic liquids in devices and systems, it is beneficial that it is locked into IL/polymer composite membranes.<sup>52</sup> Good compatibility of PIL and polymer matrix is compulsory for effective membrane fabrication.<sup>53</sup> For the fabrication of composite membranes based on different polymers as mechanical support, possessing high proton conductivity and mechanical stability, several researches have been performed.<sup>54, 55, 56, 57</sup> Among numerous developed polymers, polyimides are counted as one of the potential candidates for composite membrane matrix because of their exceptional film forming ability, good thermomechanical properties and high chemical stability.<sup>58</sup> However, simple polyimides without chemical modification were not compatible with protic ionic liquids. It was found that sulfonated polyimides (SPIs) have very good compatibility with protic ionic liquids (PILs) which prevent their desorption from the polymer matrix resulting in flexible composite membranes formation having favorable thermal and mechanical properties.<sup>59</sup> Mechanical properties can be affected badly due to the presence of sulfonic acid group on polymeric backbones.<sup>60, 61</sup> However, ionic liquid functions as a plasticizer. It was thus, preferentially incorporated into sulfonate groups of SPI and plasticizing effects were found in both the ionic and nonionic domains of the composite membrane.<sup>62</sup> These improved properties emerged due to the nanoscale phase separation among the ionic and nonionic domains, where bicontinuous phases of these domains were established.<sup>63</sup> The ionic domain in SPI comprised of the sulfonic acid group where the PIL was incorporated preferentially and promoted the ionic conduction. However, the nonionic domain mainly comprised of the aromatic sulfonate polymer structure, exhibiting rigidity and high hydrophobicity, contributing to the mechanical properties. Owing to this composite structure, the composite membranes demonstrated good mechanical strength with high ionic conductivity.<sup>63, 64</sup>

#### **1.5 Applications of sulphonated polyimides and protic ionic liquid composites**

The literature reports a number of sulphonated polyimides and their composites with protic ionic liquids having structural variations which exhibit diverse applications. Here,

the focus will be on the following three main applications of sulphonated copolyimides and their composites as these applications will be targeted in this research work.

### **1.5.1 Sulphonated copolyimides as chemosensors**

Chemosensors, molecular systems which produce a detectable signal upon interaction with a chemical species, bearing high sensitivity have attracted boosting interest in recent years.<sup>65</sup> Particularly, detection of heavy and transition metal (HTM) ions is important as they are enormously toxic for human health and environment.<sup>66, 67</sup> Water resources have been contaminated globally because of the increased heavy and transition metals discharge into the water bodies.<sup>68, 69</sup> Numerous optical sensors have been synthesized and employed for the detection of different HTM ions selectively using electronic absorption, fluorescent emission, and/or colorimetric signals.<sup>70-72</sup>

Porphyrin-based sensors have displayed great potential for heavy metal ions detection in solution, because the porphyrin compounds bear extraordinary photophysical properties. But costly, complex and time consuming organic synthesis is required for the preparation of porphyrin based optical sensors. Moreover, these porphyrin sensors are water insoluble, which greatly affects their detection ability in aqueous environment.<sup>73</sup> Consequently, finding an inexpensive, simple and water soluble optical chemical sensor capable of detecting toxic metal ions is highly desired.

Over the past 60 years, the metal-chelating properties of polymers have elicited considerable interest.<sup>74</sup> Nowadays, the use of chelating polymers for waste water remediation has attracted much attention. Chelating groups are incorporated into the polymeric side chains or backbone. The choice of the type of ligands, structure and solubility of the polymer, govern the metal ion affinity, and selectivity.<sup>75, 76</sup> Polymers containing functional groups such as -COOH, phenolic-OH and -SO<sub>3</sub>H, are capable of complexing metals.<sup>77</sup> This is believed to occur due to the formation of soluble, organic complexes of heavy metals, since polymers can be easily functionalized, with functional groups that possess the ability to interact with metals.<sup>78-80</sup>

Among the polymers, polyimides have not been used as metal chelating ligands because of their weak hydrophilicity. This shortcoming can be overcome by converting polyimides into sulfonated polyimides with the introduction of sulfonic acid group, which

makes the polymeric chains hydrophilic.<sup>81</sup> By the introduction of hydrophilic sulphonic acid groups into the PI main chain the material's hydrophilicity can be improved leading to enhanced water absorption and ion exchange properties as shown in **Figure 1.7**. The hydrophilic sulphonic acid groups are capable of complexation to metal ions.<sup>82</sup> This suggests that sulphonated polyimides can exhibit metal-responsive properties. Sulphonated polyimides can function as a versatile receptor for heavy metal ions especially Ni (II), Co (II) and Cr (III).



**Figure 1.7:** Interaction of polymers with water a) Hydrophobic polymer and b) hydrophilic polymers.<sup>83</sup>

### 1.5.2 Sulphonated copolyimides for adsorption of toxic metal ions from wastewater

Water shortage is a threatening universal problem of modern society and as a result, wastewater treatment and its reuse is worldwide urgency.<sup>84</sup> Toxic metal ions, like Pb, Cr, Cd, As, Ni, Cu and Zn are widely existing water toxins. These are poisonous to human health even at trace levels due to their bioaccumulation in human body and nonbiodegradability.<sup>85</sup> Among these metals ions, lead in particular is extremely toxic, even at very low concentrations.<sup>86</sup>

Numerous human activities produce toxic metal ions particularly the industrial waste is one of the main source of their discharge into water bodies. Therefore, treatment of contaminated wastewater before releasing into environment should be the priority. Toxic metal ions can be removed by several methods like ultrafiltration, electrodeposition, chemical precipitation, ion exchange and adsorption.<sup>87, 88</sup> Among all these techniques, ion exchange and adsorption are most popular and have been widely practiced in industrial wastewater treatment processes.<sup>89</sup> Now a days, polymeric materials are under investigation

for heavy metal ions removal by exploring the interacting capability of polymer materials with contaminating species.<sup>90</sup>

Although, polyimides (PIs) have excellent chemical resistance and thermal stability, but due to their weak hydrophilicity, PIs have not been used as adsorbents for heavy metals.<sup>91,92</sup> However, because of their weak hydrophilicity PIs have not been used as adsorbents for heavy metals. However, the introduction of sulfonic acid group on the polymeric backbone makes the polymer chains hydrophilic.<sup>93</sup> By the introduction of hydrophilic sulphonate groups into PI main chain, the polymer starts interacting with water molecules and undergo swelling, as shown in **Figure 1.8**.

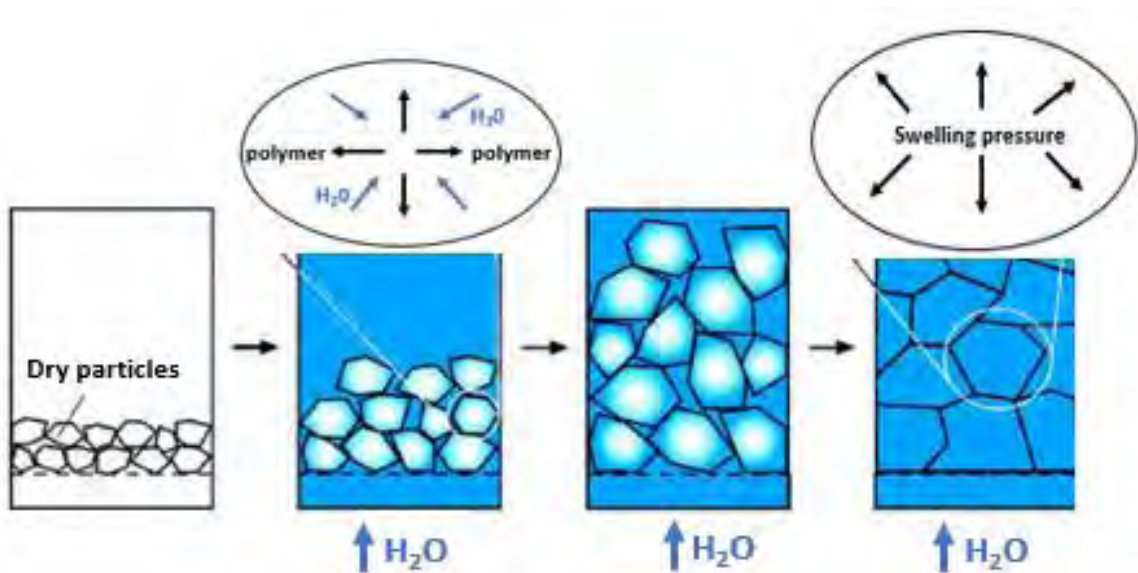


**Figure 1.8:** Swelling behaviour of polymer in water.<sup>94</sup>

The hydrophilic sulphonic acid group, an anion functional group bears strong affinity towards heavy metal ions (**Figure 1.9**).<sup>82</sup> Improvement in polymer hydrophilicity enhances the heavy metal ions adsorption capacity due to feasible access of adsorption sites. Hence, sulphonated polyimides are of immense interest in research for exploiting their possible applications in removal of toxic metal ions from water.<sup>81</sup> Sulphonated aromatic co-polyimides are efficient polymeric adsorbents for toxic metal ions.

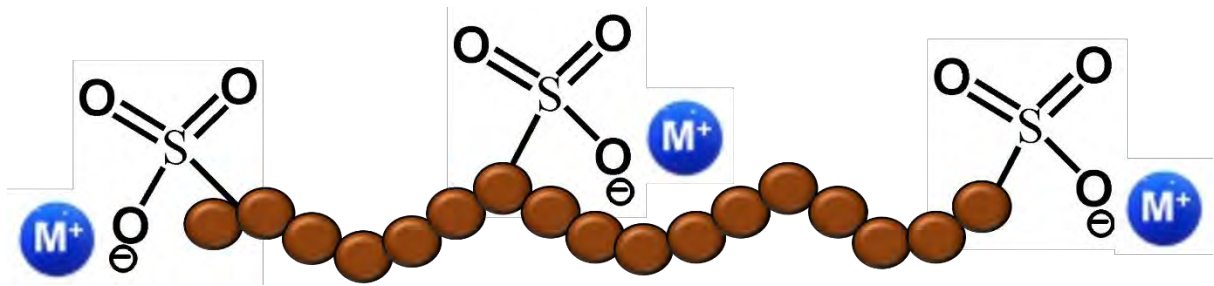


**Figure 1.9:** Interaction of sulphonic acid group with metal ions.

### 1.5.3 Polymer electrolyte membrane fuel cells (PEMFCs)

Energy is one of the basic need of a human being from the beginning of his life on earth, to make his living. As time passes, the mode, as well as the uses of energy, takes different forms (the recent one is electricity). As the population of the world is increasing day by day, the demand for energy increases. Most of our energy comes from fossil fuels (non-renewable resources), which are decreasing day by day and have a large contribution in polluting our environment. To overcome these two burning issues of energy demand and increasing pollution, fuel cells are the best option. A fuel cell is a type of an electrochemical cell in which hydrogen or any other fuel along with oxidizing agent (mostly oxygen) produces heat and electricity (**Figure 1.10**).<sup>95</sup>

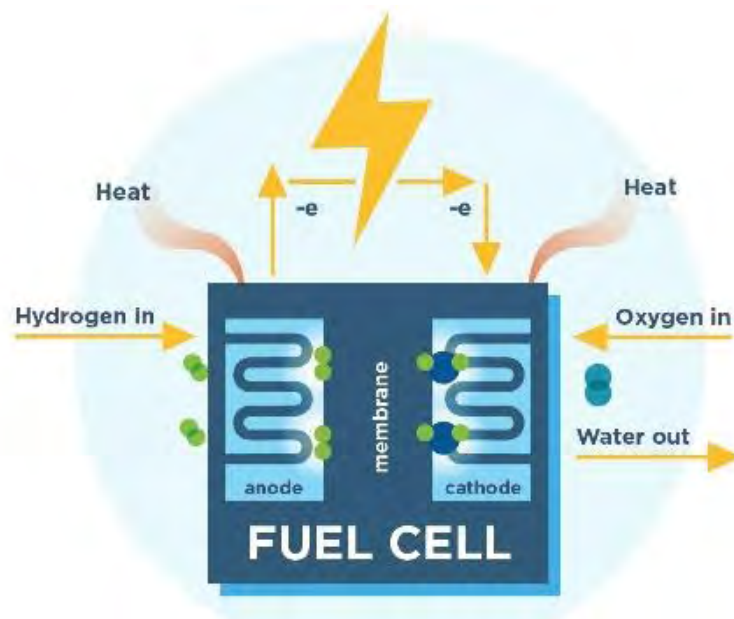


**Figure 1.10:** Pictorial representation of a fuel cell.<sup>96</sup>



A fuel cell has overpowered other energy conversion devices in a very short time due to its high efficiency, need of low maintenance charges, almost no need of fossil fuels and production of non-hazardous by-products (water commonly). All these properties lead it to be known as Green Power.<sup>97</sup>

Although fuel cell contributes a lot to the society but still needs research especially on its cell design (with a focus on efficiency, the supply of fuel, size requirement, output, heat control, and their applications).<sup>98-100</sup> Up till now, different kinds of fuel cells are in market such as solid oxide fuel cells (SOFCs), molten carbonate fuel cells (MCFCs), alkaline fuel cells (AFCs), phosphoric acid fuel cells (PAFCs), polymer electrolyte membrane fuel cells (PEMFCs) and direct methanol fuel cells (DMFCs) (**Figure 1.11**).<sup>101-103</sup>

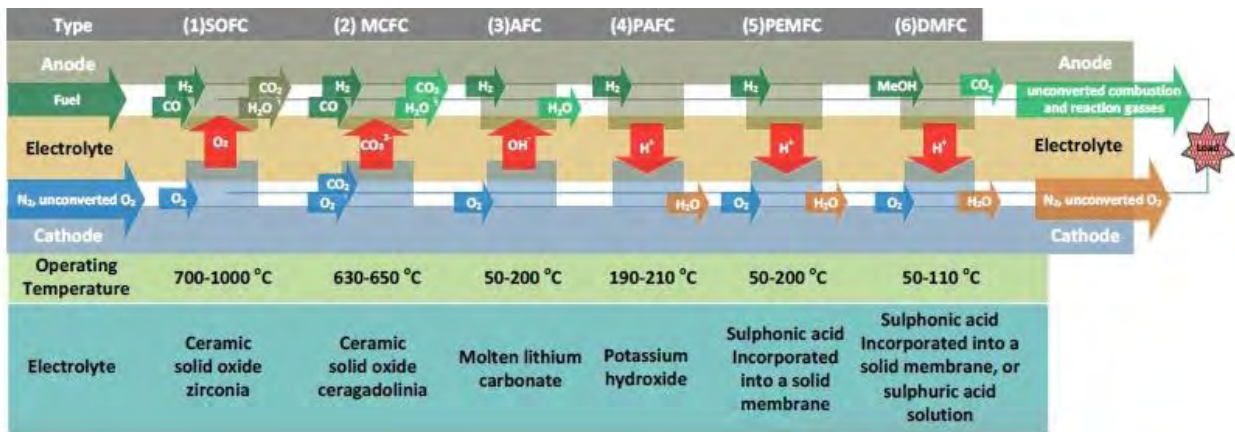


**Figure 1.11:** Types of fuel cells.<sup>104</sup>

Every type of fuel cell has its own pros and cons related to its fuel efficiency, lifetime, power output and applications. Due to the potential applications of PEMFCs in transportation, portable devices, residential power sources, and electric vehicles, a large work on this technology has been done in the last decade. Their ease of synthesis, stability, and durability made them capable of competing for the alternative technologies in the above mentioned applications. Polymer Electrolyte Membrane (PEM) is a polymer matrix which contains hydrophobic backbone and negatively or positively charged functional groups capable of ion exchange.<sup>105</sup>

Nafion® was the first commercial electrolyte membrane which made a breakthrough in the field of the fuel cell. Up till now Dow® (perfluorinated sulfonic acid ionomer membrane) and Flemion® (perfluorocarboxylic membrane) produced by Asahi Glass are some commercial membranes used in electronic devices. The working principle of PEMFCs is shown in **Figure 1.12**.

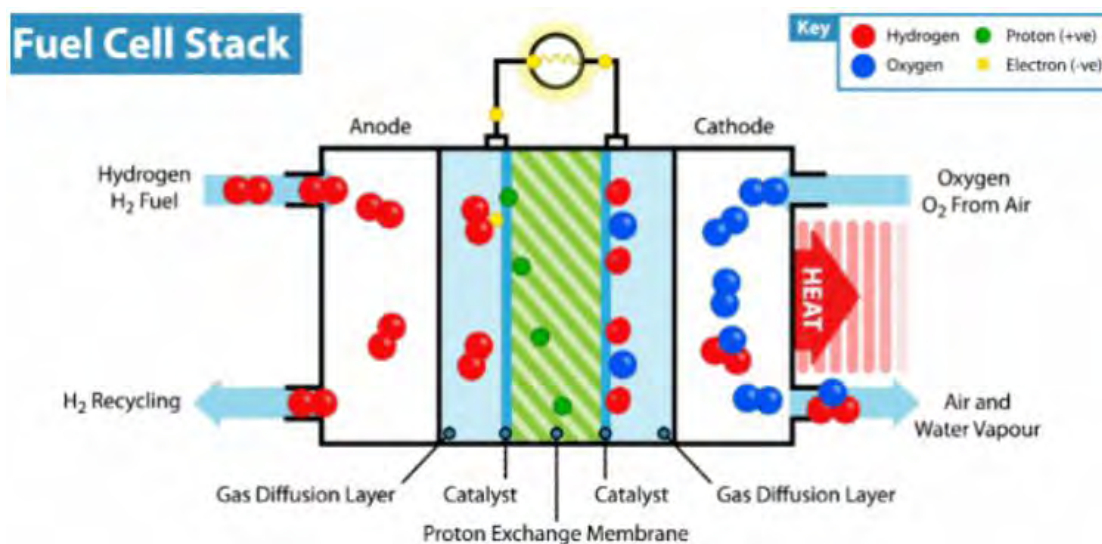


**Figure 1.12:** Schematic diagram of a polymer electrolyte membrane fuel cell. <sup>106</sup>

Drawbacks such as deterioration in conductive and mechanical properties above  $T_g$  ( $110^\circ\text{C}$ ), high cost, high gas crossover, and environment incapability made researchers develop new PEMFCs. So, the challenge in this field is to achieve a stable conductive membrane at a temperature higher than  $120^\circ\text{C}$  at a relatively low humidity level. <sup>107</sup>

Current fuel cells most often contain sulfonic acid groups bearing polymer electrolyte membranes. <sup>108, 102</sup> However, the conductivity of proton through membranes is water dependent and the membranes showed significantly high proton conductivity only in the presence of water. The water molecules solvate the protons and promote their conduction by diffusion and by vehicle-type transport and are therefore essential for the mobility of protons. <sup>109</sup> Therefore, the maximum operating temperature for fuel cells with these sulfonated membranes is restricted by the boiling point of water at atmospheric pressure. An increase in the operational temperature above  $100^\circ\text{C}$ , ideally above  $150^\circ\text{C}$ , is the crucial parameter permitting further development in polymer electrolyte membrane

fuel cell.<sup>110</sup> The use of protic ionic liquid (PIL) as a proton transport medium in the polymer membrane seems an impressive solution to the problem.

During past few years, ionic liquids (ILs) have attracted widespread attention owing to their exceptional properties, namely high solvation capacity, low volatility, large electrochemical window, high thermal stability, and good ionic conductivity.<sup>111</sup> The basic requirement for an electrolyte to be used in fuel cells is the proton conductivity therefore protic ILs (PILs) synthesized by the neutralization of Brønsted acid and base are often studied for PEMFCs. Generally, the conductivity of PILs ranges between  $1 \times 10^{-4}$  to  $1.8 \times 10^{-2}$  S/cm at room temperature.<sup>112</sup> The cations conduct the protons via the vehicle and Grotthuss mechanisms. The electrochemical reactions (i.e., hydrogen oxidation and oxygen reduction) may be further accelerated at the electrode/PILs interface.<sup>44</sup> However, the fabrication of polymer membranes based on PILs need to be prepared for their use as electrolytes because the PIL alone cannot form an electrolyte in PEMFC. Mostly, sulfonated polyimide is used as polymer matrix for protic ionic liquids composites since it contains additional proton carriers in the form of sulfonic acid groups. The polyimide based membranes possess the ability of working at high operating temperature of  $\sim 150$  °C, therefore enabling the prevention of Pt poisoning and as a result are attracting the researchers attention.<sup>60, 61</sup>

## **1.6 Literature review on sulphonated copolyimides and their composites with protic ionic liquids**

In the past few decades, sulphonated polymers have attracted enormous consideration due to their significant applications especially in fuel cell systems. The extensively studied and practically employed proton conducting polymers are sulfonated perfluoropolymers such as DuPont's Nafion membrane and Dow's membrane due to their high performance including high mechanical strength, high proton conductivity and good chemical and thermal stability. However, there are some shortcomings such as high cost, low conductivity at high temperature, and high methanol permeability which limit their further application. Therefore, special attention has been given to the development of low cost and high performance nonfluorinated hydrocarbon membrane materials. The most important approach has been the introduction of sulfonic acid groups in the polymeric

backbones of fairly stable aromatic polymers like poly(ether ether ketone) (PEEK), polysulfone (PSF) and poly(phenylene sulfide) (PPS). The sulfonic acid groups can be introduced either by direct sulfonation of the parent polymers or by the polymerization of sulfonated monomers. In recent past, sulfonated polyimides have been successfully synthesized in several laboratories.<sup>113-115</sup>

Sulfonated polyimides are attractive due to their hydrophilic nature and film forming abilities but they show difficulty in the formation of the film due to their rigid packing. Many scientists develop different methods to overcome this problem;

Guo et al, used fuming sulfuric acid (sulfonating reagent) for the synthesis of new sulfonated diamine, 9,9-*bis*(4-aminophenyl)fluorene-2,7-disulfonic acid (BAPFDS) by carrying out the direct sulfonation of parent unsulphonated diamine, 9,9-*bis*(4-aminophenyl)fluorene (BAPF). Different sulfonated copolyimides were synthesized from NTDA, BAPFDS and common unsulfonated diamines with varying degree of sulfonation. Flexible membranes were obtained due to the 'kink' in polymer backbone developed by sulphonated diamine resulting in the decreased polymer overlapping. These polyimide membranes were evaluated for the measurements of proton conductivity as a function of relative humidity and temperature. The synthesized polyimide, NTDA-BAPFDS, showed fairly close proton conductivities to Nafion 117 in entire range of humidity (RH < 100%).

116

Fang et al, carried out the sulfonation of 4,4'-diaminodiphenyl ether (ODA), a commercial diamine, for the synthesis of sulfonated diamine monomer, 4,4'-diaminodiphenyl ether-2,2'-disulfonic acid (ODADS), by using a sulfonating reagent (fuming sulfuric acid). They prepared a series of sulfonated polyimides using ODADS, common unsulfonated diamines and NTDA. They reported that newly synthesized sulfonated polyimides presented quite improved water stability than the sulphonated polyimides derived from the most commonly utilized sulfonated diamine 2,2'-benzidinedisulfonic acid (BDSA). This stability can be attributed to more flexible structure of ODADS based polyimide membranes than the corresponding BDSA based ones.<sup>60</sup>

Einsla et al. evaluated the synthesis of a novel sulfonated diamine, 3,3'-disulfonic acid-bis[4-(3-aminophenoxy)phenyl]sulfone (SA-DADPS), using *m*-aminophenol and

disodium-3,3'-disulfonate-4,4'-dichlorodiphenylsulfone. The sulfonated diamine with sulfone and ether linkages was used in one-step high temperature polycondensation reaction for the synthesis of polyimides having pendant sulfonic acid groups in *m*-cresol. Incorporation of ether, sulfonyl group causes bending in the chains as compared to those polyimides whose monomers lack these type of functionalities. Significantly improved hydrolytic stability was shown by these materials as compared to phthalimides.<sup>117</sup>

Bai et al, synthesized and characterized a series of six-member ring sulfonated polyimide (SPI) copolymers having poly(ethylene oxide) (PEO) soft segment. The SPI copolymers were prepared from NTDA, 4,4'-diaminostilbene-2,2'-disulfonic acid (DSDSA), and diamine-terminated poly(ethylene oxide) (PEO-diamine, MW = 1000 g/mol) using one-step high temperature polymerization method. In this method, the molar ratio of DSDSA to PEO-diamine was altered to control the relative ratio of the sulfonic acid-containing hard segments to the PEO-containing soft segments. Mechanically strong, transparent, flexible and free-standing membranes were obtained successfully. Addition of oxygen in the aliphatic monomer chain like polyethylene oxide gave hydrolytically stable and flexible films.<sup>118</sup>

Einsla et al. studied three sulfonated polymers having different sequence lengths of sulphonic acid groups to thoroughly understand the connection between molecular structure, morphology, and properties of proton exchange membranes and relative humidity. These random copolymers were found to have very small domain sizes due to the statistical distribution of sulfonic acid groups, whereas an alternating polymer was found to have bigger and quite isolated domains due to the evenly spaced sulfonic acid groups along the polymer chain. The multiblock copolymer depicted highly phase-separated hydrophilic and hydrophobic domains, with better long-range connectivity. Morphology of the polymer plays an important role in the dependency of working electrolyte on humidity. Multi-block co-polymer showed comparable conductivity to Nafion at 40 % humidity as compared to random and alternating ones.<sup>119</sup>

Fang et al. studied the proton conductivity and hydrolytic stability of sulphonated polyimides. It was found that proton conductivities of sulphonated copolyimide membranes depend greatly on the relative humidity and the conductivity increases swiftly

with increase in humidity. At higher values of relative humidity (> 80 %), sulphonated copolyimide membranes usually showed proton conductivity comparable to or higher than Nafion 117, that are sufficiently high for practical use ( $> 10^{-2} \text{ S cm}^{-1}$ ). Whereas, at lower values of relative humidity (< 40 %), the conductivity values of these SPI membranes were found to be very low to fulfill the requirements of practical usage. Therefore, it is a big challenge to improve the proton conductivity values of sulphonated copolyimide and other sulfonated polymer membranes upto  $10^{-2} \text{ S cm}^{-1}$  at lower relative humidities. The hydrolytic stability of SPI membranes is primarily controlled by the structure of sulfonated diamine monomers including the basicity, flexibility and configuration. High basicity, flexible structure and linear configuration caused higher hydrolytic stability of SPI membranes.<sup>120</sup>

Genies et al. used model compounds to assess the hydrolytic stability of phthalic and naphthalenic imide structures. The IR and NMR spectroscopic characterizations of the model compounds, before and after aging in water, at different temperatures, showed that some structural modifications greatly depend on imide ring structures. The lower stability of the phthalic model compound was confirmed in comparison with the naphthalenic one. This stability could be justified by various equilibria allowing the regeneration of the imide structure.<sup>121</sup>

Guo et al. used 2,2'-bis(4-aminophenoxy)biphenyl-5,5'-disulfonic acid (oBAPBDS) having nonlinear configuration, commercial unsulfonated diamines and NTDA to synthesize the novel SPIs. Water stability, liquid/vapor phase water uptake (WU) and proton conductivity of synthesized SPI membranes were examined. Due to the improved solubility stability towards water, membranes showed improved water stability.<sup>122</sup>

Zhai et al. compared the hydrolytic stability of two series of sulfonated polyimides (SPIs) based on NTDA, two different sulfonated diamine monomers, 4,4'-bis(4-aminophenoxy)benzophenone-3,3'-disulfonic acid (BAPBPDS) and 4,4'-bis(4-aminophenylthio)benzophenone-3,3'-disulfonic acid (BAPTBPDS) and common non-sulfonated diamines. BAPTBPDS based copolyimide membranes showed much improved water stability than BAPBPDS based ones due to the higher basicity of BAPTBPDS monomer because of the greater electron-donating effect of thio group.<sup>123</sup>

Tripathi et al. evaluated the use of nanocomposite polymer electrolyte membranes (PEM) containing nano-sized inorganic particles embedded in organic polymeric matrix for fuel cells applications. The organic-inorganic architecture combined the appealing properties of thermally and mechanically stable inorganic backbone and chemical reactivity, flexibility, and processability of organic polymer in a single solid membrane. Homogeneous dispersion of inorganic fillers in matrix and different characteristics (e.g., thermal stability and solubility) of the two phases were the main barriers toward appropriate strategies for membrane preparation.<sup>124</sup>

Bano et al. studied the characterizations and fabrication of nano-composite membranes of sulfonated poly(ether ether ketone) (SPEEK) reinforced and cross-linked with ethylene glycol (EG) and cellulose nanocrystals (CNCs) respectively. The solvent casting method was utilized for the preparation of thin films of cross-linked composite and the films were analysed for physicochemical and electrochemical properties to evaluate their ability as proton exchange membrane (PEM) in fuel cells. Membranes of cross-linked SPEEK having 4 wt % loading of CNCs showed a significant proton conductivity of 0.186 S/cm at 95 °C and 95 % RH which is comparable to Nafion 117.<sup>125</sup>

The proton conductivities of sulfonated polymer/protic ionic liquid membrane depend upon the type and concentration of IL and upon the sulfonic acid groups in the matrix polymer.<sup>126</sup>

Doyle et al. studied the effect of addition of various equivalent weights of 1-butyl-3-methylimidazolium trifluoromethanesulfonate in Nafion membranes. They found out that the Nafion membrane having higher concentration of sulfonic acid groups displayed quite high proton conductivity of 80 mS/cm at 150 °C that is even higher in comparison to neat IL.<sup>127</sup>

Martinez et al. and Di Noto et al. investigated the effect on proton conductivity of Nafion 117 upon addition of triethylamine based protic ionic liquids. It was observed that the IL possessing best proton conductivity did not resulted in the best composite (Nafion/IL) membrane. They postulated that alongwith the ionic liquids other factors also act as decisive parameters like IL uptake, structure, interactions with the polymer and the structuring inside the membrane. It was found that that composite membranes of Nafion

with incorporated ILs have comparatively higher ability to retain water as compared to neat Nafion at temperatures above 100 °C. <sup>128-130</sup>

Susan et al. investigated protic ionic liquids (PILs), synthesized by the reactions of different organic amines (such as imidazole) with bis(trifluoromethanesulfonyl)imide and realized that protic ionic liquids (PILs) were proton-conductive. <sup>131</sup>

Fernicola et al. evaluated the proton conductivity profile of protic ionic liquid composite membranes built on monosubstituted imidazole or pyrrolidone in a polymer matrix. <sup>55</sup>

Fatyeyeva et al. immobilized the water insoluble PIL in the porous polymer (Matrimid® 5218) film to synthesize the composite polyimide/PILs membranes. The higher proton conductivity ( $\sim 10^{-3}$  S/cm) was shown by composite membranes at higher temperatures (up to 160 °C). The acquired proton conductivity values revealed that the composite membranes (polyimide/PIL) are attractive candidates for PEMFCs at middle and high temperatures. <sup>132</sup>

## **1.7 Scope and objectives of work**

Extensive research has been carried out on wastewater treatment and clean energy production using polymeric materials because of their appealing properties. Since the successful sulphonation of polyimides, the applications of sulphonated polyimides have been investigated tremendously in these two fields. The benchmark sulphonated ionomer, Nafion, used for the toxic metal ions adsorption from aqueous media and as an electrolyte for proton conductivity in polymer electrolyte membrane fuel cells (PEMFCs) possess some drawbacks such as high cost, fluorinated backbone, excessive swelling, water loss at high temperature and low glass transition temperature (117- 127 °C).

Keeping these shortcomings of Nafion in mind, the main focus of the present study will be on the hydrocarbon based sulphonated polyimides that possess higher  $T_g$ , hydrophilic-hydrophobic domains, toxic metal adsorbing and proton conducting abilities at high temperature or in the absence of water. Therefore, in current research work the synthesis of sulphonated copolyimides and their composites with protic ionic liquids will be targeted. For composites the most attractive approach of composite synthesis, i.e.,



swelling of polymer film with PIL, will be selected. Here, the polymer possessing sufficient mechanical strength alongwith chemical and thermal stability will serve as a matrix support and mechanically strong composite thin films will be obtained. Protic ionic liquids will help in the conduction of protons and will result in an increased proton conductivity through the membranes. The fabrication of flexible films (SPIs and SPI/ IL) by introducing flexible linkages into the polyimide backbone will be under investigation. Dianhydrides and diamines with flexible linkages e.g., -O-, -CH<sub>2</sub>, will be used in this research work. It is expected that flexible membranes with good adsorption ability, hydrolytic stability and proton conductivity will be achieved.

### **1.8 Plan of work**

The current research was planned with the goal of contributing to water purification and green energy technologies. To address this goal, it was planned to synthesize and characterize the sulphonated copolyimides and their composites with protic ionic liquids which will be used as toxic metal adsorbents and electrolytes in polymer electrolyte membrane fuel cells (PEMFCs) respectively. Efficient polymeric adsorbents and proton conductors may be obtained by introducing sulphonate groups on the polymeric backbone. Flexible linkages will be introduced in the polymeric backbone to improve the processability and flexibility of the membranes. Protic ionic liquids will be added in the sulphonated polyimide matrix to facilitate the proton conductivity of sulphonated polyimides.

Different alkyl chains containing diamines will be synthesized by employing inexpensive and accessible synthetic procedures. Scheme 1.1 gives the synthetic strategy for the synthesis of diamines. Some series of polyimides will be synthesized by reacting two synthesized and three commercial diamines, containing flexible linkages, with two dianhydrides (oxydiphthalic anhydride (ODPA) and 4,4'-(hexafluoroisopropylidene) diphthalic anhydride (6FDA)) via solution polymerization.

Synthesis of sulphonated copolyimides will be carried out by reacting commercial sulphonated diamine; 4,4'-diamino-2,2'-biphenyldisulfonic acid (BDSA), unsulphonated diamines (two synthesized, three commercial) with two dianhydrides (ODPA and 6FDA) using different percentages of sulphonated diamine via solution polymerization.

Eight different protic ionic liquids will be synthesized using Brønsted acids and Brønsted bases. Protic ionic liquid composites were synthesized using sulphonated polyimides as matrix and protic ionic liquids as additives to increase the proton conductivity alongwith flexibility of membranes.

For structural compatibility and good adhesion of additive in matrix, introduction of like-like chemical interactions was planned. To achieve this target, same structural moieties, triethyl amine groups, will be introduced in matrix as well as additive. The presence of similar structural units might lead to increased interfacial interactions. The whole synthetic strategy will be divided into three parts. Part A will comprise of two steps; step 1 will be the synthesis of alkyl chains containing diamines (scheme 1.1) followed by the synthesis of ODPA and FDA based polyimides (scheme 1.2) using conventional two step thermal imidization procedure. Part B will comprise of two steps; where synthesis of triethyl ammonium salt of sulphonated diamine will be carried out in step 1 (scheme 1.3), followed by the synthesis of sulphonated copolyimides in step 2 (scheme 1.4). In part C, synthesis of protic ionic liquids will be carried out in step 1 (scheme 1.5), followed by the synthesis of composites in step 2 (scheme 1.6).

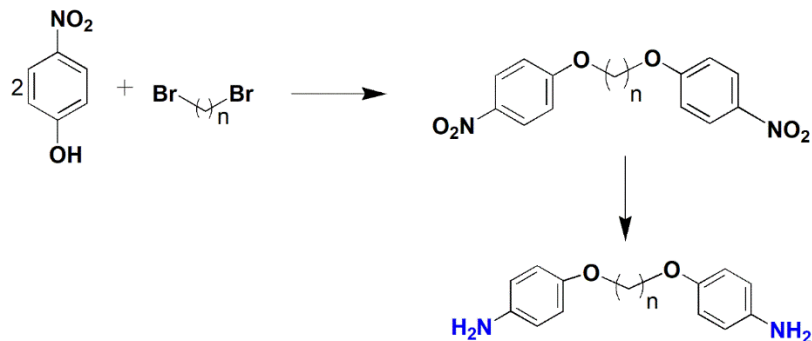
All synthesized polyimides, sulphonated copolyimides and their composites will be characterized thoroughly by conventional and modern analytical techniques for better understanding of the properties of ultimate materials.

The synthesis will be accomplished using the following schemes.

### **Part A: Synthesis of 6FDA and ODPA based polyimides**

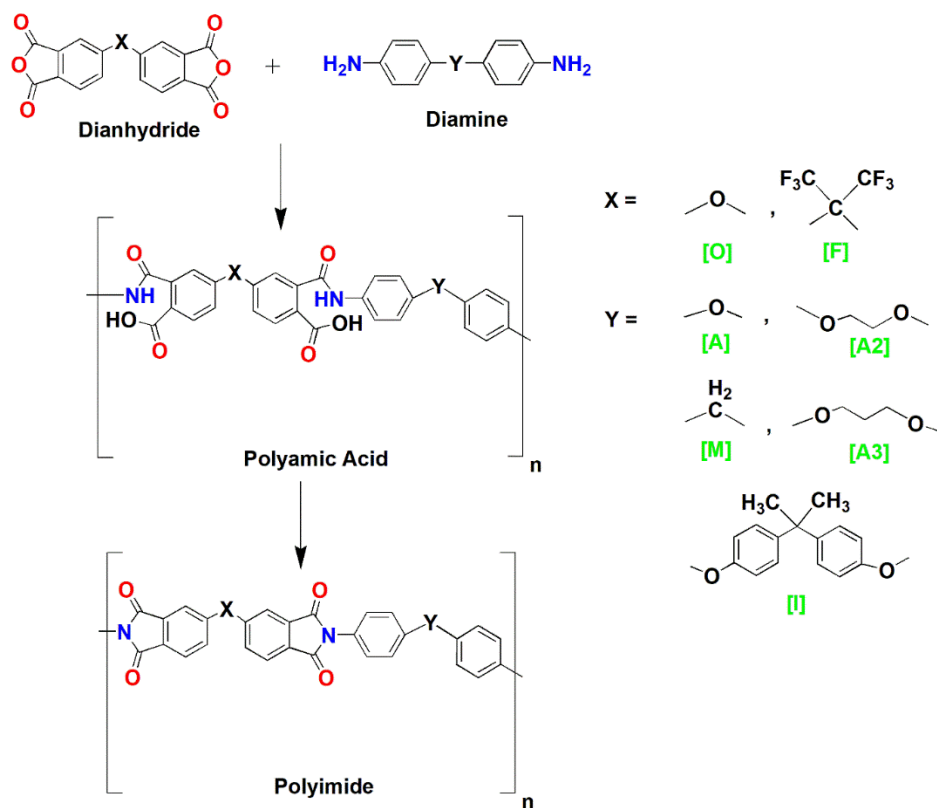
The synthesis of 6FDA and ODPA based polyimides will comprise of two steps. Step one comprises of the synthesis of diamines followed by the synthesis of polyimides in step 2. The general scheme for the synthesis of diamines is given in **Scheme 1.1** and for the polyimides in **Scheme 1.2**.

### Step 1: Synthesis of diamines



**Scheme 1.1:** General scheme for the synthesis of 4-((4-aminophenoxy)alkoxy)benzenamines.

### Step 2: Synthesis of polyimides

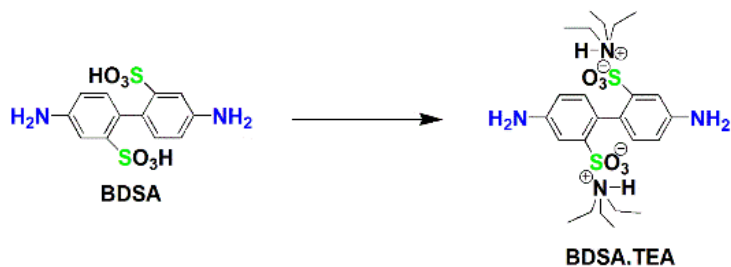


**Scheme 1.2:** General scheme for the synthesis of homopolyimides.

### Part B: Synthesis of 6FDA and ODPa based sulphonated copolyimides

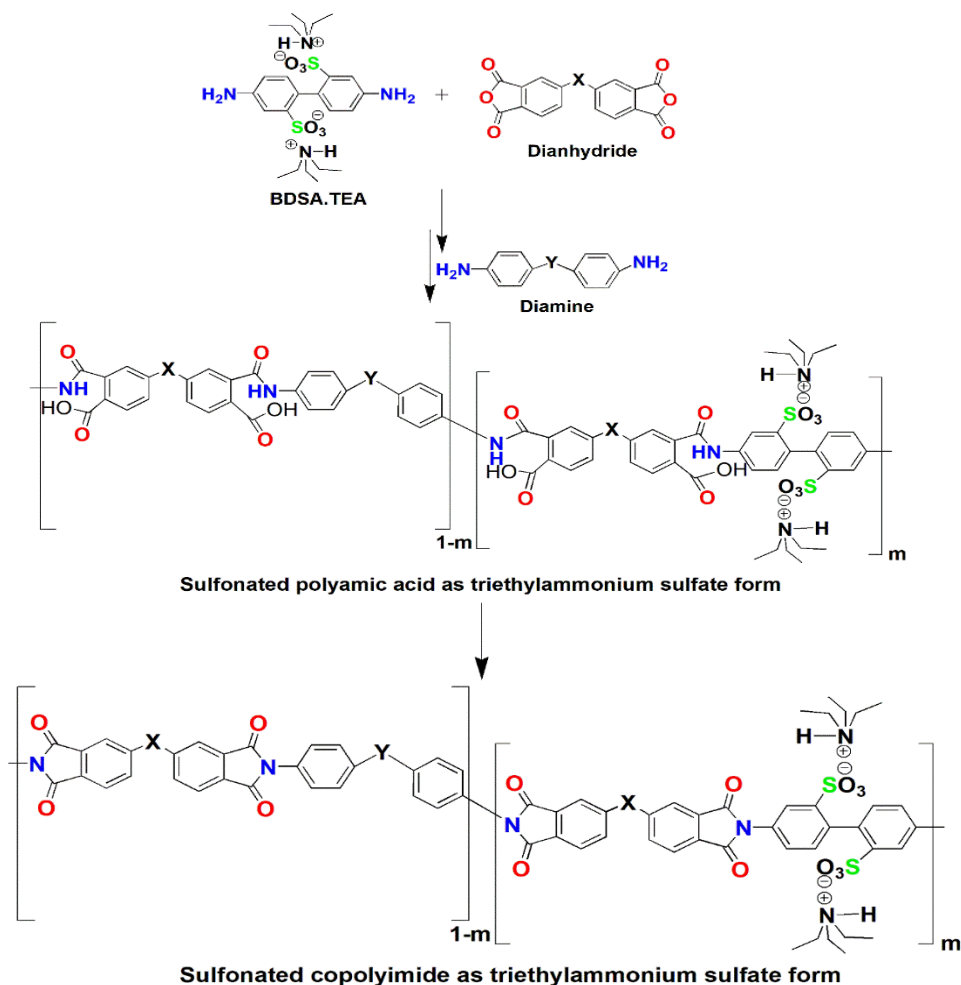
It will comprise of two steps.

**Step 1: Synthesis of triethyl ammonium salt of benzidine-2, 2'-disulphonic acid (BDSA)**



**Scheme 1.3:** General scheme for the synthesis of BDSA.TEA.

**Step 2: Synthesis of sulphonated copolyimides**

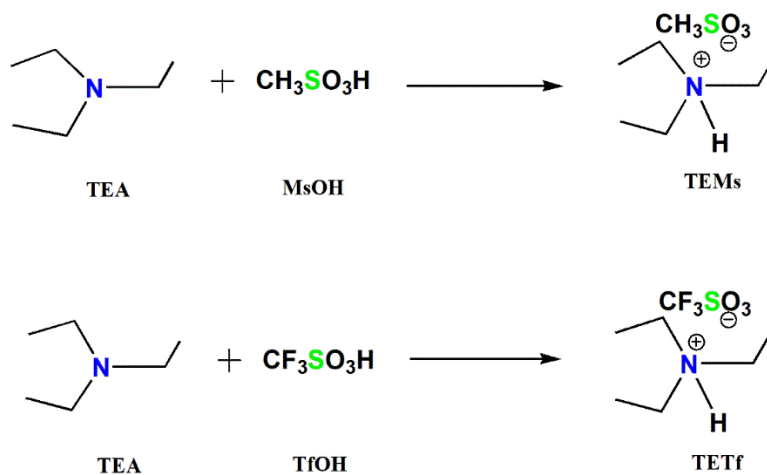


**Scheme 1.4:** General scheme for the synthesis of sulphonated copolyimides.

## Part C: Synthesis of protic ionic liquid composites

It will comprise of two steps.

### Step 1: Synthesis of protic ionic liquids



**Scheme 1.5:** Synthesis of protic ionic liquids (PILs).

### Step 2: Synthesis of composites



**Figure 1.6:** Synthesis of protic ionic liquid composites.

## 2 Experimental

All details regarding used materials and synthetic procedures employed for the synthesis of diamines, polyimides, sulphonated copolyimides, protic ionic liquids and composites alongwith the techniques used for characterization are discussed in the following chapter.

### 2.1 Materials

All commercial grade reagents and solvents were used as received, unless otherwise mentioned. These chemicals were purchased from various chemical companies such as Sigma-Aldrich (Darmstadt, Germany), Fischer scientific (Massachusetts, USA), Merck (Darmstadt, Germany) and AK Scientific Inc (Union City, USA). The chemicals include 1,2-dibromoethane (Sigma-Aldrich), 1,3-dibromopropane (Sigma-Aldrich), anhydrous potassium carbonate ( $K_2CO_3$ ) (Sigma-Aldrich), 10 % palladium charcoal (Sigma-Aldrich), hydrazine hydrate (Sigma-Aldrich), ethyl acetate (Merck), *n*-hexane (Merck), ethanol (Merck), *N,N'*-dimethylformamide (DMF, 99 %) (Merck), *m*-cresol (PG) (Sigma-Aldrich), 4,4'-oxydiphthalic anhydride (ODPA, 98%) (Sigma-Aldrich), 4,4'-(hexafluoroisopropylidene)diphthalic anhydride (6FDA, 99 %) (Sigma-Aldrich), benzidine-2, 2'-disulfonic acid (BDSA) (Sigma-Aldrich), 4, 4'-methylenedianiline (MDA) (Sigma-Aldrich), 4, 4'-oxydianiline (ODA) (Sigma-Aldrich), 4,4'-(4,4'-Isopropylidenediphenyl-1,1'-diyldioxy)dianiline (Sigma-Aldrich), *N*-methyl pyrrolidone (NMP) (Merck), deionized water, diethyl ether ( $\geq 99$  %) (Merck), triethylamine (TEA) (Fischer scientific), diethylmethyl amine (DEMA) (Fischer scientific), dimethylethyl amine (DMEA) (Fischer scientific), trimethylamine (TMA) (Fischer scientific), methane sulphonic acid (MsOH) (Fischer scientific), trifloromethane sulphonic acid (TfOH) (Fischer scientific), lead (II) nitrate ( $PbNO_3$ ) (AK Scientific Inc), nickel (II) nitrate hexahydrate [ $Ni(NO_3)_2 \cdot 6H_2O$ ] (AK Scientific Inc), cobalt (II) chloride hexahydrate [ $CoCl_2 \cdot 6H_2O$ ] (AK Scientific Inc), and chromium (III) chloride hexahydrate [ $CrCl_3 \cdot 6H_2O$ ] (AK Scientific Inc). The standard procedures of drying and purification were used for the purification of solvents.

## 2.2 Purification of solvents

The standard purification methods were employed for the drying and distillation of various solvents.

**Dimethylformamide** (DMF, boiling point 153 °C), was distilled under vacuum after drying for 12 hours using calcium hydride as drying agent.

**Ethanol** (boiling point 78 °C), was distilled under inert atmosphere of nitrogen after 6 hours reflux over CaO.

**Ethyl acetate** (boiling point 77 °C), was distilled under inert atmosphere after drying overnight with CaH<sub>2</sub>.

**n-Hexane** (boiling point 68 °C) was distilled after drying with calcium chloride as drying agent.

## 2.3 Characterization methods

Various characterization techniques have been used for the evaluation of the structures of diamines, polyimides and composites. The experimental conditions and instrumentation details are given below.

### 2.3.1 Thin layer chromatography (TLC)

To monitor the progress of different reactions, TLC was employed. For this purpose precoated silica gel aluminium plates of 0.2 mm thickness (HF-245, E. Merck) were used.

### 2.3.2 Fourier transform infrared spectroscopy (FTIR)

Fourier transform infrared spectroscopy is a well-known technique used for the structural characterization of the organic compounds. The Bruker  $\alpha$ -Alpha-P model with attenuated total reflectance transform infrared (ATR) method was used for FTIR spectroscopic characterization of polyimides, sulphonated copolyimides and composites in the range of 4000-400 cm<sup>-1</sup> at room temperature. A small amount of solid sample was used for measurements.

### 2.3.3 Ultraviolet-visible absorption spectroscopy

UV-Visible spectra and absorbance measurements of sulphonated copolyimide and metal sensing studies of sulphonated copolyimide were carried out in solution form (0.01 g polyimide in 10 mL deionized water) by using Perkin/Elmer, double-beam UV/Vis spectrophotometer Lambda 35 with diode-array detector.

### 2.3.4 Gel permeation chromatography (GPC)

The weight average molecular weight ( $M_w$ ), number average molecular weight ( $M_n$ ), and polydispersity index (PDI) of sulphonated polyimides and composites were obtained using gel permeation chromatography Agilent PL-GPC 220 high temperature system and hot filtration unit instrument having stainless steel column (7.8 mm ID and 30 cm length) calibrated with various standards of polystyrene and with chloroform as eluent. The polyimides were dissolved in hexafluoroisopropanol (HFIP) overnight.

### 2.3.5 Thermal analysis

Thermal decomposition temperature and percent weight loss for polyimides and sulphonated copolyimides were recorded using thermal gravimetric analyzer, TG209 F3, (Netzsch Germany), in an inert atmosphere of nitrogen from 30 to 800 °C at a heating rate of 10 °C min<sup>-1</sup>. All the samples were heated under vacuum for 24 h at 120 °C to ensure complete dryness prior to analysis.

Differential scanning calorimeter, Netzsch, DSC 204 was used to evaluate the glass transition temperatures ( $T_g$ ) of polyimides by heating the samples from room temperature upto 300 °C with the scanning rate of 10 °C min<sup>-1</sup>, under inert atmosphere.

### 2.3.6 Atomic absorption spectroscopy (AAS)

Lead ions adsorption and effect of contact time of lead ions with sulphonated copolyimides were investigated through the determination of residual concentration of lead ions (adsorption conditions: 0.1 g adsorbent; 50 ppm adsorbate solution; contact time 60 min; adsorption medium volume, 10 ml; 25 °C and neutral pH) using flame atomic absorption spectrophotometer (Shimadzu AA-670, Japan).

### 2.3.7 Four probe proton conductivity measurement

The proton conductivity of sulphonated copolyimides and composites was carried out using a four-probe proton conductivity setup with BT-110 Conductivity Clamp from Scribner having four platinum electrodes and Scribner 850e Fuel Cell test system, with 885 Fuel Cell Potentiostat (**Figure 2.1**). The 3×1 cm<sup>2</sup> membrane samples were soaked in water for 24 hours before test. The hydrated sample was mounted in BT-110 Conductivity Clamp from Scribner having four platinum electrodes. This conductivity clamp was then mounted



in fuel cell holder and connected with Scribner 850e Fuel Cell test system as shown in **Figure 2.1**. The steps followed for the conductivity measurement are explained below:

- i) The system stabilization was done at 60 °C and a relative humidity (RH) 20% for 2 h.
- ii) The current voltage (I-V) was recorded.
- iii) System stabilization was done for 5 min.
- iv) I-V was recorded and processes were repeated from (ii) to (iv) for 3 times.
- v) The relative humidity was increased to 40%.
- vi) System stabilization was done for 30 min.
- vii) Same steps were repeated from (ii) to (iv).
- viii) The same methodology was used for the RH of 60, 80 and 100%.
- ix) The temperature was increased to 80 °C and RH to 20%.
- x) System stabilization was done for 2 h.
- xi) Similar steps were repeated from (ii) to (viii).
- xii) The temperature was increased to 100 °C and RH to 20%.
- xiii) System stabilization was carried out for 2 h.
- xiv) Similar steps were repeated from (ii) to (viii).

The I-V was recorded between 0 and 0.8 V with a fixed 10 points/s rate. To measure I-V curve, the linear potential sweep was conducted at 1 mV/s. The 0.5 L/min flow rate was fixed for hydrogen. FCView software from Scribner was used for the analysis of data to calculate resistance (R). Eq. (2.1), was then used for the calculation of proton conductivity ( $\sigma$ ) using the value of (R)

$$\sigma = L / R \cdot A \quad (\text{Equation 2.1})$$

here, L depicts the distance between inner probes whereas A is membrane thickness.

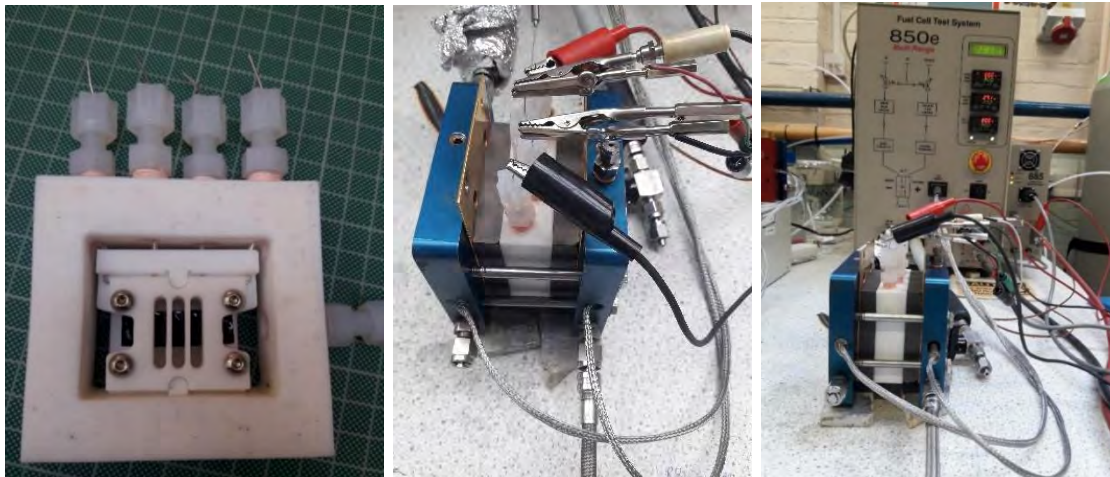


**Figure 2.1:** Four probe conductivity test using Scribner 850e Fuel Cell System.

### 2.3.8 Single fuel cell test

Single fuel cell tests were carried out for sulphonate copolyimides and their composites for catalyst coating studies using single fuel cell set up with single fuel cell holder from Scribner and Scribner 850e Fuel Cell test system, with 885 Fuel Cell Potentiostat. For the single fuel cell test, a Membrane Electrode Assembly (MEA) was fabricated using the Gas Diffusion Electrode (GDE) prepared from carbon supported catalysts (Pt nanorods). For cathode, the catalyst ink was prepared from 100  $\mu\text{L}$  water, 400  $\mu\text{L}$  IPA, 43  $\mu\text{L}$  2 wt% (synthesized SPI) FBA2-50 solution in NMP and the catalyst powder required at a Pt loading of  $0.2 \text{ mgPt cm}^{-2}$ . The sonication bath was used for 30 minutes to get a finely dispersed catalyst ink. The prepared ink was painted onto  $2 \times 2 \text{ cm}^2$  Sigracet 38 BC GDL and dried for 4 hours at  $40 \text{ }^\circ\text{C}$ .

The prepared cathode, commercial GDE ( $0.2 \text{ mgPt cm}^{-2}$ , Fuel Cell Store, USA) as anode and Nafion<sup>®</sup> 212 ( $6 \times 6 \text{ cm}^2$ ) as electrolyte membrane were hot-pressed under 4.9 MPa for 2 minutes at  $135 \text{ }^\circ\text{C}$  for the fabrication of MEA. This hot-pressed MEA was cooled down to room temperature before testing in polymer electrolyte membrane fuel cell (PEMFC). The experiment was performed at  $80 \text{ }^\circ\text{C}$  using fully humidified  $\text{H}_2/\text{O}_2$  with 1.3/1.5 stoichiometric ratios and 1.5/1.5 bar absolute pressure at both the electrodes.

## MEA testing in single fuel cell

Membrane electrode assembly (MEA) was fixed in the fuel cell single cell holder and tested in a 850e Test Stand, with 885 Fuel Cell Potentiostat. Gaskets made of polytetrafluoroethylene (PTFE, 254  $\mu\text{m}$  thickness) were used at both the electrodes sides as shown in **Figure 2.2**. This *in-situ* membrane electrode assembly test comprehends polarisation curve and EIS (electrochemical impedance spectroscopy) for explaining catalytic activities of as-prepared tested catalysts in polymer electrolyte membrane fuel cell (PEMFC) operation.

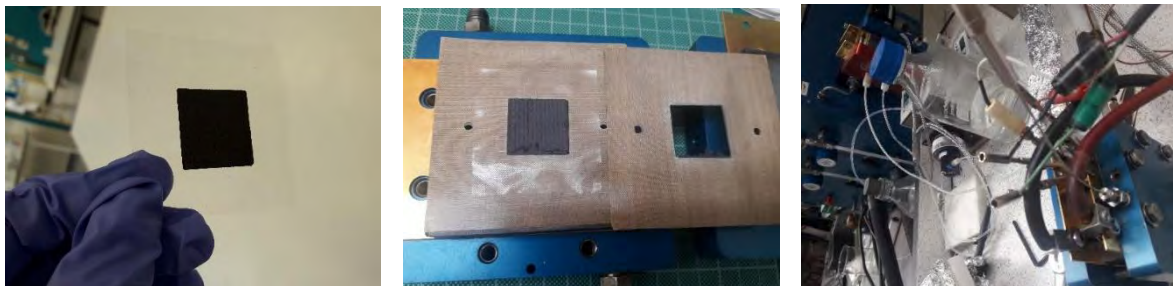


**Figure 2.2:** Single cell test setup.

### 2.3.9 Half-cell gas diffusion electrode (GDE) measurement

Half-cell GDE measurements were conducted using a FlexCell polytetrafluoroethylene (PTFE) from Gaskatel having an O-ring leading to an active area of 3  $\text{cm}^2$ . The polyimides were tested as binders in *ex-situ* GDE measurements. The catalyst loading was 0.2  $\text{mg Pt / cm}^2$  (from TKK). Catalyst ink was applied onto GDL ( $5 \times 3 \text{ cm}^2$ ), by painting a solution of 6.56 mg TKK, 43  $\mu\text{L}$  2 wt % polyimide solution in NMP, 100  $\mu\text{L}$  water and 400  $\mu\text{L}$  IPA and left to dry at 40  $^\circ\text{C}$  overnight. The GDE was inserted into the FlexCell gas compartment where it was held by O-rings leading to an active area of 3  $\text{cm}^2$ . 0.1 M  $\text{HClO}_4$  aqueous solution was used as electrolyte to fill the main and reference electrode compartments and any bubbles produced in the luggin channel (a channel connecting the RHE with main compartment containing electrolyte and as close to gas diffusion electrode (GDE) as possible) were purged out and removed with a pipette. A constant flow of 189  $\text{mLmin}^{-1}$  was fixed for nitrogen gas. A commercial HydroFlex RHE (Gaskatel) as RHE and a Pt coil counter electrode were used for the measurements, as shown in **Figure 2.3**.



**Figure 2.3:** Half cell gas diffusion electrode (GDE) test setup.

## 2.4 Synthesis

Synthesis of two diamines, ten neat polyimides, fifty sulphonated copolyimides with varying degree of sulphonation, eight protic ionic liquids and their composites with sulphonated copolyimides was carried out.

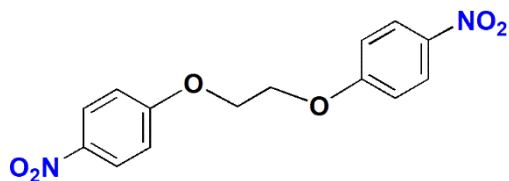
### 2.4.1 Synthesis of diamine monomers

The alkyl chains containing ether linked diamines and their precursor dinitro compounds were synthesized through Williamson ether synthesis and their characterization was carried out as follows;<sup>133</sup>

#### 2.4.1.1 General method for the synthesis of dinitro compounds

4-Nitrophenol (36 mmol) was added in a two necked round bottom flask having a mixture of 36 mmol of  $K_2CO_3$  in 50 mL of DMF under nitrogen atmosphere. The mixture was refluxed for two hours followed by the addition of 18 mmol of dibromo alkane and refluxed further for five hours as described in **scheme 3.1**. Reaction completion was monitored through TLC using solvent system; *n*-hexane: ethyl acetate (1:1). After completion, solution was poured into ice-cooled water and neutralization was done using HCl solution. Precipitates were filtered out and dried.

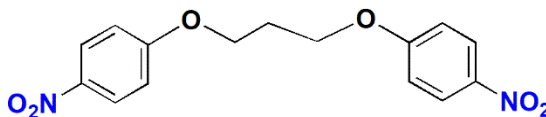
#### 2.4.1.1.1 Synthesis of 1,2-bis(4-nitrophenoxy)ethane (DN2)



1,2-bis(4-nitrophenoxy)ethane (DN2)

To synthesize DN2, 4-nitrophenol 35.97 mmol (5 g) was added to a solution of 17.81 mmol (3.384 g) 1,2-dibromo ethane along with potassium carbonate 35.97 mmol (5 g) in 50 mL of *N,N*-dimethylformamide (DMF). Pale yellow colored precipitates were obtained.  $R_f = 0.69$  (*n*-hexane: ethyl acetate, 1:1) solvent system, Yield: 80%, melting point: 148-149 °C (literature.148-149 °C).

#### 2.4.1.1.2 Synthesis of 1,2-bis(4-nitrophenoxy)propane (DN3)



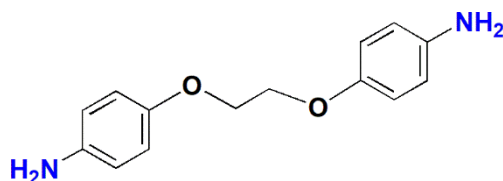
1,2-bis(4-nitrophenoxy)propane (DN3)

For the synthesis of DN3, 4-nitrophenol 35.97 mmol (5 g) was added to a solution of 17.79 mmol (3.63 g) of 1,3-dibromo propane along with potassium carbonate 35.97 mmol (5 g) in 50 mL of dimethylformamide (DMF). The off-white solid product was filtered off and washed twice with distilled water.  $R_f$  value = 0.52 using (*n*-hexane: ethyl acetate, 1:1) solvent system, Yield: 80%, melting point: 79-81 °C (literature 78 °C).

#### 2.4.1.2 General method for the reduction of dinitro compounds

In a 250 mL round bottom flask, 6.57 mmol (2 g) of dinitro compound and 0.2 g of palladium charcoal were refluxed in 60 mL of ethanol for one hour. To the reaction mixture, 7 mL of hydrazine hydrate was added and refluxed for 24 hours. The progress of reaction was checked through TLC using solvent system (*n*-hexane : ethylacetate 1:1). After completion of reaction, the boiling suspension was filtered. Precipitates were formed on the addition of ice-cooled water in the filtrate. Shiny white crystals of diamine were filtered, dried and stored in a desiccator.

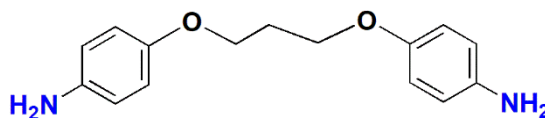
#### 2.4.1.2.1 Synthesis of 4-(2-(4-aminophenoxy)ethoxy)benzenamine (A2)



4-(2-(4-aminophenoxy)ethoxy)benzenamine (A2)

For the reduction of DN2 into 4-(2-(4-aminophenoxy)ethoxy)benzenamine (A2), 6.6 mmol (2.2 g) of 1,2-bis(4-nitrophenoxy)ethane (DN2), 0.2 g of activated charcoal and 7 mL of hydrazine hydrate was added and refluxed in 60 mL of ethanol for 24 hours. White crystalline solid was obtained.  $R_f$  value = 0.35 using (n-hexane: ethyl acetate, 1:1) solvent system, Yield: 86%, melting point: 174-176 °C (literature: 176 °C).

#### 2.4.1.2.2 Synthesis of 4-(3-(4-aminophenoxy)propoxy)benzenamine (A3)



4-(3-(4-aminophenoxy)propoxy)benzenamine (A3)

For the reduction of DN3 into 4-(3-(4-aminophenoxy)propoxy)benzenamine (A3), 6.2 mmol (2 g) of 1,3-bis(4-nitrophenoxy)propane (DN3), 0.2 g of activated charcoal and 7 mL of hydrazine hydrate was added and refluxed in 60 mL of ethanol for 24 hours. Silver white crystals were obtained.  $R_f$  value= 0.30 using (n-hexane: ethyl acetate, 1:1) solvent system, Yield: 73%, melting point: 98-100 °C (literature: 98 °C).

### 2.4.2 General procedure for the synthesis of polyimides

The polyimides were synthesized by the conventional two-step procedure via polyamic acid precursors, followed by thermal curing at elevated temperatures.<sup>134</sup> The two synthesized and three commercial diamines were reacted with two dianhydrides 6FDA and ODPA separately to synthesize two different series of polyimides based on two dianhydrides respectively. Diamine (1 mmol) was dissolved in *m*-cresol (2 mL) under anhydrous conditions in a sealed glove box. Dianhydride in stoichiometric amount (1 mmol) was added, after complete dissolution of diamine, into the diamine solution. The solution was kept under anhydrous conditions and stirred for 8 hours. As the polymerization

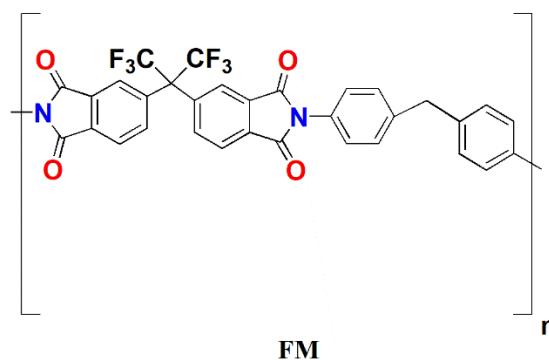
reaction started, the reaction mixture became viscous therefore some amount of *m*-cresol was added to facilitate stirring of the reaction mixture. 15 wt% solid content was maintained for polymer solution. After 18 hours stirring, very viscous polyamic acid (PAA) solution was obtained which was then heated for 12 hours at 80 °C to get PAA films. These films were subsequently heated at 100 and 150 °C and imidized at 180, 200, 250 and 300 °C each for one hour resulting in the conversion of polyamic acid films into polyimide films (as shown in scheme 1.2).

For the sake of simplicity of codes, the anhydrides 6FDA and ODPA will be abbreviated as [F] and [O] whereas diamines ODA and MDA as [A] and [M] respectively, in the following two chapters.

#### 2.4.2.1 Synthesis of neat polyimides from 4, 4'-(hexafluoroisopropylidene)diphthalic anhydride [F]

The synthesis and characterization of five neat polyimides derived by reacting 6FDA with five diamines; methylenedianiline [M], 4, 4'-oxydianiline [A], 4-(2-(4-aminophenoxy)ethoxy)benzenamine (A2), 4-(3-(4-aminophenoxy)propoxy)benzenamine (A3), 4,4'-(4,4'-Isopropylidenediphenyl-1,1'-diylldioxy)dianiline [I] is discussed below.

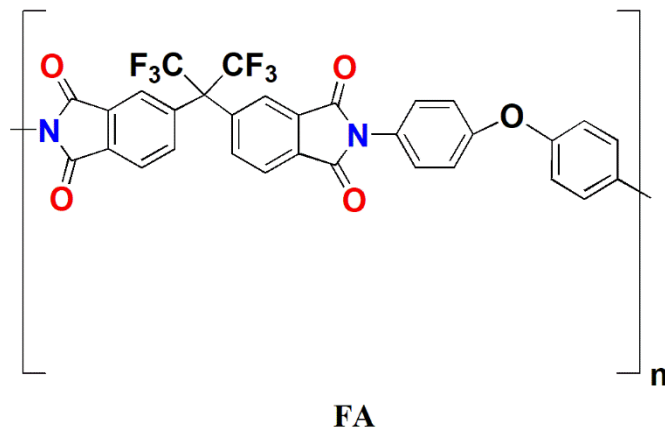
##### 2.4.2.1.1 Synthesis of neat polyimide FM



The preparation of polyimide FM was done by the solution polymerization reaction of methylene dianiline (M) with 6FDA. 1 mmol (0.448 g) of 6FDA was added in a 1 mmol (0.204 g) continuously stirred solution of M in 4 mL *m*-cresol. Polymerization reaction and the thermal imidization were done as explained in general procedure. FTIR: ( $\bar{\nu}/\text{cm}^{-1}$ ) 3052 (aryl H, stretching), 1782 (C=O asymmetric stretch, imide), 1710 (C=O symmetric stretch,

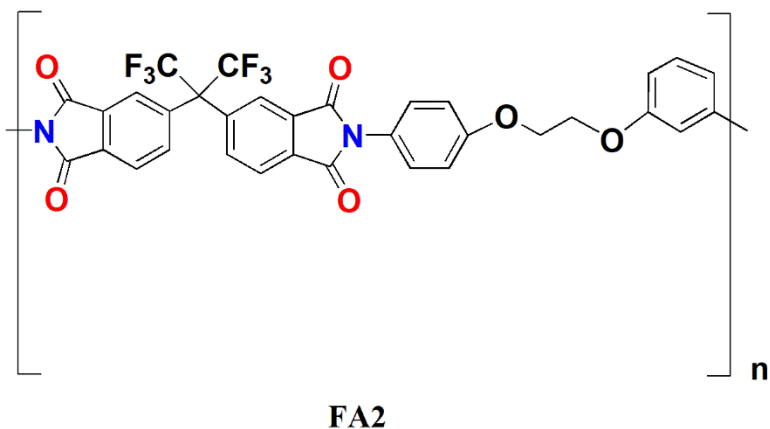
imide), 1382 (C-N stretching, imide), 1150 (C-F stretch, 6FDA) and 717 (C=O bending, imide).

#### 2.4.2.1.2 Synthesis of neat polyimide FA



The preparation of FA polyimide was carried out using the solution polymerization reaction of oxydianiline (A) with 6FDA. 1 mmol (0.448 g) of 6FDA was added in 1 mmol (0.206 g) solution of A dissolved in 4 mL *m*-cresol under continuous stirring. The above explained methodology was used to carry out polymerization reaction and the thermal imidization of FA. FTIR: ( $\bar{\nu}/\text{cm}^{-1}$ ) 3058 (aryl H, stretching), 1780 (C=O asymmetric stretch, imide), 1710 (C=O symmetric stretch, imide), 1380 (C-N stretching, imide), 1148 (C-F stretch, 6FDA) and 717 (C=O bending, imide).

#### 2.4.2.1.3 Synthesis of neat polyimide FA2

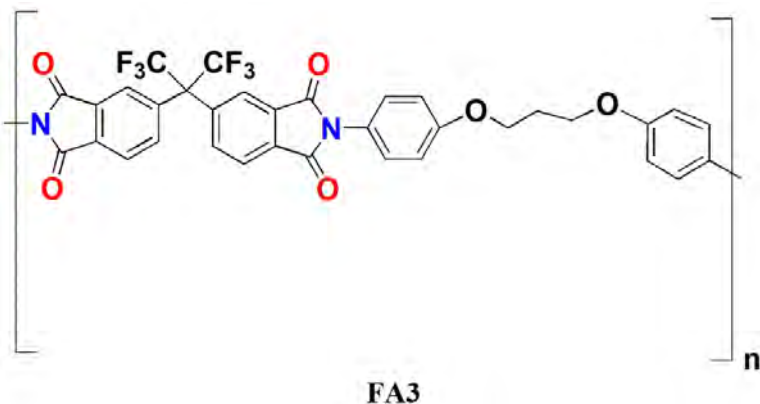


The preparation of FA2 polyimide was achieved using the solution polymerization reaction of synthesized diamine (A2) with 6FDA. 1 mmol (0.448 g) of 6FDA was added



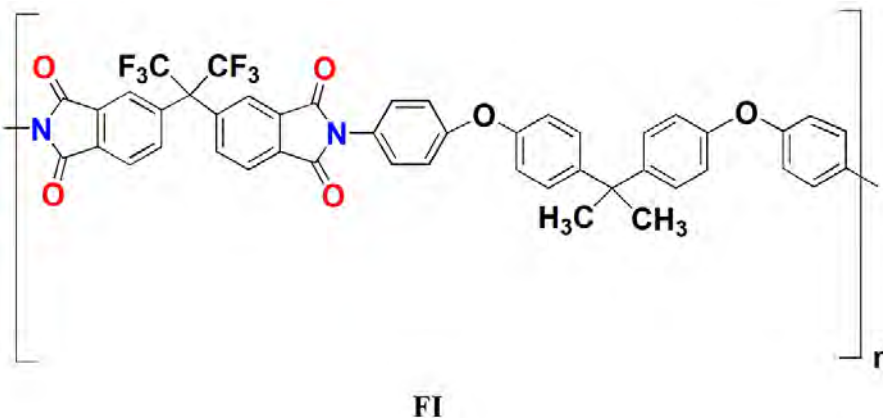
in 1 mmol (0.252 g) solution of A2 dissolved in 4 mL *m*-cresol under continuous stirring. The above explained methodology was used to carry out the polymerization reaction and the thermal imidization process. FTIR: ( $\bar{\nu}/\text{cm}^{-1}$ ) 3042 (aryl H, stretching), 1780 (C=O asymmetric stretch, imide), 1712 (C=O symmetric stretch, imide), 1383 (C-N stretching, imide), 1150 (C-F stretch, 6FDA) and 715 (C=O bending, imide).

#### 2.4.2.1.4 Synthesis of neat polyimide FA3



The FA3 polyimide was prepared using solution polymerization procedure by reacting synthesized diamine (A3) with 6FDA. 1 mmol (0.448 g) of 6FDA was added in 1 mmol (0.265 g) solution of A3 dissolved in 4 mL *m*-cresol under continuous stirring. The above explained methodology was used to carry out the polymerization reaction and the thermal imidization process. FTIR: ( $\bar{\nu}/\text{cm}^{-1}$ ) 3048 (aryl H, stretching), 1780 (C=O asymmetric stretch, imide), 1712 (C=O symmetric stretch, imide), 1382 (C-N stretching, imide), 1150 (C-F stretch, 6FDA) and 717 (C=O bending, imide).

#### 2.4.2.1.5 Synthesis of neat polyimide FI

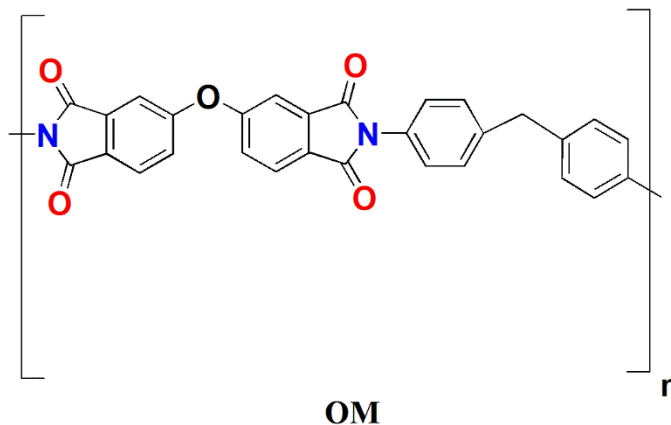


The preparation of polyimide FI was done by the solution polymerization reaction of 4,4'-(4,4'-isopropylidenediphenyl-1,1'-diyldioxy)dianiline (I) with 6FDA. The dianhydride 6FDA, 1 mmol (0.448 g) was added in 1 mmol (0.423 g) solution of I dissolved in 4 mL *m*-cresol under continuous stirring. The above explained methodology was used to carry out the polymerization reaction and the thermal imidization process. FTIR: ( $\bar{\nu}/\text{cm}^{-1}$ ) 3078 (aryl H, stretching), 1782 (C=O asymmetric stretch, imide), 1710 (C=O symmetric stretch, imide), 1382 (C-N stretching, imide), 1148 (C-F stretch, 6FDA) and 714 (C=O bending, imide).

#### 2.4.2.2 Synthesis of neat polyimides from oxydiphthalic anhydride [O]

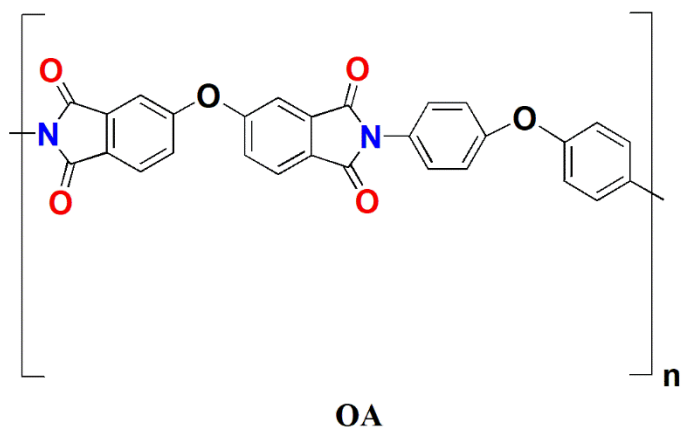
The synthesis and characterization of polyimides derived from ODPA with five diamines; methylenedianiline [M], 4'-oxydianiline [A], 4-(2-(4-aminophenoxy)ethoxy)benzenamine (A2), 4-(3-(4-aminophenoxy)propoxy)benzenamine (A3) and 4,4'-(4,4'-Isopropylidenediphenyl-1,1'-diyldioxy)dianiline [I] is discussed below.

##### 2.4.2.2.1 Synthesis of neat polyimide OM



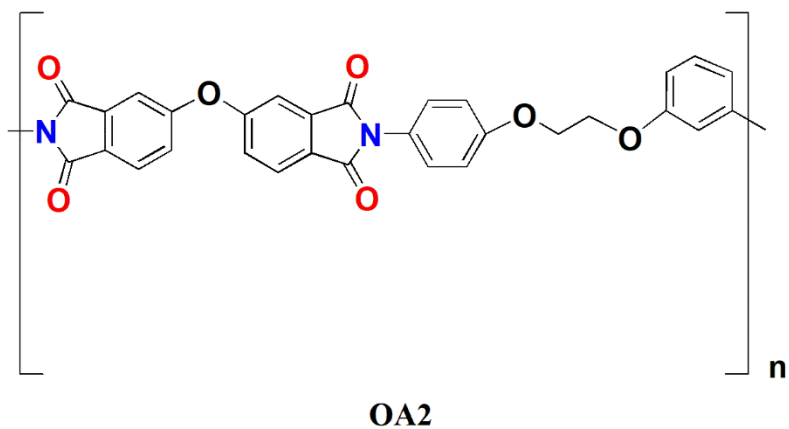
The preparation of polyimide OM was done by the solution polymerization reaction of methylene dianiline (M) with ODPA. 1 mmol (0.313 g) of ODPA was added in 1 mmol (0.204 g) solution of M dissolved in 4 mL *m*-cresol under continuous stirring. The above explained methodology was used to carry out the polymerization reaction and the thermal imidization process. FTIR: ( $\bar{\nu}/\text{cm}^{-1}$ ) 3042 (aryl H, stretching), 1776 (C=O asymmetric stretch, imide), 1716 (C=O symmetric stretching, imide), 1373 (C-N stretching, imide), 1170 (C-O stretching, ODPA) and 740 (C=O bend, imide).

#### 2.4.2.2.2 Synthesis of neat polyimide OA



The OA polyimide was prepared using solution polymerization procedure by reacting oxydianiline (A) with ODPA. 1 mmol (0.313 g) of ODPA was added in 1 mmol (0.206 g) solution of A dissolved in 4 mL *m*-cresol under continuous stirring. The above explained methodology was used to carry out the polymerization reaction and the thermal imidization process. FTIR: ( $\bar{\nu}/\text{cm}^{-1}$ ) 3060 (aryl H, stretching), 1774 (C=O asymmetric stretch, imide), 1715 (C=O symmetric stretching, imide), 1370 (C-N stretching, imide), 1165 (C-O stretching, ODPA) and 740 (C=O bend, imide).

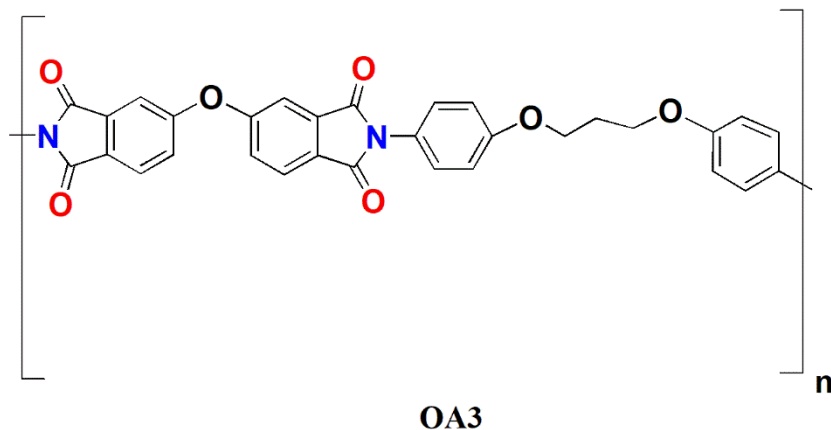
#### 2.4.2.2.3 Synthesis of neat polyimide OA2



The preparation of polyimide OA2 was done by the solution polymerization reaction of synthesized diamine (A2) with ODPA. 1 mmol (0.313 g) of ODPA was added in 1 mmol (0.252 g) solution of A2 dissolved in 4 mL *m*-cresol under continuous stirring. The above explained methodology was used to carry out the polymerization reaction and the thermal imidization process. FTIR: ( $\bar{\nu}/\text{cm}^{-1}$ ) 3048 (aryl H, stretching), 1774 (C=O

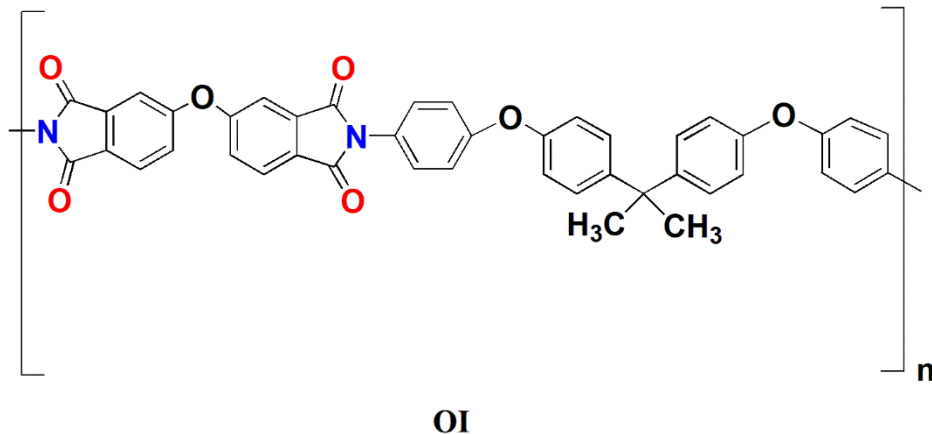
asymmetric stretch, imide), 1715 (C=O symmetric stretch, imide), 1370 (C-N stretching, imide), 1160 (C-O stretching, ODPA) and 740 (C=O bend, imide).

#### 2.4.2.2.4 Synthesis of neat polyimide OA3



The polyimide OA3 was prepared using the solution polymerization procedure by reacting synthesized diamine (A3) with ODPA. 1 mmol (0.313 g) of ODPA was added in 1 mmol (0.265 g) solution of A3 dissolved in 4 mL *m*-cresol under continuous stirring. The above explained methodology was used to carry out the polymerization reaction and the thermal imidization process. FTIR: ( $\bar{\nu}/\text{cm}^{-1}$ ) 3052 (aryl H, stretching), 1776 (C=O asymmetric stretch, imide), 1715 (C=O symmetric stretch, imide), 1368 (C-N stretching, imide), 1160 (C-O stretching, ODPA) and 740 (C=O bend, imide).

#### 2.4.2.2.5 Synthesis of neat polyimide OI



Preparation of polyimide OI was achieved using the solution polymerization reaction of 4,4'-(4,4'-isopropylidenediphenyl-1,1'-diyldioxy)dianiline (I) with ODPA. 1 mmol

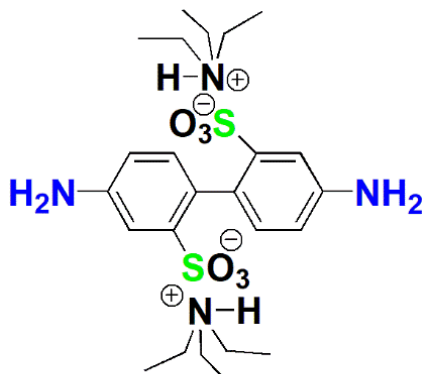
(0.313 g) ODPa was added in 1 mmol (0.423 g) solution of I dissolved in 4 mL *m*-cresol under continuous stirring. The above explained methodology was used to carry out the polymerization reaction and the thermal imidization process. FTIR: ( $\bar{\nu}/\text{cm}^{-1}$ ) 3082 (aryl H, stretching), 1774 (C=O asymmetric stretch, imide), 1718 (C=O symmetric stretch, imide), 1374 (C-N stretching, imide), 1168 (C-O stretching, ODPa) and 740 (C=O bend, imide).

### 2.4.3 General procedure for the synthesis of sulphonated copolyimides (SPIs)

The block sulphonated copolyimides were prepared by the standard two-step thermal imidization procedure via polyamic acid precursor as described above.<sup>135</sup> The two dianhydrides 6FDA and ODPa were reacted with sulphonated diamine in its triethylammonium sulfate form (BDSA.TEA) (cf: 2.4.3.1) and the other unsulphonated diamine monomer to synthesize two different series of sulphonated copolyimides. Firstly, the anhydride-terminated SPI oligomers were prepared from BDSA.TEA dissolved in *m*-cresol and stoichiometric amount of dianhydride monomer under anhydrous conditions in a sealed glove box. The reaction mixture was kept under anhydrous conditions with stirring for 8 hours at room temperature (30 °C). As the polymerization reaction started, the reaction mixture became viscous. The unsulphonated diamine was then added into the oligomer solution alongwith some *m*-cresol to facilitate stirring. The solid content of polymer solution was kept at 15 wt %. After 18 hours stirring, very viscous polyamic acid (PAA) solution was obtained which was heated in a petridish for 12 hours at 80 °C to get PAA films. These films were subsequently heated at 100, 150 °C and imidized at 180, 200, 250 and 300 °C each for one hour resulting in block sulphonated copolyimide films (as shown in scheme 1.4).

For both (6FDA and ODPa dianhydride based) series of copolyimides, initial synthesis of a sulphonated copolyimide included 90:10 mole ratio with respect to unsulphonated:sulphonated diamine. To evaluate the impact of varying degree of sulfonation, four additional copolyimides compositions were synthesized using dianhydride/unsulphonated diamine/sulphonated diamine, where the sulfonated diamine triethylammonium salt (BDSA.TEA) content was raised to 20, 30, 40 and 50 mole % respectively. The same two step thermal imidization route was followed for all the molar ratios of copolyimide synthesis.

### 2.4.3.1 Synthesis of triethyl ammonium salt (B) of benzidine-2, 2'-disulfonic acid (BDSA)



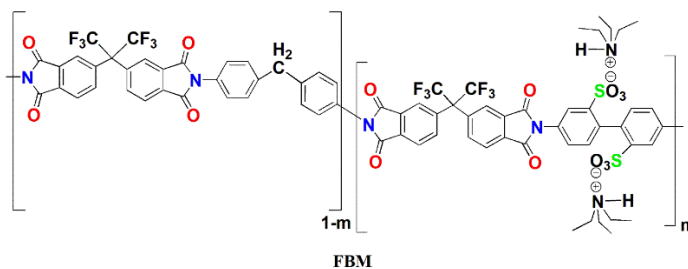
**BDSA.TEA (B)**

To synthesize the BDSA.TEA salt, the diamine BDSA (2.0 mmol) in 50 mL ethanol was added to a 3-neck round bottom flask equipped with magnetic stirrer and N<sub>2</sub> inlet. The mixture was stirred at 80 °C under N<sub>2</sub> flow, triethylamine (4.0 mmol) was added dropwise to the boiling mixture and heated until BDSA was completely dissolved. The boiling solution was hot filtered and BDSA was obtained in its triethylammonium sulphate form (BDSA.TEA). The synthesized BDSA.TEA was recrystallized from ethanol and dried under vacuum for three days. <sup>136</sup> FTIR: ( $\bar{\nu}/\text{cm}^{-1}$ ) 1084 (S=O asymmetric stretching, sulphonate), 1035 (S=O symmetric stretch, sulphonate), and 620 (C-S stretch, sulphonate).

### 2.4.3.2 Synthesis of SPIs from 4,4'-(hexafluoroisopropylidene)diphthalic anhydride [F]

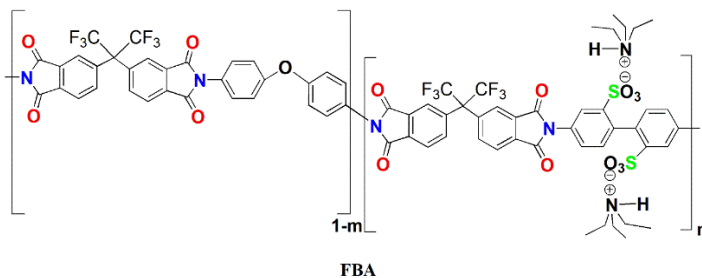
The synthesis and characterization of sulphonated copolyimides derived from 6FDA using BDSA.TEA as sulphonated diamine and five unsulphonated diamines; methylenedianiline [M], 4, 4'-oxydianiline [A], 4-(2-(4-aminophenoxy)ethoxy)benzenamine (A2), 4-(3-(4-aminophenoxy)propoxy)benzenamine (A3), 4,4'-(4,4'-Isopropylidenediphenyl-1,1'-diyldioxy)dianiline [I] in different compositions, is discussed in this section.

### 2.4.3.2.1 Synthesis of sulphonated copolyimides (FBM (10, 20, 30, 40, 50))



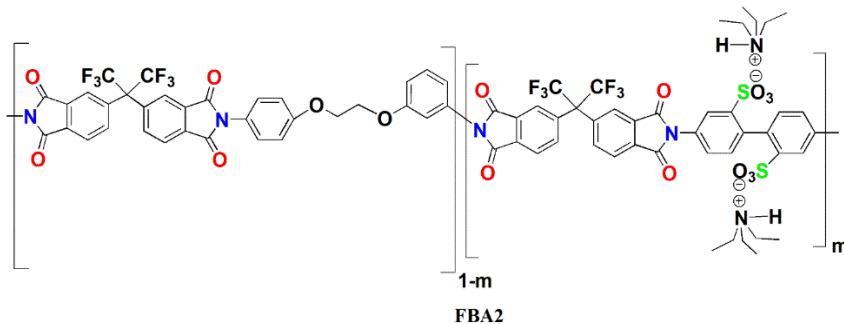
The solution polymerization was used for the synthesis of sulphonated copolyimides FBM (10, 20, 30, 40, 50) using 6FDA with sulphonated diamine BDSA.TEA and methylene dianiline (M). Firstly, five different compositions in mole % of BDSA.TEA [0.1 mmol (0.078 g), 0.2 mmol (0.156 g), 0.3 mmol (0.234 g), 0.4 mmol (0.311 g) and 0.5 mmol (0.389 g)] were dissolved in *m*-cresol (4 mL) one by one and stirred with a stoichiometric amount [1 mmol (0.448 g)] of dianhydride monomer separately for 8 hours at room temperature (30 °C), then the respective mole % of methylene dianiline (M) [0.5 mmol (0.10 g), 0.6 mmol (0.122 g), 0.7 mmol (0.143 g), 0.8 mmol (0.163 g) and 0.9 mmol (0.184 g)] were added into the oligomer solution of each mole % of BDSA.TEA along with some *m*-cresol to facilitate stirring of reaction mixture. The overall 1:1 stoichiometric ratio of dianhydride and diamines was maintained for each system. The above explained methodology was used to carry out the polymerization reaction and the thermal imidization process. FTIR: ( $\bar{\nu}/\text{cm}^{-1}$ ) 3088 (aryl H, stretching), 1782 (C=O asymmetric stretch, imide), 1710 (C=O symmetric stretch, imide), 1382 (C-N stretching, imide), 1150 (C-F stretching), 1084 (S=O asymmetric stretching, sulphonate), 1035 (S=O symmetric stretch, sulphonate), 717 (C=O bending, imide) and 620 (C-S stretch, sulphonate). (Annexure 3.1)

### 2.4.3.2.2 Synthesis of sulphonated copolyimides (FBA (10, 20, 30, 40, 50))



The solution polymerization was used for the synthesis of sulphonated copolyimides FBA (10-50) using 6FDA with sulphonated diamine BDSA.TEA and 4, 4'-oxydianiline (A). Firstly, five different mole % of BDSA.TEA [0.1 mmol (0.078 g), 0.2 mmol (0.156 g), 0.3 mmol (0.234 g), 0.4 mmol (0.311 g) and 0.5 mmol (0.389 g)] were dissolved in *m*-cresol (4 mL) one by one and stirred with a stoichiometric amount [1 mmol (0.448 g)] of dianhydride monomer separately for 8 hours at room temperature (30 °C), then the respective mole % of diamine (A) [0.5 mmol (0.10 g), 0.6 mmol (0.124 g), 0.7 mmol (0.144 g), 0.8 mmol (0.165 g) and 0.9 mmol (0.186 g)] were added into the oligomer solution of each mole % of BDSA.TEA alongwith some *m*-cresol to facilitate stirring of reaction mixture. The overall 1:1 stoichiometric ratio of dianhydride and diamines was maintained for each system. The above explained methodology was used to carry out the polymerization reaction and the thermal imidization process. FTIR: ( $\bar{\nu}/\text{cm}^{-1}$ ) 3065 (aryl H, stretching), 1780 (C=O asymmetric stretch, imide), 1710 (C=O symmetric stretch, imide), 1380 (C-N stretching, imide), 1148 (C-F stretching) 1083 (S=O asymmetric stretching, sulphonate), 1034 (S=O symmetric stretch, sulphonate), 717 (C=O bending, imide) and 620 (C-S stretch, sulphonate). (Annexure 3.2)

#### 2.4.3.2.3 Synthesis of sulphonated copolyimides (FBA2 (10, 20, 30, 40, 50))

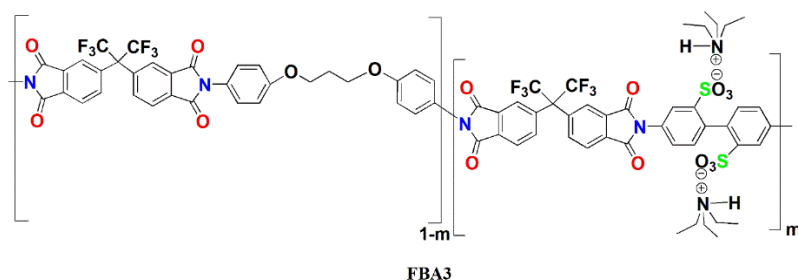


The solution polymerization was used for the synthesis of sulphonated copolyimides FBA2 (10-50) using 6FDA with sulphonated diamine BDSA.TEA and synthesized diamine (A2). Firstly, five different mole % of BDSA.TEA [0.1 mmol (0.078 g), 0.2 mmol (0.156 g), 0.3 mmol (0.234 g), 0.4 mmol (0.311 g) and 0.5 mmol (0.389 g)] were dissolved in *m*-cresol (4 mL) one by one and stirred with a stoichiometric amount [1 mmol (0.448 g)] of dianhydride monomer separately for 8 hours at room temperature (30 °C), then the respective mole % of diamine (A2) [0.5 mmol (0.126 g), 0.6 mmol (0.151 g),



0.7 mmol (0.176 g), 0.8 mmol (0.201 g) and 0.9 mmol (0.227 g)] were added into the oligomer solution of each mole % of BDSA.TEA alongwith some *m*-cresol to facilitate stirring of reaction mixture. The overall 1:1 stoichiometric ratio of dianhydride and diamines was maintained for each system. The above explained methodology was used to carry out the polymerization reaction and the thermal imidization process. FTIR: ( $\bar{\nu}/\text{cm}^{-1}$ ) 3078 (aryl H, stretching), 1780 (C=O asymmetric stretch, imide), 1712 (C=O symmetric stretch, imide), 1383 (C-N stretching, imide), 1150 (C-F stretching) and 1084 (S=O asymmetric stretching, sulphonate), 1035 (S=O symmetric stretch, sulphonate), 715 (C=O bending, imide) and 620 (C-S stretch, sulphonate). (Annexure 3.3)

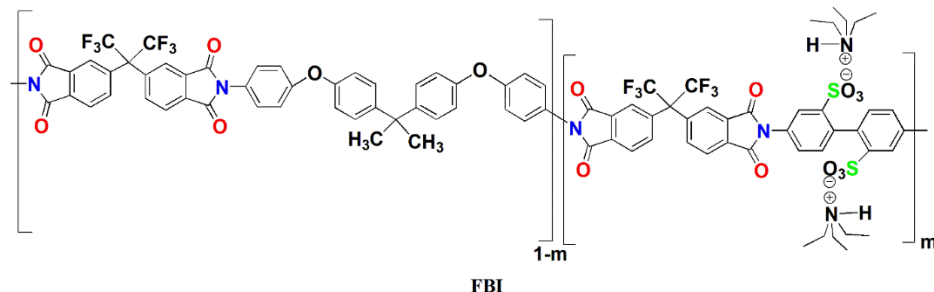
#### 2.4.3.2.4 Synthesis of sulphonated copolyimides (FBA3 (10, 20, 30, 40, 50))



The solution polymerization was used for the synthesis of sulphonated copolyimides FBA2 (10-50) using 6FDA with sulphonated diamine BDSA.TEA and synthesized diamine (A3). Firstly, five different mole % of BDSA.TEA [0.1 mmol (0.078 g), 0.2 mmol (0.156 g), 0.3 mmol (0.234 g), 0.4 mmol (0.311 g) and 0.5 mmol (0.389 g)] were dissolved in *m*-cresol (4 mL) one by one and stirred with a stoichiometric amount [1 mmol (0.448 g)] of dianhydride monomer separately for 8 hours at room temperature (30 °C), then the respective mole % of diamine (A3) [0.5 mmol (0.133 g), 0.6 mmol (0.160 g), 0.7 mmol (0.186 g), 0.8 mmol (0.213 g) and 0.9 mmol (0.239 g)] were added into the oligomer solution of each mole % of BDSA.TEA alongwith some *m*-cresol to facilitate stirring of reaction mixture. The overall 1:1 stoichiometric ratio of dianhydride and diamines was maintained for each system. The above explained methodology was used to carry out the polymerization reaction and the thermal imidization process. FTIR: ( $\bar{\nu}/\text{cm}^{-1}$ ) 3075 (aryl H, stretching), 1780 (C=O asymmetric stretch, imide), 1712 (C=O symmetric stretch, imide), 1382 (C-N stretching, imide), 1150 (C-F stretching), 1082 (S=O

asymmetric stretching, sulphonate), 1032 (S=O symmetric stretch, sulphonate), 717 (C=O bending, imide) and 620 (C-S stretch, sulphonate). (Annexure 3.4)

#### 2.4.3.2.5 Synthesis of sulphonated copolyimides (FBI (10, 20, 30, 40, 50))



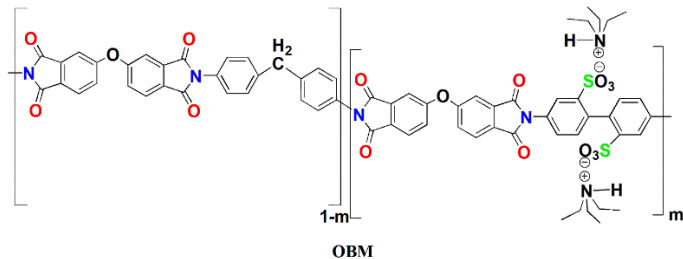
The solution polymerization was used for the synthesis of sulphonated copolyimides FBI (10-50) using 6FDA with sulphonated diamine BDSA.TEA and diamine 4,4'-(4,4'-isopropylidenediphenyl-1,1'-diylidioxy)dianiline (I). Firstly, five different mole % of BDSA.TEA [0.1 mmol (0.078 g), 0.2 mmol (0.156 g), 0.3 mmol (0.234 g), 0.4 mmol (0.311 g) and 0.5 mmol (0.389 g)] were dissolved in *m*-cresol (4 mL) one by one and stirred with a stoichiometric amount [1 mmol (0.448 g)] of dianhydride monomer separately for 8 hours at room temperature (30 °C), then the respective mole % of diamine (I) [0.5 mmol (0.212 g), 0.6 mmol (0.254 g), 0.7 mmol (0.296 g), 0.8 mmol (0.338 g) and 0.9 mmol (0.381 g)] were added into the oligomer solution of each mole % of BDSA.TEA along with some *m*-cresol to facilitate stirring of reaction mixture. The overall 1:1 stoichiometric ratio of dianhydride and diamines was maintained for each system. The above explained methodology was used to carry out the polymerization reaction and the thermal imidization process. FTIR: ( $\bar{\nu}/\text{cm}^{-1}$ ) 3086 (aryl H, stretching), 1782 (C=O asymmetric stretch, imide), 1710 (C=O symmetric stretch, imide), 1382 (C-N stretching, imide), 1148 (C-F stretching), 1084 (S=O asymmetric stretching, sulphonate), 1035 (S=O symmetric stretch, sulphonate), 714 (C=O bending, imide) and 620 (C-S stretch, sulphonate). (Annexure 3.5)

#### 2.4.3.3 Synthesis of SPIs from oxydipthalic anhydride [O]

The synthesis and characterization of sulphonated copolyimides derived from ODPDA using BDSA.TEA as sulphonated diamine and five unsulphonated diamines; methylenedianiline [M], 4'-oxydianiline [A], 4-(2-(4-aminophenoxy)ethoxy)benzenamine (A2), 4-(3-(4-aminophenoxy)propoxy)benzenamine

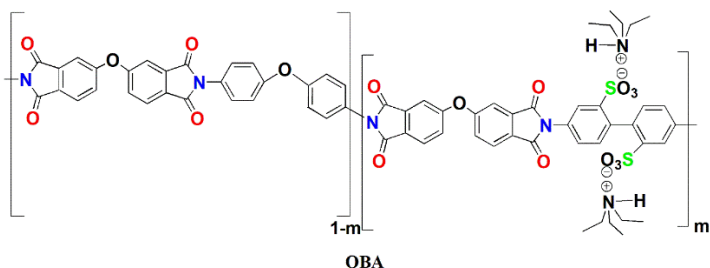
(A3), 4,4'-(4,4'-Isopropylidenediphenyl-1,1'-diyl-dioxy)dianiline [I] in different compositions is discussed in this section.

#### 2.4.3.3.1 Synthesis of sulphonated copolyimides (OBM (10, 20, 30, 40, 50))



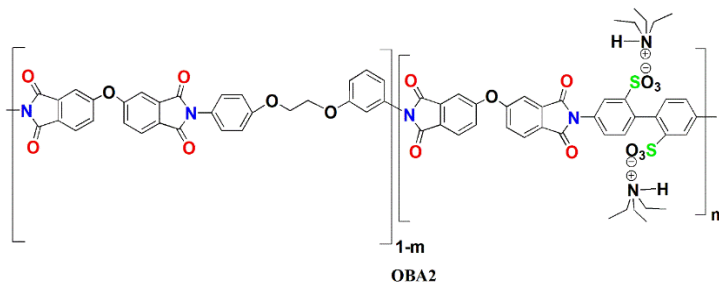
The solution polymerization was used for the synthesis of sulphonated copolyimides OBM (10-50) using ODPA with sulphonated diamine BDSA.TEA and diamine methylene dianiline (M). Firstly, five different mole % of BDSA.TEA [0.1 mmol (0.078 g), 0.2 mmol (0.156 g), 0.3 mmol (0.234 g), 0.4 mmol (0.311 g) and 0.5 mmol (0.389 g)] were dissolved in *m*-cresol (4 mL) one by one and stirred with a stoichiometric amount [1 mmol (0.313 g)] of dianhydride monomer separately for 8 hours at room temperature (30 °C), then the respective mole % of methylene dianiline (M) [0.5 mmol (0.10 g), 0.6 mmol (0.122 g), 0.7 mmol (0.143 g), 0.8 mmol (0.163 g) and 0.9 mmol (0.184 g)] were added into the oligomer solution of each mole % of BDSA.TEA along with some *m*-cresol to facilitate stirring of reaction mixture. The overall 1:1 stoichiometric ratio of dianhydride and diamines was maintained for each system. The above explained methodology was used to carry out the polymerization reaction and the thermal imidization process. FTIR: ( $\bar{\nu}/\text{cm}^{-1}$ ) 3078 (aryl H, stretching), 1776 (C=O asymmetric stretch, imide), 1716 (C=O symmetric stretch, imide), 1373 (C-N stretching, imide), 1170 (C-O stretching), 1087 (S=O asymmetric stretching, sulphonate), 1033 (S=O symmetric stretch, sulphonate), 740 (C=O bending, imide) and 620 (C-S stretch, sulphonate). (Annexure 4.1)

#### 2.4.3.3.2 Synthesis of sulphonated copolyimides (OBA (10, 20, 30, 40, 50))



The solution polymerization was used for the synthesis of sulphonated copolyimides OBA (10-50) using ODPa with sulphonated diamine BDSA.TEA and diamine 4, 4'-oxydianiline (A). Firstly, five different mole % of BDSA.TEA [0.1 mmol (0.078 g), 0.2 mmol (0.156 g), 0.3 mmol (0.234 g), 0.4 mmol (0.311 g) and 0.5 mmol (0.389 g)] were dissolved in *m*-cresol (4 mL) one by one and stirred with a stoichiometric amount [1 mmol (0.313 g)] of dianhydride monomer separately for 8 hours at room temperature (30 °C), then the respective mole % of diamine (A) [0.5 mmol (0.10 g), 0.6 mmol (0.124 g), 0.7 mmol (0.144 g), 0.8 mmol (0.165 g) and 0.9 mmol (0.186 g)] were added into the oligomer solution of each mole % of BDSA.TEA along with some *m*-cresol to facilitate stirring of reaction mixture. The overall 1:1 stoichiometric ratio of dianhydride and diamines was maintained for each system. The above explained methodology was used to carry out the polymerization reaction and the thermal imidization process. FTIR: ( $\bar{\nu}/\text{cm}^{-1}$ ) 3064 (aryl H, stretching), 1774 (C=O asymmetric stretch, imide), 1715 (C=O symmetric stretch, imide), 1370 (C-N stretching, imide), 1165 (C-O stretching), 1086 (S=O asymmetric stretching, sulphonate), 1030 (S=O symmetric stretch, sulphonate), 740 (C=O bending, imide) and 620 (C-S stretch, sulphonate). (Annexure 4.2)

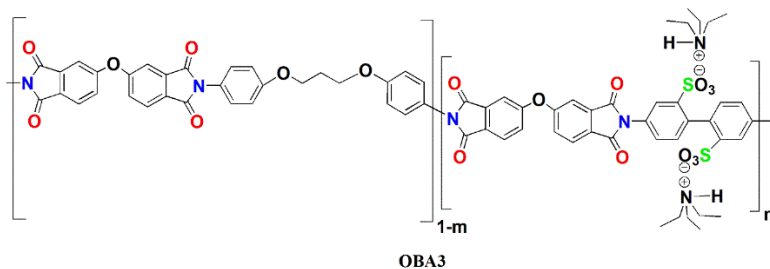
#### 2.4.3.3.3 Synthesis of sulphonated copolyimides (OBA2 (10, 20, 30,40, 50))



The solution polymerization was used for the synthesis of sulphonated copolyimides OBA2 (10-50) using ODPa with sulphonated diamine BDSA.TEA and synthesized diamine (A2). Firstly, five different mole % of BDSA.TEA [0.1 mmol (0.078 g), 0.2 mmol (0.156 g), 0.3 mmol (0.234 g), 0.4 mmol (0.311 g) and 0.5 mmol (0.389 g)] were dissolved in *m*-cresol (4 mL) one by one and stirred with a stoichiometric amount [1 mmol (0.313 g)] of dianhydride monomer separately for 8 hours at room temperature (30 °C), then the respective mole % of diamine (A2) [0.5 mmol (0.126 g), 0.6 mmol (0.151 g), 0.7 mmol (0.176 g), 0.8 mmol (0.201 g) and 0.9 mmol (0.227 g)] were added into the

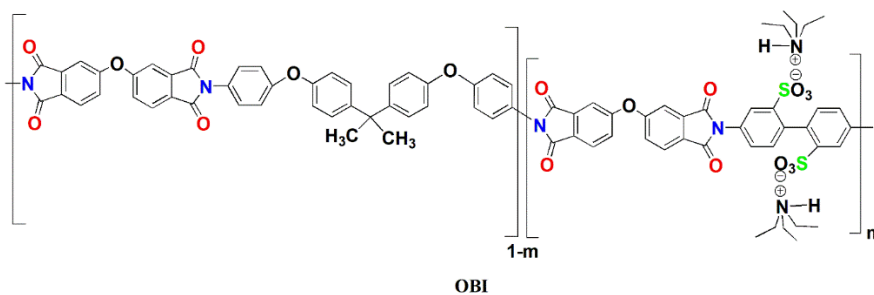
oligomer solution of each mole % of BDSA.TEA alongwith some *m*-cresol to facilitate stirring of reaction mixture. The overall 1:1 stoichiometric ratio of dianhydride and diamines was maintained for each system. The above explained methodology was used to carry out the polymerization reaction and the thermal imidization process. FTIR: ( $\bar{\nu}/\text{cm}^{-1}$ ) 3072 (aryl H, stretching), 1774 (C=O asymmetric stretch, imide), 1715 (C=O symmetric stretch, imide), 1370 (C-N stretching, imide), 1160 (C-O stretching), 1086 (S=O asymmetric stretching, sulphonate), 1030 (S=O symmetric stretch, sulphonate), 738 (C=O bending, imide) and 620 (C-S stretch, sulphonate). (Annexure 4.3)

#### 2.4.3.3.4 Synthesis of sulphonated copolyimides (OBA3 (10, 20, 30, 40, 50))



The solution polymerization was used for the synthesis of sulphonated copolyimides OBA3 (10-50) using ODPA with sulphonated diamine BDSA.TEA and synthesized diamine (A3). Firstly, five different mole % of BDSA.TEA [0.1 mmol (0.078 g), 0.2 mmol (0.156 g), 0.3 mmol (0.234 g), 0.4 mmol (0.311 g) and 0.5 mmol (0.389 g)] were dissolved in *m*-cresol (4 mL) one by one and stirred with a stoichiometric amount [1 mmol (0.313 g)] of dianhydride monomer separately for 8 hours at room temperature (30 °C), then the respective mole % of diamine (A3) [0.5 mmol (0.133 g), 0.6 mmol (0.160 g), 0.7 mmol (0.186 g), 0.8 mmol (0.213 g) and 0.9 mmol (0.239 g)] were added into the oligomer solution of each mole % of BDSA.TEA alongwith some *m*-cresol to facilitate stirring of reaction mixture. The overall 1:1 stoichiometric ratio of dianhydride and diamines was maintained for each system. The above explained methodology was used to carry out the polymerization reaction and the thermal imidization process. FTIR: ( $\bar{\nu}/\text{cm}^{-1}$ ) 3079 (aryl H, stretching), 1776 (C=O asymmetric stretch, imide), 1715 (C=O symmetric stretch, imide), 1368 (C-N stretching, imide), 1160 (C-O stretching), 1087 (S=O asymmetric stretching, sulphonate), 1033 (S=O symmetric stretch, sulphonate), 740 (C=O bending, imide) and 620 (C-S stretch, sulphonate). (Annexure 4.4)

### 2.4.3.3.5 Synthesis of sulphonated copolyimides (OBI (10, 20, 30, 40, 50))



The solution polymerization was used for the synthesis of sulphonated copolyimides OBI (10-50) using ODPA with sulphonated diamine BDSA.TEA and diamine 4,4'-(4,4'-isopropylidenediphenyl-1,1'-diyl dioxy)dianiline (I). Firstly, five different mole % of BDSA.TEA [0.1 mmol (0.078 g), 0.2 mmol (0.156 g), 0.3 mmol (0.234 g), 0.4 mmol (0.311 g) and 0.5 mmol (0.389 g)] were dissolved in *m*-cresol (4 mL) one by one and stirred with a stoichiometric amount [1 mmol (0.313 g)] of dianhydride monomer separately for 8 hours at room temperature (30 °C), then the respective mole % of diamine (I) [0.5 mmol (0.212 g), 0.6 mmol (0.254 g), 0.7 mmol (0.296 g), 0.8 mmol (0.338 g) and 0.9 mmol (0.381 g)] were added into the oligomer solution of each mole % of BDSA.TEA along with some *m*-cresol to facilitate stirring of reaction mixture. The overall 1:1 stoichiometric ratio of dianhydride and diamines was maintained for each system. The above explained methodology was used to carry out the polymerization reaction and the thermal imidization process. FTIR: ( $\bar{\nu}/\text{cm}^{-1}$ ) 3085 (aryl H, stretching), 1774 (C=O asymmetric stretch, imide), 1718 (C=O symmetric stretch, imide), 1374 (C-N stretching, imide), 1168 (C-O stretching), 1086 (S=O asymmetric stretching, sulphonate), 1032 (S=O symmetric stretch, sulphonate), 740 (C=O bending, imide) and 620 (C-S stretch, sulphonate). (Annexure 4.5)

### 2.4.4 General procedure for the synthesis of protic ionic liquids (PILs)

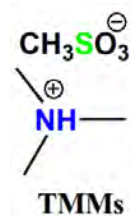
PILs were prepared according to the methods reported in the literature.<sup>137</sup> A general procedure for the synthesis of PILs is shown in **Scheme 3.5**. The synthesis was carried out under nitrogen atmosphere using two-necked round bottom flask equipped with dropping funnel and magnetic stirrer bar. Tertiary amine (0.05 mol) was diluted in 50 mL diethyl ether. Since the reaction for the formation of PILs was highly exothermic, the reaction flask was immersed in ice bath and the dropwise addition of sulphonic acid (0.05 mol) to triethyl amine was carried out through dropping funnel. Then the mixture was stirred for four hours

at  $\sim 0\text{ }^{\circ}\text{C}$ . The reaction mixture was concentrated by the evaporation of diethyl ether on rotary evaporator. The protic ionic liquids were obtained as light yellow viscous liquids.

#### 2.4.4.1 Synthesis of protic ionic liquids (PILs) using methane sulphonic acid (MsOH)

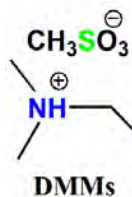
Four different protic ionic liquids were prepared by reacting methane sulphonic acid (MsOH) with four different tertiary amines; trimethyl amine (TMA), dimethylethyl amine (DMEA), diethylmethyl amine (DEMA) and triethyl amine (TEA).

##### 2.4.4.1.1 Synthesis of trimethylammonium methanesulphonate (TMMs)



TMMs was synthesized by stirring diluted triethylamine (0.05 mol) with dropwise addition of methane sulphonic acid (0.05 mol) in diethyl ether for four hours at  $\sim 0\text{ }^{\circ}\text{C}$ . Light yellow viscous liquid.

##### 2.4.4.1.2 Synthesis of dimethylethylammonium methanesulphonate (DMMs)



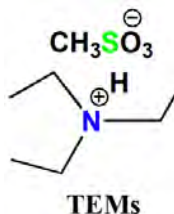
DMMs was synthesized by stirring diluted dimethylethylamine (0.05 mol) with dropwise addition of methane sulphonic acid (0.05 mol) in diethyl ether for four hours at  $\sim 0\text{ }^{\circ}\text{C}$ . Light yellow viscous liquid.

##### 2.4.4.1.3 Synthesis of diethylmethylammonium methanesulphonate (DEMs)



DEMs was synthesized by stirring diluted diethylmethylamine (0.05 mol) with dropwise addition of methane sulphonic acid (0.05 mol) in diethyl ether for four hours at  $\sim 0^\circ\text{C}$ . Light yellow viscous liquid.

#### 2.4.4.1.4 Synthesis of triethylammonium methanesulphonate (TEMs)

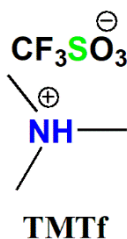


TEMs was synthesized by stirring diluted triethylamine (0.05 mol) with dropwise addition of methane sulphonic acid (0.05 mol) in diethyl ether for four hours at  $\sim 0^\circ\text{C}$ . Light yellow viscous liquid. (Annexure 10.1)

#### 2.4.4.2 Synthesis of protic ionic liquids (PILs) using trifluoromethane sulphonic acid (TfOH)

Four different protic ionic liquids were prepared by reacting trifluoromethanesulphonic acid (TfOH) with four different tertiary amines; trimethyl amine (TMA), dimethylethyl amine (DMEA), diethylmethyl amine (DEMA) and triethyl amine (TEA).

##### 2.4.4.2.1 Synthesis of trimethylammonium trifluoromethanesulphonate (TMTf)



TMTf was synthesized by stirring diluted triethylamine (0.05 mol) with dropwise addition of trifluoromethane sulphonic acid (0.05 mol) in diethyl ether for four hours at  $\sim 0^\circ\text{C}$ . Light yellow viscous liquid.

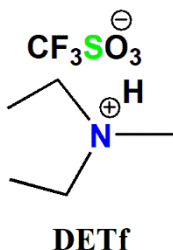


#### 2.4.4.2 Synthesis of dimethylethylammonium trifluoromethanesulphonate (DMTf)



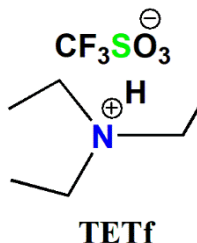
DMTf was synthesized by stirring diluted dimethylethylamine (0.05 mol) with dropwise addition of trifluoromethane sulphonic acid (0.05 mol) in diethyl ether for four hours at  $\sim 0^\circ\text{C}$ . Light yellow viscous liquid.

#### 2.4.4.2.3 Synthesis of diethylmethylammonium trifluoromethanesulphonate (DETf)



DETf was synthesized by stirring diluted diethylmethylamine (0.05 mol) with dropwise addition of trifluoromethane sulphonic acid (0.05 mol) in diethyl ether for four hours at  $\sim 0^\circ\text{C}$ . Light yellow viscous liquid.

#### 2.4.4.2.4 Synthesis of triethylammonium trifluoromethanesulphonate (TETf)



TETf was synthesized by stirring diluted triethylamine (0.05 mol) with dropwise addition of trifluoromethane sulphonic acid (0.05 mol) in diethyl ether for four hours at  $\sim 0^\circ\text{C}$ . Light yellow viscous liquid. (Annexure 11.1)

#### 2.4.5 Synthesis of sulphonated copolyimide/protic ionic liquid (SPI/IL) composites

The solution casting method was used for the synthesis of SPI/IL composites where sulphonated copolyimides were used as matrix polymer and synthesized protic ionic liquids as fillers. Appropriate amounts (weight %) of protic ionic liquids were added to a solution of completely dissolved sulphonated copolyimides in *m*-cresol in a glass vial equipped with a magnetic stirrer bar. The mixture was stirred at 80 °C for 24 hours so that PIL can dissolve properly, and it was then casted on glass petri dish. The evaporation of *m*-cresol at 80 °C gave a uniform composite membrane. The composite membranes were peeled from the petri dish, dried in a vacuum oven at 80 °C for 24 hours and then stored in an inert atmosphere.<sup>59</sup> In order to see the compatibility and stability of the composite membranes, only TEA was found to be suitable and stable. Composite membranes with varying weight percentages of protic ionic liquids (IL content: 10, 20, 30, 40, and 50 wt %) were prepared. The codes of the ionic liquids are given in **Table 2.1**.

**Table 2.1:** Synthesized composites

#	Codes
1.	FBM-20/IL (10%)
2.	FBM-20/IL (20%)
3.	FBM-20/IL (30 %)
4.	FBM-20/IL (40 %)
5.	FBM-20/IL (50 %)
6.	FBA2-10/IL (20 %)
7.	FBA2-20/IL (20 %)
8.	FBO-10/IL (20 %)
9.	FBO-20/IL (20 %)
10.	FBO-30/IL (20 %)
11.	FBO-40/IL (20 %)
12.	FBM-50/IL (20 %)
13.	FBM-10/IL (20 %)
14.	FBM-20/IL (20 %)
15.	FBM-30/IL (20 %)
16.	FBM-40/IL (20 %)
17.	FBM-50/IL (20 %)

### 3 Results and Discussion

The chapter includes two main sections.

First section details the synthesis of alkyl chains containing diamines, 4-(2-(4-aminophenoxy)ethoxy)benzenamine (A2) and 4-(3-(4-amino phenoxy)propoxy)benzenamine (A3), and synthesis, structural characterization, molecular weight determination, thermal stability and theoretical studies of various polyimides and sulphonated copolyimides to evaluate their potential applications as metal ions sensors, lead ions adsorption membranes, proton conducting membranes and catalyst coating in polymer electrolyte membrane fuel cells.

Second section includes the synthesis and characterization of composites of sulphonated copolyimides with protic ionic liquid additives. Various essential characteristics involving film formation, thermal stability and crystallinity were evaluated and compared with sulphonated copolyimide systems to elucidate the effect of ionic liquids on flexibility and proton conductivity profile of sulphonated copolyimides membranes. The whole chapter explains the experimental results and related data obtained.

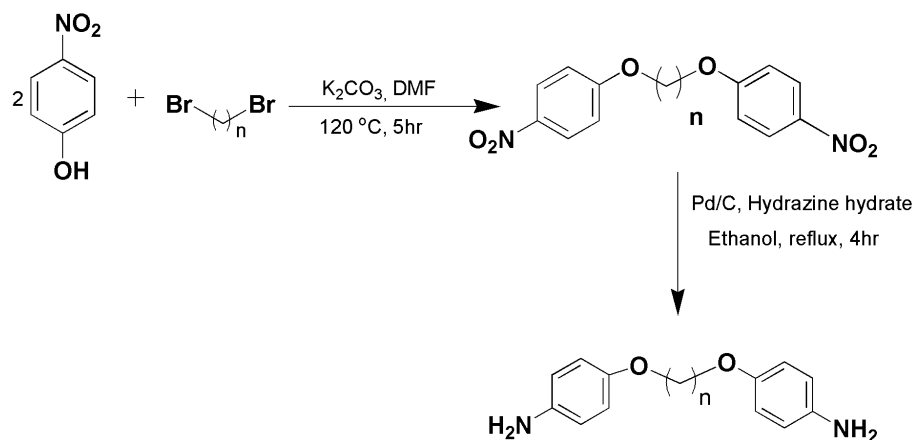
#### 3.1 Synthesis of diamines, homopolyimides, copolyimides and composites

Two diamines differing in alkyl chain lengths, five homopolyimides, fifty sulphonated copolyimides with varying degree of sulphonation and seventeen composites were synthesized and characterized.

##### 3.1.1 Synthesis of diamines

Two diamines differing in alkyl chain lengths i.e, two and three CH<sub>2</sub> units 4-(2-(4-aminophenoxy)ethoxy)benzenamine (A2) and 4-(3-(4-aminophenoxy)propoxy)benzenamine (A3) were synthesized using reported procedure (**Figure 3.2**).

The synthesis of aliphatic groups containing aromatic diamines was carried out in two steps as shown in **Scheme 3.1**.



**Scheme 3.1:** Synthesis of 4-((4-aminophenoxy)alkoxy)benzenamines.

In first step, the dinitro precursors were synthesized using Williamson ether synthesis followed by the reduction of dinitro compounds into diamines using Pd/C and hydrazine hydrate. *p*-Nitrophenol was reacted with K<sub>2</sub>CO<sub>3</sub> in DMF to generate phenoxide ion followed by the addition of aliphatic dihalides into the reaction mixture for producing dinitro compounds (DN2 and DN3) which were then reduced to their respective diamines (A2 and A3). Recrystallization was done using ethanol. The physical data of dinitro and diamines is mentioned in **Table 3.1**. The dinitro and diamines were obtained in good yields (73-86 %) and the melting points were in accordance with the reported ones.

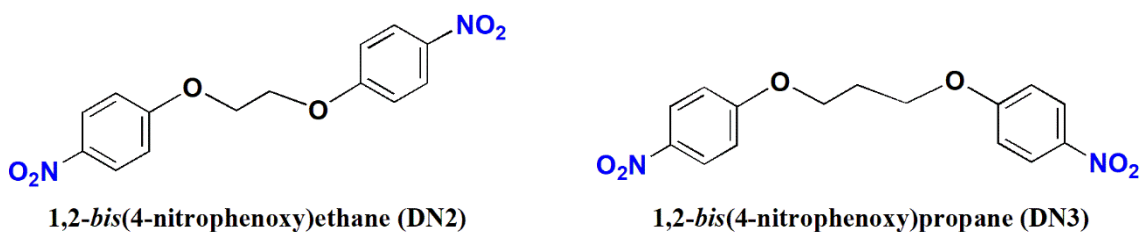


**Figure 3.1:** Structures of dinitro compounds.

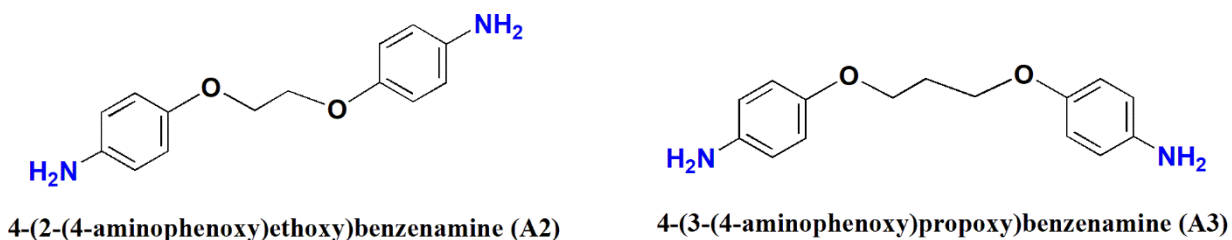


**Figure 3.2:** Structures of diamines.

**Table 3.1:** Physical data of dinitros and diamines

#	Codes	Physical Appearance	Yield (%) (reported) <sup>133</sup>	m.p. (°C) (Lit. m.p.) <sup>133</sup>	R <sub>f</sub> value*
1	DN2	Off white powder	80 (86)	148-149 (149)	0.69
2	A2	White crystals	86 (92)	174-176 (176)	0.35
3	DN3	Light yellow powder	80 (85)	79-81 (78)	0.52
4	A3	Silver white crystals	73 (78)	98-100 (98)	0.30

\*Stationary phase=silica gel 60F<sub>254</sub>; mobile phase= ethyl acetate : *n*-hexane (1:1),  $\lambda = 254$  nm

### 3.1.2 Synthesis of homo and copolyimides

Synthesis of polyimides (PIs) and sulphonated copolyimides (SPIs) was carried out via two step thermal imidization procedure. As discussed in introduction, this particular method was selected because it gives completely imidized, high molecular weight and hydrolytically stable polyimides. The benefits of this procedure were apparent, during this research, as completely imidized and high molecular weight polyimides were achieved as judged through intrinsic viscosity and gel permeation chromatography (GPC).

Series of high molecular weight wholly imidized homopolyimides were prepared using two different dianhydrides (6FDA and ODPA) and commercial and synthesized unsulphonated diamines (A, A2, A3, M, I). Series of high molecular weight wholly imidized sulphonated copolyimides with pendant sulphonic acid (-SO<sub>3</sub>H) groups in polymeric backbones were prepared using two different dianhydrides (6FDA and ODPA), commercially available sulphonated diamine (BDSA) in triethylammonium salt form (BDSA.TEA) alongwith commercial and synthesized unsulphonated diamines (A, A2, A3, M, I). The monomers used are shown in **Figure 3.3**.

In the present research, the synthesized alkyl chains containing aromatic diamines were used alongwith commercial dianhydrides and diamines, because of their easy synthesis, convenience and low cost. The monomers were selected after extensive literature review. The objective of this research was to synthesize completely cyclized, flexible film forming sulphonated copolyimides and their composites with protic ionic liquids for their use as toxic metals adsorbents and proton conducting electrolyte membranes for PEMFCs. For this high molecular weight copolyimides having pendant

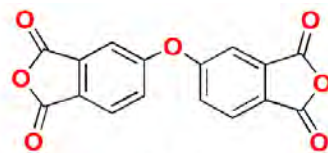
sulphonic acid groups and their composites with protic ionic liquids were prepared. In all cases, synthesis of unsulphonated homopolyimides was also carried out for the comparison of physical properties.

This section details the FTIR results, morphological studies, molecular weight determination, thermal characteristics and theoretical studies of the polyimides. UV-Visible spectroscopy results, atomic absorption spectroscopy (AAS) studies, four probe proton conductivity measurements, half-cell test and single cell test results of polyimides and their composites are discussed for heavy metal sensing, Pd (II) adsorption, proton conductivity and catalyst coating studies for fuel cell applications.

### Dianhydrides

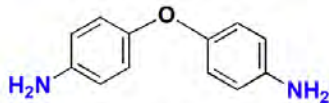


4, 4'-(Hexafluoroisopropylidene)diphthalic anhydride (6FDA) [F]

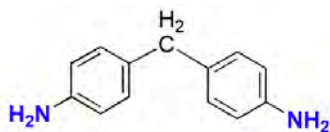


4,4'-Oxydiphthalic anhydride (ODPA) [O]

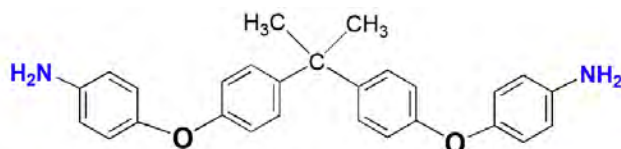
### Diamines



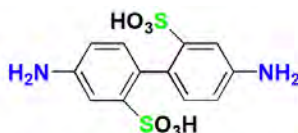
4-(4-aminophenoxy)benzenamine (A)



4-(4-aminobenzyl)benzenamine (M)



4-(4-(2-(4-(4-aminophenoxy)phenyl)propan-2-yl)phenoxy)benzenamine (I)



Benzidine-2, 2'-disulfonic acid (BDSA)  
(B)

**Figure 3.3:** Monomers used for synthesis of polyimides and sulphonated copolyimides.

### 3.1.2.1 Synthesis of polyimides (PIs)

Two commercially available dianhydrides (6FDA and ODPDA) were used in this research work. Polyimides containing 6FDA and ODPDA dianhydrides were selected due to their appealing properties of flexibility and transparency. In 6FDA, the bulky structure of two  $-CF_3$  groups and kinked arrangement hampers the close packing of adjoining polymer chains. Alongwith this, steric hindrance between *ortho* aromatic protons to isopropylidene linkage and fluorine atoms inhibits free rotation of  $(CF_3)_2 C-C (Ar)$  bond resulting in the rigid nature of this monomer. Additionally, 6FDA is renowned to improve the solubility of polyimides.<sup>138</sup>

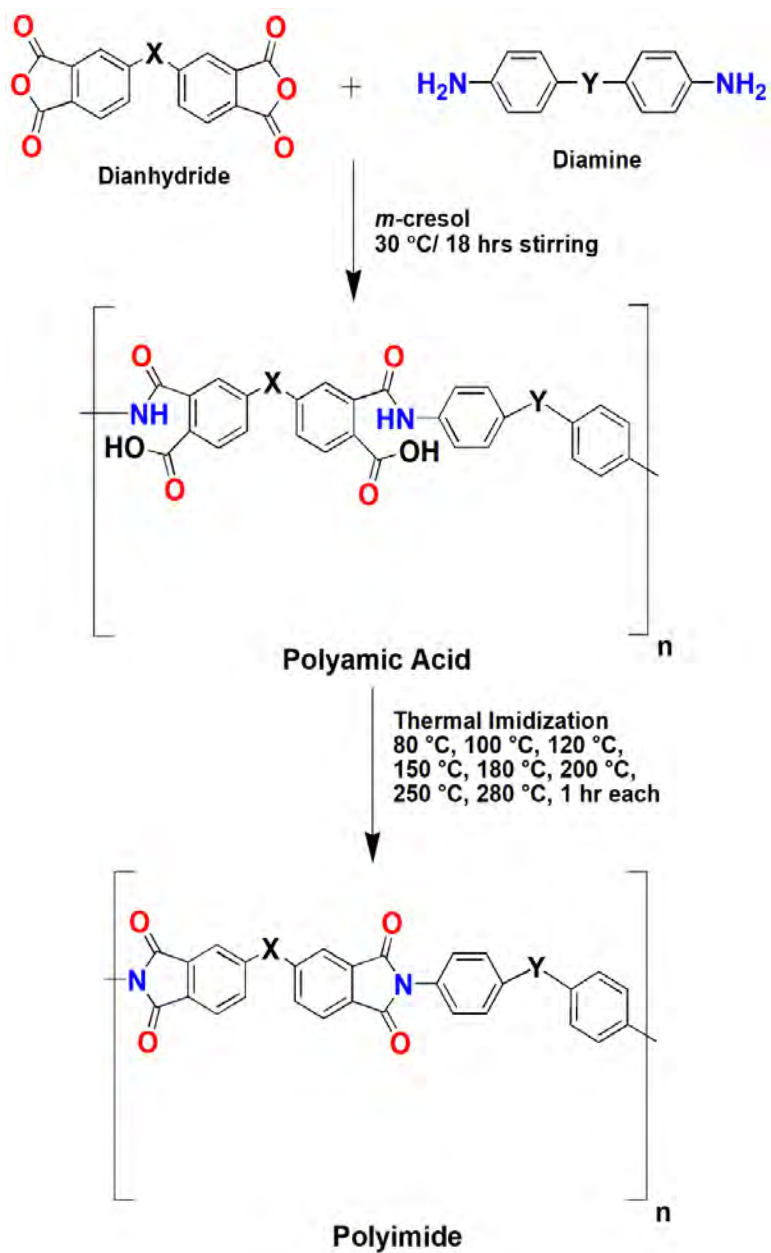
The ODPDA dianhydride has a very flexible oxygen linker between the two phthalic anhydride parts of the molecule. The ether linkage imparts extra flexibility to the polyimide backbone. Ether linkage imparted better solubility and flexibility to the polyimides which can be accredited to the distorted and bent chain structure.<sup>138</sup> Ando et al. arranged the commercially available dianhydrides according to the flexibility of polyimides with fixed diamine structures: BTDA > PMDA > BPDA > ODPDA > 6FDA.<sup>139</sup>

Moreover, for all the homopolyimides and sulphonated copolyimides prepared in this research project, one to one (1:1) monomers stoichiometry was maintained regarding mole percent of dianhydride monomer and mole percent of diamine(s) monomer in order to get high molecular weight polymers. It was not intended to control the molecular weight of polymers by using any endcapper, monofunctional monomer. Polyimides having different flexible groups and varying degree of sulphonation were employed in order to improve the flexibility of the system and enhanced metal adsorption and proton conductivity respectively.

The synthesis of polyimides was carried out by conventional two-step thermal imidization procedure (**Scheme 3.2**).

Equimolar amounts of aromatic diamine and aromatic dianhydride were reacted with 15% solids concentration in *m*-cresol. PAA solution was prepared for 18 hours at room temperature. Thermal curing of PAA solution was carried out upto 300 °C on glass petri dish to obtain the polyimide films. Ten different polyimides were synthesized using

two different dianhydrides and five different diamine (two synthesized and three commercial).



**Scheme 3.2:** Synthesis of homopolyimides.



The general structure of polyimides is given below, and codes of the synthesized polyimides are tabulated in **Table 3.2**.

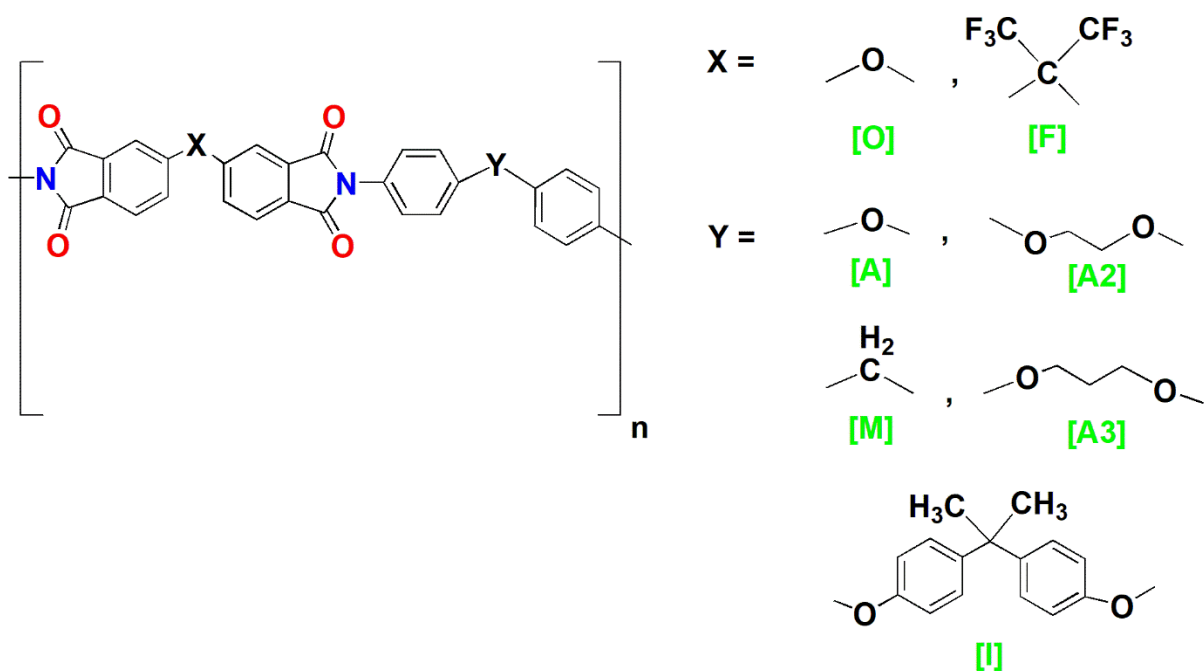


**Figure 3.4:** General structure of polyimide.

**Table 3.2:** Codes for polyimides

#	Codes	X	Y
1	OA	O	A
2	OA2	O	A2
3	OA3	O	A3
4	OI	O	I
5	OM	O	M
6	FA	F	A
7	FA2	F	A2
8	FA3	F	A3
9	FI	F	I
10	FM	F	M

### 3.1.2.1.1 FTIR Studies of polyimides (PIs)

To confirm the synthesis of polyimides (FM) and (OM), FTIR spectra were collected as shown in **Figure 3.5**. Appearance of several characteristic bands clearly indicated the successful synthesis of polyimides. The characteristic absorption bands of imide carbonyl group around 1780 (asymmetric stretching), 1710 (symmetric stretching), 1382 (C-N stretching) and 717 (C=O bending) along with some strong absorption bands around 1350-1150  $\text{cm}^{-1}$  (C-O and C-F stretching) confirmed the successful formation of polyimides.<sup>26, 140, 141</sup>

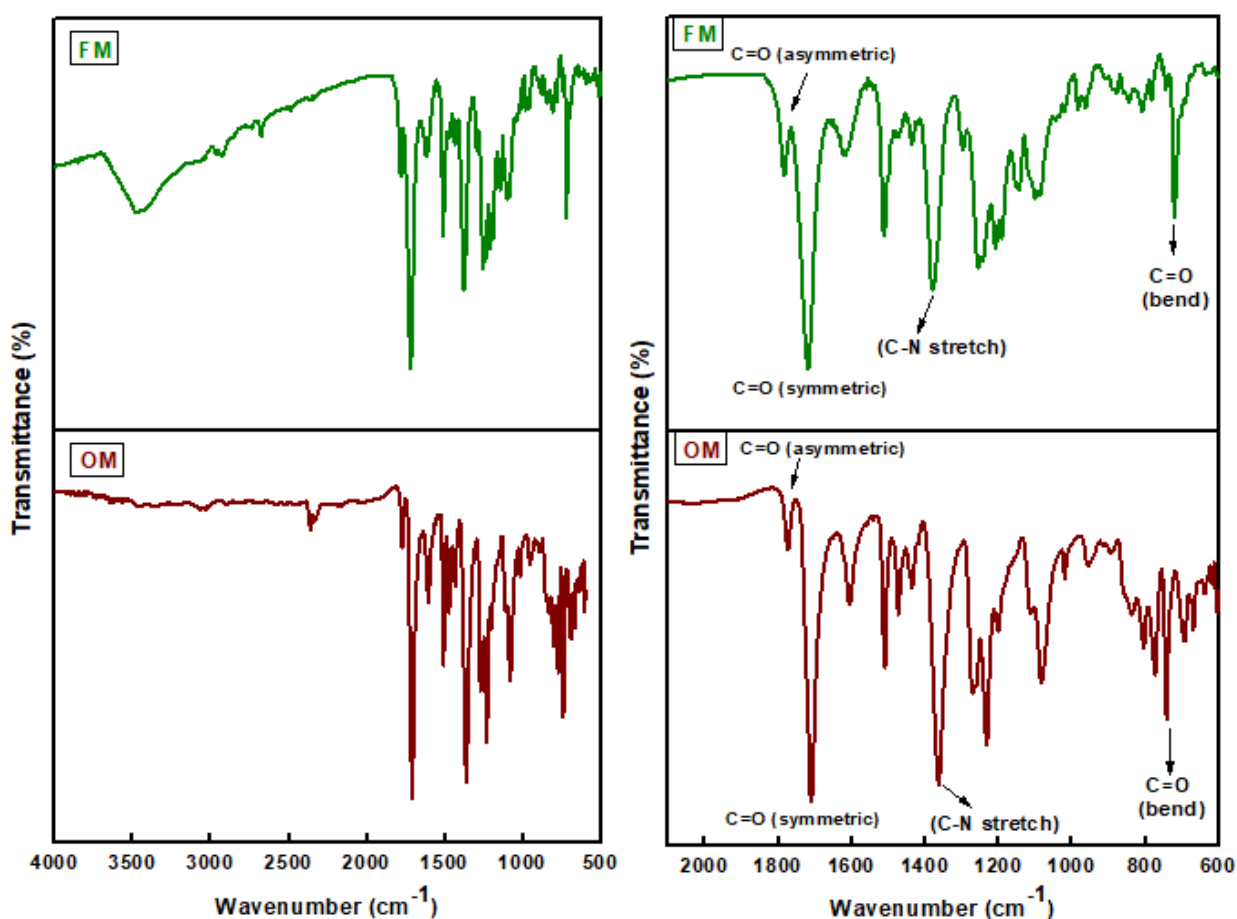


**Figure 3.5:** Full range and elaborated FTIR spectra of FM and OM.

### 3.1.2.1.2 Morphological studies of polyimides

The morphology of the PIs was analyzed by X-ray Diffraction (XRD) studies, using the polyimide films with  $2\theta$  ranging from 0 to  $60^\circ$ . The XRD patterns are shown in **Figure 3.6**.

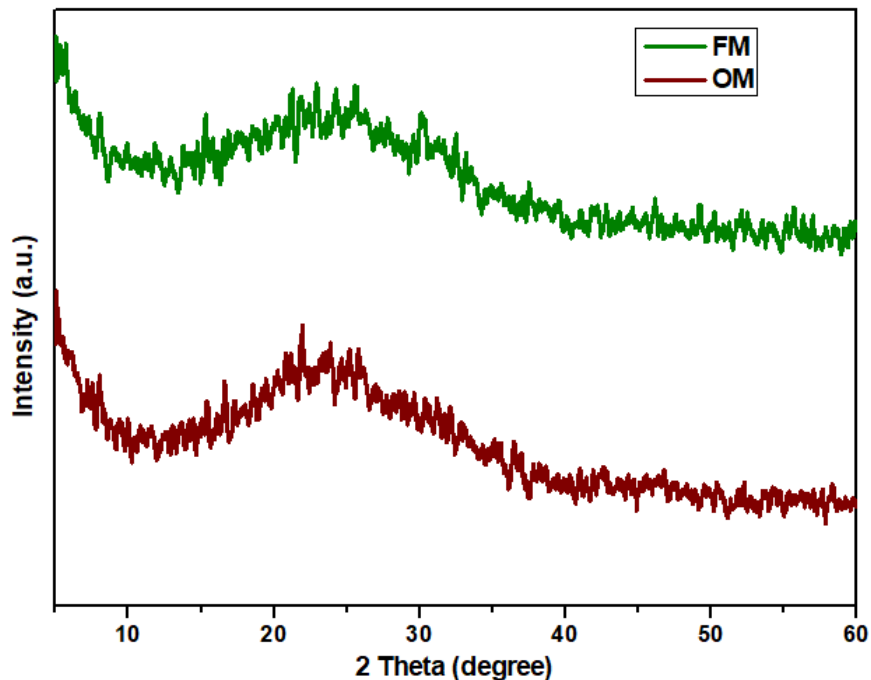


**Figure 3.6:** XRD patterns of (FM) and (OM).

The polyimides expressed broad diffraction peak at  $\sim 24^\circ$  ( $2\theta$ ), an evidence indicating the amorphous polyimides morphology, due to the presence of short flexible alkyl linkages responsible for loosening the polymer chain packing.<sup>142</sup>

### 3.1.2.1.3 Thermal properties of polyimides

Thermogravimetric analysis (TGA) and differential scanning calorimetry (DSC) were used to evaluate the thermal properties of polyimides. Thermal gravimetric analyzer was used to measure the thermal stability of polyimides because it is the most accurate method for the estimation of thermal stability of a polymer. **Figure 3.7** depicts the thermograms of polyimides FM and OM. The membranes were analyzed between 25 and 800 °C in nitrogen at heating rate of 10 °C min<sup>-1</sup> and the results are summarized in **Table 3.3**.

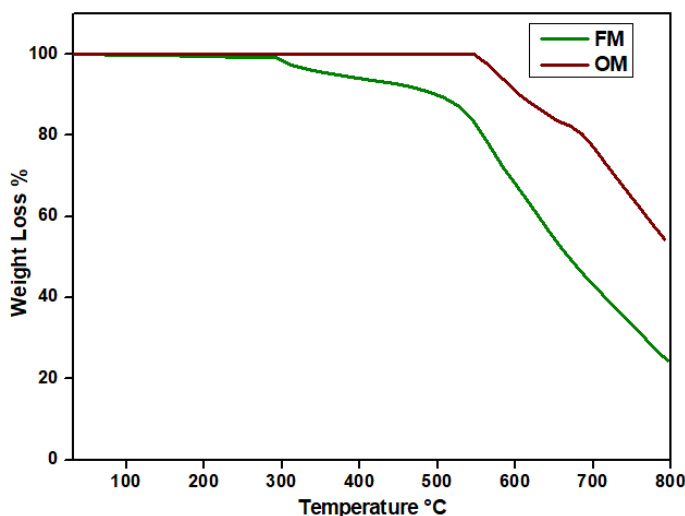


**Figure 3.7:** TGA patterns of (FM) and (OM).

The polyimides exhibited two step degradation where the first step was assigned to the removal of entrapped solvents while the second step was correlated generally to the decomposition of the polyimide backbone.<sup>60</sup> As can be seen in **Figure 3.7**, the polyimide OM showed no obvious weight loss till 570 °C, indicating no thermal decomposition took place upto this temperature. The polyimide kept on degrading till the last temperature limit i.e, 800 °C. At 800 °C, 10-54 % wt. of degradation product was recorded. OM synthesized from ODPA and MDA, gave the highest residual weight percent i.e, 54 % under nitrogen at 800 °C in comparison with other polyimides. This could be accredited to higher carbon content of polymer backbone.<sup>60</sup>

The key factors contributing to heat resistance of polymers are molecular symmetry, resonance stabilization, primary and secondary interactions and mechanism of bond cleavage. The unsulphonated polyimides based on both dianhydrides, FM and OM, showed good endurance to thermal degradation as indicated by the 5 % weight loss which took place above 350 °C and 570 °C for FM and OM respectively. Td's have been plotted as function of temperature. (Annexure 11).

TGA results clearly indicated that the obtained polyimides possess fairly good thermal stability and can be used in relatively harsh environmental conditions.

The DSC thermograms for PIs (FM) and (OM) are presented in **Figure 3.8**. Relatively moderate Tg were recorded in the range of 186-236 °C due to the flexible and

polar connecting groups.<sup>30, 143</sup> Generally, molecular packing and chain rigidity of polymer backbones determine the T<sub>g</sub> values of the polymers. As a result, PI (OM) derived from ODPDA and MDA with rigid polymer backbone exhibited higher T<sub>g</sub> whereas PI (FM), derived from 6FDA and MDA showed lower T<sub>g</sub> value. This might be attributed to the bulky -CF<sub>3</sub> groups of 6FDA decreasing the intermolecular interactions and inhibiting close packing of the polymer chains.<sup>144</sup>

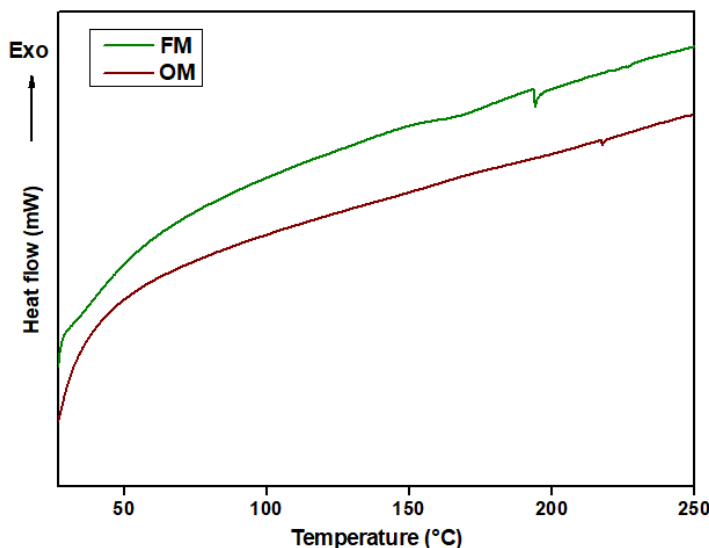


**Figure 3.8:** DSC thermograms of (FM) and (OM).

**Table 3.3:** Thermal properties of polyimides

Polyimide	T <sub>g</sub> * (°C)	T <sub>d</sub> (°C)	T <sub>5%</sub> (°C)	T <sub>10%</sub> (°C)	RW% (800 °C)
FM	194	293	352	507	24
OM	217	548	578	609	54

\* as measured by DSC, T<sub>d</sub> = onset of degradation temperature, T<sub>5%</sub> = temperature at which 5 % weight loss occurred, T<sub>10%</sub> = temperature at which 10 % weight loss occurred and RW% = residual weight % at

#### 3.1.2.1.4 Solubility and viscosities of polyimides

The solubility of synthesized polyimides in different organic solvents was checked by dissolving 10 mg polyimide in 1 mL of solvent at 30 °C. These polymers are soluble in *m*-cresol at room temperature and in NMP at heating. Polyimides are completely insoluble in all other solvents (non-polar as well as polar) even on heating. *m*-Cresol a highly protic solvent reduces/ or overcomes the chain-chain interactions and improves solubility by penetrating into the polyimide chains.

Polyimides showed very limited solubility which can be assigned to closely packed chains of the polyimides. This close packing is due to the symmetry, rigidity and regularity of polyimide backbone which is responsible for poor solubility. Intra and intermolecular interactions resulted in close packing of polymer chains and in turn in poor solubility. The bulky  $-CF_3$  groups of 6FDA inhibited close chain packing while flexible ether linkage of ODPAs are responsible for the solubility of these high molecular weight polymers in highly polar solvents.<sup>30, 36</sup>

The viscosity measurements were carried out using *m*-cresol solutions of PIs with the concentration of 0.2 gdl<sup>-1</sup> at 30 °C with U-tube Ubbelohd's viscometer. The inherent viscosities ( $\eta_{inh}$ ) were found around 1.10 and 2.166 dL/g for OM and FM respectively, depicting highly viscous nature of polymer solutions, indicative of the fact that polyimides have quite high molecular weights.<sup>30, 145</sup> The data is tabulated in **Table 3.4**.

**Table 3.4:** Viscometric data of polyimides in *m*-cresol

Polyimide	$\eta_{rel}$	$\eta_{sp}$	$\eta_{red}$	$\eta_{inh}$
FM	1.542	0.542	2.710	2.166
OM	1.2372	0.2372	1.186	1.10

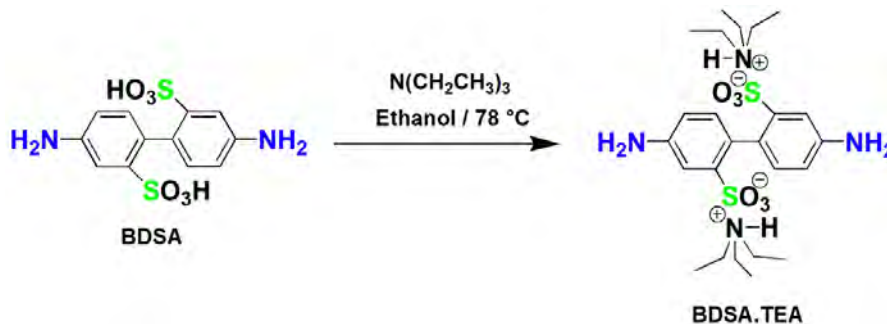
$\eta_{rel}$  = relative viscosity,  $\eta_{sp}$  = specific viscosity,  $\eta_{red}$  = reduced viscosity,  
 $\eta_{inh}$  = inherent viscosity

### 3.1.2.2 Synthesis of sulphonated copolyimides (SPIs)

The primary objective of this research work was to synthesize high molecular weight sulfonated copolyimide membranes. These single piece, free-standing films can be employed for heavy metal sensing, Pb (II) adsorption and as proton exchange membranes for polymer electrolyte membrane fuel cells (PEMFCs).

Incorporation of commercial sulphonated diamine monomer as triethylammonium salt (BDSA.TEA) in 6FDA and ODPAs based polyimides was employed as a strategy for the introduction of sulphonic acid group in polyimide backbone to increase the hydrophilicity which is the basic prerequisite to enhance the water interaction and water absorption in the polyimide membrane. As a result, improved interaction with heavy metal ions in aqueous media and proton conduction in PEMFCs are expected.

To synthesize the triethylammonium salt of BDSA, triethylamine was added dropwise to the boiling solution of BDSA in ethanol and heated until BDSA was completely dissolved (**Scheme 3.3**).<sup>136</sup>



**Scheme 3.3:** Synthesis of triethyl ammonium salt of benzidine-2, 2'-disulphonic acid.

The structural characterization of BDSA.TEA was carried out by FTIR spectroscopic technique. The comparative FTIR spectra of BDSA and BDSA.TEA showed clear change in the -S=O asymmetric (1156 cm<sup>-1</sup>) and symmetric (1033 cm<sup>-1</sup>) vibrations which confirmed the successful salt formation as can be seen in **Figure 3.9**.

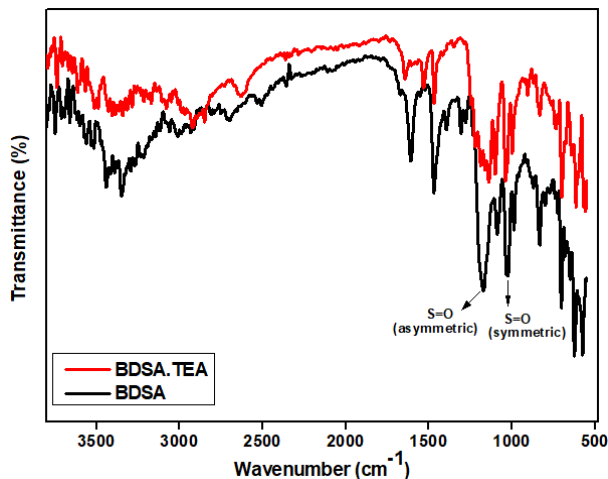
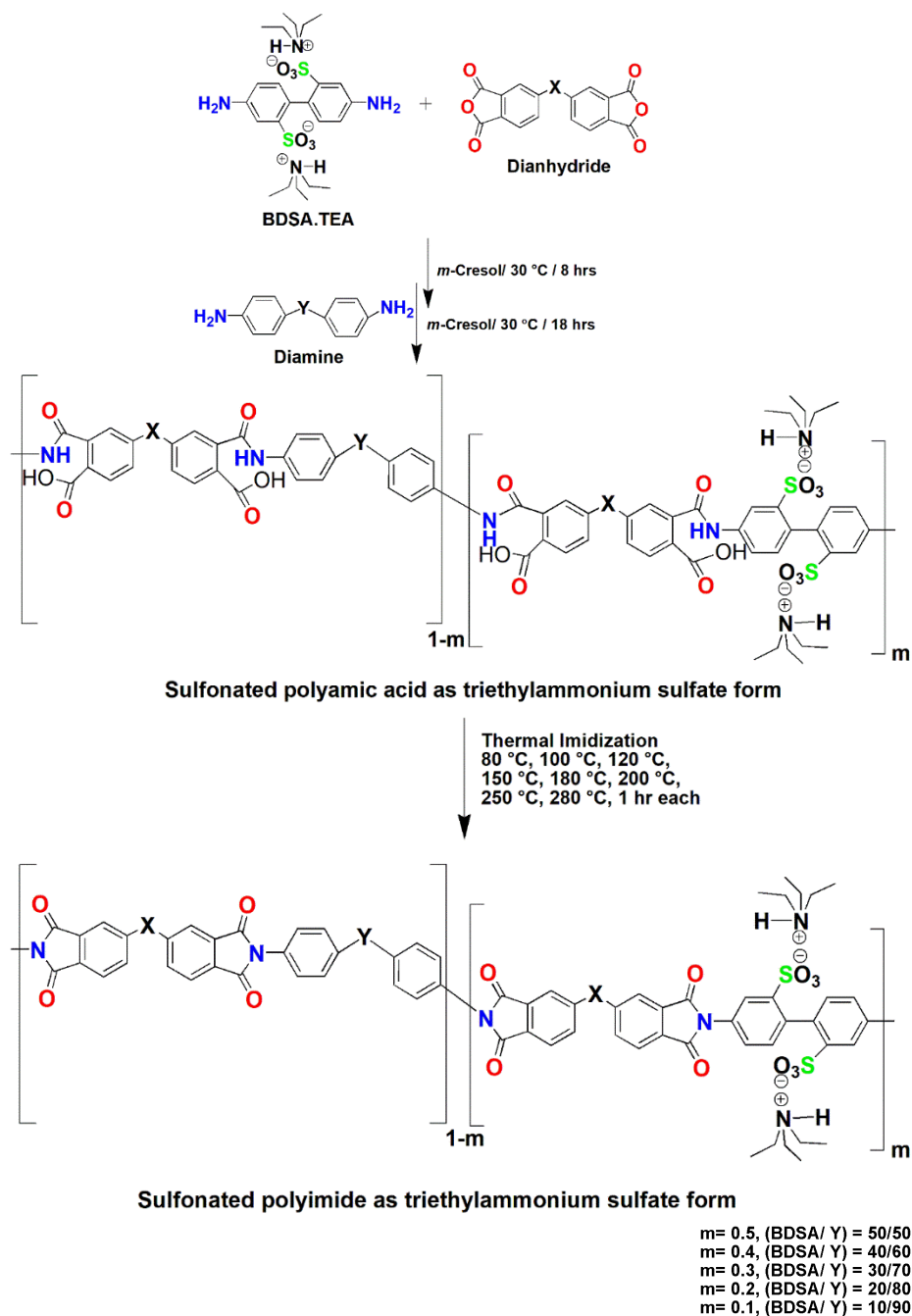


**Figure 3.9:** Comparative FTIR spectra of BDSA.TEA and BDSA.

The sulphonated diamine BDSA.TEA, non-sulphonated aromatic diamine and commercially available aromatic dianhydrides (6FDA and ODP) were reacted to give two different series (6FDA and ODP based) of sulphonated copolyimides respectively (**Scheme 3.4**).



**Scheme 3.4:** Synthesis of sulphonated copolyimide in triethyl ammonium sulfate form.

For the synthesis of sulphonated copolyimides, thermal imidization method (two step) was used. Equimolar amounts of diamine monomers and aromatic dianhydrides were reacted with 15% solid content in *m*-cresol. PAA solution was prepared for 18 hours at room temperature. Thermal curing of PAA solution was carried out upto 300 °C in glass



petri dish to obtain the sulphonated copolyimides as films. The general structure of copolyimide is shown in **Figure 3.10**.

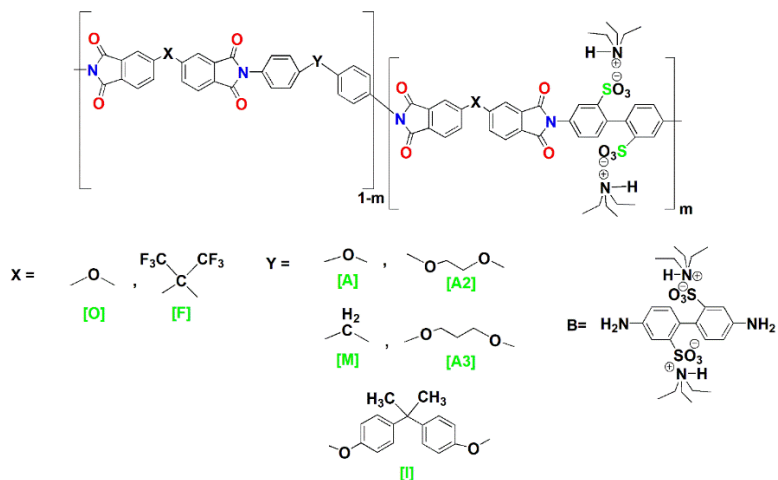


**Figure 3.10:** General structure of sulphonated copolyimide.

The synthesis of first sulphonated copolyimide comprised of 90:10 mole ratio with respect to unsulphonated:sulphonated diamine. To evaluate the impact of varying degree of sulfonation, four additional copolyimides compositions were synthesized using dianhydride/unsulphonated diamine/sulphonated diamine, by varying the sulfonated diamine triethylammonium salt (BDSA.TEA) content from 20, 30, 40 and 50 mol % respectively. For all the copolymerizations, two step thermal imidization route was employed, where PAA was thermally imidized into sulphonated copolyimide. In all the copolymerizations, the sulfonated diamine monomer (BDSA.TEA) was stirred with dianhydride for 8 hours, to get oligomerized, before the addition of unsulfonated diamine in the reaction mixture. The reason being, as the sulfonated diamine have two electron withdrawing  $-SO_3H$  groups therefore it is supposed to be weaker nucleophile (less reactive) as compared to the unsulfonated diamine to attack the dianhydride carbonyl carbon. However, it was found that increase in solubility and higher polymer solution viscosities were obtained with increased sulfonic acid content i.e; by increasing the mole percent of incorporated sulfonated diamine. Codes and compositions of 6FDA and ODPa based sulphonated copolyimides are given in **Tables 3.5** and **3.6** respectively.

**Table 3.5:** Codes and percentage compositions of 6FDA based sulphonated copolyimides (SPIs)

#	Codes	X (%)	B (%)	Y (%)
1.	FBA-50	F (100)	B (50)	A (50)
	FBA-40	F (100)	B (40)	A (60)
	FBA-30	F (100)	B (30)	A (70)
	FBA-20	F (100)	B (20)	A (80)
	FBA-10	F (100)	B (10)	A (90)
2.	FBA2-50	F (100)	B (50)	A2 (50)
	FBA2-40	F (100)	B (40)	A2 (60)
	FBA2-30	F (100)	B (30)	A2 (70)
	FBA2-20	F (100)	B (20)	A2 (80)
	FBA2-10	F (100)	B (10)	A2 (90)
3.	FBA3-50	F (100)	B (50)	A3 (50)
	FBA3-40	F (100)	B (40)	A3 (60)
	FBA3-30	F (100)	B (30)	A3 (70)
	FBA3-20	F (100)	B (20)	A3 (80)
	FBA3-10	F (100)	B (10)	A3 (90)
4.	FBI-50	F (100)	B (50)	I (50)
	FBI-40	F (100)	B (40)	I (60)
	FBI-30	F (100)	B (30)	I (70)
	FBI-20	F (100)	B (20)	I (80)
	FBI-10	F (100)	B (10)	I (90)
5.	FBM-50	F (100)	B (50)	M (50)
	FBM-40	F (100)	B (40)	M (60)
	FBM-30	F (100)	B (30)	M (70)
	FBM-20	F (100)	B (20)	M (80)
	FBM-10	F (100)	B (10)	M (90)

**Table 3.6:** Codes and percentage compositions ODPA based sulphonated copolyimides

(SPIs)				
#	Codes	X (%)	B (%)	Y (%)
<b>1.</b>	OBA-50	O (100)	B (50)	A (50)
	OBA-40	O (100)	B (40)	A (60)
	OBA-30	O (100)	B (30)	A (70)
	OBA-20	O (100)	B (20)	A (80)
	OBA-10	O (100)	B (10)	A (90)
<b>2.</b>	OBA2-50	O (100)	B (50)	A2 (50)
	OBA2-40	O (100)	B (40)	A2 (60)
	OBA2-30	O (100)	B (30)	A2 (70)
	OBA2-20	O (100)	B (20)	A2 (80)
	OBA2-10	O (100)	B (10)	A2 (90)
<b>3.</b>	OBA3-50	O (100)	B (50)	A3 (50)
	OBA3-40	O (100)	B (40)	A3 (60)
	OBA3-30	O (100)	B (30)	A3 (70)
	OBA3-20	O (100)	B (20)	A3 (80)
	OBA3-10	O (100)	B (10)	A3 (90)
<b>4.</b>	OBI-50	O (100)	B (50)	I (50)
	OBI-40	O (100)	B (40)	I (60)
	OBI-30	O (100)	B (30)	I (70)
	OBI-20	O (100)	B (20)	I (80)
	OBI-10	O (100)	B (10)	I (90)
<b>5.</b>	OBM-50	O (100)	B (50)	M (50)
	OBM-40	O (100)	B (40)	M (60)
	OBM-30	O (100)	B (30)	M (70)
	OBM-20	O (100)	B (20)	M (80)
	OBM-10	O (100)	B (10)	M (90)

### 3.1.2.2.1 Free standing film formation

6FDA and ODPDA anhydrides based free standing sulfonated copolyimide membranes utilized in this dissertation were synthesized by thermal imidization method. The polyamic acid was poured into the glass petri dish and gradually heated under vacuum from 80 upto 280 °C maintaining each temperature for one hour to get the flexible copolyimide films. Finally, the films were dried in vacuum at 80 °C for 24 hours. Polyimide films were used for almost all the characterizations unless otherwise mentioned.

The films obtained from the unsulphonated polyimides, both polyimide series based on 6FDA and ODPDA anhydrides, produced tough, flexible yellowish to brown color films upon drying (**Figure 3.11**). Similar film characteristics were produced upon introduction of lower percentages of sulfonated monomer (up to 40 %) when casted. However, with the increase in degree of sulfonation up to 50 %, though the films did not cracked during the drying process they became less flexible and comparatively more brittle as compared to their sulfonated counterparts with low level of sulfonation. These films cracked easily when folded to test for creasability. The polyimide membranes with more than 50 % sulfonated diamine in their backbones showed brittle film characteristics and cracked during drying. Brown coloration in the dry films also increased with an increase in the level of sulfonation.

Preparation of tough and flexible films (copolyimides having 0-40 % sulfonation level) is convincing evidence of formation of high molecular weight and completely imidized polyimides.

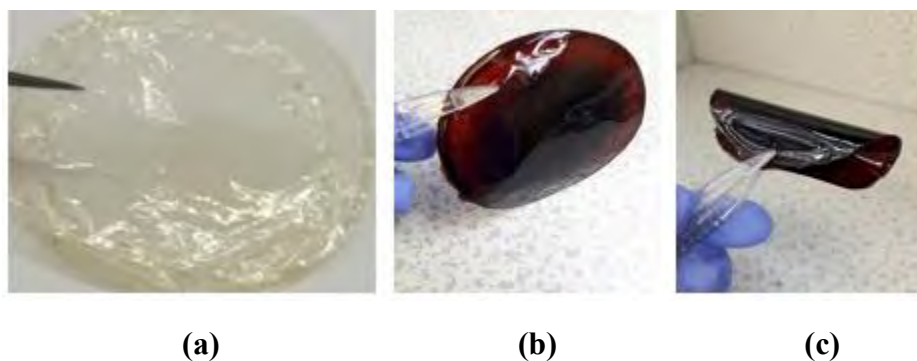


**Figure 3.11:** Physical appearance of (a) 20 % (b, c) 50 % sulphonated copolyimide films.

### 3.1.2.2.2 FTIR studies of sulphonated copolyimides (SPIs)

To confirm the synthesis of sulphonated co-polyimides FBM-50 and OBM-50 FTIR spectra were collected as shown in **Figure 3.12**. Appearance of several characteristic bands in sulphonated copolyimides spectra clearly indicated the successful introduction of  $-\text{SO}_3$  groups in the polymer chain. The characteristic absorption bands of imide carbonyl group were observed around 1780 (asymmetric stretching) and 1710  $\text{cm}^{-1}$  (symmetric stretching). Additional vibrations were observed at 1382 (C-N stretching) and 717 (C=O bending) along with some strong absorption bands around 1350-1150  $\text{cm}^{-1}$  (C-O and C-F stretching) confirmed the successful formation of imide linkage. The characteristic peaks around 1084 and 1035  $\text{cm}^{-1}$  corresponding to the asymmetric and symmetric vibrations of sulfonate group respectively and those at 620  $\text{cm}^{-1}$  corresponding to C-S vibration (stretch) provided convincing evidence of successful formation of sulphonated co-polyimides.<sup>26, 140,</sup>  
141

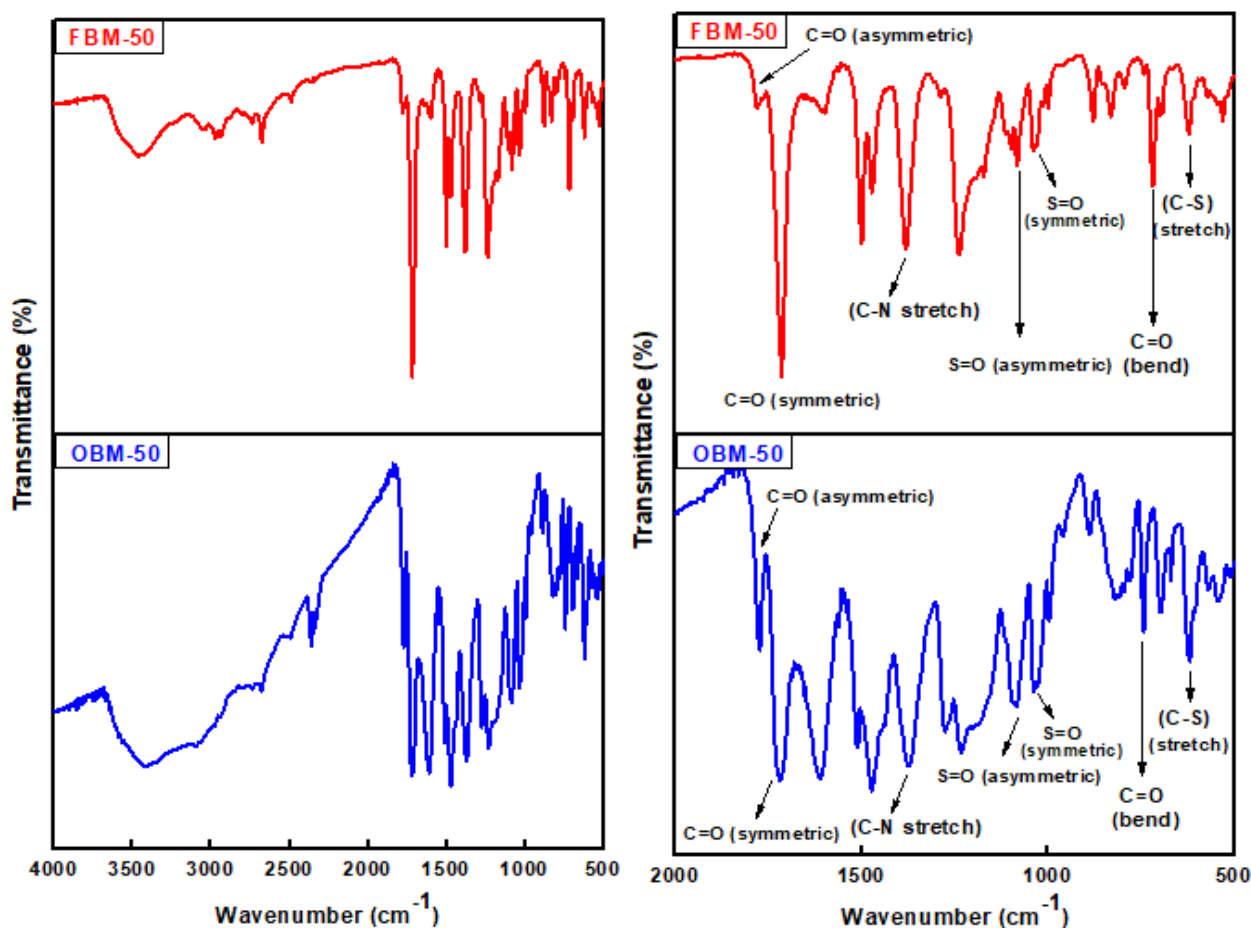


**Figure 3.12:** Full range and elaborated FTIR spectra of FBM-50 and OBM-50.

### 3.1.2.2.3 Morphological studies of sulphonated co-polyimides (SPIs)

The morphology of SPIs was analyzed by X-ray Diffraction (XRD) studies, using the polyimide films with  $2\theta$  ranging from 0 to  $60^\circ$ . The XRD patterns of sulphonated co-polyimides are shown in **Figure 3.13**.

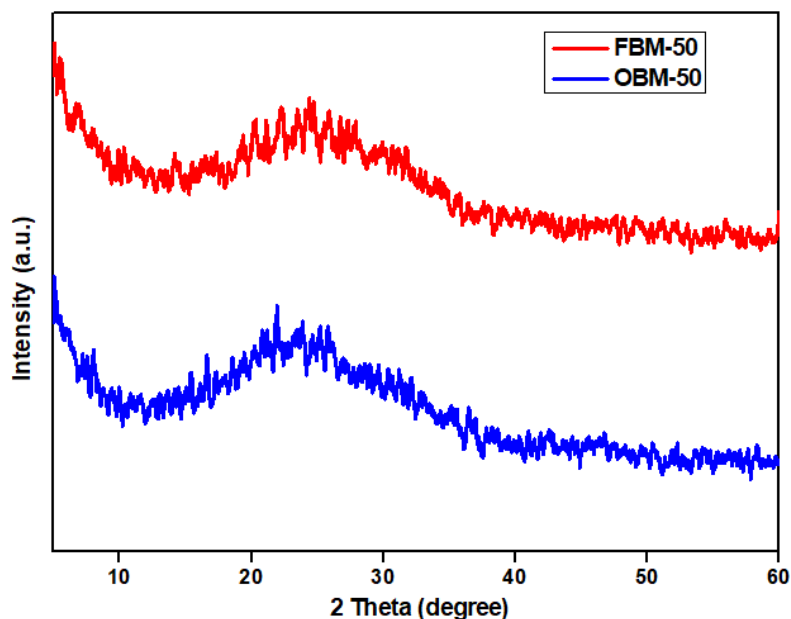


**Figure 3.13:** XRD of FBM-50 and OBM-50.

The sulphonated copolyimides expressed broad diffraction peak at  $\sim 24^\circ$  ( $2\theta$ ), an evidence indicating the amorphous polyimides morphology, due to the presence of flexible alkyl linkages responsible for loosening the polymer chain packing.<sup>142</sup>

### 3.1.2.2.4 Thermal properties of sulphonated co-polyimides (SPIs)

Thermogravimetric analysis (TGA) and differential scanning calorimetry (DSC) were used to evaluate the thermal properties of polyimides. Thermal gravimetric analyzer was used to measure the thermal stability of copolyimides. **Figure 3.14** depicts thermogravimetric analysis curves of copolyimides FBM-50 and OBM-50. The membranes were analyzed between 25 and  $800^\circ\text{C}$  in nitrogen at heating rate of  $10^\circ\text{C min}^{-1}$  and the results are summarized in **Table 3.7**.

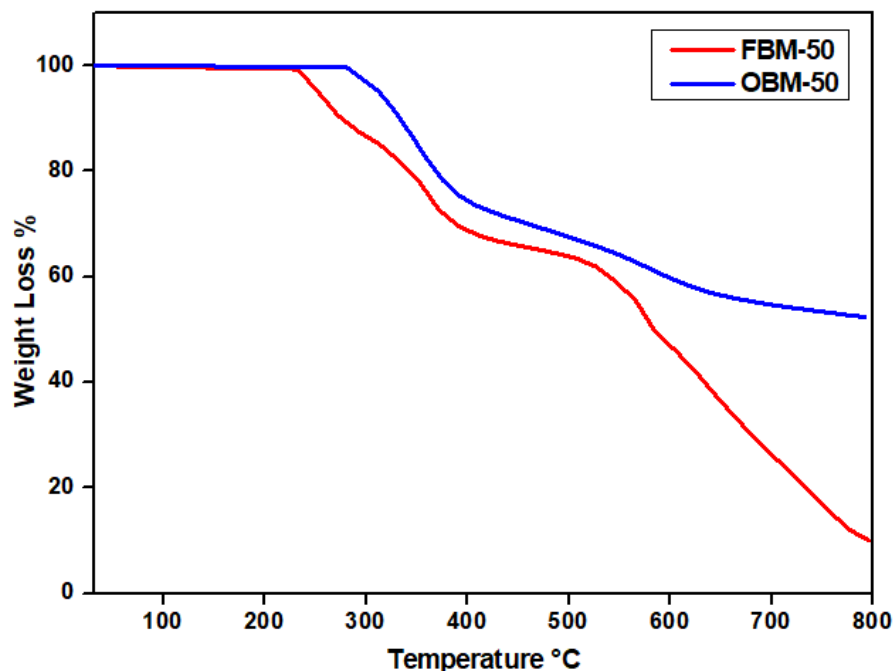


**Figure 3.14:** TGA thermograms of FBM-50 and OBM-50.

The sulphonated copolyimides exhibited three-step degradation. The first step was attributed to the removal of entrapped solvents while the second step was correlated to the degradation of sulphonic acid group leading to the discharge of sulphur monoxide and sulphur dioxide gases. It is reported that degradation of sulphonic acid group is not affected by backbone structure of sulphonated polyimides.<sup>29</sup> The third step indicated the decomposition of the polyimide backbone. As can be seen from **Figure 3.14**, the polyimide OBM-50 showed no obvious weight loss till 280 °C, suggesting no thermal decomposition took place upto this temperature. The residual weight percent was in range of 10-54% at 800 °C under nitrogen atmosphere. TGA results clearly indicated that the obtained sulphonated copolyimides possess fairly good thermal stability and can be used in relatively harsh environmental conditions due to their better thermal stability.<sup>60</sup>

The DSC thermograms for SPIs FBM-50 and OBM-50 are presented in **Figure 3.15**. Relatively moderate glass transition temperatures were recorded in the range of 170-204 °C due to the flexible and polar connecting groups.

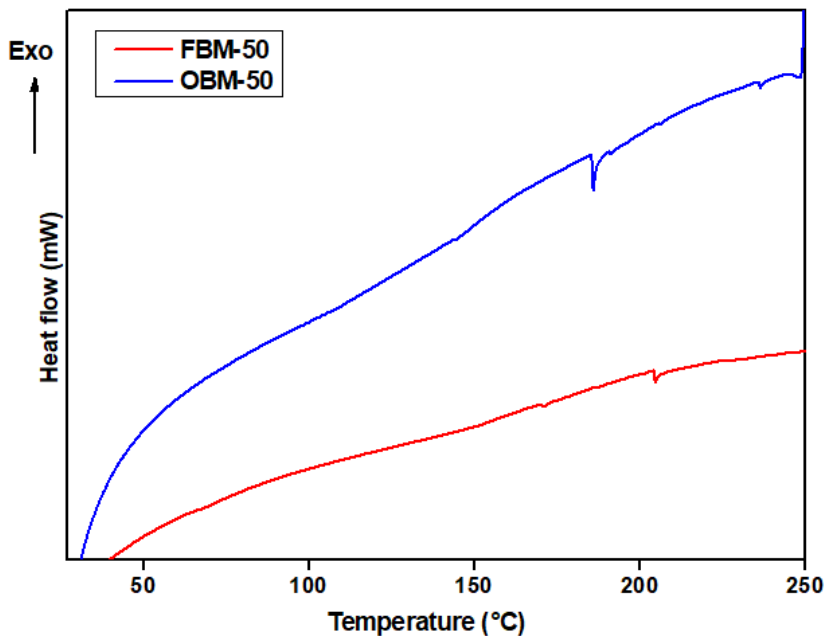


**Figure 3.15:** DSC curves of FBM-50 and OBM-50.

In copolyimides the DSC thermograms showed two distinct glass transition temperatures, the sulphonated block exhibited a higher  $T_g$  than that of the non-sulphonated block. This higher  $T_g$  may be resulted from close packing of polymer chains due to the presence of sulphonate groups onto the polymer backbone resulting in enhanced intermolecular interactions through polar ionic sites and inhibition to free rotation of the polymer chains.<sup>30, 143</sup> It is accepted that alongwith chain rigidity of polymeric backbones, the intermolecular interactions like hydrogen bonding and ionomer effects are significant factors that determine the  $T_g$  values of the polymers.<sup>144</sup>

**Table 3.7:** Thermal properties of FBM-50 and OBM-50

Copolyimide	$T_g^*$ (°C)	$T_d$ (°C)	$T_{5\%}$ (°C)	$T_{10\%}$ (°C)	RW% (800 °C)
<b>FBM-50</b>	170, 204	233	253	273	10
<b>OBM-50</b>	186, 236	281	313	329	52

\* as measured by DSC,  $T_d$  = onset of degradation temperature,  $T_{5\%}$  = temperature at which 5 % weight loss occurred,  $T_{10\%}$  = temperature at which 10 % weight loss occurred and RW% = residual weight % at



### 3.1.2.2.5 Solubility, viscosity and molecular weight analysis of sulphonated copolyimides

The solubility of synthesized sulphonated copolyimides was checked in several solvents by dissolving 10 mg polyimide in 1 mL of solvent at 30 °C. These copolyimides are soluble in *m*-cresol at room temperature and in NMP at heating. Sulphonated copolyimides are completely insoluble in all other solvents (non-polar as well as polar) even on heating. *m*-Cresol a highly protic solvent reduces/ or overcomes the chain-chain interactions and improves solubility by penetrating into the polyimide chains.

Sulphonated copolyimides showed very limited solubility which can be assigned to closely packed chains of polyimides. This close packing is responsible for symmetry, rigidity and regularity of sulphonated copolyimide backbone which is responsible for poor solubility. Intramolecular, intermolecular interactions and presence of sulphonate groups resulted in close packing of polymer chains and in turn in poor solubility. Bulky -CF<sub>3</sub> groups of 6FDA inhibited close chain packing and flexible ether linkage of ODPA are responsible for the solubility of these high molecular weight sulphonated copolyimides in highly polar solvents.<sup>30, 36</sup>

The viscosity measurements of SPIs (TEA salt form) were carried out using *m*-cresol as solvent with the concentration of 0.2 gdl<sup>-1</sup> at 30 °C using U-tube Ubbelohd's viscometer. The inherent viscosities ( $\eta_{inh}$ ) were found in the range of 1.584 to 3.250 dL/g depicting highly viscous nature of polymers solutions, indicative of the fact that sulphonated copolyimides have quite high molecular weights.<sup>30, 145</sup> The data is tabulated in **Table 3.8**.

**Table 3.8:** Viscometric data of FBM-50 and OBM-50

Polyimide	$\eta_{rel}$	$\eta_{sp}$	$\eta_{red}$	$\eta_{inh}$
FBM-50	1.915	0.915	4.576	3.250
OBM-50	1.373	0.372	1.860	1.584

$\eta_{rel}$  = relative viscosity,  $\eta_{sp}$  = specific viscosity,  $\eta_{red}$  = reduced viscosity,  
 $\eta_{inh}$  = inherent viscosity

The appreciable enhancement in viscosity with increase in the sulphonated content of the system, from unsulphonated to 50% sulphonated copolymer, was possibly due to an increased ionic content of the polymer solution and not because of an increase of molecular

weight.<sup>146</sup> Similar increase in viscosity was observed with increasing content of sulfonic acid in the polymer backbone in other polyimides investigated in this study.

#### 3.1.2.2.6 Gel permeation chromatographic analysis of sulphonated copolyimides

Molecular weight characterization of sulphonated copolyimides dissolved in hexafluoro isopropanol (HFIP) overnight, was conducted using gel permeation chromatography (GPC). The data is tabulated in **Table 3.9**. The  $M_n$  and  $M_w$  of polyimides were found in the range of 5163 - 8337 g/mol and 14978 - 22379 g/mol respectively demonstrating the high molecular weights of sulphonated copolyimides and PDI values show their polydisperse nature.<sup>60</sup>

Polymers having high molecular weights with a polydispersity index greater than one are expected for step-growth polymerizations. It is likelihood that the molecular weights attained from intrinsic viscosities and GPC may be affected by the sulfonate groups.<sup>146</sup> Undoubtedly, it is associated to increased intermolecular interactions of the polymer backbones.<sup>60</sup>

**Table 3.9:** GPC data of sulphonated copolyimides FBM and OBM copolyimides

Codes	$M_w$ (g/mol)	$M_n$ (g/mol)	PDI
<b>FBM-20</b>	14978	8337	1.7
<b>FBA2-20</b>	21748	6685	3.2
<b>FBA2-40</b>	15827	5428	2.9
<b>OBM-20</b>	22379	5163	4.3

#### 3.1.2.2.7 UV-Visible Spectrophotometric studies of sulfonated copolyimide

UV-Visible spectrophotometric studies were carried out for sulphonated copolyimide OBM-20 (0.01g film) in 10 mL deionized water, at room temperature and neutral pH. An appreciable intensity absorption band around 275 nm was observed after 12 hours and its intensity kept on increasing with passage of time which is an indication of increase in the solubility of sulphonated copolyimide in water with the passage of time. The maximum intensity signal was observed after 60 hours. The absorption bands were

recorded upto 84 hours with a time difference of 12 hours each until the absorption became constant.

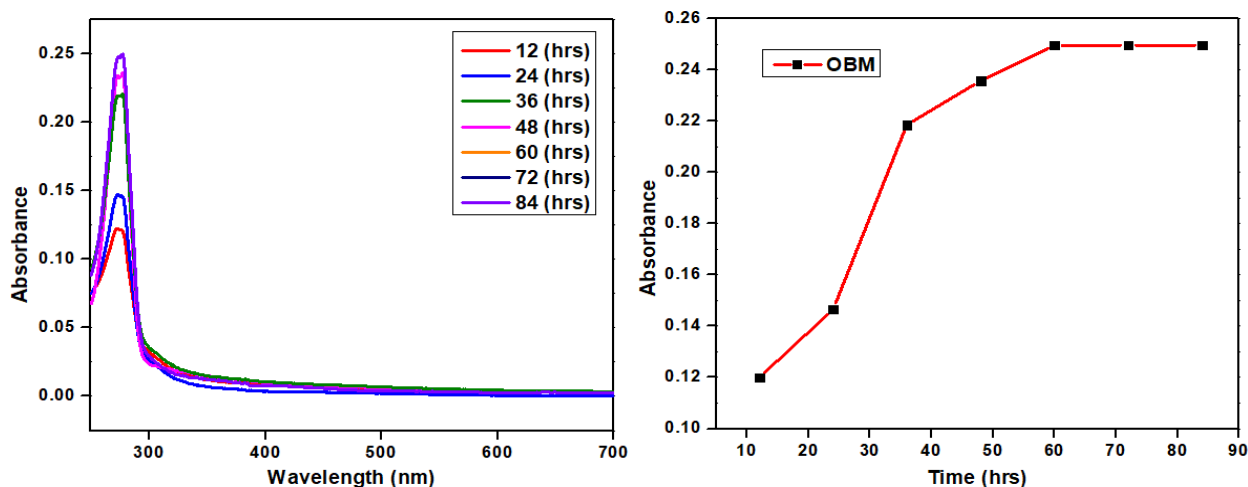


**Figure 3.16:** UV-Vis spectra of OBM-20 (a) and (b) corresponding plot showing time dependent changes in absorbance at  $\lambda_{max}$  in aqueous solution of neutral pH at 25 °C.

### 3.1.2.2.8 Computational studies of SPIs

Computational studies were carried out to theoretically assess the available hydrophilic and hydrophobic accessible surface areas of the copolyimides FBM-50 and OBM-50. Molecular Operating Environment (2016) software with MMFF94x (Hamiltonian force field) employing semi-empirical method was used for molecular surface studies. AM1 semi-empirical method was used for geometry optimization of structures and MMFF94x for energy minimization of each optimized structure.

To investigate the electrostatic behavior of SPIs, both FBM-50 and OBM-50 were drawn by MOE builder tool (**Figure 3.17**). In these figures, green dotted area represents hydrophobic part of molecule, blue area shows hydrophilic part while pink dots show hydrogen bonding part of molecules. Based on electrostatic surface map, it was found that OBM-50 has a larger hydrophilic surface area than FBM-50 hence it is more hydrophilic and will show more interactions with water as compared to FBM-50. The dipole moment, water accessible surface area and total hydrophobic surface area were calculated for these molecules and data is tabulated in **Table 3.10**. The water accessible surface area for OBM-

50 is 738.247 and that for FBM-50 is 593.259 which also confirmed the more electrostatic integrations of OBM-50 with water molecules as compared to FBM-50.

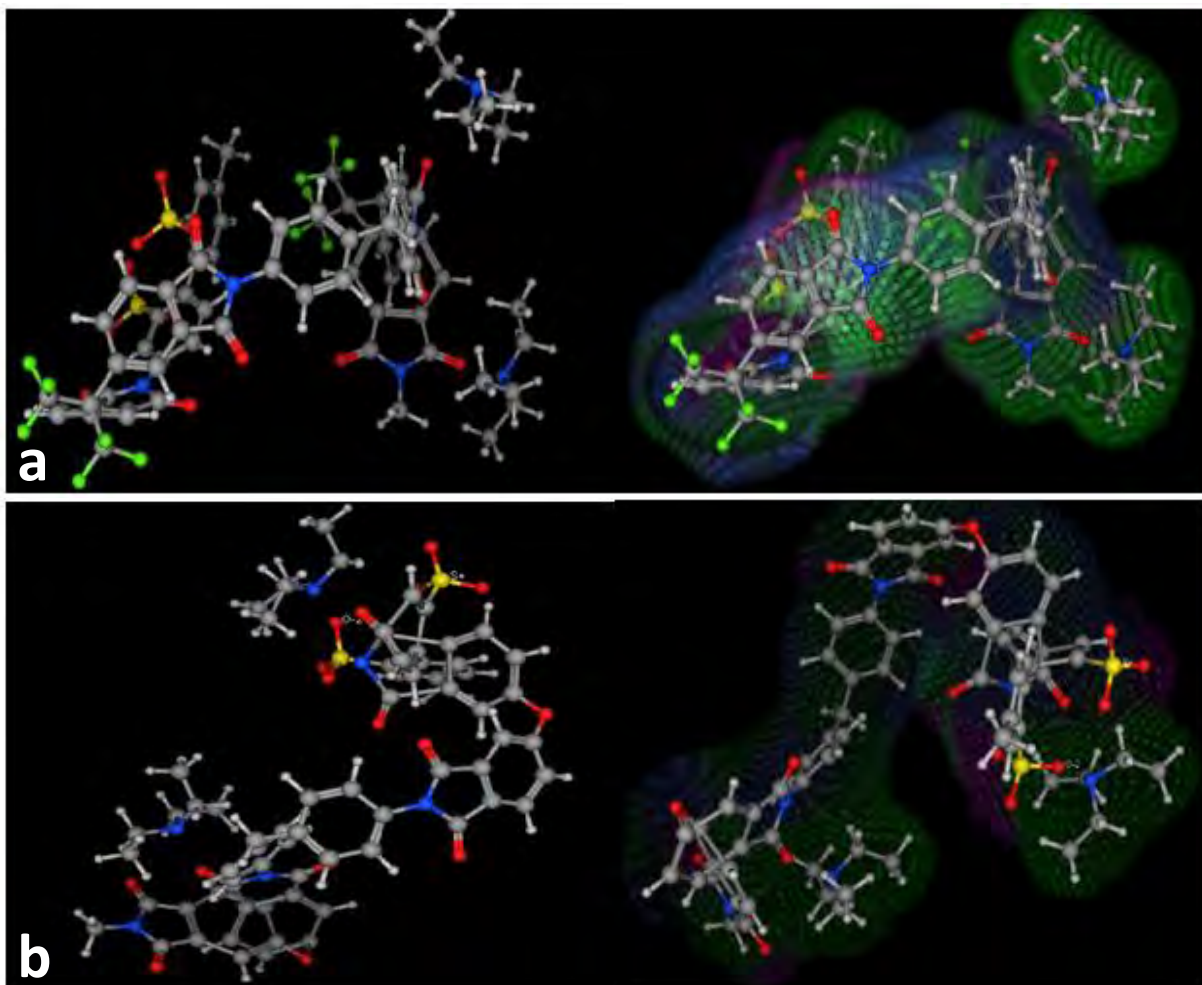


**Figure 3.17:** 3D view of (a) FBM-50 (b) OBM-50 in ball and stick and their electrostatic surface map.

**Table 3.10:** Molecular descriptors for FBM and OBM complexes

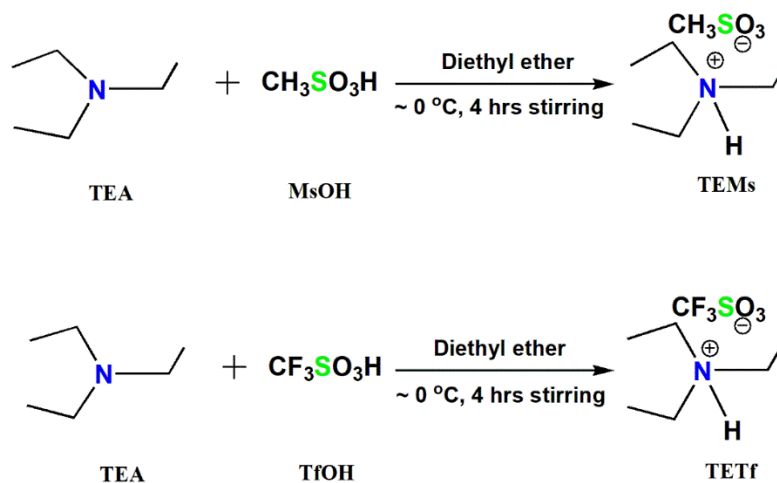
SPIs	Dipole moment	Water accessible surface area (ASA)	Accessible surface area hydrophobic (ASAH)
FBM	0.0000	593.2592	593.2592
OBM	0.0000	738.2473	356.7329

### 3.1.3 Synthesis of sulphonated copolyimides/protic ionic liquid composites

The synthesis of composites was carried out in two steps where, protic ionic liquids were synthesized in first step followed by the synthesis of protic ionic liquid composites in second step.

#### 3.1.3.1 Synthesis of protic ionic liquids

Synthesis of protic ionic liquids was carried out using equimolar combinations of Brønsted acid and Brønsted base (Scheme 3.5).



**Scheme 3.5:** Synthesis of protic ionic liquids (PILs).

Two different sulphonic acids and four tertiary amines were used to synthesize eight protic ionic liquids. Structures of sulphonic acids, tertiary amines are protic ionic liquids are given in **Figure.3.18** and codes in **Table 3.11**.

#### Sulphonic acids

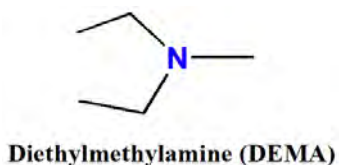
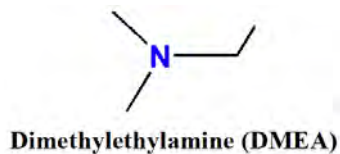
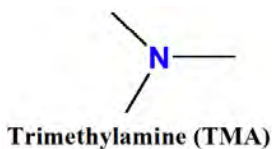


Methanesulphonic acid (MsOH)



Trifluoromethanesulphonic acid (TfOH)

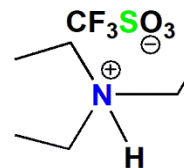
#### Tertiary amines



## Ionic Liquids



Triethylammonium methanesulphonate (TEMs)



Triethylammonium trifluoromethanesulphonate (TETf)

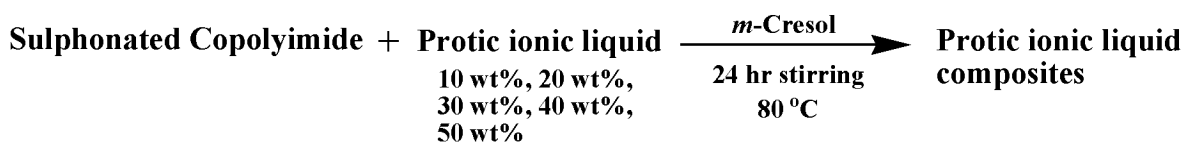
**Figure 3.18:** Structures of Brønsted acids, Brønsted bases and triethyl amine ionic liquids

**Table 3.11:** Codes for PILs

#	Codes	Amine	Acid
1	DEMs	DEMA	MsOH
2	DETf	DEMA	TfOH
3	DMMs	DMEA	MsOH
4	DMTf	DMEA	TfOH
5	TEMs	TEA	MsOH
6	TETf	TEA	TfOH
7	TMMs	TMA	MsOH
8	TMTf	TMA	TfOH

### 3.1.3.2 Synthesis of composites (SPI/IL)

The fabrication of composite membranes was achieved by solution casting method (Scheme 3.6).



**Scheme 3.6:** Synthesis of protic ionic liquid composites.

Appropriate amounts of protic ionic liquids (10, 20, 30, 40 and 50 wt%) were added to *m*-cresol solution of sulphonated copolyimide in a glass vial equipped with magnetic stirrer. Overnight stirring of the reaction mixture was carried out at 80 °C to ensure the

complete dissolution and the solution was then casted on glass petri dish. *m*-Cresol was evaporated at 80 °C for the fabrication of a uniform composite membrane. The membrane was peeled off from the petri dish, dried in vaccuum oven at 80 °C for 24 hours and then stored in an inert atmosphere (**Table 3.12**).

**Table 3.12:** Codes and percentage compositions of composites with PIL (TEMs)

#	Codes	SPI	PIL
1.	FBM-20/IL (10%)	FBM-20	TEMs (10%)
2.	FBM-20/IL (20%)	FBM-20	TEMs (20%)
3.	FBM-20/IL (30%)	FBM-20	TEMs (30%)
4.	FBM-20/IL (40%)	FBM-20	TEMs (40%)
5.	FBM-20/IL (50%)	FBM-20	TEMs (50%)
6.	FBA2-10/IL (20%)	FBA2-10	TEMs (20%)
7.	FBA2-20/IL (20%)	FBA2-20	TEMs (20%)
8.	FBO-10/IL (20%)	FBO-10	TEMs (20%)
9.	FBO-20/IL (20%)	FBO-20	TEMs (20%)
10.	FBO-30/IL (20%)	FB0-30	TEMs (20%)
11.	FBO-40/IL (20%)	FBO-40	TEMs (20%)
12.	FBM-50/IL (20%)	FBM-50	TEMs (20%)
13.	FBM-10/IL (20%)	FBM-10	TEMs (20%)
14.	FBM-20/IL (20%)	FBM-20	TEMs (20%)
15.	FBM-30/IL (20%)	FBM-30	TEMs (20%)
16.	FBM-40/IL (20%)	FBM-40	TEMs (20%)
17.	FBM-50/IL (20%)	FBM-50	TEMs (20%)

Ionic liquids with different substitutions on N of the Bronsted bases were prepared and checked. Different weight percentages of protic ionic liquids were added in the SPIs matrix ranging between 10, 20, 30, 40 and 50 wt %. These composite membranes retained upto 50 wt % [TEMs] successfully. To achieve stable composite membranes synthesis, compatibility between polyimide matrix and the PIL additive is very important.<sup>59</sup> The sulphonated copolyimides (SPIs) were employed in triethylammonium salt form in the composite membranes, since the polyimides with a triethylammonium sulfonate group showed good compatibility with TEMs. The structural similarity between the two phases contributed to good compatibility, therefore all the composites were prepared with TEMs.

### 3.1.3.2.1 FTIR Studies of composite membranes

The synthesis of composites was confirmed through FTIR spectroscopic studies. The comparative spectra of sulphonated copolyimide (FBM-20) and its ionic liquid composite [FBM(20).IL(20)] are shown in **Figure 3.19**. SPI/IL composite membrane exhibited characteristic  $\text{-CH}_3$  group absorption around  $2800\text{ cm}^{-1}$  as compared to FTIR spectrum of SPI. The appearance of broad band around  $3400\text{ cm}^{-1}$  in composite could be attributed to hydrogen bonding between  $\text{-SO}_3$  and  $\text{R}_3\text{NH}^+$  alongwith this an increase in the intensity of sulphonte group peak around  $1083\text{ cm}^{-1}$  can be observed upon additon of ionic liquid. The FTIR spectra gave a convincing indication of successful formation of SPI/IL composite.

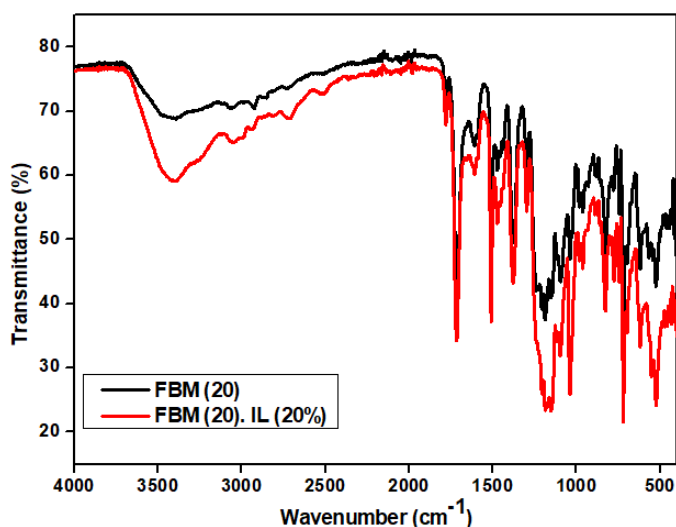


**Figure 3.19:** FTIR spectra of FBM-20/IL (20%).



### 3.1.3.2.2 Morphological studies of composites

XRD studies were carried out for the morphological studies of composite membranes. Upon addition of ionic liquids in SPI the peak intensity of SPI decreased and it kept on decreasing upon increasing the wt % of added ionic liquid as can be seen in **Figure 3.20**. The decrease in peak intensity depicts that addition of ionic liquids plasticized the SPI and as a result increased the flexibility of composite membranes.<sup>147</sup>

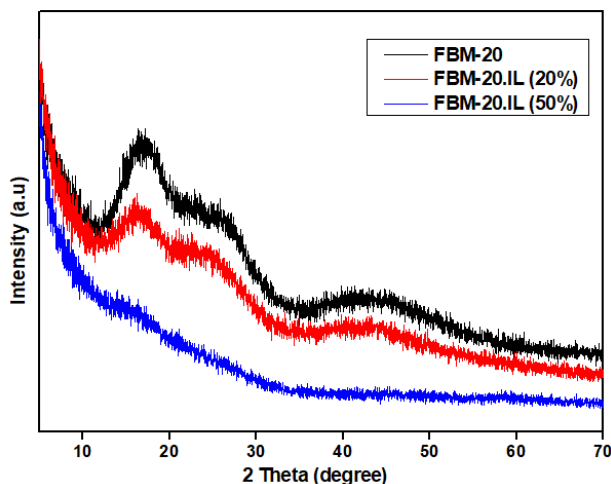


**Figure 3.20:** Comparative XRD patterns of FBM-20, FBM-20/IL (20%) and FBM-20/IL (50%).

### 3.1.3.2.3 Gel permeation chromatographic analysis of composites

Molecular weight characterization of protic ionic liquid composites dissolved in hexafluoro isopropanol (HFIP) overnight, was conducted using gel permeation chromatography (GPC) where weight and number average molecular weights and PDI were ascertained. The data is tabulated in **Table 3.13**. The  $M_n$  and  $M_w$  of polyimides were found in the range of 14045 - 21078 and 31834 - 41726 g/mol respectively demonstrating the high molecular weights of composites.

**Table 3.13:** GPC data of composites FBM-20/IL (50 %) and FBA2-20/IL (20 %)

Codes	$M_w$ (g/mol)	$M_n$ (g/mol)	PDI
FBM-20/IL (50%)	31834	21078	1.5
FBA2-20/IL (20 %)	41726	14045	2.9

### 3.2 Heavy metal sensing studies of SPI (OBM-20)

The metal sensing studies of OBM-20 towards Ni (II), Co (II) and Cr (III) were carried out using UV-Visible spectrophotometric technique. In the absence of any metal, the absorption bands and intensity of the absorption bands of OBM-20 (0.01g) in the deionized water were recorded at room temperature and at neutral pH, as shown in **Figure 3.16** (section 3.1.2.2.7). The polyimide showed an absorption band around 275 nm and its intensity kept on increasing with the passage of time that is an indication of increase in the solubility of sulphonated co-polyimide in water with passage of time and became constant after 60 hours. In the presence of metal ions an appreciable increase in the absorption intensity of these bands was observed. This increase in the absorption intensity in the presence of metal ions was examined carefully to evaluate the metal sensing behaviour of OBM-20 in aqueous media.

#### 3.2.1 Electronic absorption variations of OBM-20 by divalent and trivalent metal ions

In order to check the metal responsive behaviour of OBM-20 in aqueous media, the UV-Vis absorption spectra were recorded by adding the same amount (0.01g) of the sulphonated copolyimide (OBM-20) in 0.01 N solutions (deionized water) of three metal ions [Ni (II), Co (II) and Cr (III)] separately under the same conditions and for same time duration. The changes in the intensity of absorption spectra of the OBM-M<sup>n+</sup> complexes were monitored for the three metal ions solutions separately and shown in **Figures (3.21, 3.22 and 3.23)**. The absorption intensity of OBM-20 exhibited distinguishing increase in absorption band in the presence of metal ions. The increase in the absorption peak of OBM-20 was observed carefully and was attributed to the formation of OBM-M<sup>n+</sup> complex. The ratio of  $I_{\text{OBM}}/I_{\text{OBM-M}^{2+}}$  was increased from 0.247 to 0.285, 0.289 and 1.036 for Co (II), Cr (III) and Ni (II) respectively. An increased absorption was observed for OBM-M<sup>2+</sup>. Absorbance was increased for all the three metal ions with a marginal difference in the increased intensity of Co (II) and Cr (III), as shown in **Figures 3.21 and 3.22** respectively.

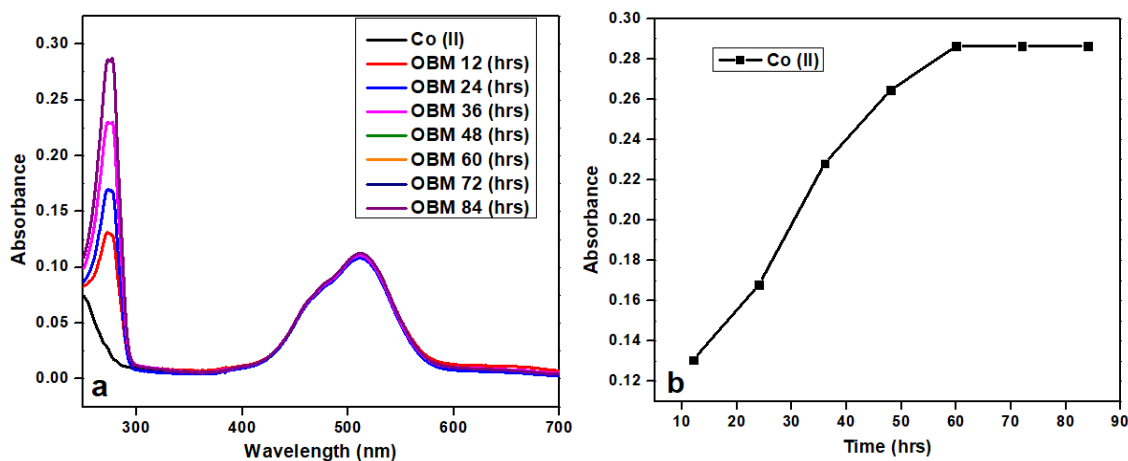


**Figure 3.21:** (a) UV-Vis spectra of OBM-20 in the presence of Co (II) and (b) corresponding plot showing time dependent changes in absorbance at  $\lambda_{max}$  in aqueous solution of neutral pH at 25 °C.

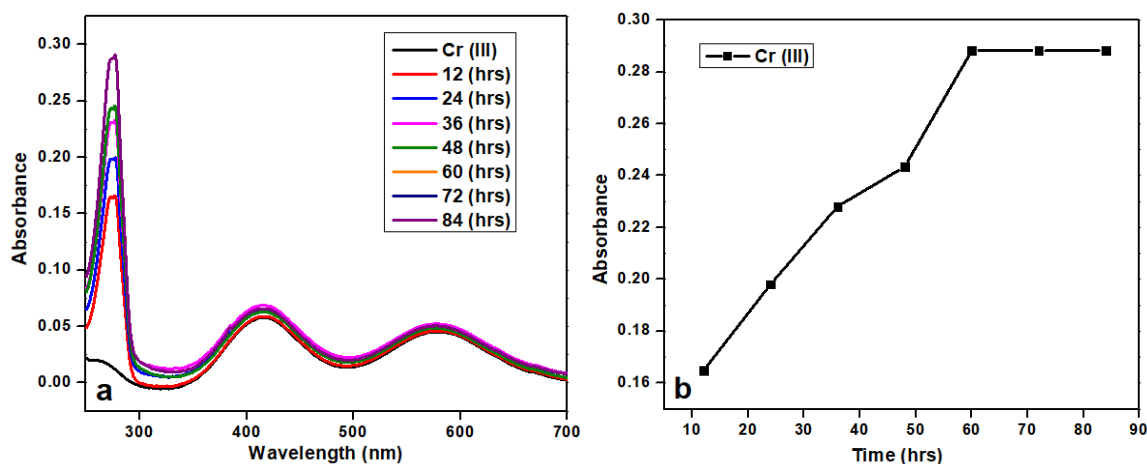


**Figure 3.22:** (a) UV-Vis spectra of OBM-20 in the presence of Cr (III) and (b) corresponding plot showing time dependent changes in absorbance at  $\lambda_{max}$  in aqueous solution of neutral pH at 25 °C.

Interestingly, Ni (II) showed an appreciable increase in the absorption of OBM-20 which can be attributed to the stronger chelation of Ni (II) with the sulphonated copolyimide resulting in more soluble metal-ligand complex as shown in **Figure 3.23**. The comparison of absorbance intensities of co-polyimide and metal complexes are given in **Table 3.14**. These results led us to postulate that Ni (II) ions form a stronger complex with OBM-20 as compared to the other ions.

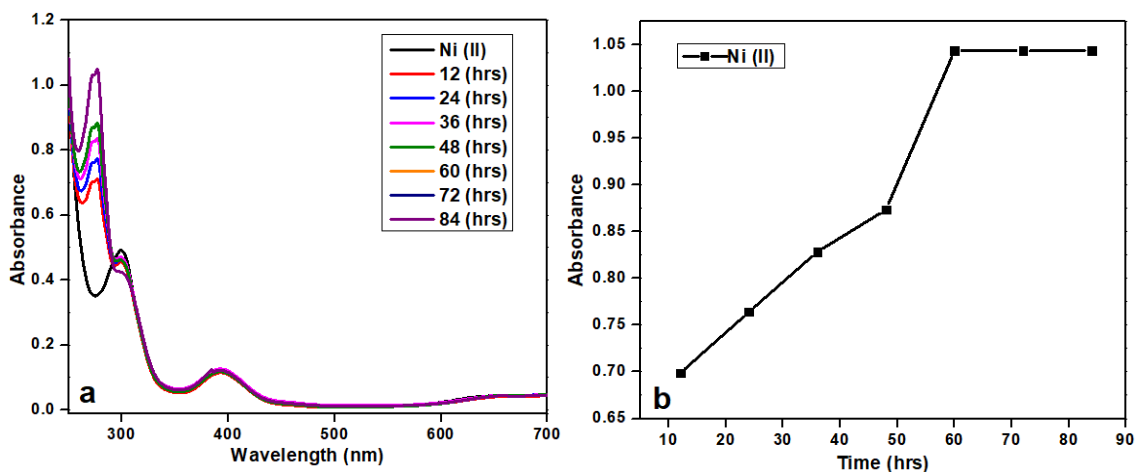


**Figure 3.23:** (a) Changes in absorption spectrum of OBM-20 in the presence of Ni (II) and (b) corresponding plot showing time dependent variation in absorbance at  $\lambda_{max}$  in neutral pH at 25 °C.

**Table 3.14:** Comparison of the absorbance intensities of OBM-20 in the absence and presence of Ni (II), Co (II) and Cr (III)

Time	OBM-20	Ni (II)[OBM-20]	Co (II)[OBM-20]	Cr (III)[OBM-20]
12 hrs	0.122	0.703	0.128	0.164
24 hrs	0.14	0.763	0.168	0.198
36 hrs	0.218	0.828	0.228	0.234
48 hrs	0.235	0.873	0.262	0.263
60 hrs	0.247	1.036	0.285	0.289
72 hrs	0.247	1.036	0.285	0.289
84 hrs	0.247	1.036	0.285	0.289

As OBM-20 complexes more effectively with Ni (II) as compared to Co (II) and Cr (III), it is thus concluded that the complexation ability of OBM-20 seems to be dependent on the ionic radii of chelating metal ions.<sup>148</sup> The dissolution of OBM-20 in water is a slow process, however, dissolved OBM-20 responds to metal ions immediately. By providing an equilibration time of 10 minutes to the solution of dissolved OBM-20 and salts of metal ions, the variation in the absorption signal of OBM-20 was used for the sensing of Ni (II), Co (II) and Cr (III) with detection limits of 0.01 nM, 1.00 nM and 0.01 nM respectively.

### 3.2.1.1 Effect of pH

To evaluate the effect of pH on the sensing potential of OBM-20 towards [Ni (II), Co (II) and Cr (III)] ions, UV-Visible spectroscopic experiments were carried out in solution of different pH (acidic, neutral and basic media). An aqueous solutions of HCl (0.1 M) and NaOH (0.1 M) were used to control the pH values. The absorption spectra were recorded at room temperature (25 °C) and the graphs were plotted between absorbance vs wavelength as shown in **Figure 3.24**.

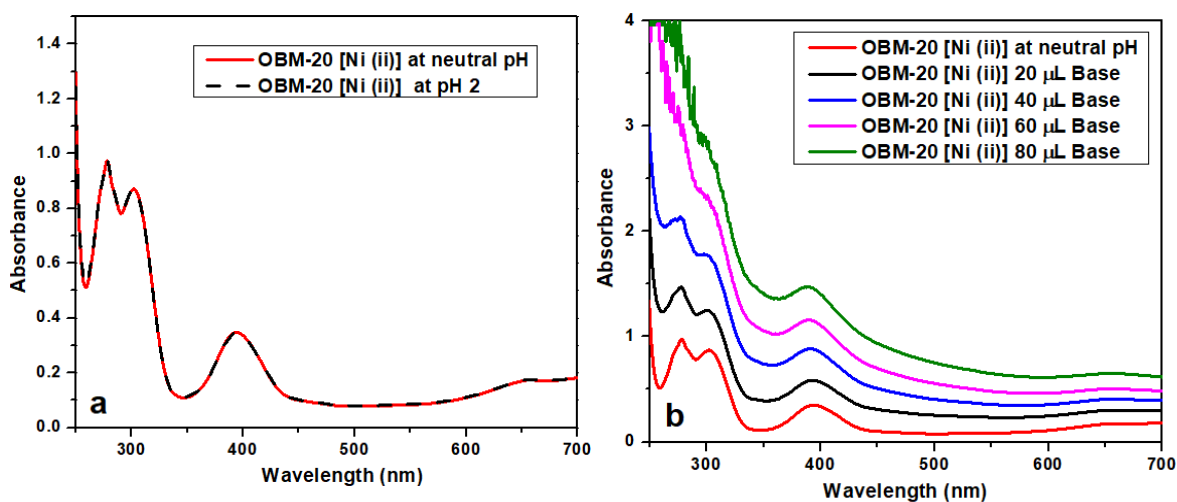


**Figure 3.24:** Absorption spectra of OBM-20 in the presence of Ni (II) a) at pH 2.0 b) at pH 8.0-9.0.

No change in absorption band or intensity was observed in acidic medium (pH = 2.0) and the two absorption bands of OBM-20 recorded in solutions of (pH = 2.0 and neutral pH) were found to be indistinguishable. Similar behavior was noticed for Co (II) and Cr (III). In basic medium at pH = 9, the solutions became turbid that can be attributed to the formation of hydroxides of respective metal ions.

### 3.2.1.2 Effect of interfering ions

Detection of targeted analyte with selectivity in the presence of other analytes is an essential property of a sensor. To check the selectivity of OBM-20 for the sensing of target metal ions, competitive experiments were performed in the presence of common interfering ions (Fe (II), Mg (II), Ca (II), K (I) and Na (I)) existing in water. These five metal ions (0.01 N) were treated under similar experimental conditions in the presence of Ni (0.01 N) and variations in the absorbance were recorded. For examining the interference effect 1

mL salt solution of competitive metal ions was added to 1 mL solution of OBM-20+Ni (II) at similar experimental conditions. Fresh solution of OBM-20+Ni (II) was used for detecting all the interfering ions. The study revealed that the presence of standard solutions of interfering ions (Na (I), K (I) Mg (II) and Ca (II)) influence the intensity of absorption band to a negligible extent except due to dilution by the addition of second salt solution. However, Fe (II) showed pronounced interference effect on the intensity of OBM-20+Ni (II). Co (II) showed same behaviour as can be seen for Ni (II) in **Figure 3.25**. and for Co (II) in **Figure 3.26 (a)** whereas Ca (II) and Mg (II) alongwith Fe (II) affected the intensity of OBM-20+Cr (III) (**Figure 3.26 (b)**). This difference in the interference effects of different metal ions can be attributed to the different charge and atomic radius of chromium ion than nickel and cobalt ions. Therefore, on the basis of these results it can be concluded that OBM-20 is selective for the sensing of Ni (II) and Co (II) in the presence of common interfering ions except Fe (II).

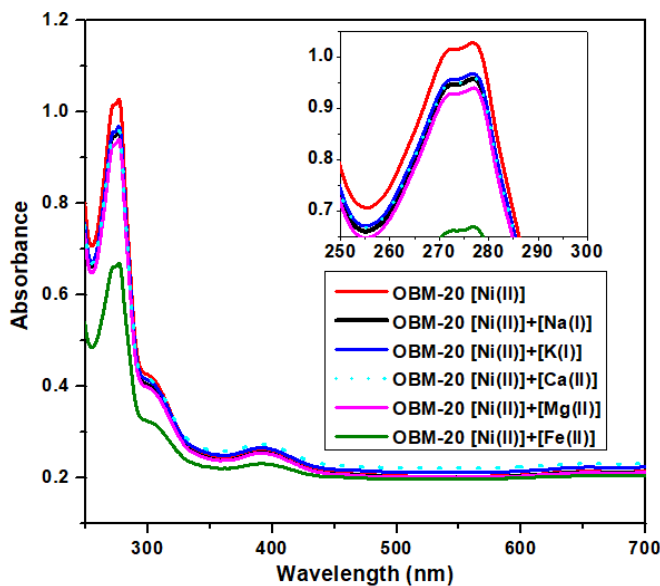


**Figure 3.25:** Selectivity of OBM-20 towards Ni (II) in the presence of interfering ions [Na (I), K(I), Ca (II), Mg (II), Fe (II)].

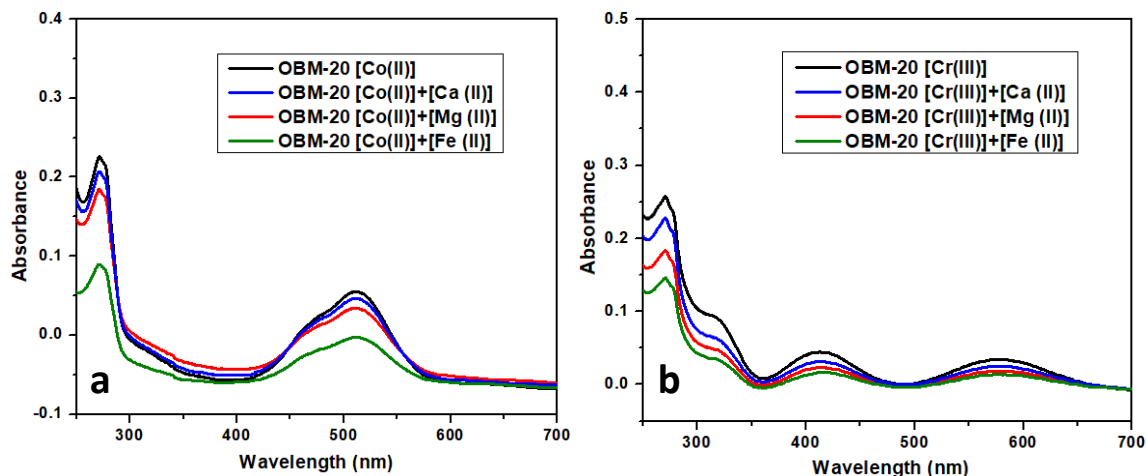


**Figure 3.26:** Selectivity of OBM-20 towards a) Co (II) b) Cr (III) in presence of interfering ions [Ca (II), Mg (II), Fe (II)].

### 3.2.1.3 Limit of Detection (LOD)

To study the sensitivity of OBM-20 towards metal ions concentration, UV-Visible titration experiments were performed in deionized water at room temperature and neutral pH. For this purpose, in the solution of OBM-20 (0.01 g / 10 mL), the molar concentration of metal ions was varied from 0.01 nM to 0.01 M for Ni (II) and Cr (III) and from 1.00 nM to 0.01 M for Co (II). The corresponding spectra can be seen in **Figure 3.27** and **Figure 3.28 (a), (b)** respectively. An observation of **Figure 3.28** revealed that the absorption band of OBM-20 (275 nm) having absorption intensity of 0.318 could be observed in 0.01 nM solution of Ni (II). The increase in the solubility of OBM-20 after 12 hours from 0.122 to 0.138 can be attributed to the stronger chelation of Ni (II) with the sulphonated copolyimide resulting in more soluble metal-ligand complex (see table 3.13). These results depicted that OBM-20 can sense the nanomolar concentration of Ni (II). It can also be seen that increasing the concentration of metal ions results in increased absorption intensity of OBM-20. Similar behaviour was shown by Co (II) (**Figure 3.28 (a)**) and Cr (III) (**Figure 3.28 (b)**) with LOD values of 1.00 nM and 0.01 nM respectively. Consequently, it can be inferred that the designed polymer can be employed to sense the tested metal ions upto nanomolar concentration.

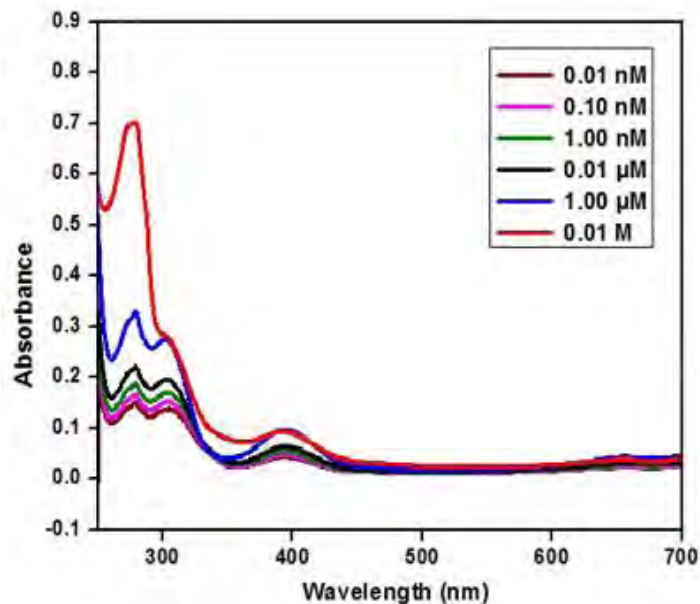


**Figure 3.27:** Absorption spectra of OBM-20 in various concentrations (0.01 nM-0.01 M) of Ni (II).

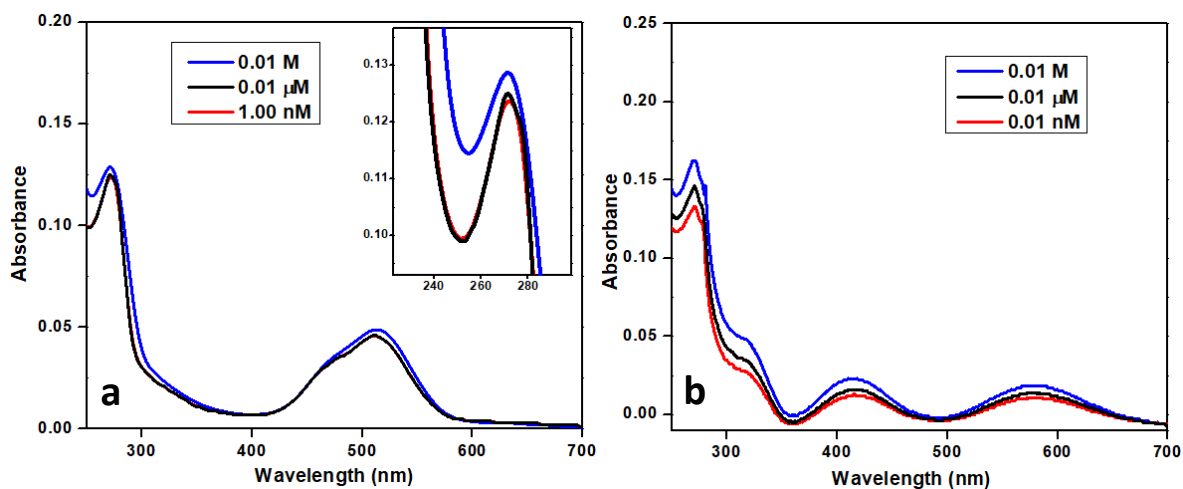


**Figure 3.28:** Absorption spectra of OBM-20 in various concentrations of a) Co (II) (1 nM-0.01 M) b) Cr (III) (0.01 nM-0.01 M).

All these results indicated that sulphonated copolyimide (OBM-20) can be used as a chemical sensor at neutral pH and could be applied for spectrophotometric determination of the metal ions under study in nanomolar concentration with negligible effect of common interfering ions except iron.



### 3.3 Lead ions adsorption studies of SPIs (FBM-50 and OBM-50)

Lead (II) adsorption studies were carried out for both 6FDA and ODPDA dianhydrides based sulphonated copolyimides (FBM-50 and OBM-50) using atomic absorption spectroscopy. The experimental parameters were optimized for efficient adsorption conditions. In addition, quantum chemistry calculations using Molecular Operating Environment (MOE) software were performed, to scrutinize the experimental results for molecular surface studies. A good correlation was observed between computational and experimental findings.

#### 3.3.1 Optimization of parameters

Lead salt solution was prepared by dissolving  $\text{Pb}(\text{NO}_3)_2$  in deionized water. Adsorption process was performed using adsorbent dose in range of 0.01 to 2 g while all other conditions were kept constant (adsorption conditions: contact time 60 min; adsorption medium volume, 10 ml; 25 °C and neutral pH). The adsorbent dose dependent  $q_e$  of Pb (II) is shown in **Figure 3.29 (a)**. It was observed that lead ions removal increased as the adsorbent dose was increased upto a limit (0.1 g). In fact, available active sites for adsorption of lead ions increased with an increase in adsorbent dose due to which removal of lead ions was also increased. After certain adsorbent dose, maximum number of metal ions were adsorbed and further increase in its amount did not influence the value of metal ions removal due to the establishment of equilibrium between metal ions in solution and metal ions adsorbed over adsorbent surface. Therefore, 0.1 g adsorbent was used for further experimentation.

The next step was to change the metal ions concentration to evaluate the optimum concentration of adsorbate. **Figure 3.29 (b)** shows an increase in metal ions concentration increased the removal at ambient temperature. However, at very high metal ions concentration, saturation of adsorption sites of the adsorbent was achieved thus no more increase in adsorption of metal ions was observed. The maximum percentage removal of 99 and 30 was obtained by OBM-50 and FBM-50 respectively, at 50 ppm metal ions concentration.

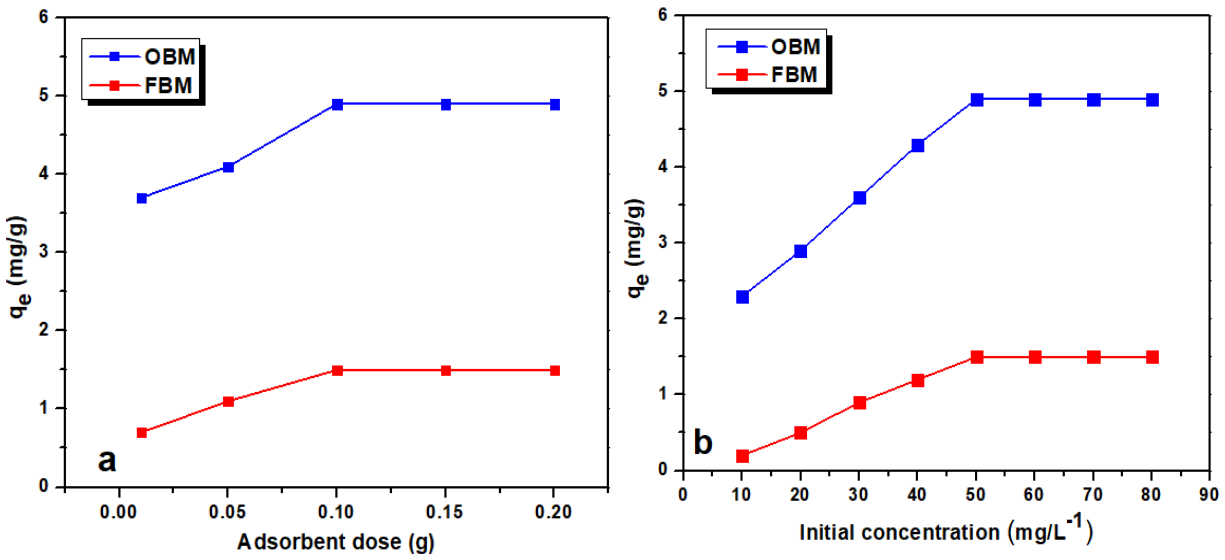


**Figure 3.29:** (a) Effect of adsorbent dose (b) initial ions concentration on the adsorption capacity of sulphonated copolyimides (FBM-50 and OBM-50). Adsorption conditions: contact time 60 min; adsorption medium volume, 10 ml; 25 °C and neutral pH.

The adsorption of metal ions was thoroughly investigated above and below 50 ppm particularly at 40 ppm and 60 ppm concentration (**Figure 3.30**). All the experiments were repeated thrice, and average values were calculated with maximum standard deviation of  $\pm 0.04$ . After comparing all the results for the effect of initial ions concentration, 50 ppm metal ions concentration was selected for further experimentation.

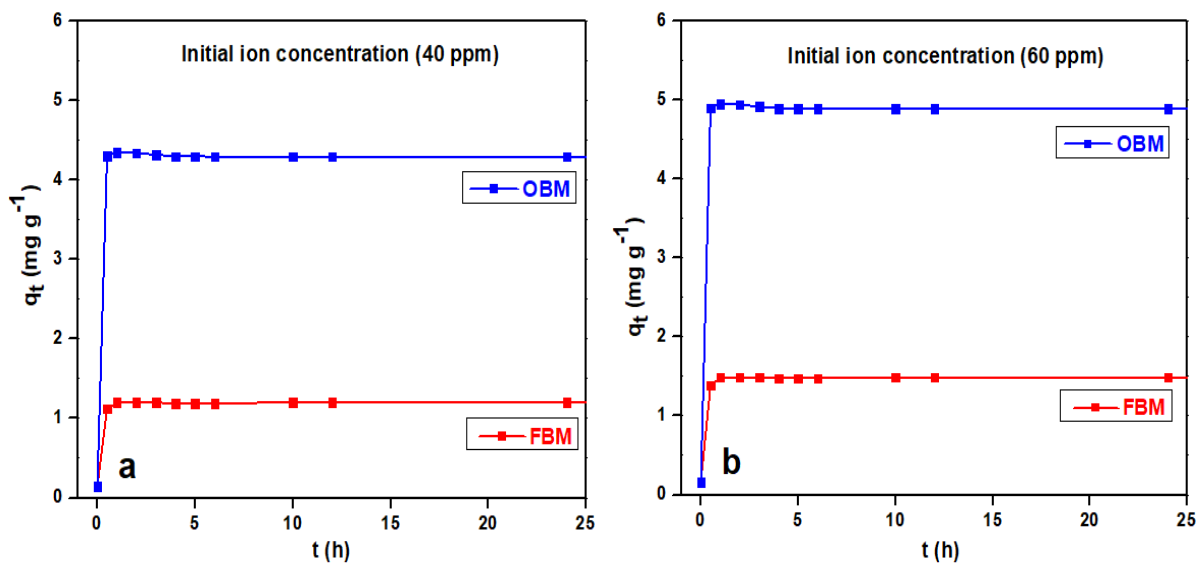


**Figure 3.30:** Time course for the adsorption of heavy metal ions on sulphonated polyimides. Adsorption conditions: (a) 40 ppm concentration, (b) 60 ppm concentration, adsorption medium volume, 10 ml; 25 °C and neutral pH.

It is well known that the charge on adsorbent (copolyimide) and on adsorbate (metal ions) depends upon pH of medium which alternatively affects the adsorption rate of metal ions. **Figure 3.31** shows the effect of pH on adsorption of lead ions.

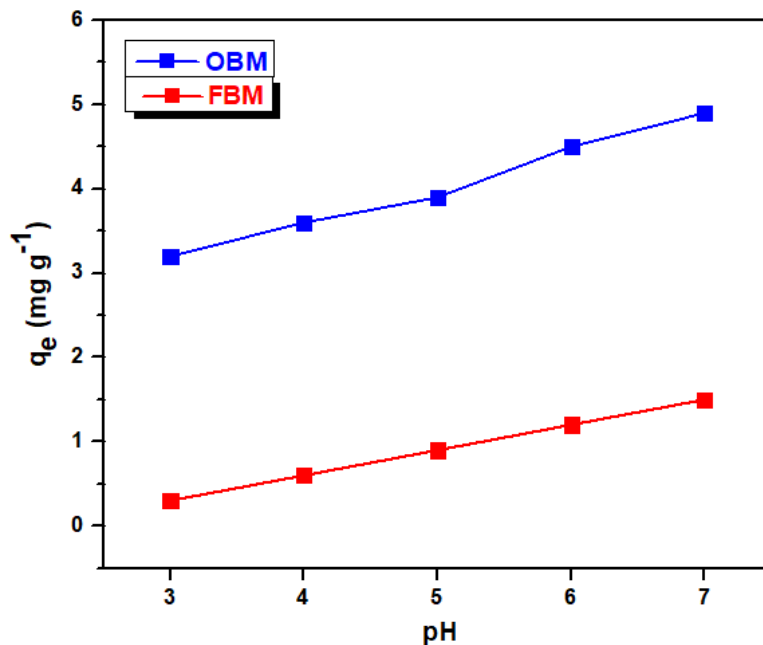


**Figure 3.31:** The effect of change in pH of adsorption medium on the adsorption capacity of sulphonated copolyimides (FBM and OBM). Adsorption conditions: contact time 60 min; adsorption medium volume, 10 ml; 25 °C and neutral pH.

It can be seen from **Figure 3.31**, that the adsorption of lead ions increases with an increase in pH of the medium with maximum adsorption obtained at pH 7. At low pH sulphonic acid groups of copolyimides are protonated and positively charged lead ions are hindered to be adsorbed on the surface. Thus, the percentage removal of metal ions as well as adsorption capacity of copolyimides is decreased at low pH of medium. At neutral pH the sulphonic acid groups are deprotonated and adsorption of metal ions is increased. Thus, free sulphonic acid groups form complexes with positively charged lead ions via electrostatic interactions and result in maximum adsorption. But in basic medium, at high pH precipitation occurred which can be attributed to hydrolysis of Pb (II) ions to  $\text{Pb}(\text{OH})_2$ . Thus, neutral pH was found optimum for maximum lead ions adsorption and further experiments were carried out at neutral pH. All the experiments were repeated three times and average values were calculated. The maximum uncertainty was found to be 4%.

### 3.3.2 Adsorption kinetics of lead ions

Kinetics of lead ions adsorption was studied using 50 ppm adsorbate solution. The adsorbent (0.1 g) was added to 10 mL of adsorbate solution and samples were analyzed after 0.5, 1, 2, 3, 4, 5, 6, 10, 12, and 24 h of contact. To ensure the removal of any suspended material centrifugation was done. After that, centrifuged liquid was examined for the determination of residual concentration of lead ions by AAS. Quantity of adsorbed lead ions by sulphonated copolyimides  $q_e$  ( $\text{mg g}^{-1}$ ) and adsorption percentage were calculated by means of Eq. (3.1) and Eq. (3.2) respectively: <sup>21</sup>

$$q_e M = V(C_o - C_e) \quad (\text{Equation 3.1})$$

$$\text{Metal ions adsorbed (\%)} = C_o - C_e / C_o \times 100 \quad (\text{Equation 3.2})$$

Where, M is the amount of adsorbent used (g), V is the volume of the solution (L) and  $C_o$  and  $C_e$  are the initial and final heavy metal ion concentrations in solution ( $\text{mg L}^{-1}$ ) respectively. <sup>21, 149</sup>

Pseudo-first and pseudo-second-order rate equations were used to analyze the lead ions adsorption rate onto sulfonated polyimide adsorbent. Pseudo 1<sup>st</sup> order rate equation Eq. (3.3) in linear form is represented as follow <sup>21</sup>

$$\ln(q_1 - q_t) = \ln q_1 - k_1 t \quad (\text{Equation 3.3})$$

Where,  $q_1$  ( $\text{mg g}^{-1}$ ) is adsorbed amount at equilibrium,  $q_t$  ( $\text{mg g}^{-1}$ ) is amount of Pb ions adsorbed at time t and  $k_1$  is pseudo-first-order rate constant ( $\text{h}^{-1}$ ). By the linear plot of  $\ln(q_1 - q_t)$  versus t,  $k_1$  can be determined.

For the calculations of pseudo 2<sup>nd</sup> order parameters, pseudo 2<sup>nd</sup> order rate equation Eq.(3.4) was employed in its linear form; <sup>150</sup>

$$t/q_t = 1/k_2 q_2^2 + (1/q_2)t \quad (\text{Equation 3.4})$$

where  $k_2$  ( $\text{g mg}^{-1}\text{h}^{-1}$ ) is the second-order rate constant of adsorption,  $q_2$  ( $\text{mg g}^{-1}$ ) is the amount of adsorbate [Pb (II)] adsorbed at equilibrium, and  $q_t$  ( $\text{mg g}^{-1}$ ) is the adsorbate contacting the adsorbent at any time t. The linear variation of  $t/q_t$  versus t was employed to calculate  $k_2$  and  $q_2$ . Comparison between calculated and experimental  $q_e$  confirmed the rationality of the calculated equation and assumed order of reaction.

### 3.3.2.1 Adsorption kinetics and contact time effects

For the determination of optimum contact time for the adsorption of Pb (II) on SPIs, the outcome of contact time on lead ions adsorption was investigated. Removal of the maximum amount of metal ions from solution with the saturation of membrane ionic sites refers to the adsorption capacity. **Figure 3.32 (a)** shows the effect of adsorption time of Pb (II) on SPIs (FBM-50 and OBM-50). Fast adsorption kinetics was observed within first 50 mins with adsorption equilibrium attained in 60 mins. Therefore, 60 min was set as the optimum equilibration time. Maximum adsorption capacities in SPIs were found to be 99 and 30% with values of  $q_e$  4.9 and 1.5 mg/g for OBM-50 and FBM-50 respectively.

The intercepts of plot of  $t/q_t$  vs  $t$  were employed to calculate pseudo 2<sup>nd</sup> order rate constants, shown in **Figure 3.32 (b)**. For Pb (II) adsorption on OBM-50 and FBM-50, the values of  $R^2$  (0.999, 0.999) obtained by using pseudo 2<sup>nd</sup> order kinetic equations were closer to unity in comparison to those  $R^2$  (0.215, 0.323) for pseudo 1<sup>st</sup> order kinetics respectively. These results indicated the best explanation of lead ions adsorption phenomenon by 2<sup>nd</sup> order rate equation. Higher values for  $k_2$  were obtained for Pb (II) ions adsorption as compared to  $k_1$ . Thus, results indicated adsorption of lead ions followed pseudo 2<sup>nd</sup> order kinetics, as shown in **Figure 3.32**.

Kinetic parameters for pseudo 2<sup>nd</sup> and pseudo 1<sup>st</sup> order rate equations are given in **Table 3.15**.

According to literature, for a chelating polymer, kinetics is significantly controlled by polymeric backbone characteristics, as it relies on the presence of chelating functional groups and their accessibility without steric hindrance.<sup>151</sup> Efficient metal ions adsorption on SPIs can be credited to the presence of sulfonate groups. These groups interact by electrostatic attractions with lead ions and are responsible for hydrophilic and strongly acidic nature of adsorbents. In this study, time required to attain equilibrium for adsorption of Pb (II) ions on SPIs (60 minutes) seems suitable from kinetic considerations when compared with results stated in literature where time required to attain equilibrium ranged from 30 min to 7 h.<sup>152, 153</sup>

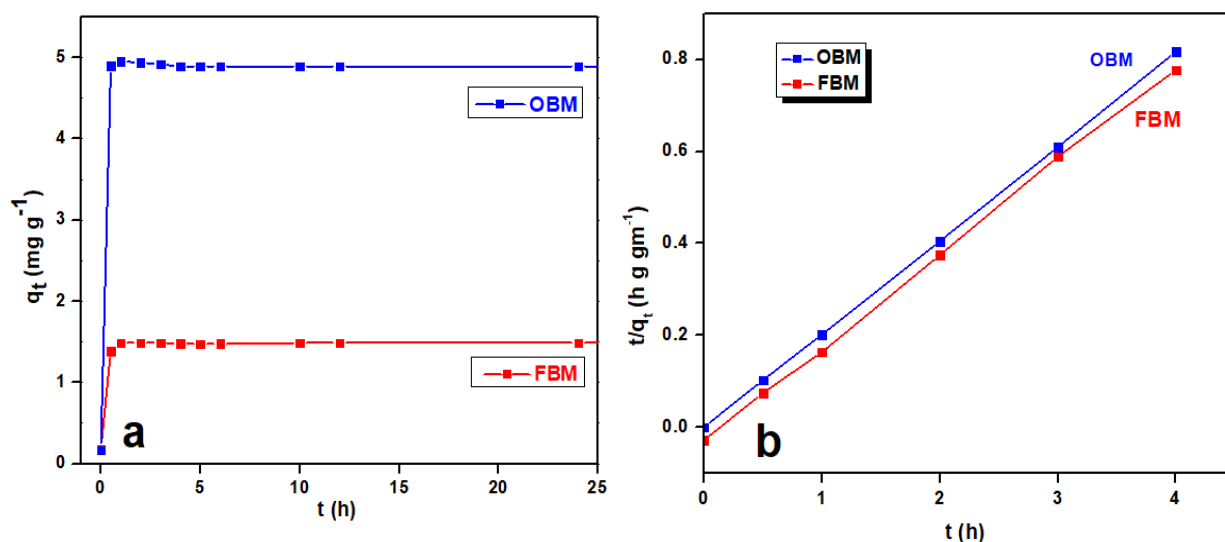


**Figure 3.32:** Adsorption kinetics (a) Time course for the adsorption of heavy metal ions on sulphonated polyimides. Adsorption conditions: 50 ppm concentration, adsorption medium volume, 10 ml; 25 °C and neutral pH (b) Pseudo 2nd order model for metal ions adsorption at ambient temperature.

**Table 3.15:** Kinetic parameters for Pb (II) ions adsorption on SPIs

SPI	Pseudo 1 <sup>st</sup> order model			Pseudo 2 <sup>nd</sup> order model		
	$k_1$ (h <sup>-1</sup> )	$q_1$ (mg g <sup>-1</sup> )	R <sup>2</sup>	$k_2 \times 10^2$ (g mg <sup>-1</sup> h <sup>-1</sup> )	$q_2$ (mg g <sup>-1</sup> )	R <sup>2</sup>
<b>OBM</b>	0.2259	0.659	0.215	0.35	4.899	0.999
<b>FBM</b>	0.1496	0.572	0.323	0.68	1.405	0.999

These results were compared with adsorption capacity results of various types of reported polymeric adsorbents. **Table 3.16** shows a comparison of lead ions adsorption capacity of different materials reported in literature. It can be seen from Table 3.15 that synthesized sulphonated copolyimides prepared in this study showed comparable adsorption capacities with other adsorbents, revealing that these sulphontaed copolyimides are suitable for the removal of Pb (II) ions from aqueous media.

**Table 3.16:** Comparison of lead ions adsorption capacity of different materials in literature

<b>Adsorbent</b>	<b>Pb (II) adsorption capacity (mg g<sup>-1</sup>)</b>	<b>Physical Form</b>	<b>pH</b>	<b>Reference</b>
<b>Nafion 117</b>	58.0	Membrane	5.9	154
<b>Lignin derived biochar</b>	950.3	Particles	5	155
<b>Polyacrylamide/ attapulgit</b>	30.4	Particles	4	156
<b>Chitosan</b>	26.0	Particles	7	157
<b>Thiacalix[4]arene-loaded resin</b>	25.9	Particles	6	158
<b>Poly(VP-PEGMA-EGDMA)</b>	18.2	Beads	6	159
<b>Poly(PET-g-AAm)</b>	14.0	Fibers	5.5	160
<b>Rice husk ash</b>	9.8	Particles	5.8	161
<b>Poly(ethylene terephthalate)</b>	1.3	Fibers	5.5	160
<b>MBT-clay</b>	0.7	Particles	3.5	162
<b>FBM 50</b>	1.5	Membrane	7	This study
<b>OBM 50</b>	4.9	Membrane	7	This study

### 3.3.3 Theoretical calculations for adsorption

Our interest in quantum chemistry calculations was to identify the structural factors influencing the lead ions adsorption on SPI adsorbents using MOE software. Interactions of both OBM-50 and FBM-50 with Pb (II) were studied using surface and map tool. Five different descriptors were selected for both these complexes. Sum of dipole moment, atomic polarizabilities (apol), water accessible surface area (ASA), total hydrophobic surface area (ASAH) and electrostatic energy (Eele) profile were calculated for these complexes.

On the basis of electrostatic surface map, it was found that OBM-50 has large hydrophilic surface area than FBM-50 hence it is more hydrophilic and will show more interactions with water as compared to FBM complex as shown in **Figure 3.33** and **Figure 3.34**. Water accessible surface area for OBM is 738.2473 and that for FBM is 593.2592 which also confirmed the more electrostatic integrations with water molecules. Similarly, electrostatic energy profile for OBM-50 was calculated as -1343.89 kcal/mol and that for FBM-50 as -1205.01 kcal/mol. These descriptors data confirmed the greater affinity of OBM-50 towards water as compared to FBM-50. On the basis of surface area studies and electronic descriptors calculations, it is confirmed that both FBM-50 and OBM-50 have the ability to extract Pb from water and OBM-50 is more suitable for capturing Pb (II) as compared to FBM-50. <sup>163</sup> Molecular descriptors data is given in **Table 3.17**.

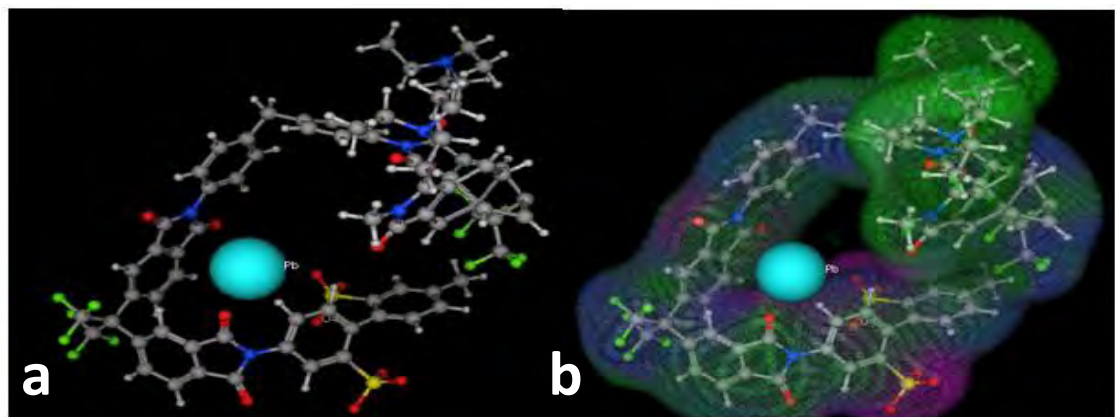


**Figure 3.33:** (a) 3D view of complex of FBM with Pb in ball and stick (b) Hydrophobic (green dots) and hydrophilic part (blue & purple) of FBM complex with Pb.

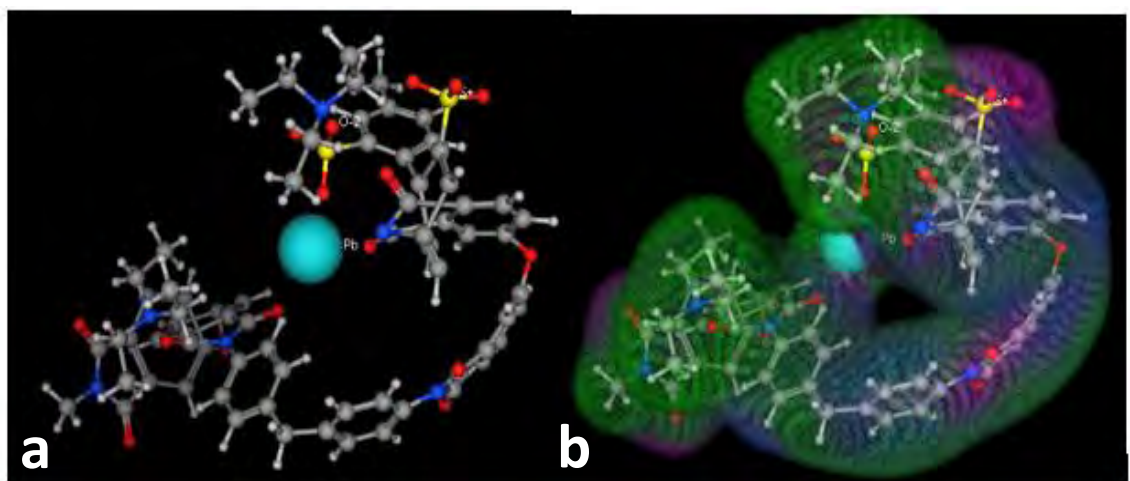


**Figure 3.34:** (a) 3D view of complex of OBM with Pb in ball and stick (b) Hydrophobic (green dots) and hydrophilic part (blue & purple) of OBM complex with Pb.



**Table 3.17:** Molecular descriptors for FBM-50 and OBM-50 complexes

Complex	Dipole moment	Eele (kcal/mol)	apol	ASA	ASAH
<b>FBM-50</b>	0.0000	-1205.0101	192.8667	593.2592	593.2592
<b>OBM-50</b>	0.0000	-1343.8864	208.5067	738.2473	356.7329

### 3.4 Four probe proton conductivity measurements

For conductivity measurements, 3x1 cm<sup>2</sup> membrane samples of FBA2-20 and FBA2-40 were immersed in water for 24 hours for hydration prior to the proton conductivity test whereas the sample of FBA2-20/IL (20 %), was tested without hydration. The in-plane proton conductivity of membranes was measured through a four-probe system fitted with platinum electrodes using three different temperatures (60, 80 and 100 °C) with five different values of relative humidity (RH - 20, 40, 60, 80 and 100%). Eq. (3.5) was used to calculate the proton conductivity ( $\sigma$ ) of membranes;

$$\sigma = L / R \cdot A \quad (\text{Equation 3.5})$$

Here, L indicates the distance of inner probes while R is ohmic resistance whereas A is membrane cross-sectional area.<sup>164</sup> Proton conductivity results carried out for FBA2-40 at three temperatures and five different relative humidities are shown in **Figure 3.35**.

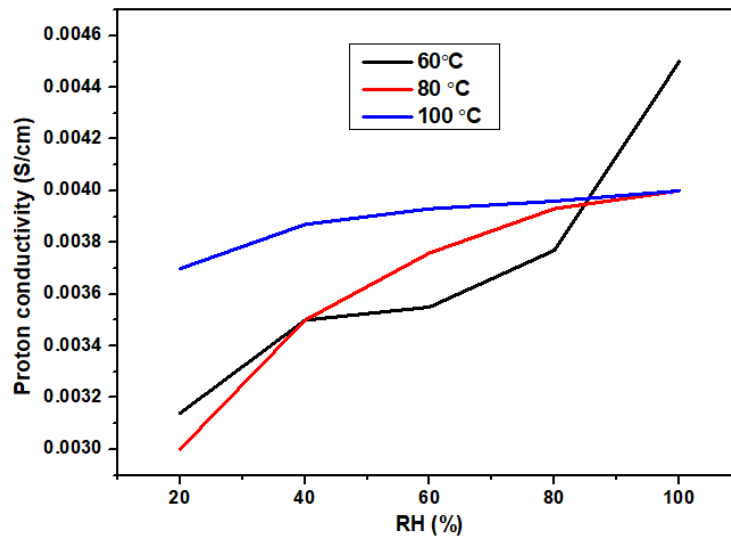


**Figure 3.35:** Proton conductivity of FBA2-40 at 60 °C, 80 °C and 100 °C.

At all the three temperatures, proton conductivity increases with the increase in RH. At 60 °C, the highest proton conductivity was observed at 100% relative humidity whereas at 80 and 100 °C, the proton conductivity values are quite close to each other at 80 % and 100 % RH. At 100 °C, the highest proton conductivities were observed at lower relative humidities (20-60%) as compared to those at lower temperatures (60 °C and 80 °C) where the highest proton conductivity was observed at 100% relative humidity. These results depicted that FBA2-40 membranes can conduct protons at 100 °C even at lower relative humidities (20-40%) and at lower temperatures (60 °C, 80 °C) proton conduction is possible at higher relative humidities (80-100%). All the membranes showed the same trend i.e., the proton conductivity increased with the increase in temperature and relative humidity. Bayer et al. demonstrated that the proton resistance of electrolyte membranes reduces with the increase of temperature and humidity.<sup>165</sup> It was proposed that, the decrease in the distance between activated sites takes place with the increased amount of water, which depicts that every sulphonic acid group holds either water or another sulphonic acid group next to it. Therefore, protons can follow an easier path through the membrane having conducting sites all the way long. Similarly, in the current study, the membrane resistance decreased with the increase in temperature and humidity resulting in an increase in the proton conductivity across the membrane.

Proton conductivity measurements of sulphonated polyimide (FBA2-20) and its composite with 20 wt % protic ionic liquid [FBA2-20/IL (20 %)] were carried out at 80 °C and five different relative humidity conditions. The comparative proton conductivity curves of sulphonated polyimide and its composite are shown in **Figure 3.36** and their comparison with Nafion 212 is displayed in **Figure 3.37**.

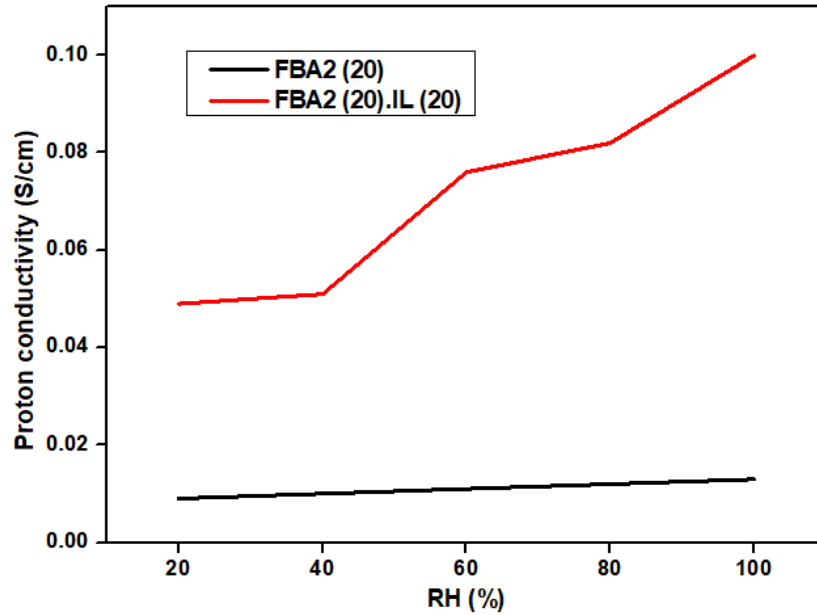


**Figure 3.36:** Proton conductivity of FBA2 (20) and FBA2-20 /IL (20 %) at 80 °C.

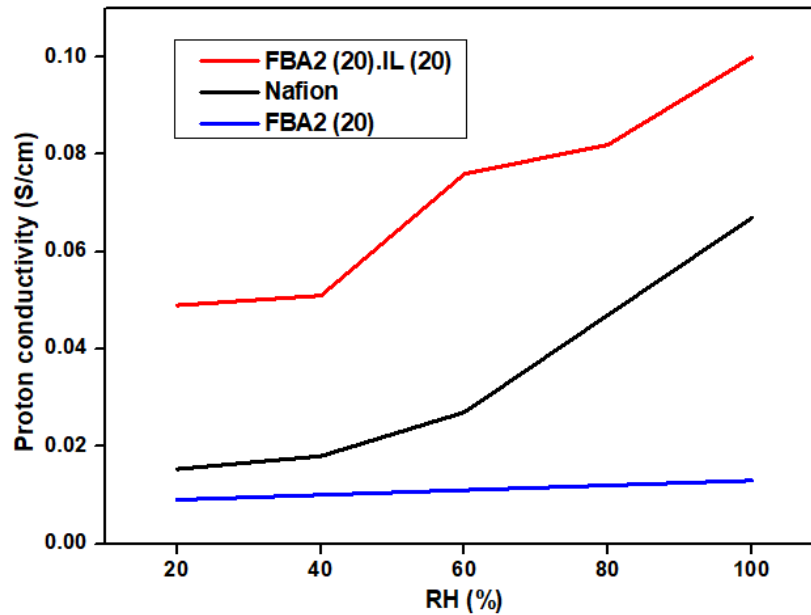


**Figure 3.37:** Proton conductivity of FBA2-20, Nafion 212 and FBA2-20/IL (20 %) at 80 °C.

These figures depict that composite membranes exhibited the highest proton conductivity as compared to the sulphonated polyimide and Nafion 212 at 80 °C, at all relative humidity values, which is the practical operating temperature of Nafion-based PEMFCs. These proton conductivities obtained here demonstrated that the sulphonated copolyimides (SPIs) and their protic ionic liquid composites can conduct protons at higher

temperatures and at 100 % relative humidity whereas the ionic liquid composite membrane showed superior proton conductivity as compared to sulphonated polyimides. The higher proton conductivity value of the composite membrane (0.1 S/cm) at 100% RH than Nafion (0.07 S/cm) under same conditions indicated that sulphonated polyimide/protic ionic liquid composites could be suitable for high temperature PEMFCs.

The high proton conductivity of the composite membrane is attributed to Grotthus-type mechanism, in which reorganization of hydrogen bonds plays a vital role in protic ionic liquid composites. The presence of protic ionic liquid could provide a more facile hopping of protons, which in turn contributes to increasing the proton transport.<sup>166, 147</sup>

### 3.5 Single fuel cell test

For single fuel cell test, the membrane electrode assemblies (MEAs) having a 4 cm<sup>2</sup> area were prepared where gas diffusion layer (GDL) was used as a support and the platinum nanorods as catalyst (at a catalyst loading of 0.2 mg Pt/cm<sup>2</sup>).<sup>167</sup>

The hydration of membrane was performed at a fixed voltage of 0.6 V for at least 12 hours or until a stable current was reached and then the polarization curve was recorded (**Figure 3.38**), and the power density curve is shown in **Figure 3.39**.

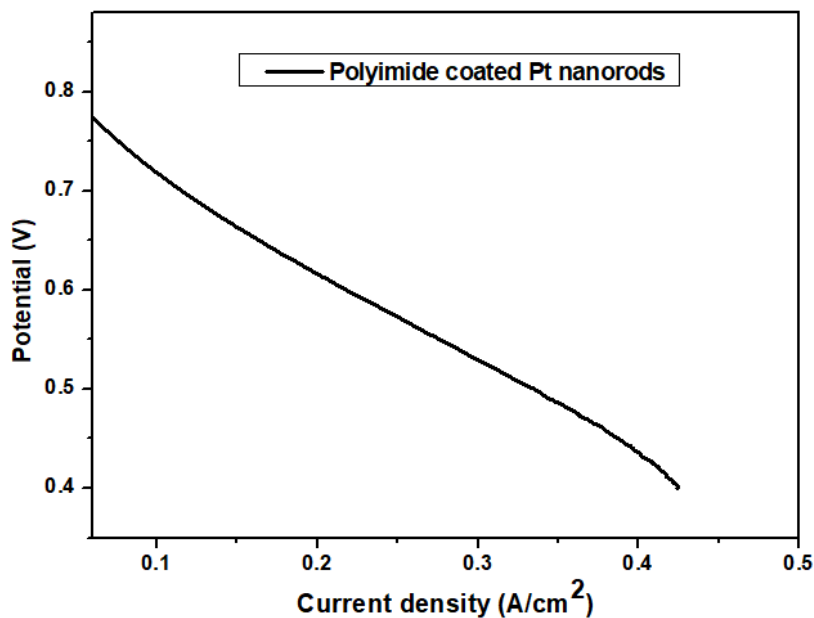


**Figure 3.38:** Polarization curve of FBA2-50 at 80 °C and 100 % RH coated platinum nanorods.

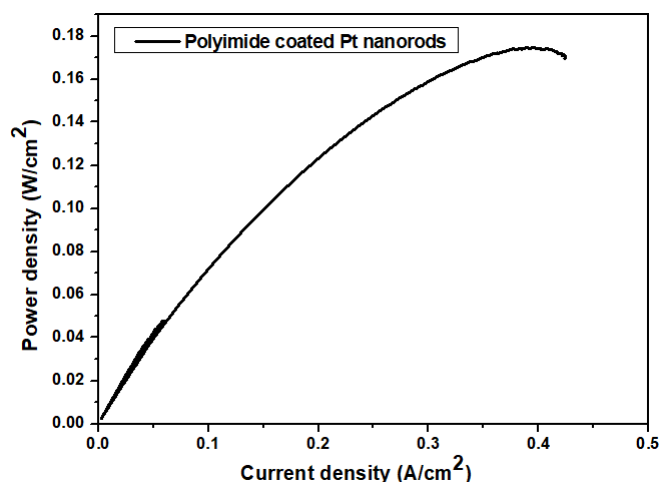


**Figure 3.39:** Power density of FBA2-50 coated platinum nanorods.

The usual Nyquist plots obtained by EIS measurements are shown in **Figure 3.40**.

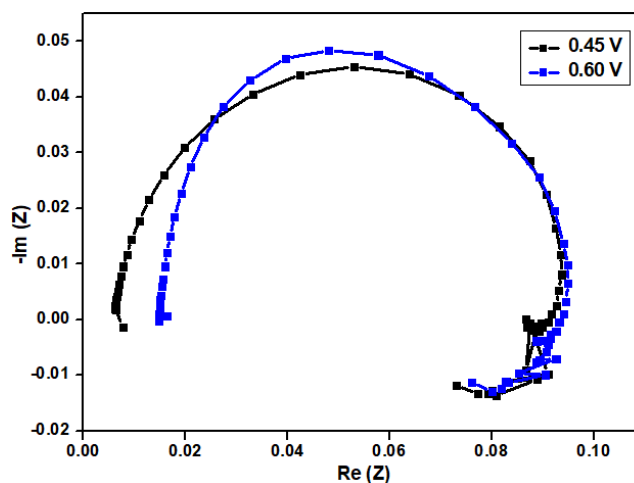


**Figure 3.40.** EIS of FBA2-50 coated platinum nanorods.

The presence of single semi-circle loop depicts the loss caused by the interfacial kinetics of electrochemical process, that normally happens at a region of low current density.<sup>168</sup> At high and low frequencies, the intercept of the arc with real axis is related to the internal ohmic ( $R_{\Omega}$ ) and charge transfer resistance ( $R_{CT}$ ) respectively. One of the important parameters of single cell test is the peak power density, and its value is around  $0.18 \text{ W/cm}^2$  for the as-prepared single cell (**Figure 3.39**).

### 3.6 Half Cell Gas Diffusion Electrode (GDE) measurements

The FlexCell polytetrafluoroethylene (PTFE) from Gaskatel was used for the conduction of *ex-situ* GDE measurements.<sup>169</sup> Cyclic voltammetry (CV) scans were

performed for the GDEs made with various ionomers. The electrochemical surface area (ECSA) was calculated based on the hydrogen adsorption and desorption areas. The desorption areas were quite smaller as compared to the adsorption areas. This difference was more pronounced in composites as compared to the sulphonated copolyimides. The results are shown below for Nafion (**Figure 3.41**), FBA2-50 (**Figure 3.41**), FBM-20 (**Figure 3.42**), and [FBM-20/ IL (50 %)] (**Figure 3.42**) coated Pt/C.

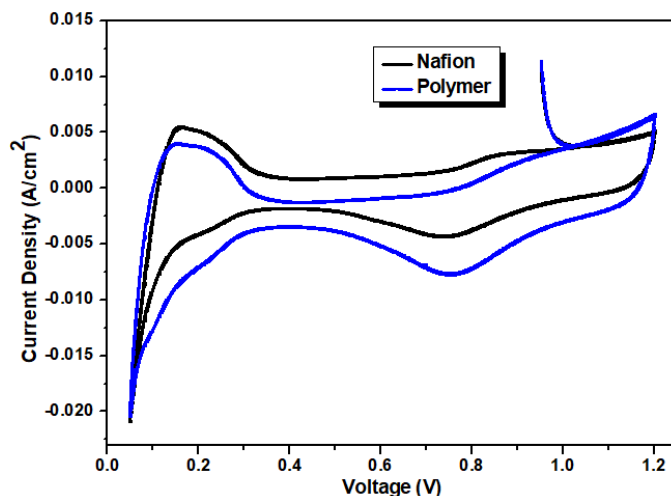


**Figure 3.41:** Comparative cyclic voltammograms of Nafion and FBA2-50 coated Pt/C.

The ECSAs for Nafion and FBA2-50 coated Pt/C came out to be 11.234 cm<sup>2</sup> and 8.351 cm<sup>2</sup> respectively. The ECSA of synthesized sulphonated copolyimides coated Pt/C are smaller than the Nafion (a commercial binder) coated Pt/C.

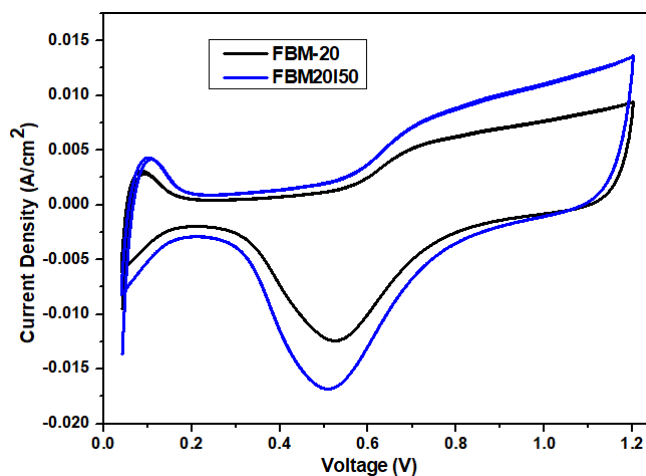


**Figure 3.42:** Comparative cyclic voltammograms of FBM-20 and FBM-20/IL (50 %) coated Pt/C.

The values for ECSAs for [FBM (20)] and [FBM (20)/ IL (50)] coated Pt/C are 10.249 cm<sup>2</sup> and 14.249 cm<sup>2</sup> respectively. These results indicated that the sulphonated polyimides and their protic ionic liquid composites can work as effective Pt catalyst binders.

## Conclusions

---

The thesis summarizes efforts in developing synthetic approaches focusing on the polymer design of sulphonated copolyimides and their composites with protic ionic liquids for efficient toxic metal adsorption and proton conduction. The introduction of hydrophilic sulphonic acid group in polyimide main chain, enhances the hydrophilicity and proton exchange abilities of the sulphonated copolyimides. These properties resulted in good metal adsorption abilities and proton exchange membranes (PEMs) with good electrochemical fuel cell performance in medium temperature proton exchange membrane fuel cell (PEMFC). Sulfonated hydrocarbon PEMs are alternatives to commercially available perfluorosulfonic acid ionomers (PFSA, e.g., Nafion<sup>®</sup>) that inevitably lose proton conductivity when exposed to harsh operating conditions.

To achieve the desired results, two series of homo and sulphonated copolyimides were successfully prepared using two synthesized and three commercial diamines having flexible linkages, two different commercial dianhydrides namely oxydiphthalic anhydride (ODPA) and 4,4'-(hexafluoroisopropylidene)diphthalic anhydride (6FDA) along with varying percentages of commercial sulphonated diamine, 4,4'-diamino-2,2' - biphenyldisulfonic acid (BDSA). The structural characteristics of synthesized diamines and resultant polyimides were evaluated by the physical data, FTIR spectroscopy, UV-Visible spectroscopy and XRD. Molecular weights of the synthesized polyimides were evaluated through viscosity measurements and gel permeation chromatographic (GPC) studies. Theoretical studies were carried out using Molecular operating software (2016). UV-Visible and atomic absorption spectroscopic (AAS) studies were carried out for heavy metal sensing and lead ions adsorption studies in aqueous media. Furthermore, eight different protic ionic liquids were synthesized using two different Brønsted acids and four different Brønsted bases. These ionic liquids were used as additives in the synthesized sulphonated copolyimide matrices for the synthesis of proton conductive composites. The composites were characterized through FTIR and XRD analytical techniques. Four probe proton conductivity measurements were carried out for proton conductivity studies of fabricated membranes. Half cell measurements and single cell tests were carried out for



catalyst coating studies for polymer electrolyte membrane fuel cells. These analyses have headed to the following conclusions.

- The solubility results demonstrated that polyimides and their sulphonated analogs are soluble in *m*-cresol at room temperature and in NMP upon heating and can be processed.
- The viscosity measurements ( $\eta_{inh} = 1.10 - 3.25$  dL/g) and GPC results depicted that weight average molecular weight (Mw) and polydispersity index of sulphonated copolyimides and composites varied between 12379-42726 g/mol and 1.5-4.3 respectively. The results showed that the copolyimides derived from FDA dianhydride have high molecular weights as compared to ODPa derived copolyimides. This might be attributed to the high molecular weight of 6FDA monomer as compared to ODPa monomer.
- 6FDA derived copolyimides are thermally stable, amorphous materials resulting in light coloured flexible films which in turn increases their efficiency for practical polymer electrolyte membrane fuel cells (PEMFCs)
- The thermal properties of synthesized polyimides were assessed by thermal gravimetric analysis (TGA) and differential scanning calorimetry (DSC). The results showed that ODPa based polyimides are thermally more stable and manifested higher glass transition temperatures as compared to 6FDA based polyimides. This can be attributed to better molecular interactions and compact chain packing in ODPa based polyimides as compared to 6FDA based polyimide where bulky  $-CF_3$  groups of 6FDA decreases the intermolecular interactions and inhibit close packing of the polymer chains.
- UV Visible spectroscopic studies along with theoretical studies (MOE software) displayed that the sulphonated copolyimides are hydrophilic in nature, ODPa based polyimides interacted with water molecules more efficiently as compared to 6FDA based polyimides. This increased hydrophilic character of ODPa based polyimides can be attributed to strong hydrogen bonding between the highly electronegative oxygen atom and surrounding water molecules. By inductive effect, oxygen atoms acquire partial negative charge by withdrawing electrons from the neighboring carbon atoms in the polymer chains making these polyimides more

hydrophilic as compared to 6FDA based polyimides. The experimental results were scrutinized by theoretical results where higher water accessible surface areas were obtained for ODPA based polyimides as compared to FDA based polyimides.

- The ODPA based sulphonated copolyimide (OBM-20) was evaluated for heavy metal sensing studies in aqueous media. The results depicted that OBM-20 can sense Ni (II), Co (II) and Cr (III) in nanomolar concentrations and it interacts more preferentially with Ni (II) as compared to Co (II) and Cr(III) at room temperature and neutral pH.
- Lead ions adsorption studies were carried out for both 6FDA (FBM-50) and ODPA (OBM-50) based copolyimides using atomic absorption spectroscopy (AAS) in aqueous media. The experimental results were confirmed through theoretical studies using MOE software. The results revealed that both FBM-50 and OBM-50 have the ability to extract Pb from water. OBM-50 was found to be more suitable for capturing Pb with higher  $q_e = 4.9 \text{ mg g}^{-1}$  as compared to FBM-50 with lower  $q_e = 1.5 \text{ mg g}^{-1}$ , due to its more hydrophilic nature; a prerequisite for adsorption.
- To evaluate the proton conductivity of sulphonated copolyimides and protic ionic liquid composites, four probe proton conductivity measurements were carried out. The results depicted that these membranes can efficiently conduct protons upto 100 °C with 100 % relative humidity and the conductivity of composites (0.1 S/cm) at 80 °C is quite high as compared to sulphonated copolyimides (0.004 S/cm) and Nafion 212 (0.05 S/cm) under same reaction conditions. It is thus concluded that these membranes can be used as electrolytes for polymer electrolyte membrane fuel cells upto 100 °C.
- Single fuel cell test and half cell test studies were carried out for catalyst coating studies in PEMFCs. These results revealed that these ionomers can coat the catalysts effectively and can function as catalyst binders like Nafion.

## Future Recommendations

---

- The synthesized sulphonated copolyimides can be used for adsorption of various toxic metal ions from water.
- The synthesized sulphonated copolyimides and their composites can be used as electrolytes for high temperature polymer electrolyte fuel cells working at higher temperatures  $\geq 120$  °C.
- The sulphonated copolyimides and their composites can be evaluated as coaters and binders for different fuel cell catalysts working at higher temperatures as these are thermally stable at high temperatures.
- The alkyl chains containing diamines can be used for the preparation of more flexible and mechanically stable proton conducting membranes for PEMFCs.

## References

---

- (1) Zhang, P.; Zhang, K.; Dou, S.; Zhao, J.; Yan, X.; Li, Y. Mechanical, Dielectric, and Thermal Attributes of Polyimides Stemmed Out of 4, 4'-Diaminodiphenyl Ether. *Crystals* **2020**, *10* (3), 173.
- (2) Lee, J.; Yoo, S.; Kim, D.; Kim, Y. H.; Park, S.; Park, N. K.; So, Y.; Kim, J.; Park, J.; Ko, M. J. Intrinsic Low-Dielectric Constant and Low-Dielectric Loss Aliphatic-Aromatic Copolyimides: The Effect of Chemical Structure. *Mater. Today Commun.* **2022**, *33*, 104479.
- (3) Bogert, M. T.; Renshaw, R. R. 4-Amino-o-phthalic acid and some of its derivatives. *J. Am. Chem. Soc.* **1908**, *30* (7), 1135–1144.
- (4) Sroog, C. E.; Endrey, A. L.; Abramo, S. V; Berr, C. E.; Edwards, W. M.; Olivier, K. L. Aromatic Polypyromellitimides from Aromatic Polyamic Acids. *J. Polym. Sci. Part A Polym. Chem.* **1996**, *34* (11), 2069–2086.
- (5) Lian, M.; Lu, X.; Lu, Q. Synthesis of Superheat-Resistant Polyimides with High Tg and Low Coefficient of Thermal Expansion by Introduction of Strong Intermolecular Interaction. *Macromolecules* **2018**, *51* (24), 10127–10135.
- (6) Li, X.; Al-Ostaz, A.; Jaradat, M.; Rahmani, F.; Nouranian, S.; Rushing, G.; Manasrah, A.; Alkhateb, H.; Finckenor, M.; Lichtenhan, J. Substantially Enhanced Durability of Polyhedral Oligomeric Silsequioxane-Polyimide Nanocomposites against Atomic Oxygen Erosion. *Eur. Polym. J.* **2017**, *92*, 233–249.
- (7) Li, T.; Liu, J.; Zhao, S.; Chen, Z.; Huang, H.; Guo, R.; Chen, Y. Microporous Polyimides Containing Bulky Tetra-o-Isopropyl and Naphthalene Groups for Gas Separation Membranes. *J. Memb. Sci.* **2019**, *585*, 282–288.
- (8) Iwan, A.; Malinowski, M.; Sikora, A.; Tazbir, I.; Pasciak, G.; Grabiec, E. Nafion-115/Aromatic Poly (etherimide) with Isopropylidene Groups/Imidazole Membranes for Polymer Fuel Cells. *J. Appl. Polym. Sci.* **2015**, *132* (34), 42436.
- (9) Likhatchev, D.; Alexandrova, L.; Tlenkopatchev, M.; Martinez-Richa, A.; Vera-Graziano, R. One-step Synthesis of Aromatic Polyimides Based on 4, 4'-

- Diaminotriphenylmethane. *J. Appl. Polym. Sci.* **1996**, *61* (5), 815–818.
- (10) Mehdipour-Ataei, S.; Bahri-Laleh, N.; Amirshaghghi, A. Comparison of One-Step and Two-Step Methods of Polyimidization and Substitution Effect in the Synthesis of New Poly (Ester-Imide) s with Bulky Pendent Group. *Polym. Degrad. Stab.* **2006**, *91* (11), 2622–2631.
  - (11) Sroog, C. E. Polyimides. *Prog. Polym. Sci.* **1991**, *16* (4), 561–694.
  - (12) Liaw, D. J.; Liaw, B. Y.; Yu, C. W. Synthesis and Characterization of New Organosoluble Polyimides Based on Flexible Diamine. *Polymer (Guildf)*. **2001**, *42* (12), 5175–5179.
  - (13) Pravednikov, A. N.; Kardash, I. Y.; Glukhoyedov, N. P.; Ardashnikov, A. Y. Some Features of the Synthesis of Heat-Resistant Heterocyclic Polymers. *Polym. Sci. USSR* **1973**, *15* (2), 399–410.
  - (14) Ardashnikov, A. Y.; Kardash, I. Y.; Pravednikov, A. N. The Nature of the Equilibrium in the Reaction of Aromatic Anhydrides with Aromatic Amines and Its Role in Synthesis of Polyimides. *Polym. Sci. USSR* **1971**, *13* (8), 2092–2100.
  - (15) Kaas, R. L. Autocatalysis and Equilibrium in Polyimide Synthesis. *J. Polym. Sci. Polym. Chem. Ed.* **1981**, *19* (9), 2255–2267.
  - (16) Gunduz, N. Synthesis and Characterization of Sulfonated Polyimides as Proton Exchange Membranes for Fuel Cells. Virginia Tech 2001.
  - (17) Harris, F. W. **1990**, Synthesis of Aromatic Polyimides from Dianhydrides and Diamines. *Polyimides*; Springer Dordrecht, Germany.
  - (18) Dine-Hart, R. A.; Wright, W. W. Preparation and Fabrication of Aromatic Polyimides. *J. Appl. Polym. Sci.* **1967**, *11* (5), 609–627.
  - (19) Facinelli, J. V; Gardner, S. L.; Dong, L.; Sensenich, C. L.; Davis, R. M.; Riffle, J. S. Controlled Molecular Weight Polyimides from Poly (Amic Acid) Salt Precursors. *Macromolecules* **1996**, *29* (23), 7342–7350.
  - (20) Sroog, C. E. Polyimides. *J. Polym. Sci. Macromol. Rev.* **1976**, *11* (1), 161–208.

- (21) Brink, M. H.; Bandom, D. K.; Wilkes, G. L.; McGrath, J. E. Synthesis and Characterization of a Novel '3F'-Based Fluorinated Monomer for Fluorine-Containing Polyimides. *Polymer (Guildf)*. **1994**, *35* (23), 5018–5023.
- (22) Kreuz, J. A.; Endrey, A. L.; Gay, F. P.; Sroog, C. E. Studies of Thermal Cyclizations of Polyamic Acids and Tertiary Amine Salts. *J. Polym. Sci. Part A-1 Polym. Chem.* **1966**, *4* (10), 2607–2616.
- (23) Vinogradova, S. V; Vygodskii, Y. S.; Vorob'ev, V. D.; Churochkina, N. A.; Chudina, L. I.; Spirina, T. N.; Korshak, V. V. Chemical Cyclization of Poly (Amido-Acids) in Solution. *Polym. Sci. USSR* **1974**, *16* (3), 584–589.
- (24) Ratta, V. Crystallization, Morphology, Thermal Stability and Adhesive Properties of Novel High Performance Semicrystalline Polyimides. Virginia Polytechnic Institute and State University 1999.
- (25) Hiesgen, R.; Helmly, S.; Galm, I.; Morawietz, T.; Handl, M.; Friedrich, K. A. Microscopic Analysis of Current and Mechanical Properties of Nafion® Studied by Atomic Force Microscopy. *Membranes (Basel)*. **2012**, *2* (4), 783–803.
- (26) Jalani, N. H.; Datta, R. The Effect of Equivalent Weight, Temperature, Cationic Forms, Sorbates, and Nanoinorganic Additives on the Sorption Behavior of Nafion®. *J. Memb. Sci.* **2005**, *264* (1–2), 167–175.
- (27) Kusoglu, A.; Weber, A. Z. New Insights into Perfluorinated Sulfonic-Acid Ionomers. *Chem. Rev.* **2017**, *117* (3), 987–1104.
- (28) Banerjee, S.; Curtin, D. E. Nafion® Perfluorinated Membranes in Fuel Cells. *J. Fluor. Chem.* **2004**, *125* (8), 1211–1216.
- (29) Feng, M.; Qu, R.; Wei, Z.; Wang, L.; Sun, P.; Wang, Z. Characterization of the Thermolysis Products of Nafion Membrane: A Potential Source of Perfluorinated Compounds in the Environment. *Sci. Rep.* **2015**, *5* (1), 1–8.
- (30) EPA, U. Long-Chain Perfluorinated Chemicals (PFCs) Action Plan. Available at [left angle Brac. [http://www.epa.gov/opptintr/existingchemicals/pubs/pfcs-action\\_plan1230\\_09.pdf](http://www.epa.gov/opptintr/existingchemicals/pubs/pfcs-action_plan1230_09.pdf) [right angle Brac. **2009**. (accessed 23/03/2023)

- (31) Park, C. H.; Lee, C. H.; Guiver, M. D.; Lee, Y. M. Sulfonated Hydrocarbon Membranes for Medium-Temperature and Low-Humidity Proton Exchange Membrane Fuel Cells (PEMFCs). *Prog. Polym. Sci.* **2011**, *36* (11), 1443–1498.
- (32) Jutemar, E. P.; Jannasch, P. Influence of the Polymer Backbone Structure on the Properties of Aromatic Ionomers with Pendant Sulfo benzoyl Side Chains for Use as Proton-Exchange Membranes. *ACS Appl. Mater. Interfaces* **2010**, *2* (12), 3718–3725.
- (33) Cornet, N.; Diat, O.; Gebel, G.; Jousse, F.; Marsacq, D.; Mercier, R.; Pineri, M. Sulfonated Polyimide Membranes: A New Type of Ion-Conducting Membrane for Electrochemical Applications. *J. New Mater. Electrochem. Syst.* **2000**, *3* (1), 33–42.
- (34) Lei, Z.; Chen, B.; Koo, Y.-M.; MacFarlane, D. R. Introduction: Ionic Liquids. *Chemical Reviews*. ACS Publications 2017, pp 6633–6635.
- (35) Watanabe, M.; Thomas, M. L.; Zhang, S.; Ueno, K.; Yasuda, T.; Dokko, K. Application of Ionic Liquids to Energy Storage and Conversion Materials and Devices. *Chem. Rev.* **2017**, *117* (10), 7190–7239.
- (36) Murray, S. M.; O'Brien, R. A.; Mattson, K. M.; Ceccarelli, C.; Sykora, R. E.; West, K. N.; Davis Jr, J. H. The Fluid-mosaic Model, Homeoviscous Adaptation, and Ionic Liquids: Dramatic Lowering of the Melting Point by Side-chain Unsaturation. *Angew. Chemie Int. Ed.* **2010**, *49* (15), 2755–2758.
- (37) Sinensky, M. Homeoviscous Adaptation—a Homeostatic Process That Regulates the Viscosity of Membrane Lipids in Escherichia Coli. *Proc. Natl. Acad. Sci.* **1974**, *71* (2), 522–525.
- (38) Hamaguchi, H. O.; Ozawa, R. Structure of Ionic Liquids and Ionic Liquid Compounds: Are Ionic Liquids Genuine Liquids in the Conventional Sense. *Adv. Chem. Phys* **2005**, *131*, 85–104.
- (39) Earle, M. J.; Seddon, K. R. Ionic Liquids. Green Solvents for the Future. *Pure Appl. Chem.* **2000**, *72* (7), 1391–1398.
- (40) Greaves, T. L.; Drummond, C. J. Protic Ionic Liquids: Properties and Applications.

*Chem. Rev.* **2008**, *108* (1), 206–237.

- (41) Angell, C. A.; Byrne, N.; Belieres, J.-P. Parallel Developments in Aprotic and Protic Ionic Liquids: Physical Chemistry and Applications. *Acc. Chem. Res.* **2007**, *40* (11), 1228–1236.
- (42) Parker, A. J. The Effects of Solvation on the Properties of Anions in Dipolar Aprotic Solvents. *Q. Rev. Chem. Soc.* **1962**, *16* (2), 163–187.
- (43) Mirjafari, A.; Pham, L. N.; McCabe, J. R.; Mobarrez, N.; Salter, E. A.; Wierzbicki, A.; West, K. N.; Sykora, R. E.; Davis, J. H. Building a Bridge between Aprotic and Protic Ionic Liquids. *RSC Adv.* **2013**, *3* (2), 337–340.
- (44) Xu, W.; Angell, C. A. Solvent-Free Electrolytes with Aqueous Solution-like Conductivities. *Science* (80-. ). **2003**, *302* (5644), 422–425.
- (45) Noda, A.; Susan, M. A. B. H.; Kudo, K.; Mitsushima, S.; Hayamizu, K.; Watanabe, M. Brønsted Acid– Base Ionic Liquids as Proton-Conducting Nonaqueous Electrolytes. *J. Phys. Chem. B* **2003**, *107* (17), 4024–4033.
- (46) Miran, M. S.; Yasuda, T.; Susan, M. A. B. H.; Dokko, K.; Watanabe, M. Binary Protic Ionic Liquid Mixtures as a Proton Conductor: High Fuel Cell Reaction Activity and Facile Proton Transport. *J. Phys. Chem. C* **2014**, *118* (48), 27631–27639.
- (47) Belieres, J.-P.; Angell, C. A. Protic Ionic Liquids: Preparation, Characterization, and Proton Free Energy Level Representation. *J. Phys. Chem. B* **2007**, *111* (18), 4926–4937.
- (48) Mann, J. P.; McCluskey, A.; Atkin, R. Activity and Thermal Stability of Lysozyme in Alkylammonium Formate Ionic Liquids—Influence of Cation Modification. *Green Chem.* **2009**, *11* (6), 785–792.
- (49) Estager, J.; Holbrey, J. D.; Swadźba-Kwaśny, M. Halometallate Ionic Liquids—Revisited. *Chem. Soc. Rev.* **2014**, *43* (3), 847–886.
- (50) Beyersdorff, T.; Schubert, T. J. S.; Welz-Biermann, U.; Pitner, W. Synthesis of



Ionic Liquids. *Electrodepos. from Ion. Liq.* **2008**, 2, 15.

- (51) Hayes, R.; Warr, G. G.; Atkin, R. Structure and Nanostructure in Ionic Liquids. *Chem. Rev.* **2015**, 115 (13), 6357–6426.
- (52) Susan, M. A. B. H.; Kaneko, T.; Noda, A.; Watanabe, M. Ion Gels Prepared by in Situ Radical Polymerization of Vinyl Monomers in an Ionic Liquid and Their Characterization as Polymer Electrolytes. *J. Am. Chem. Soc.* **2005**, 127 (13), 4976–4983.
- (53) Schauer, J.; Sikora, A.; Plíšková, M.; Mališ, J.; Mazúr, P.; Paidar, M.; Bouzek, K. Ion-Conductive Polymer Membranes Containing 1-Butyl-3-Methylimidazolium Trifluoromethanesulfonate and 1-Ethylimidazolium Trifluoromethanesulfonate. *J. Memb. Sci.* **2011**, 367 (1–2), 332–339.
- (54) Dahi, A.; Fatyeyeva, K.; Langevin, D.; Chappey, C.; Rogalsky, S. P.; Tarasyuk, O. P.; Marais, S. Polyimide/Ionic Liquid Composite Membranes for Fuel Cells Operating at High Temperatures. *Electrochim. Acta* **2014**, 130, 830–840.
- (55) Fernicola, A.; Panero, S.; Scrosati, B. Proton-Conducting Membranes Based on Protic Ionic Liquids. *J. Power Sources* **2008**, 178 (2), 591–595.
- (56) Chu, F.; Lin, B.; Yan, F.; Qiu, L.; Lu, J. Macromolecular Protic Ionic Liquid-Based Proton-Conducting Membranes for Anhydrous Proton Exchange Membrane Application. *J. Power Sources* **2011**, 196 (19), 7979–7984.
- (57) Tigelaar, D. M.; Waldecker, J. R.; Peplowski, K. M.; Kinder, J. D. Study of the Incorporation of Protic Ionic Liquids into Hydrophilic and Hydrophobic Rigid-Rod Elastomeric Polymers. *Polymer (Guildf)*. **2006**, 47 (12), 4269–4275.
- (58) Pu, H.; Wang, D. Studies on Proton Conductivity of Polyimide/H<sub>3</sub>PO<sub>4</sub>/Imidazole Blends. *Electrochim. Acta* **2006**, 51 (26), 5612–5617.
- (59) Lee, S. Y.; Yasuda, T.; Watanabe, M. Fabrication of Protic Ionic Liquid/Sulfonated Polyimide Composite Membranes for Non-Humidified Fuel Cells. *J. Power Sources* **2010**, 195 (18), 5909–5914.

- (60) Fang, J.; Guo, X.; Harada, S.; Watari, T.; Tanaka, K.; Kita, H.; Okamoto, K. Novel Sulfonated Polyimides as Polyelectrolytes for Fuel Cell Application. 1. Synthesis, Proton Conductivity, and Water Stability of Polyimides from 4, 4'-Diaminodiphenyl Ether-2, 2'-Disulfonic Acid. *Macromolecules* **2002**, *35* (24), 9022–9028.
- (61) Deligöz, H.; Vatansever, S.; Öksüzömer, F.; Koç, S. N.; Özgümüş, S.; Gürkaynak, M. A. Preparation and Characterization of Sulfonated Polyimide Ionomers via Post-sulfonation Method for Fuel Cell Applications. *Polym. Adv. Technol.* **2008**, *19* (8), 1126–1132.
- (62) Ito, A.; Yasuda, T.; Ma, X.; Watanabe, M. Sulfonated Polyimide/Ionic Liquid Composite Membranes for Carbon Dioxide Separation. *Polym. J.* **2017**, *49* (9), 671–676.
- (63) Yasuda, T.; Nakamura, S.; Honda, Y.; Kinugawa, K.; Lee, S.-Y.; Watanabe, M. Effects of Polymer Structure on Properties of Sulfonated Polyimide/Protic Ionic Liquid Composite Membranes for Nonhumidified Fuel Cell Applications. *ACS Appl. Mater. Interfaces* **2012**, *4* (3), 1783–1790.
- (64) Ito, A.; Yasuda, T.; Yoshioka, T.; Yoshida, A.; Li, X.; Hashimoto, K.; Nagai, K.; Shibayama, M.; Watanabe, M. Sulfonated Polyimide/Ionic Liquid Composite Membranes for Carbon Dioxide Separation: Transport Properties in Relation to Their Nanostructures. *Macromolecules* **2018**, *51* (18), 7112–7120.
- (65) Lvova, L. Chemical Sensors for Heavy Metals/Toxin Detection. *Chemosensors* **2020**, *8* (1), 14.
- (66) Zaynab, M.; Al-Yahyai, R.; Ameen, A.; Sharif, Y.; Ali, L.; Fatima, M.; Khan, K. A.; Li, S. Health and Environmental Effects of Heavy Metals. *J. King Saud Univ.* **2022**, *34* (1), 101653.
- (67) Wang, L.; Zheng, P.; Zhang, W.; Xu, M.; Jia, K.; Liu, X. Detection of Cu<sup>2+</sup> Metals by Luminescent Sensor Based on Sulfonated Poly (Arylene Ether Nitrile)/Metal-Organic Frameworks. *Mater. Today Commun.* **2018**, *16*, 258–263.
- (68) Ali, M. M.; Rahman, S.; Islam, M. S.; Rakib, M. R. J.; Hossen, S.; Rahman, M. Z.;

- Kormoker, T.; Idris, A. M.; Phoungthong, K. Distribution of Heavy Metals in Water and Sediment of an Urban River in a Developing Country: A Probabilistic Risk Assessment. *Int. J. Sediment Res.* **2022**, *37* (2), 173–187.
- (69) Kumar, V.; Parihar, R. D.; Sharma, A.; Bakshi, P.; Sidhu, G. P. S.; Bali, A. S.; Karaouzas, I.; Bhardwaj, R.; Thukral, A. K.; Gyasi-Agyei, Y. Global Evaluation of Heavy Metal Content in Surface Water Bodies: A Meta-Analysis Using Heavy Metal Pollution Indices and Multivariate Statistical Analyses. *Chemosphere* **2019**, *236*, 124364.
- (70) Yang, D.; Li, F.; Luo, Z.; Bao, B.; Hu, Y.; Weng, L.; Cheng, Y.; Wang, L. Conjugated Polymer Nanoparticles with Aggregation Induced Emission Characteristics for Intracellular Fe<sup>3+</sup> Sensing. *J. Polym. Sci. Part A Polym. Chem.* **2016**, *54* (12), 1686–1693.
- (71) Kumar, A.; Sahoo, P. R.; Kumar, S. Colorimetric and Fluorescence-Based Detection of Mercuric Ion Using a Benzothiazolinic Spiropyran. *Chemosensors* **2019**, *7* (3), 35.
- (72) Tan, R. X.; Ibsen, M.; Tjin, S. C. Optical Fiber Refractometer Based Metal Ion Sensors. *Chemosensors* **2019**, *7* (4), 63.
- (73) Ermakova, E. V.; Koroleva, E. O.; Shokurov, A. V.; Arslanov, V. V.; Bessmertnykh-Lemeune, A. Ultra-Thin Film Sensors Based on Porphyrin-5-phosphonate Diesters for Selective and Sensitive Dual-Channel Optical Detection of Mercury (II) Ions. *Dye. Pigment.* **2021**, *186*, 108967.
- (74) Waheed, A.; Baig, N.; Ullah, N.; Falath, W. Removal of Hazardous Dyes, Toxic Metal Ions and Organic Pollutants from Wastewater by Using Porous Hyper-Cross-Linked Polymeric Materials: A Review of Recent Advances. *J. Environ. Manage.* **2021**, *287*, 112360.
- (75) Dzhardimalieva, G. I.; Uflyand, I. E. Design Strategies of Metal Complexes Based on Chelating Polymer Ligands and Their Application in Nanomaterials Science. *J. Inorg. Organomet. Polym. Mater.* **2018**, *28* (4), 1305–1393.

- (76) Max, J. B.; Nabiyani, A.; Eichhorn, J.; Schacher, F. H. Triple-Responsive Polyampholytic Graft Copolymers as Smart Sensors with Varying Output. *Macromol. Rapid Commun.* **2021**, *42* (7), 2000671.
- (77) Ge, Q.; Liu, H. Tunable Amine-Functionalized Silsesquioxane-Based Hybrid Networks for Efficient Removal of Heavy Metal Ions and Selective Adsorption of Anionic Dyes. *Chem. Eng. J.* **2022**, *428*, 131370.
- (78) Oral, I.; Abetz, V. A Highly Selective Polymer Material Using Benzo-9-Crown-3 for the Extraction of Lithium in Presence of Other Interfering Alkali Metal Ions. *Macromol. Rapid Commun.* **2021**, *42* (9), 2000746.
- (79) Sezer Hicyilmaz, A.; Celik Bedeloglu, A. Applications of Polyimide Coatings: A Review. *SN Appl. Sci.* **2021**, *3* (3), 1–22.
- (80) Chen, C. K.; Lin, Y. C.; Hsu, L. C.; Ho, J. C.; Ueda, M.; Chen, W. C. High Performance Biomass-Based Polyimides for Flexible Electronic Applications. *ACS Sustain. Chem. Eng.* **2021**, *9* (8), 3278–3288.
- (81) Santiago, A. A.; Ibarra-Palos, A.; Cruz-Morales, J. A.; Sierra, J. M.; Abatal, M.; Alfonso, I.; Vargas, J. Synthesis, Characterization, and Heavy Metal Adsorption Properties of Sulfonated Aromatic Polyamides. *High Perform. Polym.* **2018**, *30* (5), 591–601.
- (82) Zhang, H.; Zhu, S.; Yang, J.; Ma, A.; Chen, W. Enhanced Removal Efficiency of Heavy Metal Ions by Assembling Phytic Acid on Polyamide Nanofiltration Membrane. *J. Memb. Sci.* **2021**, *636*, 119591.
- (83) <https://www.sigmaaldrich.com/GB/en/products/materials-science/biomedical-materials/hydrophilic-polymers> (accessed 24/02/2023).
- (84) Omer, A. M.; Dey, R.; Eltaweil, A. S.; Abd El-Monaem, E. M.; Ziora, Z. M. Insights into Recent Advances of Chitosan-Based Adsorbents for Sustainable Removal of Heavy Metals and Anions. *Arab. J. Chem.* **2022**, *15* (2), 103543.
- (85) Wang, W.; Yu, F.; Ba, Z.; Qian, H.; Zhao, S.; Liu, J.; Jiang, W.; Li, J.; Liang, D. In-Depth Sulfhydryl-Modified Cellulose Fibers for Efficient and Rapid Adsorption of

Cr (VI). *Polymers (Basel)*. **2022**, *14* (7), 1482.

- (86) Lu, W.; Levin, R.; Schwartz, J. Lead Contamination of Public Drinking Water and Academic Achievements among Children in Massachusetts: A Panel Study. *BMC Public Health* **2022**, *22* (1), 1–14.
- (87) Wei, P.; Lou, H.; Xu, X.; Xu, W.; Yang, H.; Zhang, W.; Zhang, Y. Preparation of PP Non-Woven Fabric with Good Heavy Metal Adsorption Performance via Plasma Modification and Graft Polymerization. *Appl. Surf. Sci.* **2021**, *539*, 148195.
- (88) Tang, L.; Huang, S.; Wang, Y.; Liang, D.; Li, Y.; Li, J.; Wang, Y.; Xie, Y.; Wang, W. Highly Efficient, Stable, and Recyclable Hydrogen Manganese Oxide/Cellulose Film for the Extraction of Lithium from Seawater. *ACS Appl. Mater. Interfaces* **2020**, *12* (8), 9775–9781.
- (89) Giri, D. D.; Alhazmi, A.; Mohammad, A.; Haque, S.; Srivastava, N.; Thakur, V. K.; Gupta, V. K.; Pal, D. B. Lead Removal from Synthetic Wastewater by Biosorbents Prepared from Seeds of *Artocarpus Heterophyllus* and *Syzygium Cumini*. *Chemosphere* **2022**, *287*, 132016.
- (90) Masoumi, H.; Ghaemi, A.; Gilani, H. G. Evaluation of Hyper-Cross-Linked Polymers Performances in the Removal of Hazardous Heavy Metal Ions: A Review. *Sep. Purif. Technol.* **2021**, *260*, 118221.
- (91) Li, Y.; Zhao, J. Q.; Yuan, Y. C.; Shi, C. Q.; Liu, S. M.; Yan, S. J.; Zhao, Y.; Zhang, M. Q. Polyimide/Crown Ether Composite Films with Necklace-like Supramolecular Structure and Improved Mechanical, Dielectric, and Hydrophobic Properties. *Macromolecules* **2015**, *48* (7), 2173–2183.
- (92) Xu, Z.; Croft, Z. L.; Guo, D.; Cao, K.; Liu, G. Recent Development of Polyimides: Synthesis, Processing, and Application in Gas Separation. *J. Polym. Sci.* **2021**, *59* (11), 943–962.
- (93) Rusanov, A. L.; Bulycheva, E. G.; Bugaenko, M. G.; Leikin, A. Y.; Shevelev, S. A.; Dutov, M. D.; Serushkina, O. V.; Voitekunas, V. Y.; Abadi, M. New Sulfonated Polynaphthylimides: Synthesis and Investigation. *Polym. Sci. Ser. C* **2009**, *51* (1),

3–7.

- (94) Wack, H.; Bertling, J. Water-Swellable Materials—Application in Self-Healing Sealing Systems. In *Proceedings of the First International Conference on Self Healing Materials*; Springer Dordrecht, The Netherlands, 2007; Vol. 9.
- (95) Perry, M. L.; Fuller, T. F. A Historical Perspective of Fuel Cell Technology in the 20th Century. *J. Electrochem. Soc.* **2002**, *149* (7), S59.
- (96) <https://www.fchea.org/h2-day-2019-events-activities/2019/8/1/fuel-cell-amp-hydrogen-energy-basics> (accessed 24/02/2023).
- (97) Guangyao, M.; Wanyu, L.; Dingkun, P. New Solid State Fuel Cells—Green Power Source for 21st Century. *Ionics (Kiel)*. **1998**, *4*, 451–462.
- (98) Stambouli, A. B.; Traversa, E. Solid Oxide Fuel Cells (SOFCs): A Review of an Environmentally Clean and Efficient Source of Energy. *Renew. Sustain. Energy Rev.* **2002**, *6* (5), 433–455.
- (99) Chen, L.; Yuh, C.-Y. Hardware Materials in Molten Carbonate Fuel Cell: A Review. *Acta Metall. Sin. (English Lett.)* **2017**, *30*, 289–295.
- (100) Lin, B. Y. S.; Kirk, D. W.; Thorpe, S. J. Performance of Alkaline Fuel Cells: A Possible Future Energy System? *J. Power Sources* **2006**, *161* (1), 474–483.
- (101) Sammes, N.; Bove, R.; Stahl, K. Phosphoric Acid Fuel Cells: Fundamentals and Applications. *Curr. Opin. solid state Mater. Sci.* **2004**, *8* (5), 372–378.
- (102) Smitha, B.; Sridhar, S.; Khan, A. A. Solid Polymer Electrolyte Membranes for Fuel Cell Applications—a Review. *J. Memb. Sci.* **2005**, *259* (1–2), 10–26.
- (103) Kamarudin, S. K.; Achmad, F.; Daud, W. R. W. Overview on the Application of Direct Methanol Fuel Cell (DMFC) for Portable Electronic Devices. *Int. J. Hydrogen Energy* **2009**, *34* (16), 6902–6916.
- (104) Vaghari, H.; Jafarizadeh-Malmiri, H.; Berenjian, A.; Anarjan, N. Recent Advances in Application of Chitosan in Fuel Cells. *Sustain. Chem. Process.* **2013**, *1* (1), 1–12.
- (105) Zhang, H.; Shen, P. K. Recent Development of Polymer Electrolyte Membranes for

Fuel Cells. *Chem. Rev.* **2012**, *112* (5), 2780–2832.

- (106) <https://www.unmannedsystemstechnology.com/company/intelligent-energy/> (accessed 24/02/2023).
- (107) Asano, N.; Miyatake, K.; Watanabe, M. Hydrolytically Stable Polyimide Ionomer for Fuel Cell Applications. *Chem. Mater.* **2004**, *16* (15), 2841–2843.
- (108) Rikukawa, M.; Sanui, K. Proton-Conducting Polymer Electrolyte Membranes Based on Hydrocarbon Polymers. *Prog. Polym. Sci.* **2000**, *25* (10), 1463–1502.
- (109) Agmon, N. The Grotthuss Mechanism. *Chem. Phys. Lett.* **1995**, *244* (5–6), 456–462.
- (110) Saito, M.; Arimura, N.; Hayamizu, K.; Okada, T. Mechanisms of Ion and Water Transport in Perfluorosulfonated Ionomer Membranes for Fuel Cells. *J. Phys. Chem. B* **2004**, *108* (41), 16064–16070.
- (111) Susan, M. A. B. H.; Noda, A.; Watanabe, M. Brønsted Acid-Base Ionic Liquids as Fuel Cell Electrolytes under Nonhumidifying Conditions; ACS Publications, 2005.
- (112) Diaz, M.; Ortiz, A.; Ortiz, I. Progress in the Use of Ionic Liquids as Electrolyte Membranes in Fuel Cells. *J. Memb. Sci.* **2014**, *469*, 379–396.
- (113) Liu, X.; Zhang, Y.; Deng, S.; Li, C.; Dong, J.; Wang, J.; Yang, Z.; Wang, D.; Cheng, H. Semi-Interpenetrating Polymer Network Membranes from SPEEK and BPPO for High Concentration DMFC. *ACS Appl. Energy Mater.* **2018**, *1* (10), 5463–5473.
- (114) Yuan, Z.; Li, X.; Zhao, Y.; Zhang, H. Mechanism of Polysulfone-Based Anion Exchange Membranes Degradation in Vanadium Flow Battery. *ACS Appl. Mater. Interfaces* **2015**, *7* (34), 19446–19454.
- (115) Miyatake, K.; Iyotani, H.; Yamamoto, K.; Tsuchida, E. Synthesis of Poly (Phenylene Sulfide Sulfonic Acid) via Poly (Sulfonium Cation) as a Thermostable Proton-Conducting Polymer. *Macromolecules* **1996**, *29* (21), 6969–6971.
- (116) Guo, X. X.; Fang, J. H.; Watari, T.; Tanaka, K.; Kita, H.; Okamoto, K. I. Novel Sulfonated Polyimides as Polyelectrolytes for Fuel Cell Application. 2. Synthesis and Proton Conductivity, of Polyimides from 9,9-Bis(4-Aminophenyl)Fluorene-

2,7-Disulfonic Acid. *Macromolecules* **2002**, *35* (17), 6707–6713.

- (117) Einsla, B. R.; Hong, Y.; Seung Kim, Y.; Wang, F.; Gunduz, N.; McGrath, J. E. Sulfonated Naphthalene Dianhydride Based Polyimide Copolymers for Proton-exchange-membrane Fuel Cells. I. Monomer and Copolymer Synthesis. *J. Polym. Sci. Part A Polym. Chem.* **2004**, *42* (4), 862–874.
- (118) Bai, H.; Ho, W. S. W. New Poly(Ethylene Oxide) Soft Segment-Containing Sulfonated Polyimide Copolymers for High Temperature Proton-Exchange Membrane Fuel Cells. *J. Memb. Sci.* **2008**, *313* (1–2), 75–85.
- (119) Einsla, M. L.; Kim, Y. S.; Hawley, M.; Lee, H. S.; McGrath, J. E.; Liu, B.; Guiver, M. D.; Pivovar, B. S. Toward Improved Conductivity of Sulfonated Aromatic Proton Exchange Membranes at Low Relative Humidity. *Chem. Mater.* **2008**, *20* (17), 5636–5642.
- (120) Fang, J.; Guo, X.; Xu, H.; Okamoto, K. ichi. Sulfonated Polyimides: Synthesis, Proton Conductivity and Water Stability. *J. Power Sources* **2006**, *159* (1 SPEC. ISS.), 4–11.
- (121) Genies, C.; Mercier, R.; Sillion, B.; Petiaud, R.; Cornet, N.; Gebel, G.; Pineri, M. Stability Study of Sulfonated Phthalic and Naphthalenic Polyimide Structures in Aqueous Medium. *Polymer (Guildf)*. **2001**, *42* (12), 5097–5105.
- (122) Guo, X.; Fang, J.; Tanaka, K.; Kita, H.; Okamoto, K. Synthesis and Properties of Novel Sulfonated Polyimides from 2, 2'-bis (4-aminophenoxy) Biphenyl-5, 5'-disulfonic Acid. *J. Polym. Sci. Part A Polym. Chem.* **2004**, *42* (6), 1432–1440.
- (123) Zhai, F.; Guo, X.; Fang, J.; Xu, H. Synthesis and Properties of Novel Sulfonated Polyimide Membranes for Direct Methanol Fuel Cell Application. *J. Memb. Sci.* **2007**, *296* (1–2), 102–109.
- (124) Tripathi, B. P.; Shahi, V. K. Organic–Inorganic Nanocomposite Polymer Electrolyte Membranes for Fuel Cell Applications. *Prog. Polym. Sci.* **2011**, *36* (7), 945–979.
- (125) Bano, S.; Negi, Y. S.; Illathvalappil, R.; Kurungot, S.; Ramya, K. Studies on Nano Composites of SPEEK/Ethylene Glycol/Cellulose Nanocrystals as Promising



- Proton Exchange Membranes. *Electrochim. Acta* **2019**, *293*, 260–272.
- (126) Che, Q.; Sun, B.; He, R. Preparation and Characterization of New Anhydrous, Conducting Membranes Based on Composites of Ionic Liquid Trifluoroacetic Propylamine and Polymers of Sulfonated Poly (Ether Ether) Ketone or Polyvinylidene fluoride. *Electrochim. Acta* **2008**, *53* (13), 4428–4434.
- (127) Doyle, M.; Choi, S. K.; Proulx, G. High-temperature Proton Conducting Membranes Based on Perfluorinated Ionomer Membrane-ionic Liquid Composites. *J. Electrochem. Soc.* **2000**, *147* (1), 34.
- (128) Martinez, M.; Molmeret, Y.; Cointeaux, L.; Iojoiu, C.; Leprêtre, J.-C.; El Kissi, N.; Judeinstein, P.; Sanchez, J.-Y. Proton-Conducting Ionic Liquid-Based Proton Exchange Membrane Fuel Cell Membranes: The Key Role of Ionomer–Ionic Liquid Interaction. *J. Power Sources* **2010**, *195* (18), 5829–5839.
- (129) Di Noto, V.; Negro, E.; Sanchez, J.-Y.; Iojoiu, C. Structure-Relaxation Interplay of a New Nanostructured Membrane Based on Tetraethylammonium Trifluoromethanesulfonate Ionic Liquid and Neutralized Nafion 117 for High-Temperature Fuel Cells. *J. Am. Chem. Soc.* **2010**, *132* (7), 2183–2195.
- (130) Neves, L. A.; Benavente, J.; Coelho, I. M.; Crespo, J. G. Design and Characterisation of Nafion Membranes with Incorporated Ionic Liquids Cations. *J. Memb. Sci.* **2010**, *347* (1–2), 42–52.
- (131) Susan, M. A. B. H.; Noda, A.; Mitsushima, S.; Watanabe, M. Brønsted Acid–Base Ionic Liquids and Their Use as New Materials for Anhydrous Proton Conductors. *Chem. Commun.* **2003**, No. 8, 938–939.
- (132) Fatyeyeva, K.; Rogalsky, S.; Makhno, S.; Tarasyuk, O.; Soto Puente, J. A.; Marais, S. Polyimide/Ionic Liquid Composite Membranes for Middle and High Temperature Fuel Cell Application: Water Sorption Behavior and Proton Conductivity. *Membranes (Basel)*. **2020**, *10* (5), 82.
- (133) Eastmond, G. C.; Paprotny, J. Polyimides with Main-Chain Ethylene Oxide Units: Synthesis and Properties. *Polymer (Guildf)*. **2002**, *43* (12), 3455–3468.

- (134) Guan, Y.; Wang, C.; Wang, D.; Dang, G.; Chen, C.; Zhou, H.; Zhao, X. High Transparent Polyimides Containing Pyridine and Biphenyl Units: Synthesis, Thermal, Mechanical, Crystal and Optical Properties. *Polymer (Guildf)*. **2015**, *62*, 1–10.
- (135) Yin, Y.; Suto, Y.; Sakabe, T.; Chen, S.; Hayashi, S.; Mishima, T.; Yamada, O.; Tanaka, K.; Kita, H.; Okamoto, K. Water Stability of Sulfonated Polyimide Membranes. *Macromolecules* **2006**, *39* (3), 1189–1198.
- (136) Kasianova, I. Organic Polymer Compound, Optical Film and Method of Production Thereof. Google Patents July 29, 2010.
- (137) Shmukler, L. E.; Gruzdev, M. S.; Kudryakova, N. O.; Fadeeva, Y. A.; Kolker, A. M.; Safonova, L. P. Thermal Behavior and Electrochemistry of Protic Ionic Liquids Based on Triethylamine with Different Acids. *RSC Adv.* **2016**, *6* (111), 109664–109671.
- (138) Susa, A.; Bijleveld, J.; Hernandez Santana, M.; Garcia, S. J. Understanding the Effect of the Dianhydride Structure on the Properties of Semiaromatic Polyimides Containing a Biobased Fatty Diamine. *ACS Sustain. Chem. Eng.* **2018**, *6* (1), 668–678.
- (139) Ando, S.; Matsuura, T.; Sasaki, S. Coloration of Aromatic Polyimides and Electronic Properties of Their Source Materials. *Polym. J.* **1997**, *29* (1), 69–76.
- (140) Ye, X.; Bai, H.; Ho, W. S. W. Synthesis and Characterization of New Sulfonated Polyimides as Proton-Exchange Membranes for Fuel Cells. *J. Memb. Sci.* **2006**, *279* (1–2), 570–577.
- (141) Yang, S.; Jang, W.; Lee, C.; Shul, Y. G.; Han, H. The Effect of Crosslinked Networks with Poly (Ethylene Glycol) on Sulfonated Polyimide for Polymer Electrolyte Membrane Fuel Cell. *J. Polym. Sci. Part B Polym. Phys.* **2005**, *43* (12), 1455–1464.
- (142) Patil, Y. S.; Salunkhe, P. H.; Mahindrakar, J. N.; Ankushrao, S. S.; Kadam, V. N.; Ubale, V. P.; Ghanwat, A. A. Synthesis and Characterization of Aromatic

- Polyimides Containing Tetraphenylfuran-Thiazole Moiety. *J. Therm. Anal. Calorim.* **2019**, *135* (6), 3057–3068.
- (143) In, I.; Kim, S. Y. Soluble Wholly Aromatic Polyamides Containing Unsymmetrical Pyridyl Ether Linkages. *Polymer (Guildf)*. **2006**, *47* (2), 547–552.
- (144) Bender, T. P.; Wang, Z. Y. Synthesis of Polyimides and Segmented Block Copolyimides by Transimidization. *J. Polym. Sci. Part A Polym. Chem.* **2000**, *38* (21), 3991–3996.
- (145) Fatima, K.; Gul, A.; Akhter, Z.; Rahman, R. Ferrocene Based Azo Chromophore Functionalized Polyesters and Its Organic Analogue: Synthesis, Structural Elucidation, Thermal Behavior and IR Characterization. *J. Inorg. Organomet. Polym. Mater.* **2017**, *27* (2), 474–480.
- (146) Lundberg, R. D.; Makowski, H. S. Solution Behavior of Ionomers. I. Metal Sulfonate Ionomers in Mixed Solvents. *J. Polym. Sci. Polym. Phys. Ed.* **1980**, *18* (8), 1821–1836.
- (147) Chen, B. K.; Wu, T. Y.; Kuo, C. W.; Peng, Y. C.; Shih, I. C.; Hao, L.; Sun, I. W. 4, 4'-Oxydianiline (ODA) Containing Sulfonated Polyimide/Protic Ionic Liquid Composite Membranes for Anhydrous Proton Conduction. *Int. J. Hydrogen Energy* **2013**, *38* (26), 11321–11330.
- (148) Tabata, M.; Tanaka, M. Kinetics and Mechanism of Cadmium (II) Ion Assisted Incorporation of Manganese (II) into 5, 10, 15, 20-Tetrakis (4-Sulphonatophenyl) Porphyrinate (4). *J. Chem. Soc. Dalt. Trans.* **1983**, No. 9, 1955–1959.
- (149) Mahmoud, N. M.; Saidi, H.; Ujang, Z.; MOHD D. K. Z. Removal of Metal Ions from Aqueous Solutions Using Crosslinked Polyethylene-GTMFJ-Polystyrene Sulfonic Acid Adsorbent Prepared by Radiation Grafting. *J. Chil. Chem. Soc.* **2010**, *55* (4), 421–427.
- (150) Naseem, K.; Begum, R.; Wu, W.; Usman, M.; Irfan, A.; Al-Sehemi, A. G.; Farooqi, Z. H. Adsorptive Removal of Heavy Metal Ions Using Polystyrene-Poly (N-Isopropylmethacrylamide-Acrylic Acid) Core/Shell Gel Particles: Adsorption

Isotherms and Kinetic Study. *J. Mol. Liq.* **2019**, *277*, 522–531.

- (151) Kantipuly, C.; Katragadda, S.; Chow, A.; Gesser, H. D. Chelating Polymers and Related Supports for Separation and Preconcentration of Trace Metals. *Talanta* **1990**, *37* (5), 491–517.
- (152) Denizli, A.; Tanyolaç, D.; Salih, B.; Özdural, A. Cibacron Blue F3GA-Attached Polyvinylbutyral Microbeads as Novel Magnetic Sorbents for Removal of Cu (II), Cd (II) and Pb (II) Ions. *J. Chromatogr. A* **1998**, *793* (1), 47–56.
- (153) Varsha, M.; Kumar, P. S.; Rathi, B. S. A Review on Recent Trends in the Removal of Emerging Contaminants from Aquatic Environment Using Low-Cost Adsorbents. *Chemosphere* **2022**, *287*, 132270.
- (154) Nasef, M. M.; Yahaya, A. H. Adsorption of Some Heavy Metal Ions from Aqueous Solutions on Nafion 117 Membrane. *Desalination* **2009**, *249* (2), 677–681.
- (155) Wu, F.; Chen, L.; Hu, P.; Wang, Y.; Deng, J.; Mi, B. Industrial Alkali Lignin-Derived Biochar as Highly Efficient and Low-Cost Adsorption Material for Pb (II) from Aquatic Environment. *Bioresour. Technol.* **2021**, *322*, 124539.
- (156) Zhou, S.; Xue, A.; Zhao, Y.; Wang, Q.; Chen, Y.; Li, M.; Xing, W. Competitive Adsorption of  $Hg^{2+}$ ,  $Pb^{2+}$  and  $Co^{2+}$  Ions on Polyacrylamide/Attapulgate. *Desalination* **2011**, *270* (1–3), 269–274.
- (157) Tabakci, M.; Yilmaz, M. Synthesis of a Chitosan-Linked Calix [4] Arene Chelating Polymer and Its Sorption Ability toward Heavy Metals and Dichromate Anions. *Bioresour. Technol.* **2008**, *99* (14), 6642–6645.
- (158) Hu, X.; Li, Y.; Wang, Y.; Li, X.; Li, H.; Liu, X.; Zhang, P. Adsorption Kinetics, Thermodynamics and Isotherm of Thiocalix [4] Arene-Loaded Resin to Heavy Metal Ions. *Desalination* **2010**, *259* (1–3), 76–83.
- (159) Duran, A.; Soylak, M.; Tuncel, S. A. Poly (Vinyl Pyridine-Poly Ethylene Glycol Methacrylate-Ethylene Glycol Dimethacrylate) Beads for Heavy Metal Removal. *J. Hazard. Mater.* **2008**, *155* (1–2), 114–120.

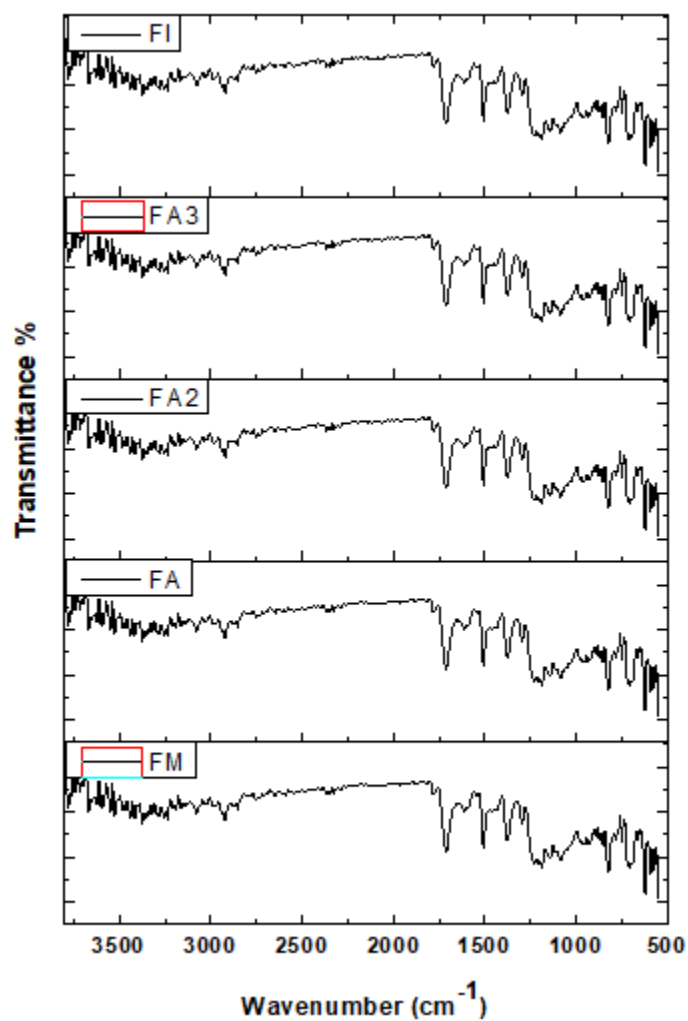
- (160) Coskun, R.; Soykan, C. Lead (II) Adsorption from Aqueous Solution by Poly (Ethylene Terephthalate)-g-Acrylamide Fibers. *J. Polym. Res.* **2006**, *13* (1), 1–8.
- (161) Feng, Q.; Lin, Q.; Gong, F.; Sugita, S.; Shoya, M. Adsorption of Lead and Mercury by Rice Husk Ash. *J. Colloid Interface Sci.* **2004**, *278* (1), 1–8.
- (162) Dias Filho, N. L.; Polito, W. L.; Gushikem, Y. Sorption and Preconcentration of Some Heavy Metals by 2-Mercaptobenzothiazole-Clay. *Talanta* **1995**, *42* (8), 1031–1036.
- (163) Munir, N.; Masood, S.; Liaqat, F.; Tahir, M. N.; Yousuf, S.; Kalsoom, S.; Mughal, E. U.; Sumrra, S. H.; Maalik, A.; Zafar, M. N. Synthesis of New Pro-PYE Ligands as Co-Catalysts toward Pd-Catalyzed Heck–Mizoroki Cross Coupling Reactions. *RSC Adv.* **2019**, *9* (65), 37986–38000.
- (164) Branco, C. M. Multilayer Membranes for Intermediate Temperature Polymer Electrolyte Fuel Cells. School of Chemical Engineering, University of Birmingham (PhD Dissertation) **2017**.
- (165) Bayer, T.; Bishop, S. R.; Nishihara, M.; Sasaki, K.; Lyth, S. M. Characterization of a Graphene Oxide Membrane Fuel Cell. *J. Power Sources* **2014**, *272*, 239–247.
- (166) Kumar, R.; Xu, C.; Scott, K. Graphite Oxide/Nafion Composite Membranes for Polymer Electrolyte Fuel Cells. *Rsc Adv.* **2012**, *2* (23), 8777–8782.
- (167) Fidiani, E.; Thirunavukkarasu, G.; Li, Y.; Chiu, Y. L.; Du, S. Au Integrated AgPt Nanorods for the Oxygen Reduction Reaction in Proton Exchange Membrane Fuel Cells. *J. Mater. Chem. A* **2021**, *9* (9), 5578–5587.
- (168) Yuan, X. Z.; Song, C.; Wang, H.; Zhang, J. **2010**, Fundamentals and Applications: Electrochemical Impedance Spectroscopy in PEM Fuel Cells; Springer London.
- (169) Mardle, P.; Thirunavukkarasu, G.; Guan, S.; Chiu, Y. L.; Du, S. Comparative Study of PtNi Nanowire Array Electrodes toward Oxygen Reduction Reaction by Half-Cell Measurement and PEMFC Test. *ACS Appl. Mater. Interfaces* **2020**, *12* (38), 42832–42841.

## List of Publications and Conference Presentations

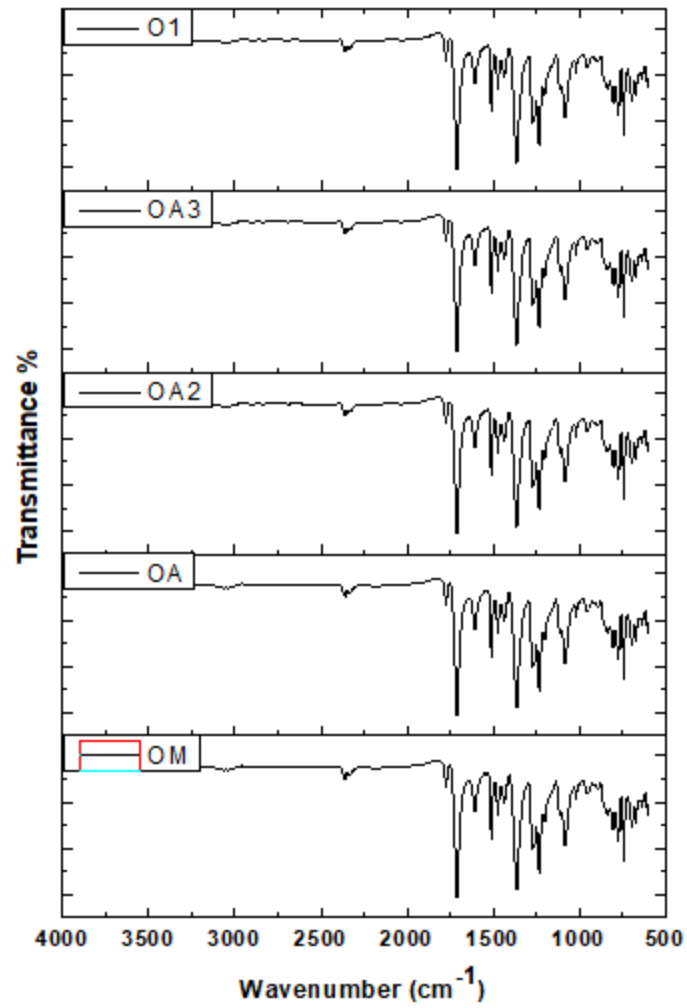
---

1. **Manzoor, A.**, Kalsoom, S., Khan, Y. K., Siddiqi, H. M., & Shah, M. H. (2022). Synthesis of Sulfonated Copolyimides by Thermal Imidization for Efficient Lead Ion Adsorption from Aqueous Media. *ACS Applied Polymer Materials*, 4(8), 5660-5669.
2. **Manzoor, A.**, Siddiqi, H. M., & Shah, A. (2022). Development of sulphonated copolyimide based sensor for metal ions detection in aqueous media. *Inorganic Chemistry Communications*, 146, 110088.
3. **Manzoor, A.**, Siddiqi, H. M. Synthesis and characterization of sulphonated copolyimides for lead ions adsorption from aqueous media. *3<sup>rd</sup> International Conference on Water, Energy, and Environment for Sustainability - 2023 (IC-WEES 2023)*. 16-18<sup>th</sup> August 2023, School of Natural Sciences, National University of Sciences and Technology (NUST) Islamabad, Pakistan. (Oral Presentation)
4. **Manzoor, A.**, Siddiqi, H. M., & Du, S. Preparation of sulphonated polyimide membranes as electrolytes for polymer electrolyte membrane fuel cells (PEMFCS). *21<sup>st</sup> International, 1<sup>st</sup> Inter-Islamic and 33<sup>rd</sup> National Chemistry Conference on Chemical Sciences: Technology, Innovation and Sustainability - 2023 (CHEMCON 2023)*. 23-25<sup>th</sup> October 2023, Department of Chemistry, Quaid-i-Azam University (QAU) Islamabad, Pakistan. (Oral Presentation)

## Annexure 1: FTIR-ATR of polyimides and sulphonated copolyimides

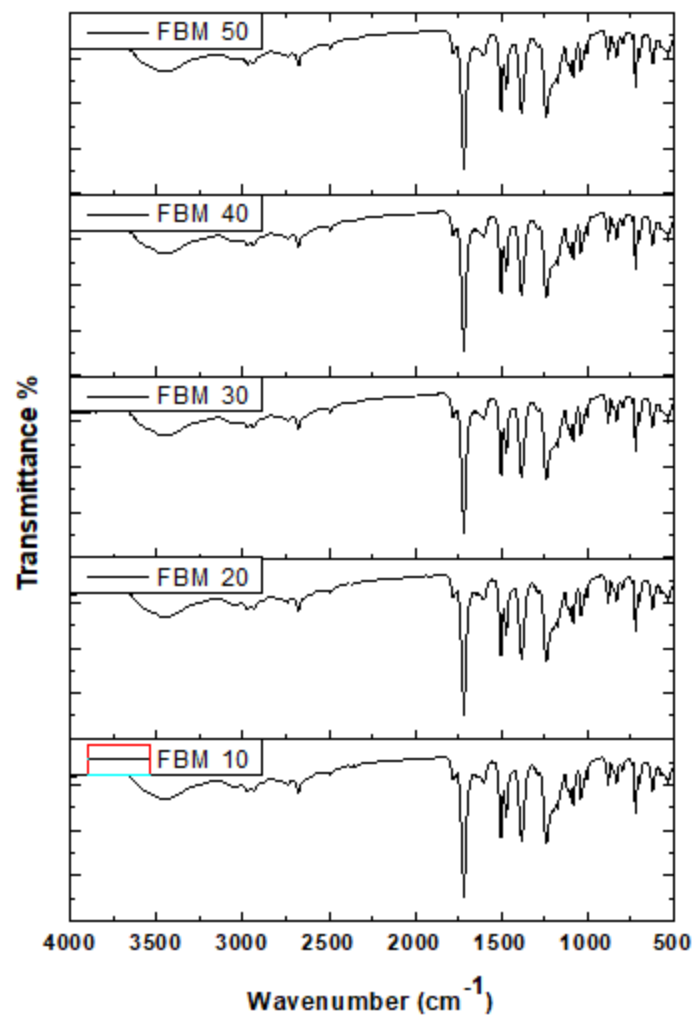


Annexure 1.1: Comparative FTIR Spectra of 6FDA based polyimides

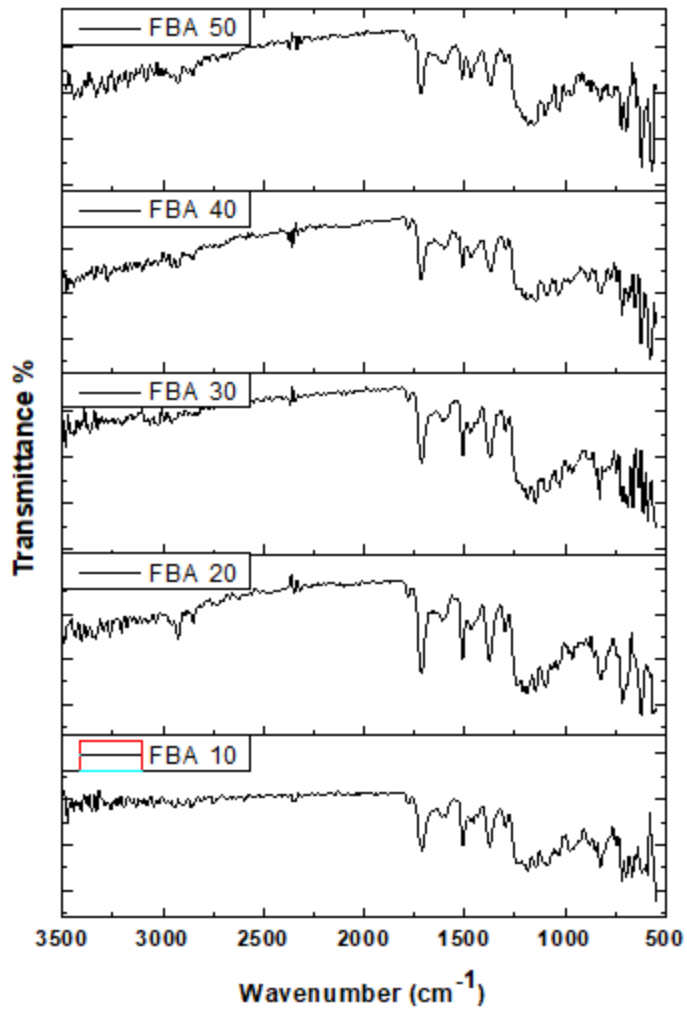


**Annexure 2.1: Comparative FTIR Spectra of ODPA based polyimides**

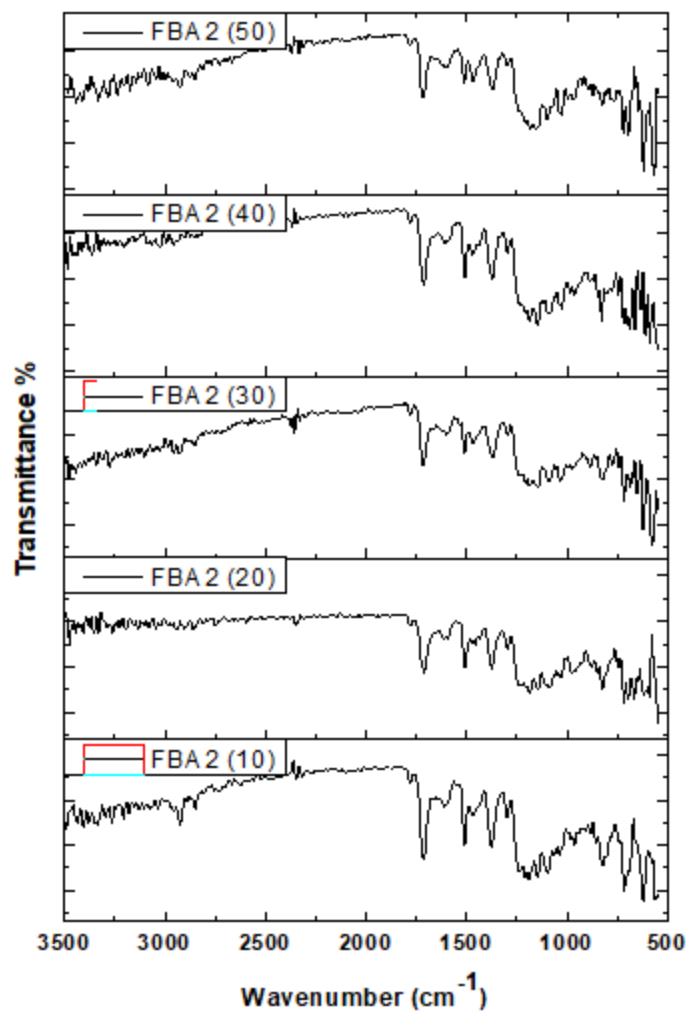




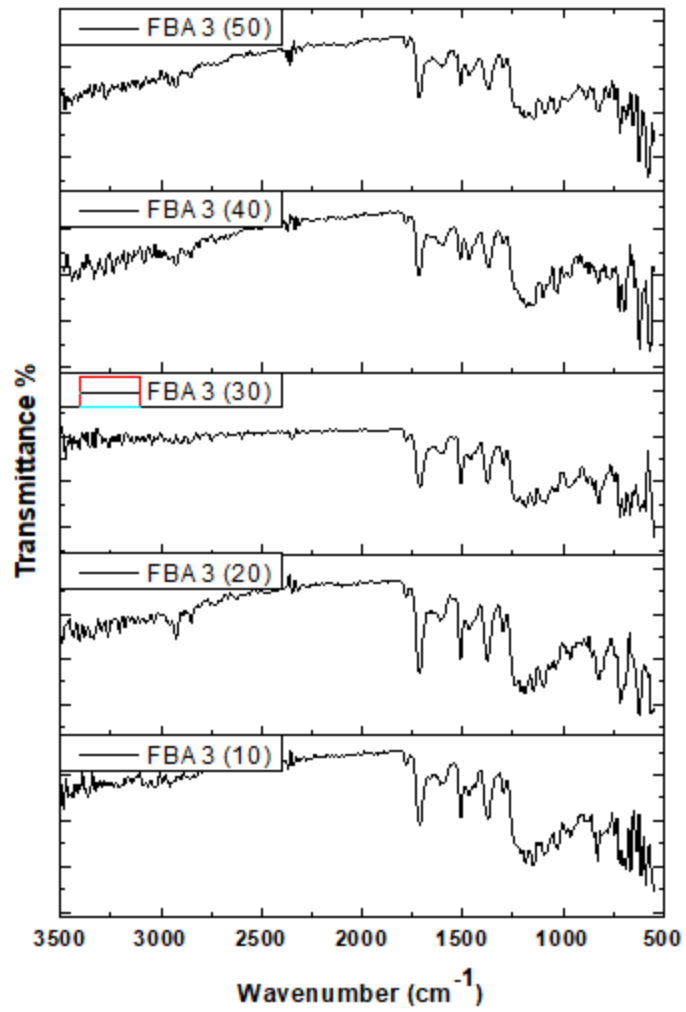
**Annexure 3.1: Comparative FTIR Spectra of FBM (10, 20, 30, 40, 50)**



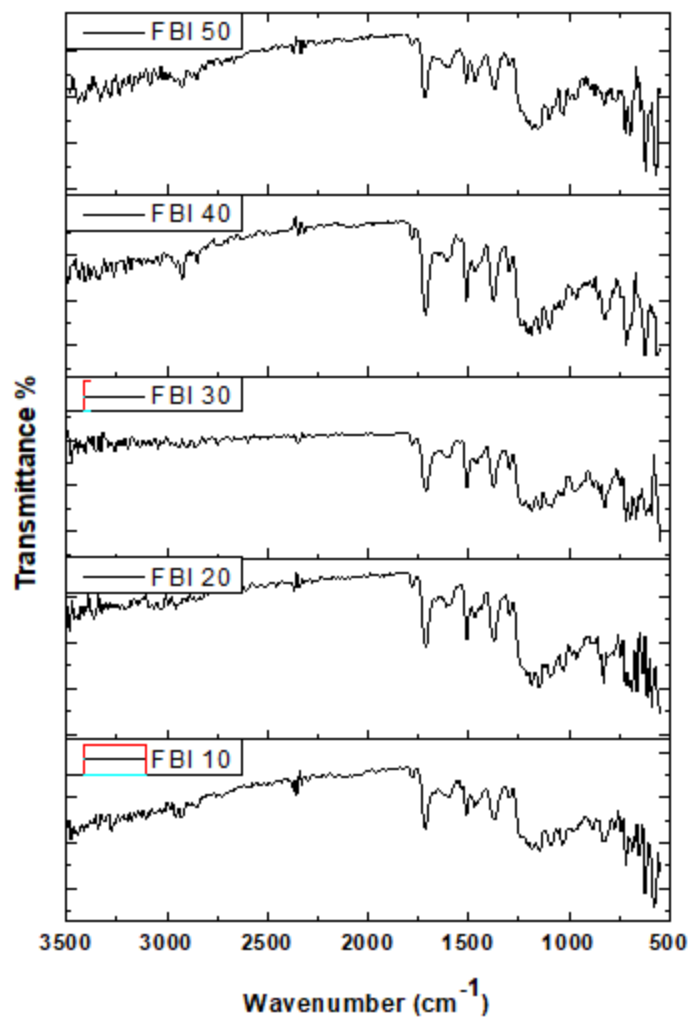
**Annexure 3.2: Comparative FTIR Spectra of FBA (10, 20, 30, 40, 50)**



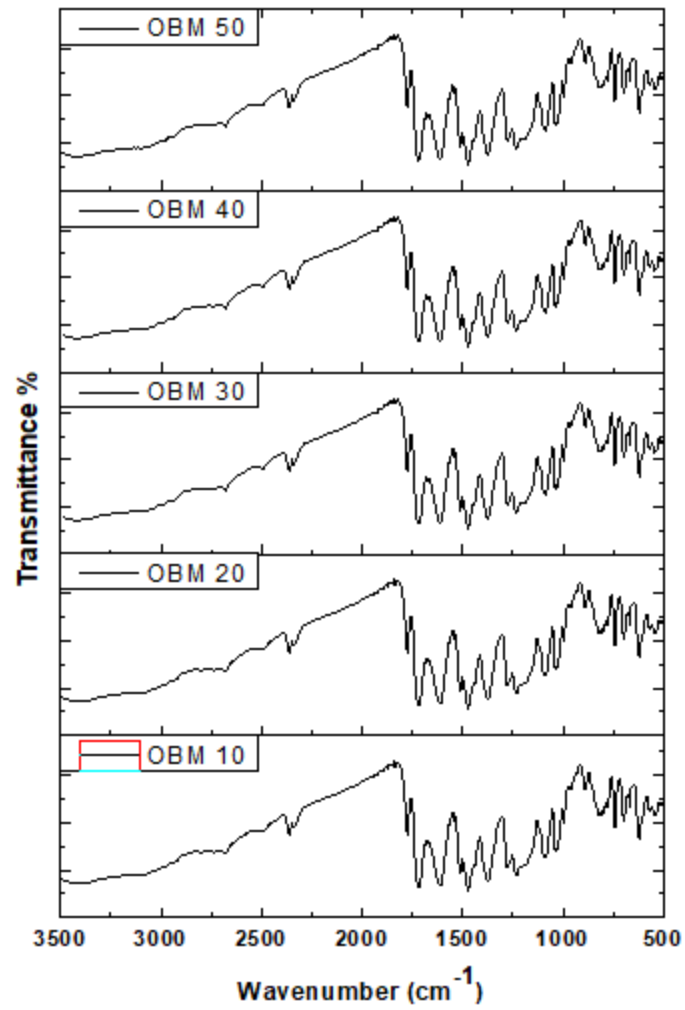
**Annexure 3.3: Comparative FTIR Spectra of FBA2 (10, 20, 30, 40, 50)**



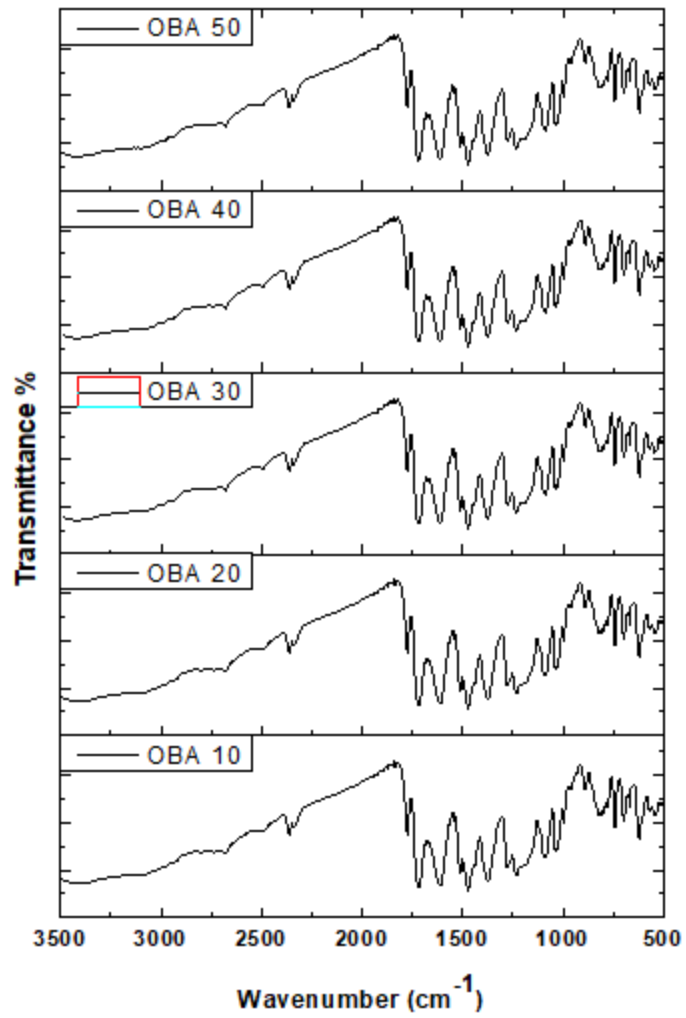
**Annexure 3.4: Comparative FTIR Spectra of FBA3 (10, 20, 30, 40, 50)**



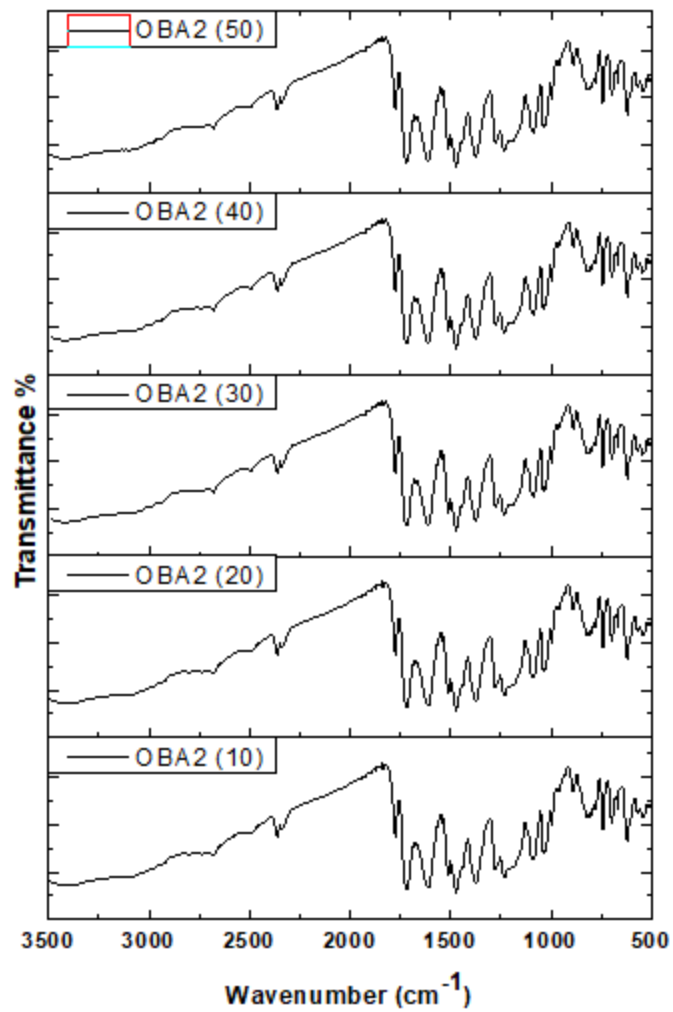
**Annexure 3.5: Comparative FTIR Spectra of FBI (10, 20, 30, 40, 50)**



**Annexure 4.1: Comparative FTIR Spectra of OBM (10, 20, 30, 40, 50)**

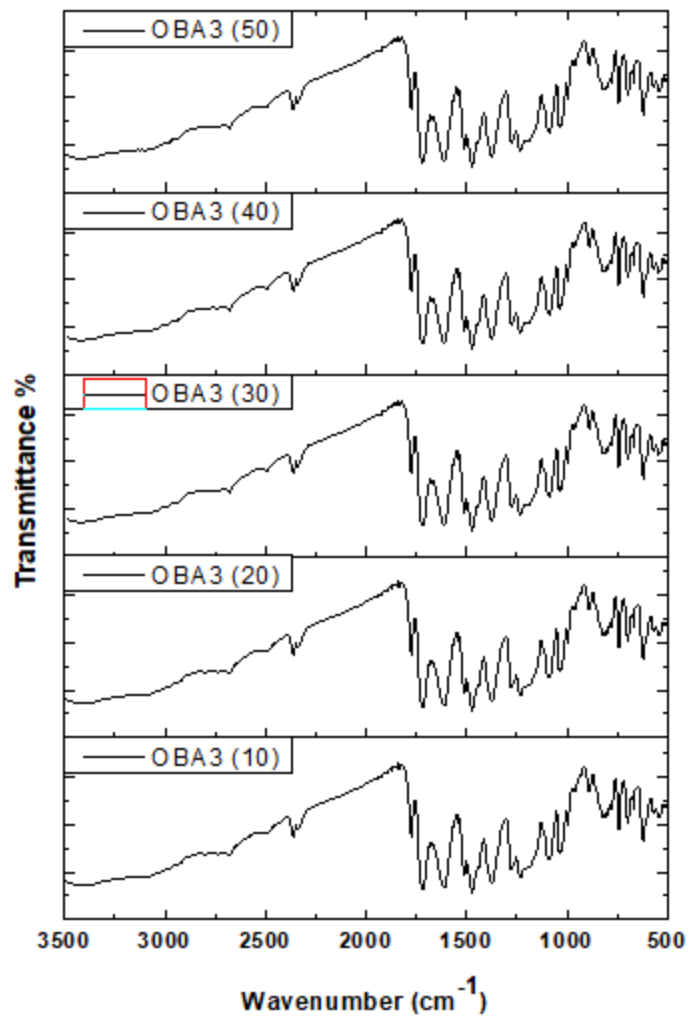


**Annexure 4.2: Comparative FTIR Spectra of OBA (10, 20, 30, 40, 50)**

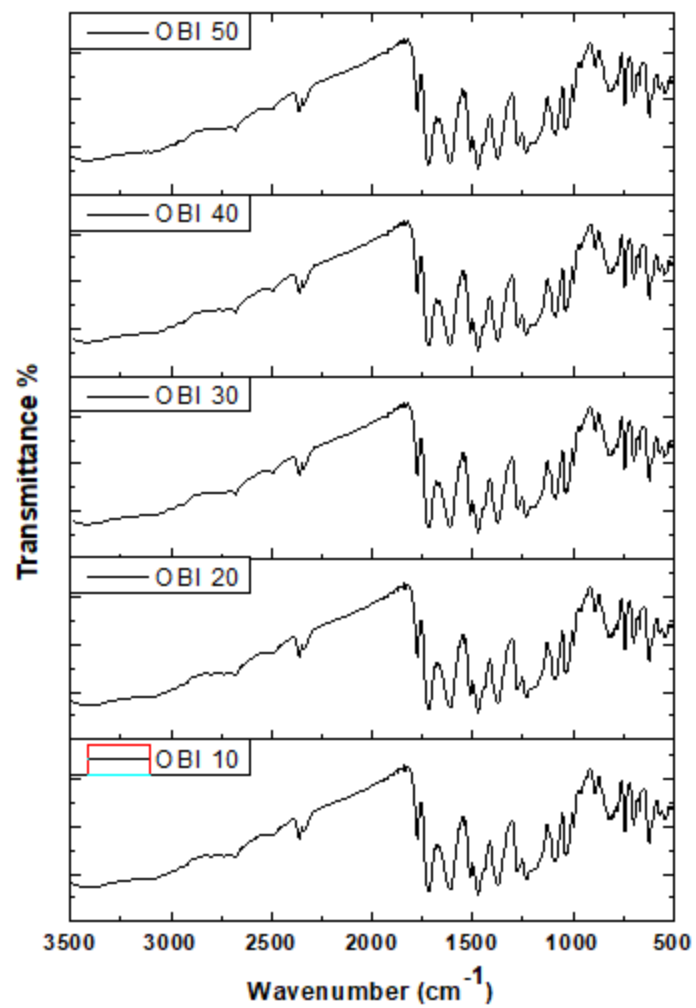


**Annexure 4.3: Comparative FTIR Spectra of OBA2 (10, 20, 30, 40, 50)**

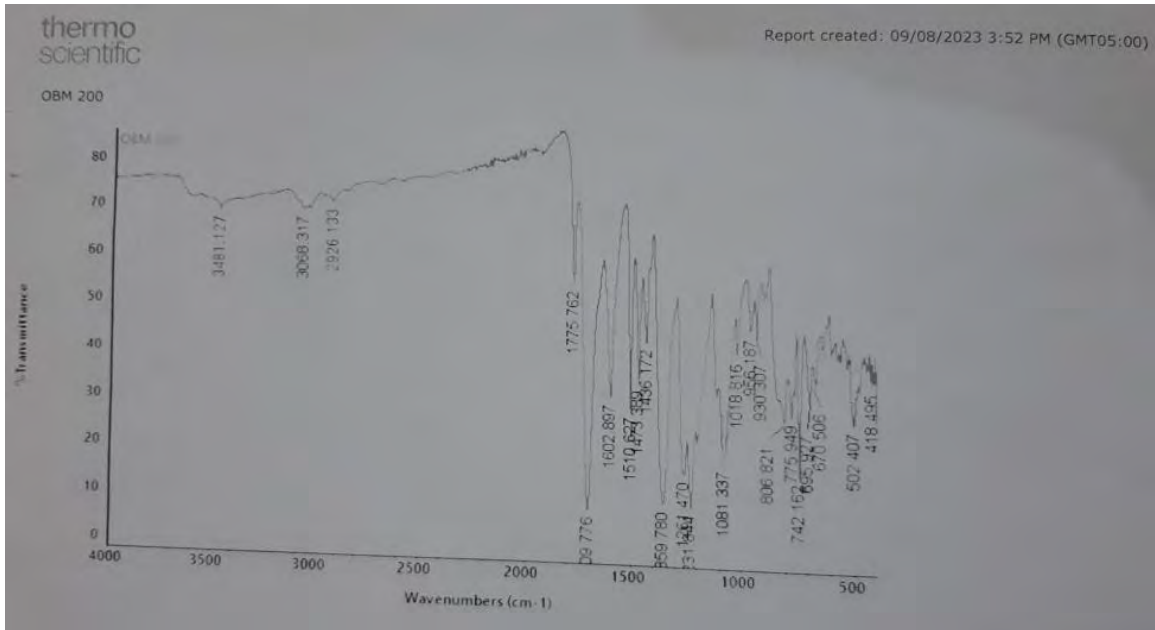




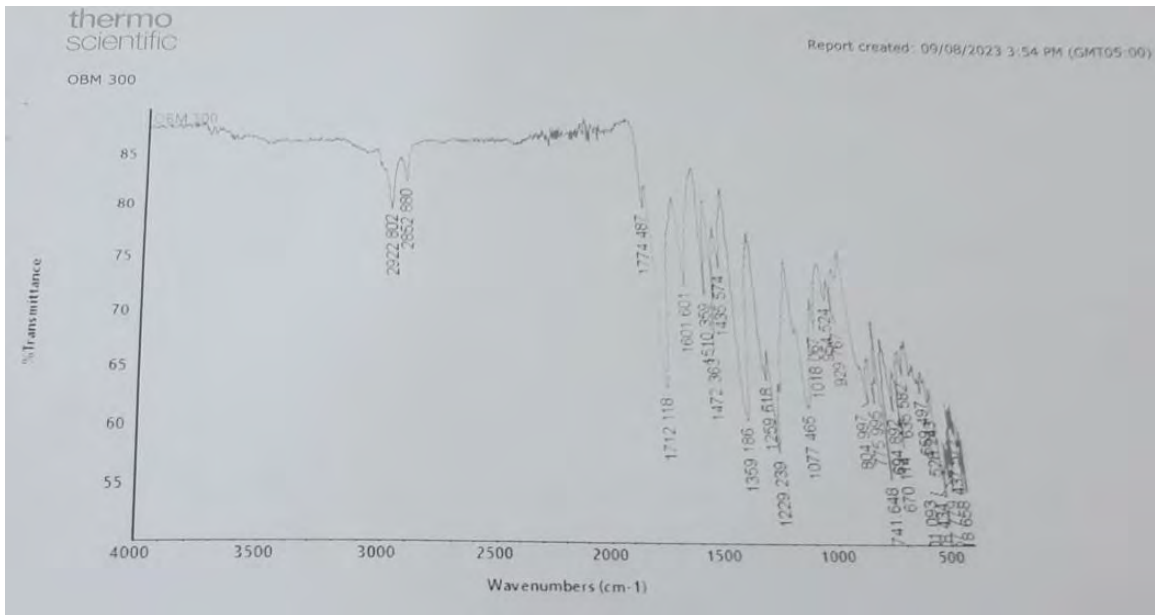
**Annexure 4.4: Comparative FTIR Spectra of OBA3 (10, 20, 30, 40, 50)**



**Annexure 4.5: Comparative FTIR Spectra of OBI (10, 20, 30, 40, 50)**

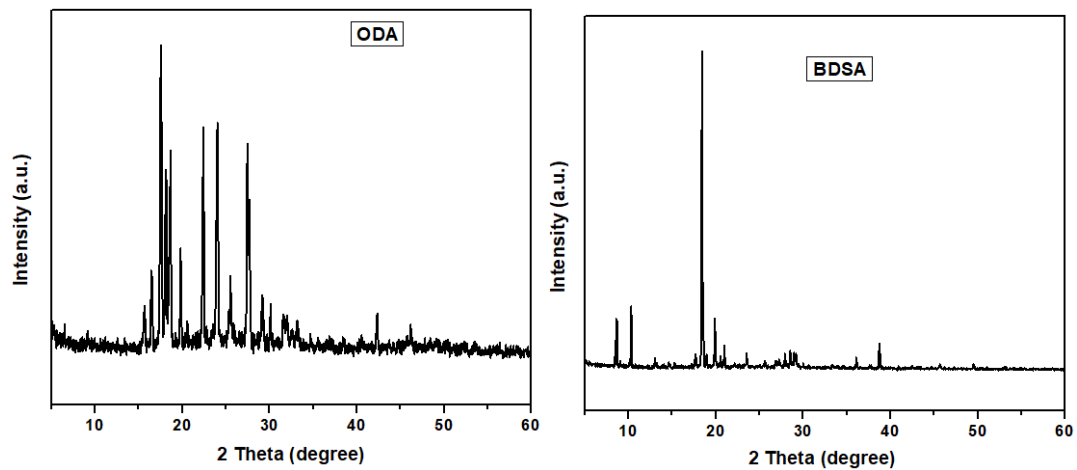


**Annexure 5.1: FTIR Spectrum of OM at 200 °C**

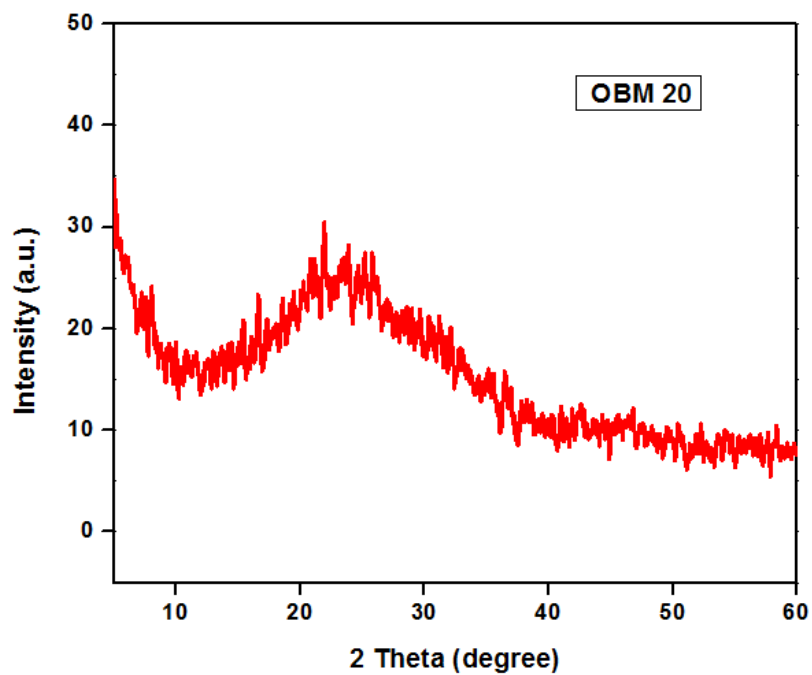


**Annexure 5.2: FTIR Spectrum of OM at 300 °C**

## Annexure 2: XRD patterns of diamines and sulphonated copolyimide

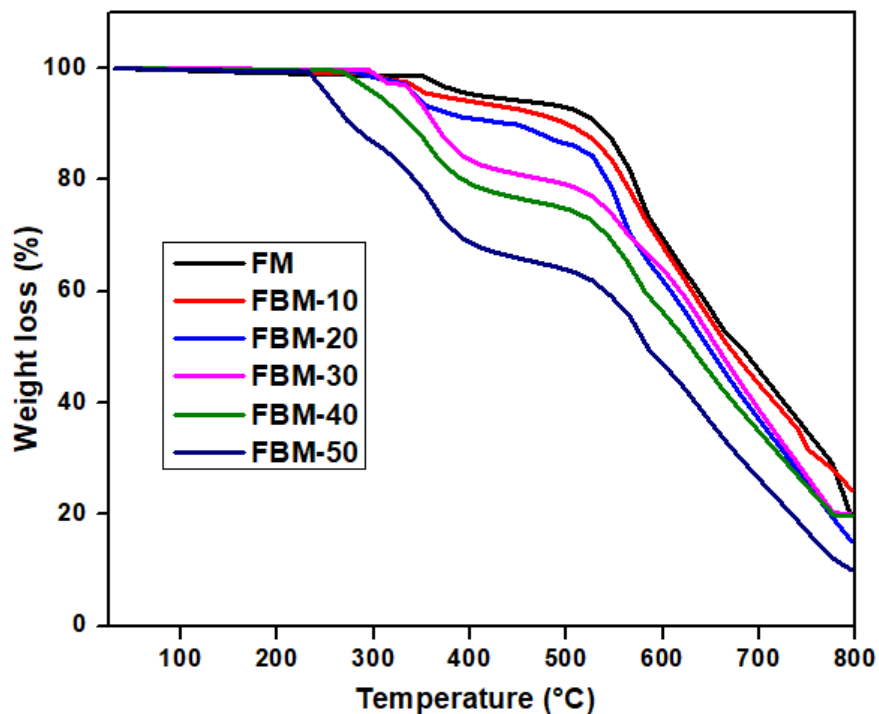


Annexure 6.1: XRD of ODA and BDSA diamines

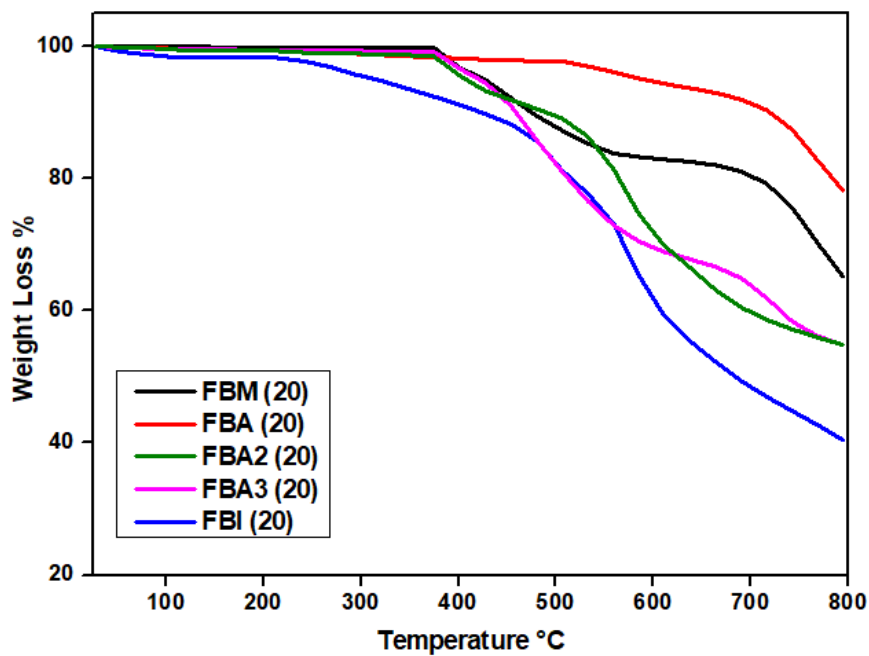


Annexure 7.1: XRD of OBM-20

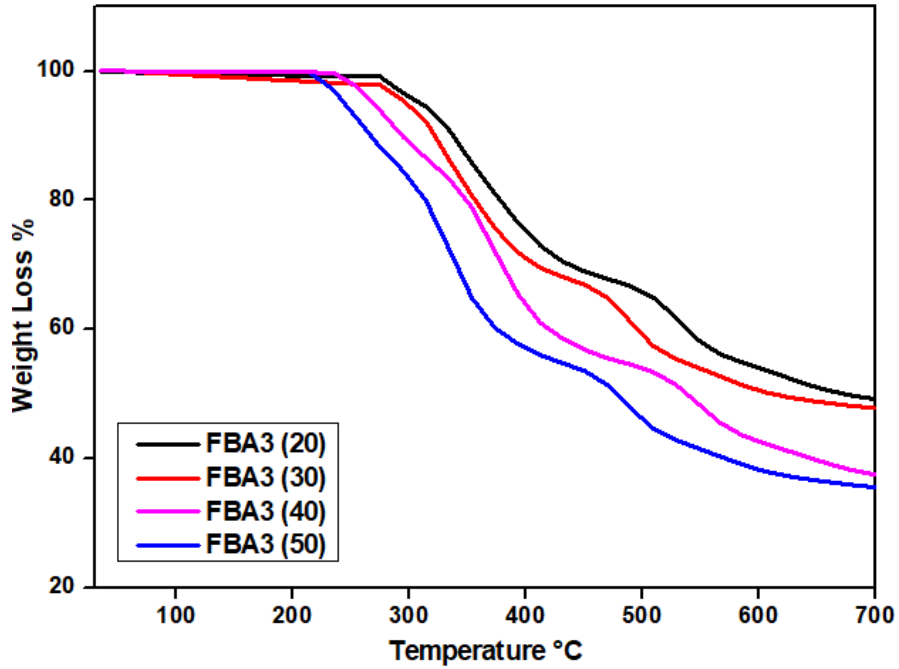
### Annexure 3: TGA curves of polyimides and sulphonated copolyimides



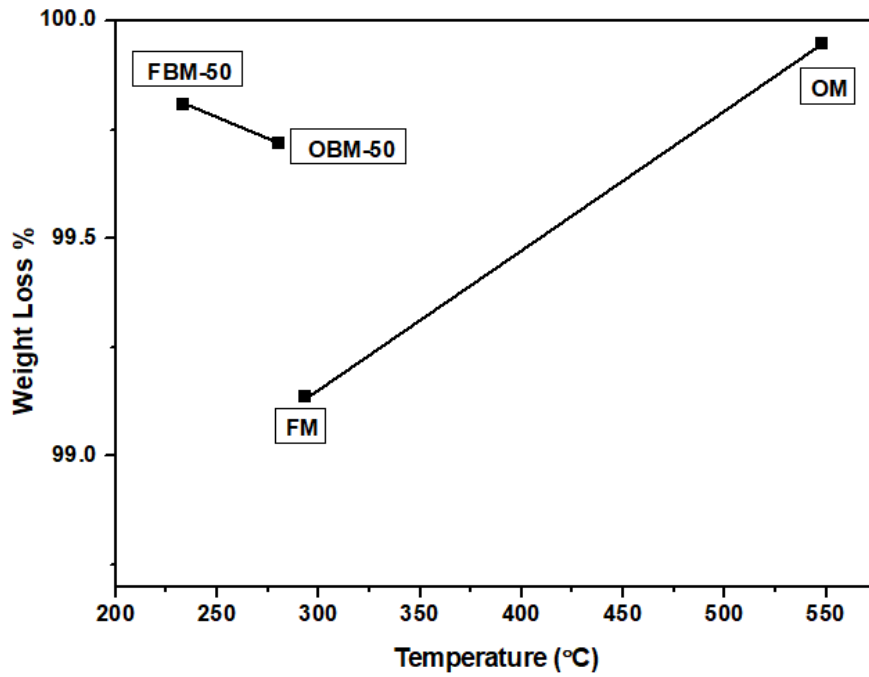
### Annexure 8.1: Comparative TGA curves of FM and its sulphonated analogs



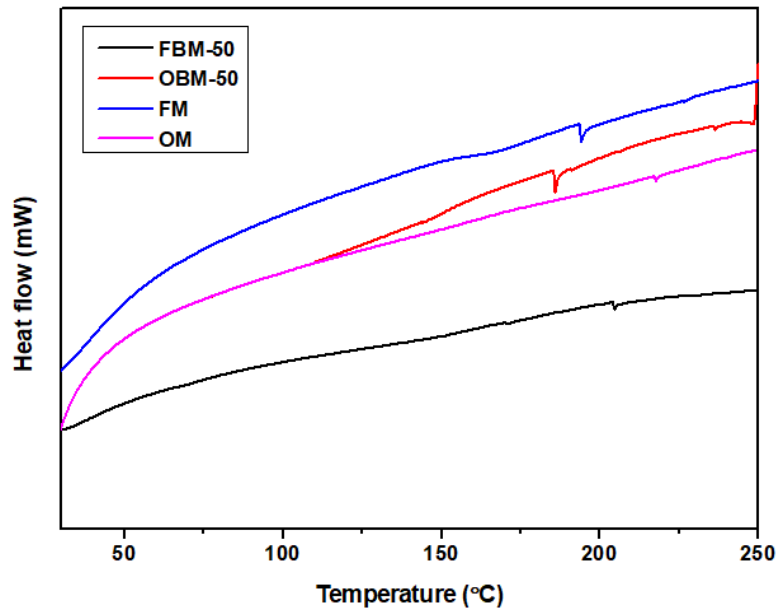
### Annexure 9.1: Comparative TGA curves of copolyimides with different diamine monomers



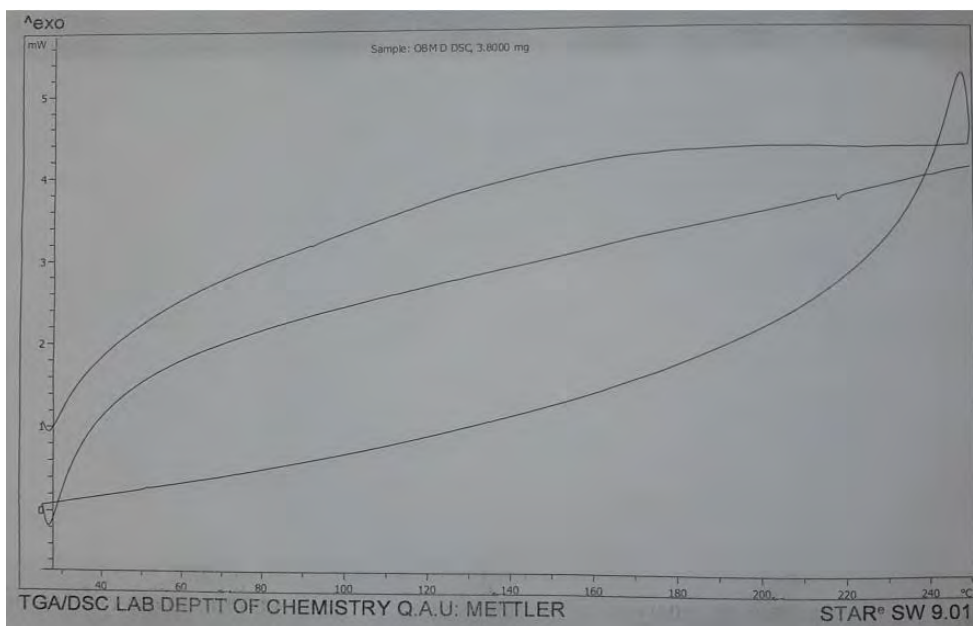
Annexure 10.1: Comparative TGA curves of FBA3-20, FBA3-30, FBA3-40 and FBA3-50



Annexure 11.1: T<sub>d</sub>'s of OM, FM, OBM-50 and FBM-50 as a function of temperature

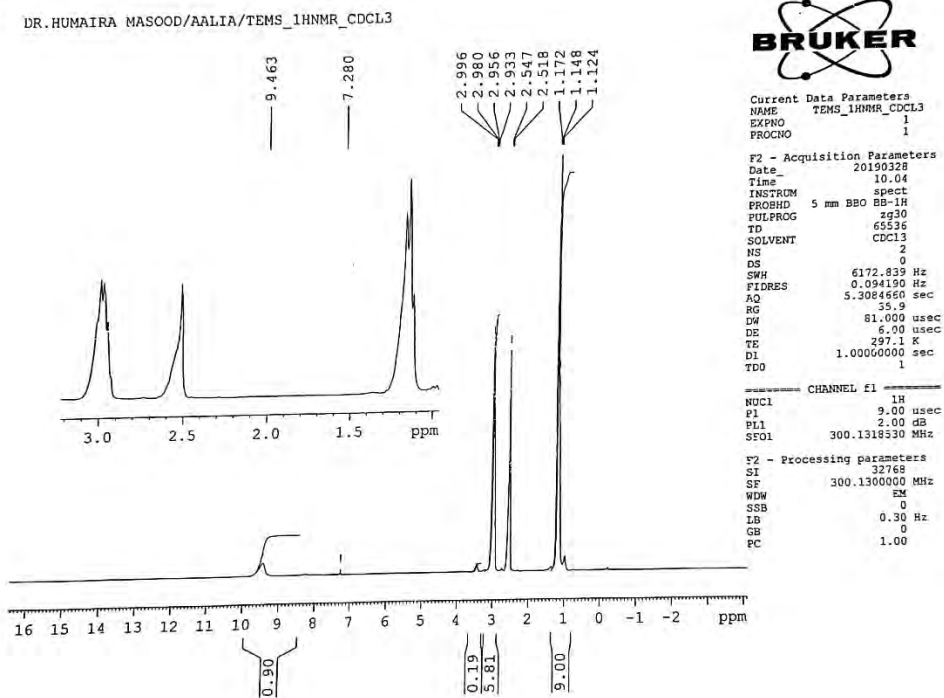


**Annexure 12.1: Comparative Tg's of OM, FM, OBM-50 and FBM-50**

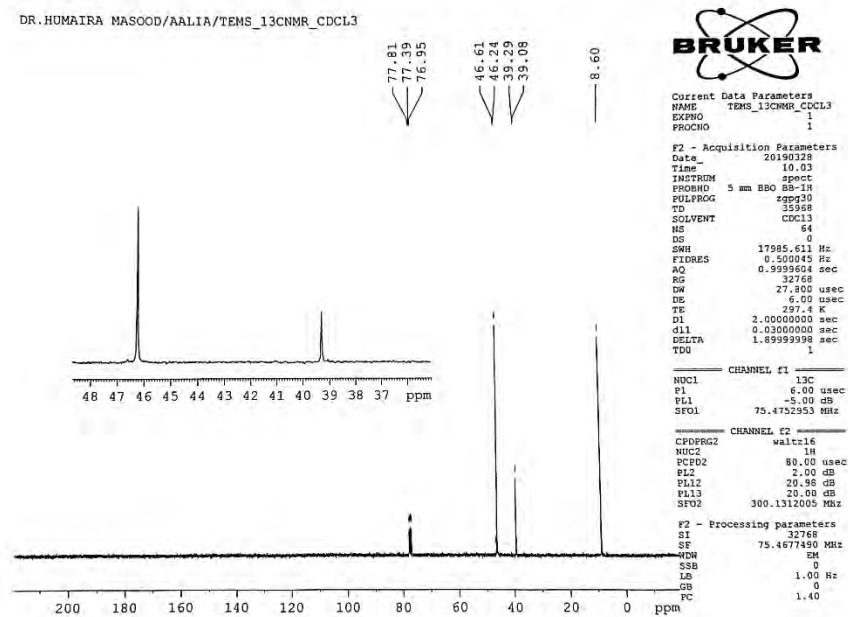


**Annexure 13.1: Tg of OM**

## Annexure 4: NMR spectra of protic ionic liquids



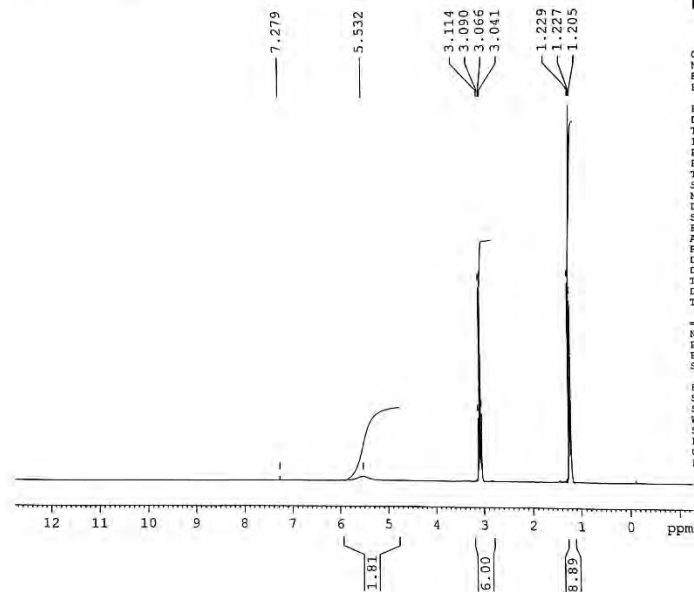
## Annexure 14.1: <sup>1</sup>H NMR spectrum of TEMs



## Annexure 14.2: <sup>13</sup>C NMR spectrum of TEMs



DR.HUMAIRA MASOOD/AALIA/TETFMS\_1HNMR\_CDCL3



Current Data Parameters  
 NAME TETFMS\_1HNMR\_CDCL3  
 EXPNO 1  
 PROCNO 1

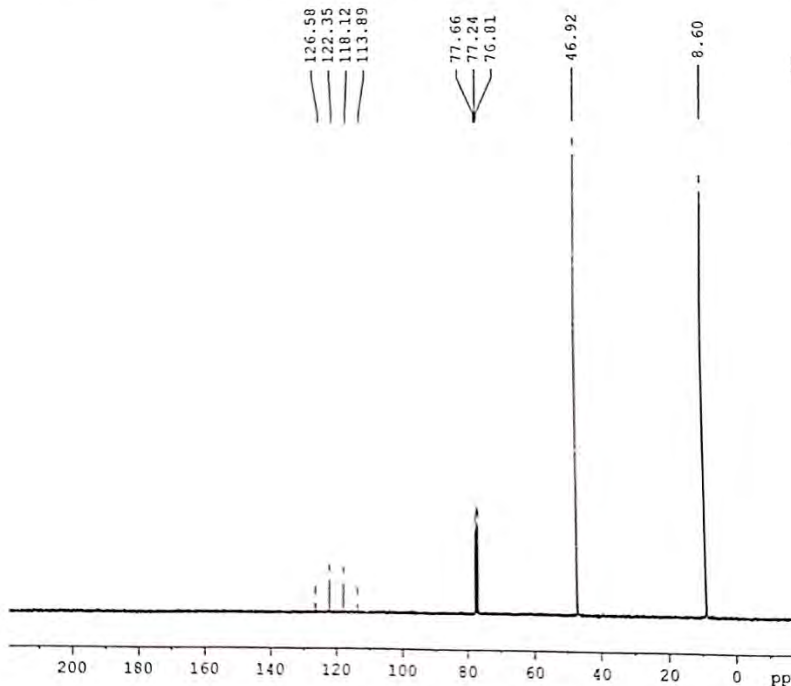
F2 - Acquisition Parameters  
 Date\_ 20190328  
 Time 10.16  
 INSTRUM spect  
 PROBHD 5 mm BBO BB-1H  
 PULPROG zg30  
 TD 65536  
 SOLVENT CDCl3  
 NS 2  
 DS 0  
 SWH 6172.839 Hz  
 FIDRES 0.094190 Hz  
 AQ 5.3084660 sec  
 RG 35.9  
 DW 81.000 usec  
 DE 6.00 usec  
 TE 298.8 K  
 D1 1.0000000 sec  
 TDO 1

CHANNEL f1  
 NUC1 1H  
 P1 9.00 usec  
 PL1 2.00 dB  
 SFO1 300.1318534 MHz

F2 - Processing parameters  
 SI 32768  
 SF 300.1300000 MHz  
 WDW EM  
 SSB 0  
 LB 0.30 Hz  
 GB 0  
 FC 1.00

Annexure 15.1: <sup>1</sup>H NMR spectrum of TETf

DR.HUMAIRA MASOOD/AALIA/TETFMS\_13CNMR\_CDCL3



Current Data Parameters  
 NAME TETFMS\_13CNMR\_CDCL3  
 EXPNO 1  
 PROCNO 1

F2 - Acquisition Parameters  
 Date\_ 20190328  
 Time 10.14  
 INSTRUM spect  
 PROBHD 5 mm BBO BB-1H  
 PULPROG zgpg30  
 TD 35968  
 SOLVENT CDCl3  
 NS 128  
 DS 0  
 SWH 17985.611 Hz  
 FIDRES 0.500045 Hz  
 AQ 0.9999604 sec  
 RG 32768  
 DW 27.800 usec  
 DE 6.00 usec  
 TE 297.1 K  
 D1 2.0000000 sec  
 d11 0.0300000 sec  
 DELTA 1.8999999 sec  
 TDO 1

CHANNEL f1  
 NUC1 13C  
 P1 6.00 usec  
 PL1 -5.00 dB  
 SFO1 75.4752953 MHz

CHANNEL f2  
 CPDPRG2 waltz16  
 NUC2 1H  
 PCPD2 80.00 usec  
 PL2 2.00 dB  
 PL12 20.98 dB  
 PL13 20.00 dB  
 SFO2 300.1312005 MHz

F2 - Processing parameters  
 SI 32768  
 SF 75.4677490 MHz  
 WDW EM  
 SSB 0  
 LB 1.00 Hz  
 GB 0  
 FC 1.40

Annexure 15.2: <sup>13</sup>C NMR spectrum of TETf